THE UNIVERSITY OF HULL

NOVEL STABILISATION OF EMULSIONS WITH

POLYELECTROLYTE COMPLEXES

being a Thesis submitted for the Degree of Doctor of Philosophy

in the University of Hull

by

Ana María Bago Rodríguez

MSc (IQS, Ramon Llull University)

BSc (IQS, Ramon Llull University)

September 2018

ACKNOWLEDGEMENTS

LIST OF PUBLICATIONS, PATENTS AND PRESENTATIONS

The work contained in this thesis has been published or will be submitted for publication:

1. A.M. Bago Rodriguez, B.P. Binks and T. Sekine, Novel stabilization of emulsions by soft particles: polyelectrolyte complexes, *Faraday Discuss.*, 2016, **191**, 255-285.

2. A.M. Bago Rodriguez, B.P. Binks and T. Sekine, Emulsion stabilization by complexes of oppositely charged synthetic polyelectrolytes, *Soft Matter*, 2018, **14**, 239-254.

3. Patent: "Novel Emulsion Emulsifiers", *US Pat.*, (provisional application number) 2017-096. (Inventors: B.P. Binks, A.M. Bago Rodriguez and T. Sekine).

4. Patent: "Oil in Water Emulsion Composition", *US Pat.*, (provisional application number) 2018-188. (Inventors: B.P. Binks, A.M. Bago Rodriguez and T. Sekine).

Poster and oral presentations have been undertaken at the following events:

1. Poster presentation 1st prize: "Novel stabilisation of emulsions by soft particles: polyelectrolyte complexes", Postgraduate Research Colloquium, 20 – 21 July 2016, University of Hull, U.K.

2. Oral presentation: "Emulsions stabilised by polyelectrolyte complexes (PEC)", UK Colloids 2017, 10 – 12 July 2017, Manchester, U.K.

3. Oral presentation: "Emulsions stabilised by polyelectrolyte complexes (PEC)", Postgraduate Research Colloquium, 22nd January 2018, University of Hull, U.K.

4. Oral presentation: "Emulsions stabilised by polyelectrolyte complexes (PEC)", 16th Conference of the International Association of Colloid and Interface Scientists (IACIS), 21 – 25 May 2018, Rotterdam, The Netherlands.

ABSTRACT

The concept of a novel stabiliser of oil-water emulsions has been put forward, being the polyelectrolyte complex (PEC) formed between oppositely charged water-soluble polymers in cases where either polymer alone is incapable of stabilising an emulsion. Four oppositely charged synthetic polyelectrolytes (strong and weak) are selected, which allowed four polymer mixtures to be studied. The behaviour of their mixtures in water is correlated with that of emulsions after addition of oil.

Aqueous polymer mixtures are investigated *via* dynamic light scattering to determine the size of the aggregates. Moreover, various optical techniques are used to identify the type of associative phase separation (precipitation or complex coacervation) and their shape. The effects of polyelectrolyte (PEL) mixing ratio, pH, [PEL] and salt content are studied in detail. In general, PEC particles are obtained as a result of a strong electrostatic interaction while complex coacervates arise from weak interactions. Around equal mole fractions of the two polymers, the zeta potential of the aggregates reverses in sign. Spherical complexes of diameters of few hundreds nanometres are obtained at low polyelectrolyte concentration. However, by increasing the initial [PEL], primary particles aggregate. Aggregated PEC particles have an irregular shape while coacervate droplets, which contain high amounts of water, are spherical and have no special internal structure, as observed from TEM images. Under specific conditions, coacervate droplets completely coalesce giving rise to the formation of the so-called coacervate phase. The effect of increasing the salt concentration is comparable in both PEC precipitates and coacervates and causes an initial destabilisation of the aqueous dispersion due to complex aggregation, followed by dissolution of the electrostatic complex at high salt concentrations.

For the emulsion study, the same parameters as for aqueous PEC dispersions are evaluated, as well as the oil volume fraction (ϕ_o). The complete study is carried out with dodecane despite oils of different chemistry and polarity have also been considered throughout this thesis. The most stable emulsions to both creaming and coalescence are prepared with aqueous PEC dispersions containing complexes of almost neutral charge. By increasing the polyelectrolyte concentration, emulsions become more stable. However, at high [PEL], aggregation levels are relatively high and emulsion stability is slightly worse as big particles can easily be dislodged from

the oil-water interface compared to smaller ones. From cryo-SEM images, close-packed particle layers are detected at drop interfaces as well as particle aggregation in the continuous phase. By increasing the oil volume fraction in the emulsion, the droplet diameter increases constantly up until a point where oil droplets appear to be deformed and the viscosity of the emulsion increases substantially. This suggests the formation of high internal phase emulsions (HIPEs), which is rare in particle-stabilised systems, where catastrophic phase inversion is the usual outcome. Taking advantage of the intrinsic fluorescence of the used PEL, confocal microscopy turns out to be a useful technique to visualise where PEC particles are placed upon homogenisation. At high oil volume fractions, particles are only detected around oil droplets, whereas at low oil volume fractions, excess particles remain at the continuous aqueous phase providing extra stability against coalescence. As for aqueous PEC dispersions, the concentration of salt has a remarkable effect on emulsion stability. For emulsions stabilised with PEC particles, by increasing the aggregation level, emulsions become completely unstable. However, at a relatively high salt content, emulsions re-stabilise due to adsorption of uncharged individual polymer molecules. Emulsions with coacervate droplets can be prepared by the addition of oil stepwise and multiple homogenisation steps. However, unlike PEC particles, the system is sensible to the oil type. The feasibility of the coacervate phase to spread at the oil-water interface is discussed in terms of the relevant spreading coefficients and predictions are compared with experiments for a range of oils. We encounter oils whose drops become engulfed by the coacervate phase as well as oils where no engulfing occurs.

Therefore, from the findings obtained from four different polyelectrolyte combinations, we can claim that emulsion stability is given by the presence of PEC at the oil-water interface as individual PEL are not surface-active on their own. Despite this work being a complete starting point for the basic understanding of emulsions stabilised by mixtures of oppositely charged polymers, we are not yet in a position to predict definite rules of behaviour in both aqueous PEC dispersions and emulsions containing them. Further investigation of other polyelectrolyte combinations is required to develop a better understanding of this area.

CONTENTS

CHAPTER 1 – INTRODUCTION

1.1 Industrial relevance of current research

This research project was funded by Shiseido, a Japanese multinational personal care company producing skin and hair care products, cosmetics and fragrances.

Their interest in this project lies in understanding whether emulsions could be prepared using polyelectrolyte complexes (PEC) as stabilisers. In general, cosmetic products contain surfactants, which can cause irritation or burning sensations of the skin. Therefore, the introduction of PEC in the development of future formulations could be of great interest to overcome this issue. Moreover, the use of this novel type of stabilisers could generate emulsions with special characteristics. From the common findings raised from the investigation of different polyelectrolyte combinations containing strong and weak polyelectrolytes, the final aim would be to elucidate a general rule that could predict the best conditions to prepare stable emulsions, which could help in the design of future formulations.

1.2 Phase separation in polymer mixtures

A polymer can be defined as a macromolecule whose structure is composed of repeating units (monomers) that chemically interact in a polymerisation reaction. Mixtures between two or more polymers gained special attention many years ago due to their potential applications. When mixing two polymer solutions, different types of phase separation can occur, which are depicted in Figure 1.1 and explained below.

Figure 1.1. Types of phase separation upon mixing aqueous solutions of polymers. Classification taken from ref. 1.
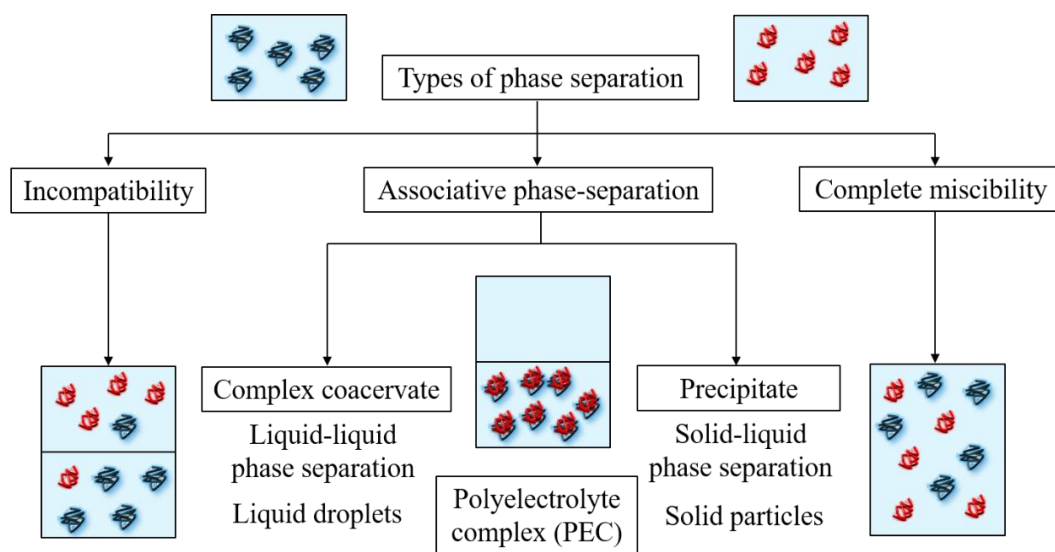
If polymers are incompatible (*i.e.* they repel each other), segregative phase separation takes place and each polymer is collected (predominantly) in a different phase. This is the most common scenario that arises upon mixing two polymer solutions and one example is the two phases formed by mixing dextran and methylcellulose in water (Figure 1.2).[1]

Figure 1.2. Composition of the two phases formed by a mixture of 1.1% dextran and 0.36% methylcellulose in water. Redrawn from ref. 1.

0.39% dextran
0.65% methylcellulose
98.96% water

1.58% dextran
0.15% methylcellulose
98.27% water
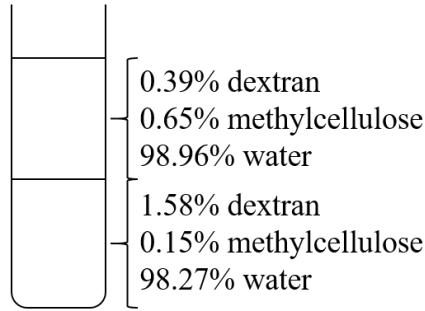
Flory and Huggins presented the first statistical thermodynamic model of polymer blends in their lattice fluid theory.[2-6] According to this theory, each polymer chain consists of a number of segments covalently bonded to each other and it is considered that each lattice site is occupied by a chain segment (Figure 1.3).[6,7]

Figure 1.3. Schematic representation of polymer-polymer arrangements in a lattice of N cells; visual illustration of combinatorial entropy. Redrawn from ref. 8.
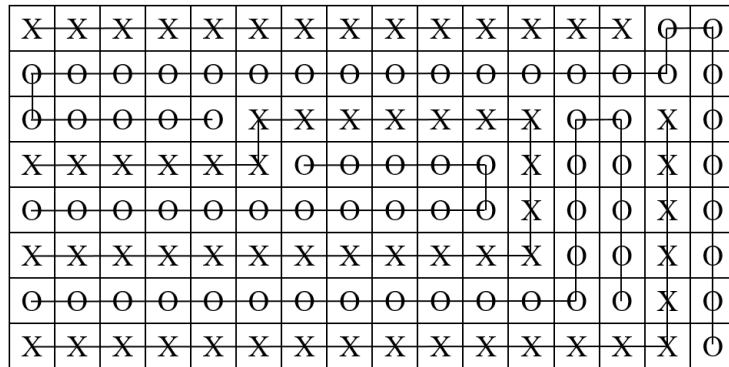
The free energy of mixing, ΔG_m, is given by,

$$\frac{\Delta G_m}{k_B T} = \frac{\varphi_1}{r_1}\ln\varphi_1 + \frac{\varphi_2}{r_2}\ln\varphi_2 + \chi_{12}\varphi_1\varphi_2 \tag{1.1}$$

where k_B is the Boltzmann constant, T is the temperature, r_i is the degree of polymerisation of the component i, φ_i is the volume fraction of the component i and χ_{12} is the Flory-Huggins interaction parameter, which is calculated as,

$$\chi_{12} = \frac{z\Delta w_{12}}{k_B T} \tag{1.2}$$

where z is the coordination number of the lattice and represents the total number of contacts between a polymer molecule and all of its neighbours.[6] Δw_{12} is the change in energy due to the formation of a 1-2 interaction from initial 1-1 and 2-2 interactions (equation 1.3).

$$\Delta w_{12} = w_{12} - (w_{11} + w_{22})/2 \qquad (1.3)$$

The first two logarithmic terms in equation 1.1 correspond to the combinatorial entropy, which is calculated by enumerating the number of arrangements of the molecules on a lattice.[9] The third term is the enthalpy of the mixing contribution and it is related to specific interactions between the components of the mixture.[9] As shown from equation 1.1, the entropic term becomes negligible for high molecular weight polymers because of their high degree of polymerisation. Since the enthalpy term is normally positive, owing to unfavourable interactions between unlike pairs of molecules, $\Delta G_m > 0$, indicating why high molecular weight polymers become less likely to mix.[9]

Complete miscibility occurs in exceptional cases and gives rise to a homogeneous solution. For complete miscibility to occur, ΔG_m must be negative. Therefore, the entropic contribution must exceed the enthalpic one; that is only exothermic mixing ensues in a miscible mixture. As a result, specific interactions might exist between the components of the mixture.[7] One example is the mixture between polystyrene and poly(2,6-dimethyl-1,4-phenylene oxide) (Figure 1.4).[10] The formation of a miscible blend in this case is explained by the π-staking of the aromatic rings.

Figure 1.4. Chemical structures of (a) poly(2,6-dimethyl-1,4-phenylene oxide) and (b) polystyrene.
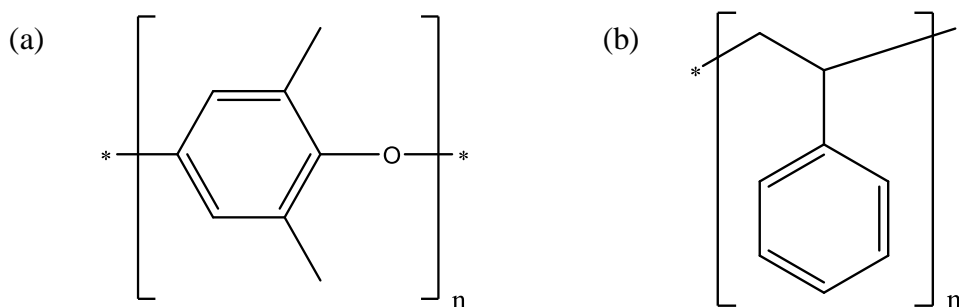
Finally, if the polymers show net attraction, usually through electrostatic interactions, associative phase separation occurs. In this case, the two polymers are collected in one

phase while the other phase consists almost entirely of solvent. This interaction can lead either to the formation of a complex coacervate (liquid-liquid type of phase separation) or a precipitate (solid-liquid type of phase separation). Both complexation mechanisms are driven by an increase of entropy due to the release of the counterions initially bound to the PEL backbone chain. Although the factors that dictate the nature of each type of associative phase separation are not fully elucidated, it is generally assumed that strong interactions between PEL yield precipitates while in coacervation the interactions are relatively weak.[11,12] The distinction between these two types of associative phase separation is not clear in the literature and the general term polyelectrolyte complex (PEC) is adopted for both scenarios. However, optical microscopy is a simple and useful technique to distinguish between precipitation (amorphous solid particles) and complex coacervation (micron-sized droplets).[11,12]

1.3 Polyelectrolyte complexes (PEC)

1.3.1 Polyelectrolyte (PEL): definition and classification

A polyelectrolyte (PEL, also called polyion) can be defined as a polymer consisting of a macromolecule bearing numerous ionisable groups (either cationic or anionic) and low molecular weight counterions to ensure electroneutrality.[13-15] Due to the charges along the polymer chain, they are hydrophilic and water-soluble. This feature makes them suitable to use in a wide range of applications, such as drug delivery, water treatment, paper making processes, cosmetic industry and food industry, amongst others.[13,14]

According to their origin, PEL can be categorized into natural, modified or synthetic. Biomacromolecules like DNA, proteins or charged polysaccharides are examples of natural polyelectrolytes, whereas synthetic polymers include poly(diallyldimethylammonium chloride) (PDADMAC) and poly(4-styrenesulfonate) sodium salt (PSSNa).[13] Figure 1.5 includes the structures of sodium carboxymethyl cellulose and PSSNa, an artificial-nature and a synthetic polyelectrolyte, respectively. Regarding the nature of the bound ions, polyions can be classified into polycations (positively charged groups), polyanions (negatively charged groups) and polyampholytes (the main backbone chain contains both cationic and anionic groups).[13] In terms of the degree of ionization and how it is affected by pH-changes, PEL can be classed as strong or weak.[13] Strong polyelectrolytes, such as PSSNa,

dissociate completely in the entire pH range. Therefore, the total charge is solely given by the polymer structure. On the other hand, weak polyelectrolytes (polyacids and polybases), *e.g.* poly(acrylic acid), PAA, have a degree of dissociation that depends on the pH. Finally, regarding the functionality, PEL can either be pendant (ionic groups on the side chain) or integral (ionic groups on the main backbone chain).[13]

Figure 1.5. Structures of (a) sodium carboxymethyl cellulose, an artificial-nature polyelectrolyte derived from cellulose, and (b) synthetic polyelectrolyte (poly(4-styrenesulfonate) sodium salt, PSSNa).
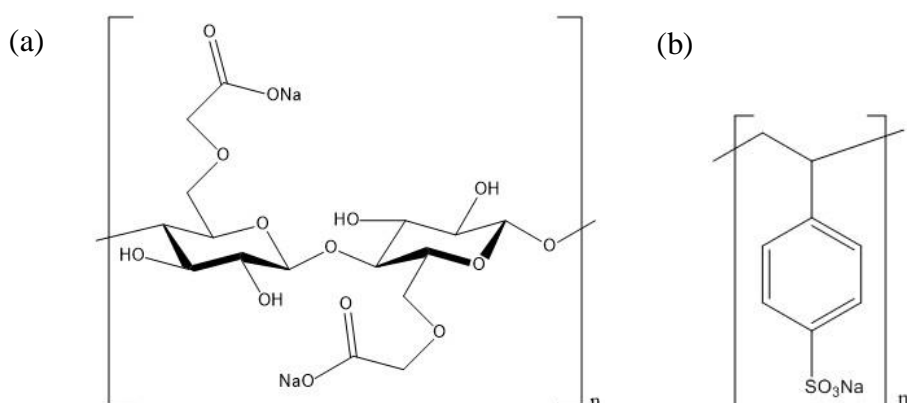
By dissolving the polyelectrolyte in a polar solvent, dissociation of the ion pairs is achieved. The counterions redistribute along the chain thereby charging the polyelectrolyte. If the solution is free of added electrolytes, *i.e.* in distilled water, the polymer coil is greatly expanded due to the strong electrostatic repulsion between charged backbone domains.[16] Addition of salt makes the polyelectrolyte behave like a nonionic polymer and chain coiling is achieved, as a result of the reduction of electrostatic repulsion between the charged units within a chain.[16,17]

One peculiarity of highly charged polyelectrolytes is the so-called counterion condensation phenomenon, described in Manning's theory.[18] When the charge density of the polyelectrolyte is small, counterions are uniformly distributed in the solution. However, with the increase of the charge density of the polyelectrolyte, the counterions condense at the surface of the macroion backbone, thereby reducing the effective charge of the polyion.[13]

It is well known that polyelectrolytes are ionized when in solution.[15] This enables them to form complexes with oppositely charged polyelectrolytes, leading to the formation of the so-called polyelectrolyte complexes (PEC). As introduced in section 1.2, it is generally accepted that the formation of a precipitate or a complex coacervate will depend mainly on the strength of the electrostatic interaction between oppositely charged polyelectrolytes.

PEC formation can be considered an entropy driven process as it implies the release of low molecular weight counterions initially bound to the ionic groups of the polymer backbone chain.[12,13] Therefore, an increase of the system entropy is achieved. The formation can also be explained in terms of Coulomb interactions, *i.e.* by electrostatic interactions between charged domains of the oppositely charged polyelectrolytes.[13] Besides this, additional inter-macromolecular interactions, such as van der Waals, hydrogen bonding and hydrophobic and dipole interactions, are involved in complex formation but are not, as such, the driving force for complexation.[13]

Recent computer simulations and experiments support the idea that the PEC formation process can be sub-divided into two steps. Firstly, an initial rapid formation (less than 5 ms) of molecular or primary complex particles with a hydrodynamic radius between 5-20 nm is achieved (Figure 1.6).[19,20]

Figure 1.6. Scheme of polyelectrolyte complex formation process. Redrawn from ref. 19.

PEL   primary PEC   secondary PEC
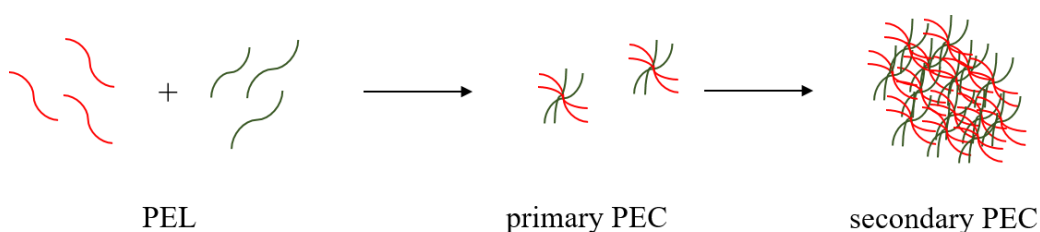
This first stage is controlled by the counterion kinetic diffusion and depends on molecular size differences and stereo-chemical fitting. Therefore, the driving force in this step is claimed to be the gain of entropy when the counterions are released from the polyelectrolyte chain. This initial ion pairing is followed by a slower stage in which further cross-links are attained in order to obtain a PEC conformation closer to

equilibrium.[13] With this step, primary particles held together by short range dispersive interactions form the so-called secondary particles. This process seems to be slightly enthalpic (exothermic) as no gain of entropy is expected.[19]

Ostwald ripening theory transferred to colloidal systems can be applied to gain a better insight into the aggregation process.[21] From this theory, it can be stated that a dispersion of small primary colloid particles under a specific size is not stable. Therefore, they re-arrange to form bigger aggregates in order to decrease the surface area.[19,21] Due to the fact that this secondary macroparticle is in a lower energy state than the primary particle, it could be discussed whether the process should be of enthalpic nature.[19] The classical DLVO theory (named after Derjaguin, Landau, Verwey and Overbeek) in 1941 and 1948 also explains the strong tendency of particles in a dispersion to aggregate by combining the effects of van der Waals attraction and electrostatic repulsion due to the so-called double layer of counterions.[22,23] This theory states that the overall potential energy of interaction (V_T) is the sum of the repulsive (electrostatic) (V_R) and the attractive (van der Waals) (V_A) potential energies,

$$V_T = V_R + V_A \tag{1.4}$$

When two particles approach, the change in overall potential energy of interaction determines whether they experience an attractive (decrease in energy) or repulsive (increase in energy) force. The potential energy of attraction for spherical particles of radius r in vacuum is given by,

$$V_A = \frac{-Hr}{12s} \tag{1.5}$$

where H is the Hamaker constant and s is the inter-particle separation.

The repulsive potential arises from the interpenetration of the diffuse double layers surrounding the particles. Therefore, this force is only experienced if the two particles are close enough. The DLVO theory considers that the two particle surfaces are identical and that the surface potential is constant throughout the approach. Approximate solutions for V_R are given by Hunter,[24]

$$V_R = 2\pi\varepsilon r \Psi_o^2 \exp(-s/\kappa^{-1}) \qquad \text{for } \kappa r \ll 1 \tag{1.6}$$

$$V_R = 2\pi\varepsilon r \Psi_o^2 ln\big(1 + \exp(-s/\kappa^{-1})\big) \qquad \text{for } \kappa r \gg 1 \tag{1.7}$$

where ε is the absolute permittivity, Ψ_o is the potential at the surface of the particles and κ^{-1} is the reciprocal of the Debye length defined by,

$$\kappa^{-1} = \sqrt{\frac{\varepsilon k_B T}{2e^2 N_A I}} \qquad (1.8)$$

where, e is the elementary charge, N_A is the Avogadro constant and I is the ionic strength.

The overall potential energy of interaction obtained from the addition of van der Waals attraction and electrostatic repulsion energies (equation 1.4) can be plotted as a function of the inter-particle separation as shown in Figure 1.7.

Figure 1.7. Overall potential energy of interaction in units of kT (black line) between two particles of radius, $r = 50$ nm, in water ($\varepsilon = 6.95 \cdot 10^{-10}$ F m^{-1} at 298 K) with a ionic strength $I = 50$ mol m^{-3}) and a $\Psi_o = 20$ mV as a function of the inter-particle separation (s) obtained from the addition of the contributions from the van der Waals attraction (red dotted line) and the electrostatic repulsion (blue dotted line). Inset plot: expansion of the plot to see the secondary minimum. Green line used as a guide.
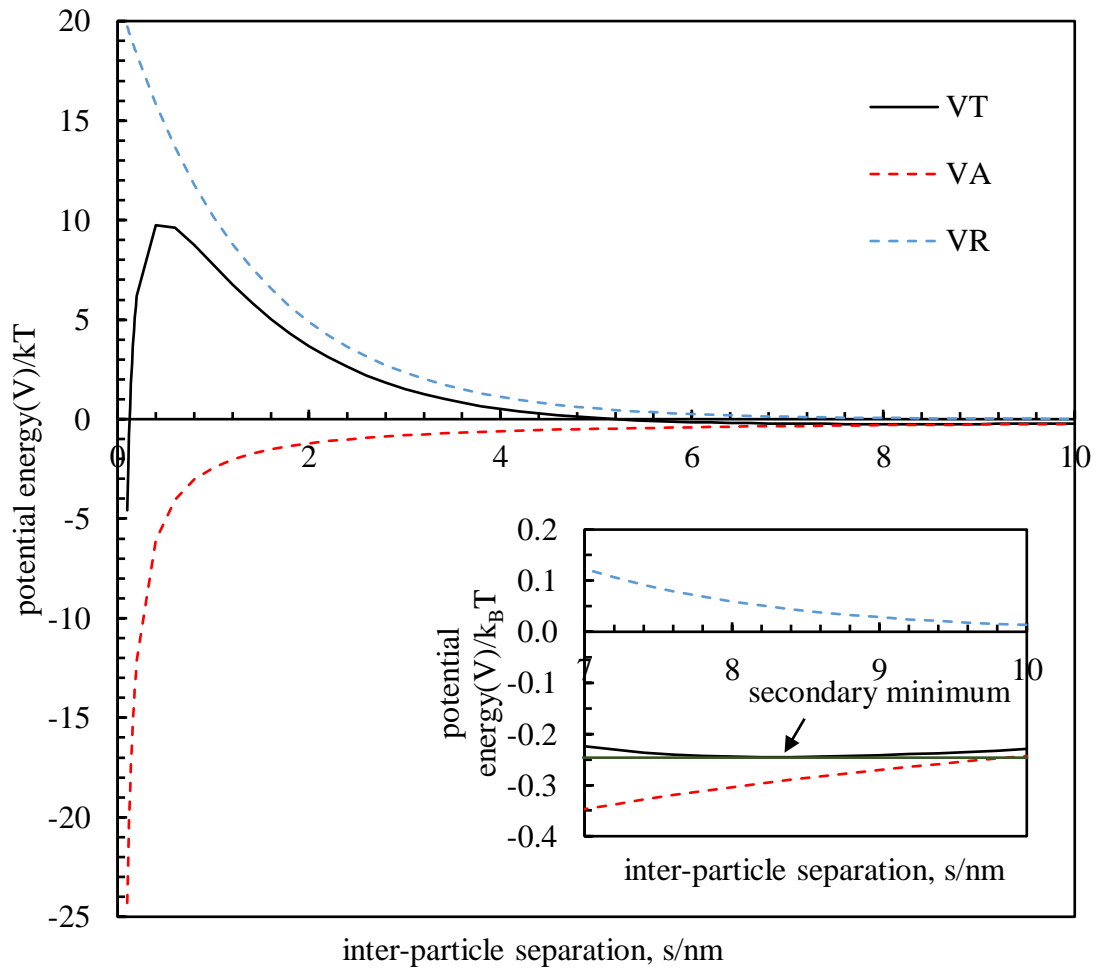
The maximum in the overall potential energy curve is the energy barrier that the particles must overcome to coagulate. The second minimum is due to the van der Waals attraction being greater than the double layer repulsion at relatively large separations. At this point particles may aggregate (flocculation).

Overbeek and Voorn developed the first theoretical description of complex coacervation between weakly charged polymers by estimating the total free energy as a sum of entropy terms (Flory-Huggins approximation) and electrostatic contribution

(Debye-Hückel approximation).[25] However, this theory is only valid at low charge densities, the correlation effects at high salt concentration and monomeric units are neglected and ion pairing effects such as counterion condensation are not taken into account.[26]

Studies on PEC date back to 1896 with the works of Kossel, in which the precipitation of egg albumin with protamine was carried out.[27] He found that the electrostatic interaction between two oppositely charged polyions could be the driving force for precipitation. The first insights on the complexation processes with synthetic polyelectrolytes were not until the 1960s, with the works of Michaels and co-workers.[28,29] They determined the interaction characteristics between PSSNa and poly(vinylbenzyltrimethylammonium chloride) (VBTAC), two strongly ionized polyelectrolytes of high charge density. The groups of Tsuchida[30] and Kabanov[31] studied PEC formation with synthetic polyelectrolytes in the framework of water-soluble complexes. Moreover, Kabanov and co-workers carried out comprehensive studies on soluble polyelectrolyte complexes dealing with the kinetics and exchange reactions between PEC and other polyelectrolytes.[32,33] Polyelectrolyte complexes prepared from natural polyelectrolytes have also been extensively investigated.[34-37]

As pointed out previously, the distinction between a precipitate and a complex coacervate is not carefully addressed in the literature and the general term polyelectrolyte complex (PEC) is adopted for both scenarios. The coacervation phenomena was first observed in 1911 by Tiebackx,[38] followed by Bungenberg de Jong[39] who first systematically investigated the phase behaviour of the natural polymers gelatin (weakly positively charged protein) and gum Arabic (weakly negatively charged polysaccharide). In 1977, Oparin, a Russian Biochemist, popularized coacervates outside the colloid area as he proposed that life was first formed in coacervate droplets.[40] However, this idea has been already displaced by modern theories, particularly after the discovery of DNA.

The term coacervation was coined by Bungenberg de Jong and Kruyt in 1929 and derives from Latin "co" (together) and "acerv" (a heap or aggregate).[39] In coacervation, a dense polymer-rich phase (coacervate phase) and a very dilute polymer-deficient phase (aqueous phase) coexist.[41] Coacervates are subdivided into "simple" and "complex" depending on the number of polymers that take part on the associative

23

phase separation phenomena. In simple coacervation, one macromolecule is present and the associative process is induced by the addition of a dehydrating agent such as salts, alcohols or a change in the temperature or the pH of the medium. One example is the mixture of polyethylene glycol, potassium phosphate and water, in which the bottom phase is rich in salt and the top phase is rich in the polymer.[1] On the other hand, in complex systems, two oppositely charged species are involved in an associative phase separation. As a result, two immiscible (and hence incompatible) liquid phases arise. The upper phase (supernatant) consists almost entirely of solvent and the bottom phase embodies a dense clear liquid phase (coacervate) which is concentrated in macromolecules. Before reaching this steady state, a biphasic system formed by a metastable suspension of macroion-rich droplets (coacervate suspension) is present.[41]

Coacervates hold higher amounts of water compared to precipitates. Jha *et al.* determined the weight fraction of water in the coacervate system containing poly(acrylic acid) (PAA) as the polyacid and poly(N,N-dimethylaminoethyl methacrylate) (PDMAEMA) or poly(diallyldimethylammonium chloride) (PDADMAC) as the polybases.[42] The weight fraction of water in absence of salt varied from 0.30 to 0.80 in both systems. Another special feature of the coacervate phase is that it displays a much higher viscosity compared to the initial polyelectrolyte solutions. Liu and co-workers reported an increase by three orders of magnitude in the viscosity of the coacervate phase between PAA and PDADMAC compared to the individual PEL solutions.[12] Finally, ultra-low interfacial tensions (γ) (around 1 mN m^{-1} or lower) between the coacervate phase and the coexistent supernatant phase have been constantly reported by different authors.[43-46] De Ruiter and Bungenberg de Jong were the first who measured γ between the coacervate phase and its equilibrium aqueous phase using the capillary rise method.[46] They pointed out the inaccuracy of the results for several reasons. The main drawback is that the capillaries need to be very narrow for those low interfacial tensions to be measured. Hence, frequent obstruction by small particles or aggregates can occur. More recently, the colloidal probe AFM[43] and the surface force apparatus (SFA)[44] have confirmed these findings of extremely low γ.

1.3.3   Factors affecting PEC formation

PEC formation can be influenced by numerous factors including polyelectrolyte characteristics (*i.e.* charge density, molecular weight, architecture and rigidity of polymer chain) and external parameters such as ionic strength, pH (for weak polyelectrolytes), temperature or the mixing procedure, amongst others. A recent comprehensive review on PEC from Meka and co-workers cites some of these factors.[47] In this section, the influence of some of the above parameters on the formation of PEC are briefly presented.

(a) Influence of salt

Salt plays an important role in the complexation process. At high salt concentration, aggregation of primary complexes occurs leading to macroscopic flocculation. In the case of relatively concentrated saline solutions, the electrostatic interaction is completely broken so transparency is regained as free polymer molecules remain in solution.[48,49] The influence of the valence of the salt on the complexation process was investigated by Michaels *et al. via* conductimetry for the complexation between salts of poly(styrene sulfonate) and poly(vinylbenzyltrimethylammonium chloride).[50] When NaCl was present, the conductivity of the reaction mixture was equal to that expected for a stoichiometric reaction involving complete release of the counterions. However, in the presence of divalent salts such as $CaCl_2$, the conductivity decreased compared to the expected value. This indicated that a certain fraction of the ionic groups did not react with the oppositely charged polyelectrolyte. They explained this behaviour by steric restrictions arised from a more tightly coiled conformation of one PEL.[50] Recently, Zhang and co-workers studied the colloidal stability and temporal evolution of PEC prepared between two strong polyelectrolytes (PDADMAC and PSSNa).[49]

(b) Influence of the mixing procedure

PEC formation depends on the mixing procedure and device.[19] However, despite its importance, this feature is not extensively investigated in the literature. PEC solutions are often prepared by mixing the polycation and polyanion solutions with a magnetic stirrer at a fixed velocity, as in the work presented here. The most widespread protocol for PEC formation is the colloid titration, which consists on the stepwise addition of

one polyelectrolyte (< 1 mL min^{-1}) into a solution containing the oppositely charged polyelectrolyte, while stirring at a fixed velocity. However, some drawbacks must be taken into consideration including the dilution effect along the titration, the difficulty in controlling the mixing and the titrant addition rate.

In the last few years, a new method called "jet mixing" was suggested by Johnson and Prud'homme.[51] This device generates two opposing flows which collide in a mixing chamber at high velocity and pressure, resulting in mixing times around 10 milliseconds. Ankerfors and co-workers used this device for the complexation of poly(allylamine hydrochloride) (PAH) and PAA.[52] In a comparative study between the jet mixing and the colloid titration method, they found that smaller PEC were obtained with the jet mixing method.[52] Sæther *et al.* reported the influence of mixing speed on the particle size of the obtained PEC between chitosan and alginate using an Ultra-Turrax device.[34] In this case, homogenization at high speed and with a large dispersing element diameter produced the smallest particles. Schatz and co-workers compared dropwise addition with one-shot addition for the PEC between chitosan and dextran sulphate.[35] As reported, one-shot mixing gave more stable particles with lower sizes compared with the dropwise mixing method.

Another important point to take into consideration is the order of addition. Several authors reported that the addition of the minor component into the major ('minor-to-major') or major component into the minor ('major-to-minor') has an influence on the PEC structure.[19,35-37] A speculative explanation supported by Müller[19] points out that for the minor-to-major scenario, either cationic or anionic, secondary particles are "electrostatically" stabilised by the excess like-charged component. However, for the major-to-minor event, once all the charges have been compensated, the excess charged component can "cross-link" the secondary particles creating colloidal networks. Therefore, the 'minor-to-major' case leads to the formation of more "equilibrated" PEC structures as the charge sign never reverses, while the major-to-minor addition might result in "unequilibrated" and looser PEC structures.

(c) Effect of the molecular weight

In general, by increasing the molecular weight of the polyelectrolytes, the PEC particle size increases.[53,54] Hu and co-workers found that by increasing the M_w of chitosan from 12,000 to 46,000 g mol^{-1}, the PEC particle size increased from 135 to 279 nm.[54]

Contradictory results were presented by Dautzenberg for the complex between PDADMAC (250 kg mol^{-1}) and a series of PSSNa of different M_w (8-1,000 kg mol^{-1}).[14] With this study, no systematic changes regarding the size were revealed.

(d) Role of stiffness-flexibility of macromolecules

When two flexible macromolecular chains (like PSSNa and PDADMAC) are associated through electrostatic interactions, scrambled-egg-like globules are formed (Figure 1.8(a)). This shrinkage into the scrambled-egg structure is due to the decrease of the total charge of PEC compared to the polyelectrolytes alone. Moreover, the solubility decreases due to the increase of hydrophobicity. On the other hand, the association between stiff and flexible macromolecular chains bearing oppositely charged groups, leads into a ladder-like structure (Figure 1.8(b)). In this case, the electrostatic attraction between chains do not induce the shrinkage but the stiff macromolecules provide a framework for a three-dimensional network, while the flexible ones act as cross-linkers giving a more extended and stable structure.[55]

Figure 1.8. (a) Formation of the scrambled-egg-like globule by the interaction of two flexible polyelectrolytes. (b) Ladder-like structure from the association of stiff and flexible chains.
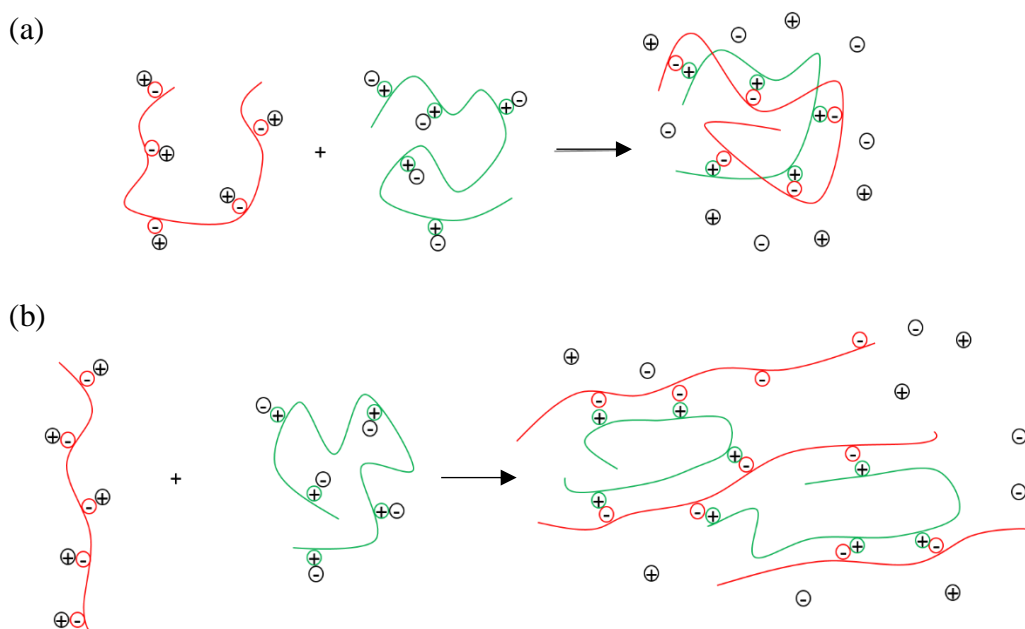
The influence of the molecule's stiffness has been evaluated in PEC between alginate and a cationic hydroxyethyl cellulose derivative (HEC).[56] Alginate is a copolymer of

two uronic acids, β-D-mannuronic (M) and α-L-guluronic (G) interconnected through diequatorial and diaxial links, respectively. This different configuration modifies the block conformations and their stiffness. Shchipunov and Postnova worked with two sodium alginate samples: one containing only mannuronic residues and the other one having both mannuronic and guluronic units.[56] Coils were obtained between HEC and mannuronate, while a ladder-like structure was prepared when alginate was used instead.

The complex formation in solutions of oppositely charged polyelectrolytes has been widely studied with Monte Carlo simulations by different authors, but particularly by the group of Linse. In ref. 57 it is mentioned that the final PEC structure depends strongly on the stiffness of the individual polyelectrolytes. Complexes prepared with flexible chains are placed close to each other. However, as soon as the chain becomes stiffer, complexes are more linearly arranged and separated.

1.3.4   *Methods of characterisation*

Dynamic and static light scattering (DLS, SLS), atomic force microscopy (AFM), scanning electron microscopy (SEM) and transmission electron microscopy (TEM) are the main methods to determine the size and evaluate the shape of PEC.[19] Colloid titration is a powerful analytical technique to determine the number or molar concentration of charges in a sample. It consists of titrating a given PEL solution with an oppositely charged low molecular weight strong PEL (PDADMAC or poly(vinylsulfate) (PVC)) until a zeta potential of zero is reached.[19] Turbidimetry is a valuable tool applicable to all systems to determine the turbidimetric endpoint along the mole fraction range.[58] As the formation of PEC is accompanied by the release of counterions into the solution, conductometric measurements can be applied to determine the electrochemical titration endpoint and to gain additional information on the complexation process *via* changes in conductivity.[58] Viscosimetry and sedimentation of the dispersion in a centrifuge can be used to estimate the amount of non-complexed residual polymer in the system.[58] UV-Visible spectrometry is of special interest for approaching problems of preferential binding and for obtaining information on conformational changes. For assessing the molecular composition of isolated PEC, elemental analysis can be used after a thorough elimination of low molecular weight salt by washing or dialysis.[58] Other techniques used for their

characterisation include: fourier transform infrared (FTIR), ^{1}H, and ^{13}C nuclear magnetic resonance, wide-angle X-ray diffraction (WAXD), differential scanning calorimetry (DSC) and thermogravimetric analysis (TGA).

Some of the techniques listed above will be used throughout this thesis and the basics are explained in Chapter 2.

1.4 Emulsions

A simple emulsion can be defined as an heterogeneous system of two immiscible liquid phases in which one of the phases (dispersed phase) is dispersed into the other (continuous phase) as drops of microscopic or colloidal size.[59,60] The boundary between these phases is called the interface. Depending on which phase contains the drops, two types of simple emulsions can be distinguished. Oil droplets dispersed in water form the so-called oil-in-water emulsions (o/w) while water droplets dispersed in oil constitute water-in-oil (w/o) emulsions. The simplest way to distinguish between o/w and w/o emulsions is the drop test, which consists in checking the miscibility of the emulsion with water and oil. If a small volume of the emulsion mixes readily with water, the continuous phase is aqueous whereas, w/o emulsions mix easily in oil. Electrical conductivity measurements can be used as well to determine the emulsion type by taking into account that an aqueous continuous phase displays higher conductivity values than an oil continuous phase.[60,61] Emulsions are thermodynamically unstable and there is a tendency with time for them to revert to the separated liquid phases. Therefore, in order to protect the formed drops from coalescence, a surface-active material or emulsifier should be added rendering the emulsions kinetically stable.[59]

Emulsions are inherently non-equilibrium systems because of their interfacial free energy, which would be released during the emulsion breaking. Based on equation 1.9, the change in the Gibbs free energy of the system (ΔG) can be expressed by,

$$\Delta G = \Delta H - T\Delta S \qquad (1.9)$$

where ΔH is the change in enthalpy, ΔS is the change in entropy. ΔS is a measure of the disorder in a system and in this case measures the size reduction of the dispersed phase. During the emulsification process, disorder increases which gives a $\Delta S > 0$

contributing to stability. ΔH can be considered as the energy input needed to achieve a certain average droplet size and is equal to,

$$\Delta H = \Delta U + P\Delta V \quad (1.10)$$

where ΔU is the change in the internal energy, P is the pressure and ΔV is the change in volume. If a volume change during emulsification is neglected, the enthalpy corresponds to the internal energy. The internal energy in this case is the sum of the work required to increase the interfacial area (ΔW) and an amount of heat, which results from wasting part of the energy input. The work required to increase the interfacial area can be used to measure the thermodynamic instability of an emulsion and is defined as stated in equation 1.11,

$$\Delta W = \gamma \Delta A \quad (1.11)$$

where γ is the interfacial tension and ΔA is the change in the interfacial area. Therefore, equation 1.9 can be re-written as,

$$\Delta G = \gamma \Delta A - T\Delta S \quad (1.12)$$

This suggests that emulsion stability is accomplished if the term $\gamma\Delta A$ is smaller than the entropy contribution. This is due to either a low interfacial tension or bigger droplets (lower surface area).[62,63] During the emulsification process (Figure 1.9), an increase in the interfacial area is achieved due to the formation of small droplets by the input of considerable amount of mechanical energy. This leads to an increase of the term $\gamma\Delta A$ and consequently ΔG will be > 0. Therefore, the system will evolve to recover its stable state by the so-called breaking of the emulsion.

Figure 1.9. Thermodynamics of the emulsification process.

$\downarrow\Delta A \rightarrow \Delta G < 0$ $\uparrow\Delta A \rightarrow \Delta G > 0$ $\downarrow\Delta A \rightarrow \Delta G < 0$

$+$ emulsifier

$\uparrow\Delta A, \downarrow\gamma \rightarrow \Delta G < 0$
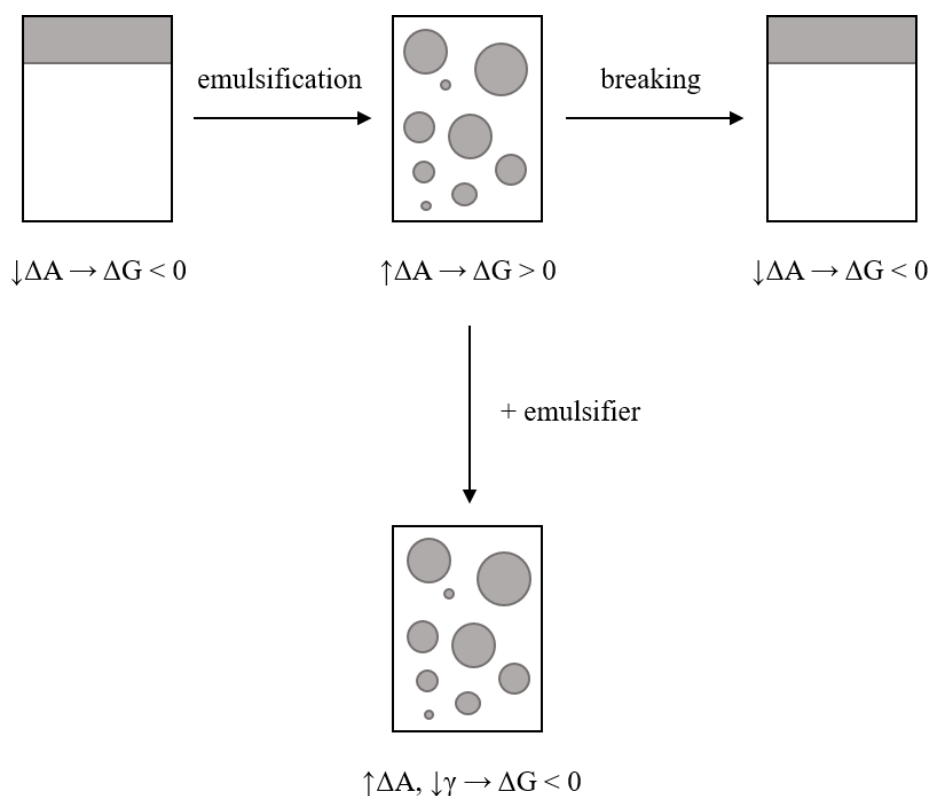
Despite emulsions being thermodynamically unstable, kinetic stability can be achieved by the adsorption of an emulsifier at the liquid-liquid interface. These compounds are surface-active materials that decrease the interfacial tension, help to make small drops and reduce the thermodynamic driving force towards coalescence.[61,62]

1.4.1 Types of emulsifiers and stabilisation mechanism

Different types of emulsifiers are encountered in the literature and the mechanism of stabilisation is different in each case. A brief explanation of each type is given in the following sections.

1.4.1.1 Surfactant

Emulsions can be stabilised by surfactants. A surfactant is a surface-active material constituted by a hydrophobic tail and a hydrophilic headgroup. Hence, they are amphiphilic molecules. The mechanism of stabilisation consists in the reduction of the interfacial tension between two immiscible phases by the adsorption at the oil-water interface.[62] When adsorbed, the hydrophobic group is within the oil phase whereas the

hydrophilic group is placed in the aqueous phase (Figure 1.10). As a result, a film at the new liquid-liquid interface is formed that prevents or retards droplet flocculation or coalescence.[64]

Figure 1.10. Schematic representation of surfactant molecules at the oil-water interface.
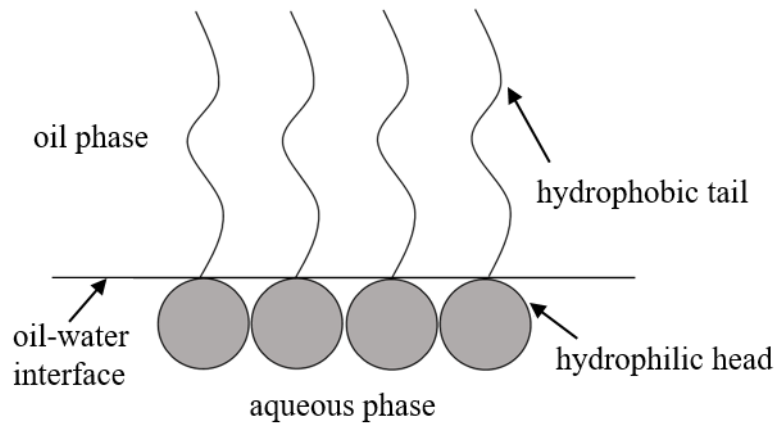
As the surfactant concentration increases, the surfactant layer at the interface becomes more concentrated, in accordance with the Gibbs adsorption equation,

$$\Delta\gamma = -\tau_s \Delta\mu_s \qquad (1.13)$$

where $\Delta\gamma$ is the change in the interfacial tension, τ_s is the surface concentration of the surfactant and $\Delta\mu_s$ is the change in the chemical potential of the surfactant. However, when a certain concentration is achieved, surfactant molecules start to associate in the bulk of one of the phases forming aggregates (micelles). This is known as the critical micelle concentration (CMC) and at this point the interfacial tension is the lowest possible under given experimental conditions.[59] This process is outlined in Figure 1.11.

Figure 1.11. On the upper part, disposition of surfactant molecules at the o-w interface with the increase in surfactant concentration. On the lower part, evolution of the surface tension values with surfactant concentration. When all the interface is covered by surfactant molecules, the lowest surface tension value is obtained. After this point, surfactant molecules form micelles.
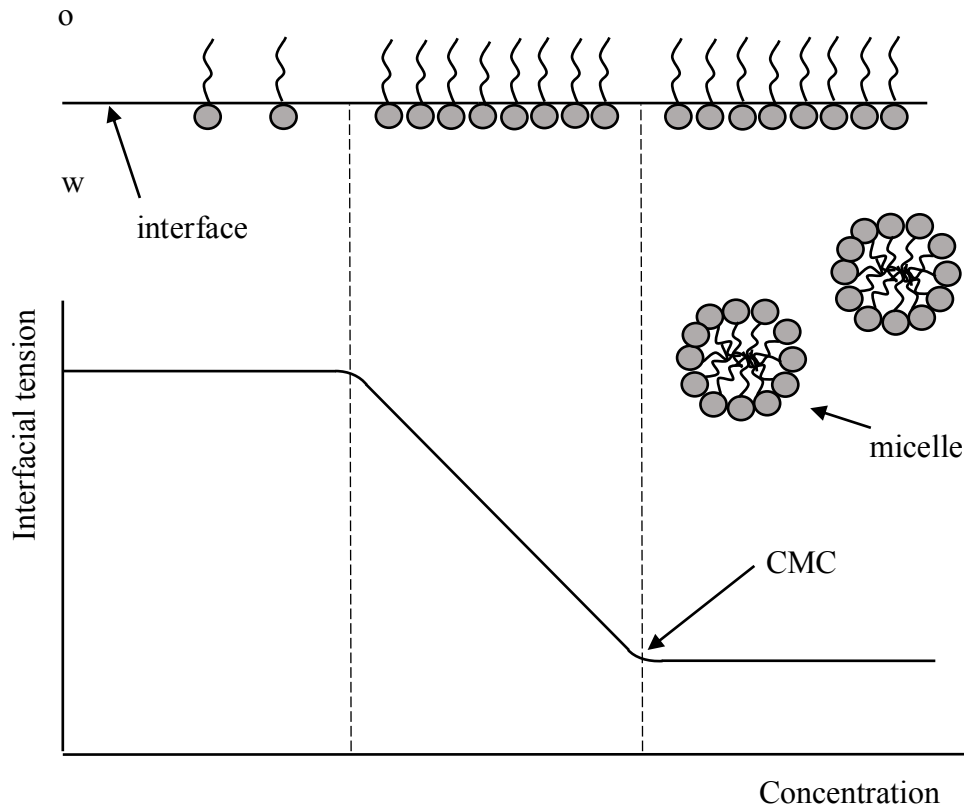
The emulsion type can easily be determined with the Bancroft rule, which states that the phase in which the emulsifier is more soluble forms the continuous phase of the resulting emulsion.[65] Therefore, a water-soluble surfactant tends to stabilise an o/w emulsion while w/o emulsions are stabilised by oil-soluble surfactants. Another way of predicting the emulsion type is with the hydrophilic-lipophilic balance (HLB). This classification is based on the surfactant structure and was first introduced by Griffin in the late 1940s.[66] The HLB is a quantitative method that assigns a number between 0 and 20 to the surfactant. This number is given by taking into account the balance between hydrophilic and hydrophobic moieties of the molecule. A hydrophobic surfactant (glycerol monooleate) has a low HLB and stabilises a w/o emulsion. Conversely, a hydrophilic surfactant (polysorbate) presents a high HLB and it is predicted to stabilise o/w emulsions.

1.4.1.2 Surface-active polymer

Emulsions can also be stabilised by surface-active polymers as they have hydrophobic and hydrophilic parts. Here, polymers form structured interfacial films that prevent the coalescence of oil drops. The formation of such layers requires the migration of the polymer to the interface followed by its adsorption.[67] Examples of polymer-stabilised emulsions have been found with hydroxypropyl methylcellulose (HPMC)[67] or PEO-PPO-PEO block copolymers[68].

Proteins and polysaccharides are natural polymers of great interest in the food industry.[69] Due to their balanced hydrophilic/lipophilic structure, proteins place themselves at the boundary between an oil and a water phase, thereby contributing to the suppression of the interfacial tension.[70] Their amphiphilic nature, together with the formation of a viscoelastic film at the interface, provides electrostatic and steric stabilisation of emulsions.[70,71] Many proteins such as caseins,[72,73] whey proteins,[72,74,75] ovalbumins[76] and bovine serum albumin[77] have been known for decades as emulsifiers. Table 1 in ref. 70 gives a summary of proteins of different sources used as emulsifiers. On the other hand, water-soluble polysaccharides are not considered true emulsifiers by colloid scientists as they do not adsorb at liquid interfaces.[78-80] Only certain hydrocolloids, such as gum Arabic, are known to exhibit emulsification properties.[78] Their surface activity is related to hydrophobic proteinaceous moieties bonded to the polysaccharide backbone.[79] Garti and Leser also demonstrated however that certain hydrophilic polysaccharides can display emulsification properties even after the removal of protein residues.[79]

1.4.1.3 Solid particles

Solid particles comprise the third group of emulsifiers. Particle-stabilised emulsions, whose discovery was attributed to Pickering in 1907,[81] gained special attention due to the enhanced stability to coalescence compared to common surfactant-stabilised emulsions.[82] Moreover, as certain particles are biologically compatible and environmentally friendly, their use has spread rapidly in the food, biomedicine, pharmaceutical and cosmetic industries. Pickering conducted the first extensive study on emulsions stabilised by solid particles, hence the term 'Pickering emulsions'.[81] However, in 1903, Ramsden already mentioned that a membrane of solid particles could stabilise emulsions and foams.[83]

The stabilisation mechanism is based on the strategic location of solid particles at the interface. This leads to the formation of a rigid barrier that prevents or inhibits coalescence. Such an effect is explained by the partial wettability of the particles at the oil-water interface as described by Finkle *et al.*[84] Particles more wetted by water (such as silica) were more susceptible to stabilise o/w emulsions while particles more wetted by oil (*i.e.* carbon black) would rather stabilise w/o emulsions. The stabilisation is linked to the contact angle that the particle makes with the oil-water interface.[85] Schulman and Leja studied the influence of the three-phase contact angle, θ, on the emulsion type and stability.[85] They found out that particles with a θ lower than 90° stabilise o/w emulsions while particles which exhibit a θ greater than 90° stabilise w/o emulsions. Moreover, they point out that particles with either an extremely low or extremely high contact angle were poor emulsifying agents as they preferred to remain dispersed within the water or the oil, respectively. Figure 1.12 illustrates the influence of the three-phase contact angle on the emulsion type.

Figure 1.12. (Upper) Position of a small spherical particle at a planar fluid-water interface for a contact angle (measured through the aqueous phase) lower than 90° (left), equal to 90° (centre) and greater than 90° (right). (Lower) Corresponding probable positioning of particles at a curved fluid-liquid interface. For $\theta < 90°$, solid-stabilised aqueous foams or o/w emulsions may form (left). For $\theta > 90°$, solid-stabilised aerosols or w/o emulsions may form (right). Redrawn from ref. 86.
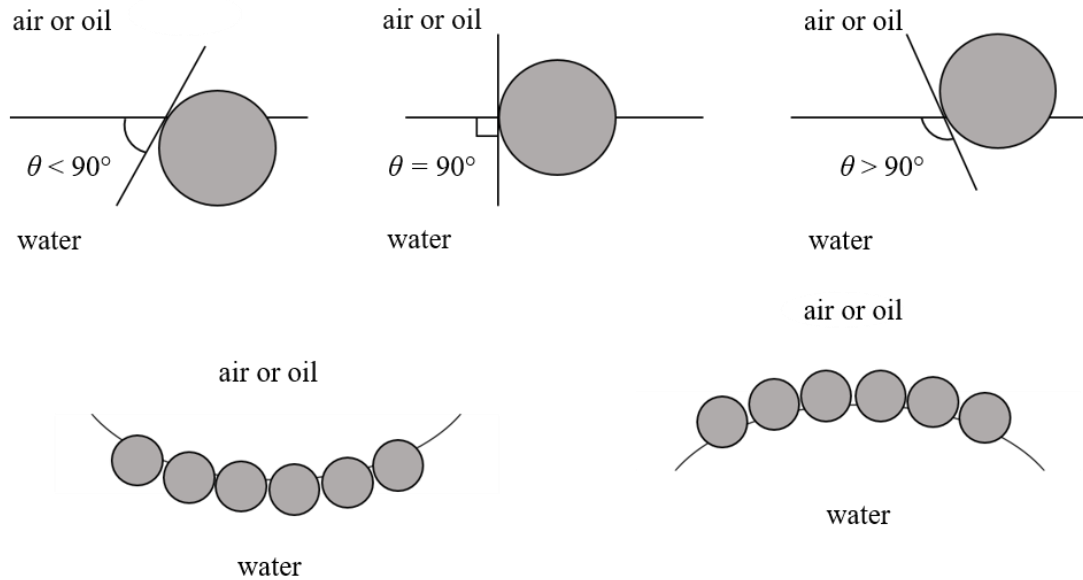
Colloidal particles can stabilise emulsions by different mechanisms summarised below. The stability of droplets is often attributed to the formation of a dense film of particles around the interface that acts as a mechanical barrier, giving rise to a very stable emulsion by providing steric hindrance against droplet coalescence.[87] However, other authors[88,89] showed that stable emulsions can be achieved even if the droplets are scarcely covered with particles. Another mechanism of stabilisation is due to the formation of a particle bridge between two adjacent drops.[90] This explains how emulsions can be stabilised against coalescence even when droplets are not fully covered by particles. Finally, some authors also introduce the idea of the formation of a 3-D network in which particles are trapped in a framework of additional particles that enhances stability by an increase of viscosity.[91] This network traps the oil droplets and protects them against coalescence and creaming (sedimentation).

Unlike surfactants, solid particles may irreversibly attach to the oil-water interface. The strength of attachment with which a particle is held at the oil-water interface is related not only to θ but also to the tension of the interface, γ_{ow}.

Figure 1.13. Representation of a spherical solid particle in its equilibrium position at an oil-water interface. The effect of gravity is assumed to be negligible for small particles (< 5 μm) so that the oil-water interface remains planar up until the contact line with the particle. Redrawn from ref. 92.
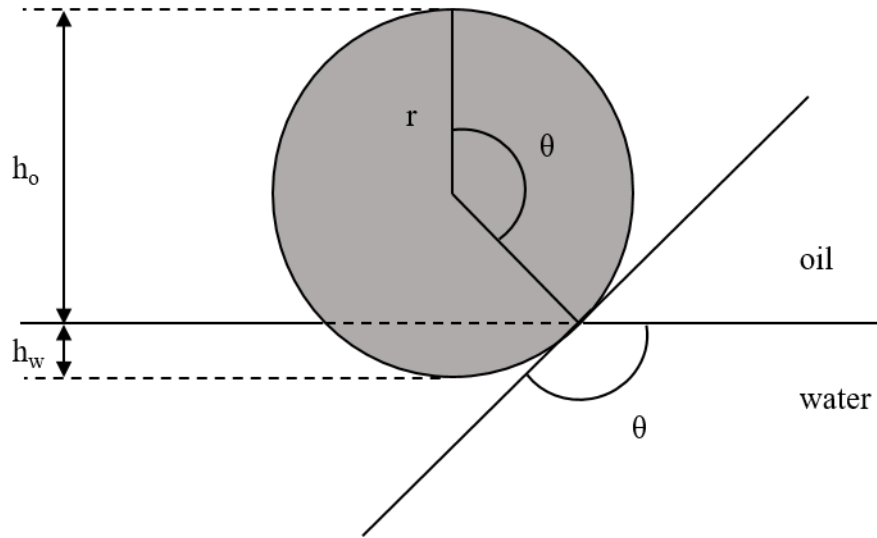
If we consider a single spherical particle of radius r, adsorbed at an oil-water interface with a contact angle θ measured through the aqueous phase (Figure 1.13), then the depth of immersion into water, h_w, equals to $r(1 + cos\theta)$. The surface area of the particle in contact with water, $A_{sw} = 2\pi r h_w = 2\pi r^2 (1 + cos\theta)$. On the other hand, the area of oil-water interface removed by the particle upon its adsorption (A_{ow}) is given by,

$$A_{ow} = \pi r^2 (1 - cos^2\theta) \qquad (1.14)$$

Hence, the energy required to detach the particle from the oil-water interface into the oil phase (ΔG_{det}) is given by,

$$\Delta G_{det} = 2\pi r^2 (1 + \cos\theta)(\gamma_{so} - \gamma_{sw}) + \gamma_{ow}\pi r^2 (1 - cos^2\theta) \qquad (1.15)$$

where γ is the interfacial tension and the subscripts s, o and w, refer to solid, oil and water, respectively. By applying Young equation ($\gamma_{so} - \gamma_{sw} = \gamma_{ow} \cos\theta$) to equation 1.15, a simplified version can be written,

37

$$\Delta G_{det} = \pi r^2 \gamma_{ow}(1 + \cos \theta)^2 \qquad (1.16)$$

For the removal of the particle from the interface to the water phase, the sign before $\cos \theta$ in equation 1.16 becomes negative,

$$\Delta G_{det} = \pi r^2 \gamma_{ow}(1 - \cos \theta)^2 \qquad (1.17)$$

As seen from equations 1.16 and 1.17, the energy needed to detach a spherical particle from the oil-water interface increases proportionally with the γ_{ow} and markedly with the particle radius (as r^2). The free energies for the detachment of a particle of radius, $r = 10$ nm from the dodecane-water interface into the oil and water phases calculated by equations 1.16 and 1.17, respectively, are plotted against the contact angle in Figure 1.14. For a hydrophobic particle ($\theta > 90°$), the free energy of particle detachment into the oil phase (squares) is smaller than that into the water phase (circles), whereas the reverse is true for a hydrophilic particle ($\theta < 90°$). The minimum energy of particle detachment is represented with the black line in Figure 1.14. The energy needed to remove the particle from the oil-water interface is maximum at $\theta = 90°$ and falls rapidly at either side. In fact, for a contact angle between 0 and 20° or between 160 and 180°, this energy is relatively small (< 15 kT). Hence, particles are too hydrophilic (low θ) or too hydrophobic (high θ) and cannot stabilise emulsions as they are easily removed from the interface. For a θ around 90°, the energy of detachment is several orders of magnitude higher than the thermal energy (kT) and so particles are thought to be irreversibly adsorbed at interfaces. However, if the particle radius is comparable to the size of most surfactant molecules (r < 1 nm), the energy of detachment is only several kT and therefore they might not be effective stabilisers.[93]

Figure 1.14. Free energy of detachment of a spherical particle of radius r = 10 nm at the planar dodecane-water interface (γ_{ow} = 52.5 mN m^{-1} at 298 K) into oil (squares) and into water (circles) *versus* particle contact angle, θ.
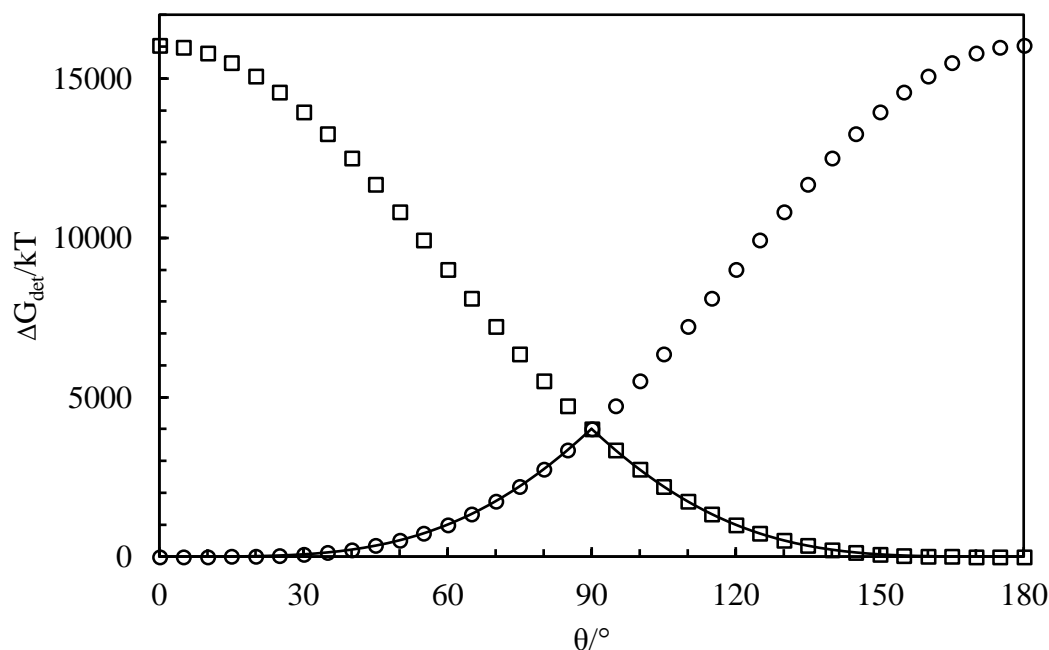
Emulsion stabilisation by hard or non-deformable particles has been extensively studied and many examples are available in the literature spanning inorganic materials such as silica,[94-96] metal,[97,98] carbon[99-101] and clay[102-104] particles. On the contrary, reports on emulsions stabilised by soft or deformable particles like microgels are relatively recent.[105] Microgels can be defined as cross-linked polymer particles that are swollen by a solvent.[106] The principles of Pickering emulsions cannot be applied entirely to microgel-stabilised emulsions. Due to their softness, microgels behave differently compared to rigid particles as they become deformed at the oil-water interface.[107] This deformability is crucial in understanding the emulsion stability in such systems.[108] Richtering and co-workers have evaluated such behaviour using their own synthesized microgel of poly(N-isopropylacrylamide)-*co*-methacrylic acid (PNIPAM-*co*-MAA).[108-111] Destribats *et al.* have worked with a whey protein microgel[112] as well as microgels made of PNIPAM of variable crosslinking degrees.[113-115] Microgel synthesis is however quite involved and some of the monomers are expensive. Finally, the use of mixtures of particles of opposite charge to form aggregates of low overall charge has been shown to be an effective way of

preparing surface-active particles *in situ*, capable of stabilising emulsions.[102,116-118] In these cases, the separate particles of negative or positive charge were too hydrophilic to enable emulsion stabilisation.

1.4.1.4 Polyelectrolyte complexes

As introduced in section 1.3, polyelectrolyte complexes can be prepared between anionic polysaccharides and proteins at pH values below the protein isoelectric point as they will carry a net positive charge. Bungenberg de Jong first reported the use of polysaccharide-protein coacervates as emulsifiers.[39] After that, emulsions stabilised with protein-polysaccharide complexes have been extensively investigated. Table 2 in ref. 119 gives recent examples of emulsion stabilisation with electrostatic polysaccharide-protein conjugates. Two different preparations are described.[119] The first consists of the addition of oil to an aqueous solution containing protein-polysaccharide complexes followed by homogenisation. The second involves the formation first of a primary emulsion stabilised by protein, followed by the addition of the polysaccharide which adsorbs onto the protein layer forming a bilayer/multilayer. Jourdain *et al.*[120] found an improvement in emulsion stability by using the complexes prepared in water instead of adding the protein and the polysaccharide in two homogenisation steps. Bridging flocculation occurred with the second method while discrete dispersed oil droplets were achieved by using the complexes formed before homogenisation. They related these differences to the structure of the composite biopolymer at the interface that varies depending on the method employed.

Despite the numerous examples of emulsions stabilised by protein–polysaccharide mixtures encountered in the literature,[120-123] in all cases the protein acts as a good emulsifier alone, *i.e.* is surface-active, and in some cases so does the polysaccharide. The complex at the emulsion droplet surface can enhance emulsion stability compared with emulsions of protein alone by the formation of a thick layer around the droplets that improves the steric stabilisation. The presence of the polysaccharide during the emulsification process leads to a reduction of the droplet size, which causes a decrease in the rate of creaming.[124]

Emulsions destabilise *via* a number of processes which may occur simultaneously or consecutively. The process by which an emulsion separates into its constituent phases can be effected by four different mechanisms shown in Figure 1.15. They are known as: creaming (or sedimentation), flocculation, coalescence and Ostwald ripening (or disproportionation).[59]

Figure 1.15. Schematic representation of different ways by which an emulsion can become unstable.
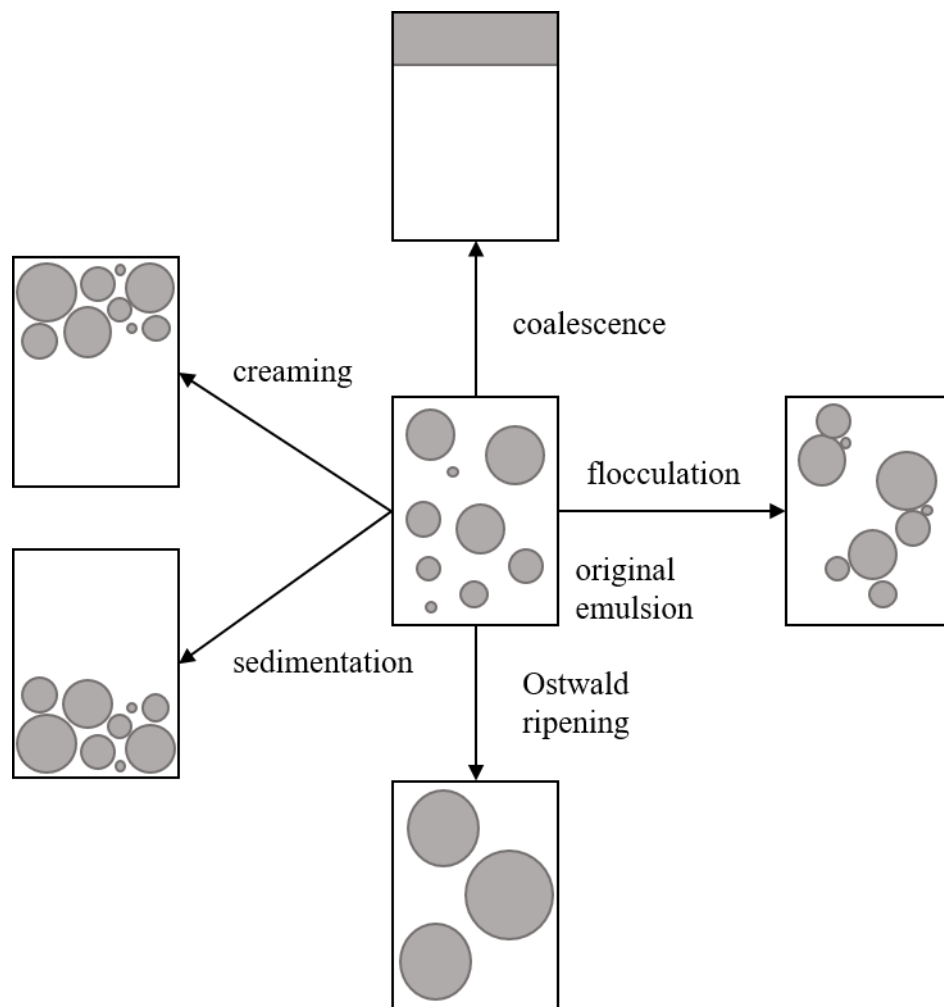
(a) Creaming: In a o/w emulsion, creaming is a process by which drops of the dispersed phase move under gravity to form a concentrated layer at the top of the sample (cream) which is richer in the dispersed phase than the bottom part (depleted serum). This is observed in o/w emulsions, as the oil phase is usually less dense than the aqueous phase. In this destabilisation mechanism, there is

41

no change in the drop size distribution. The equivalent phenomenon for a w/o emulsion is called sedimentation. Creaming/sedimentation is the principal process by which the disperse phase separates from an emulsion and is typically the precursor to coalescence. The creaming rate (v) of an isolated, spherical drop can be estimated by Stokes' law,[125]

$$v = \frac{2\, r^2\, (\rho_0 - \rho)\, g}{9\eta_0}$$ (1.18)

where r is the radius of the drop, ρ_0 is the density of the continuous phase, ρ is the density of the dispersed phase, η_0 is the viscosity of the continuous phase and g is the acceleration due to gravity. Stokes' equation indicates that creaming in very dilute emulsions is retarded by reducing the radius of emulsion drops, by increasing the viscosity of the continuous phase or by decreasing the density differences between the immiscible phases.[59]

(b) Flocculation: Flocculation consists of the aggregation of emulsion drops without merging, due to attractive forces. Therefore, all droplets remain as totally separate entities as there is no rupture of the stabilising layer at the interface. Flocculation usually leads to enhanced creaming as flocs rise faster due to their larger effective radius compared with individual drops.[59]

(c) Coalescence: Coalescence, unlike creaming and flocculation, is an irreversible process induced by the rupture of the film between two emulsion drops, which leads them to merge in a single larger drop with a subsequent reduction of the surface free energy.[59,62] This process, if not halted, results in complete phase separation of an emulsion into the two bulk liquid phases as shown in Figure 1.15.

(d) Ostwald ripening (disproportionation): Ostwald ripening is a process which involves the molecular diffusion of dispersed phase from smaller to larger droplets through the continuous phase.[59] The driving force is due to the solubility differences of molecular species between drops of different size. The solubility of a substance in the form of spherical particles increases as the drop size decreases according to Kelvin equation,[126]

$$c(r) = c(\infty)\exp\left(\frac{2\gamma V_m}{rRT}\right)$$ (1.19)

where $c(r)$ is the continuous phase solubility of the dispersed phase contained within a drop of radius r, $c(\infty)$ is the solubility in a system with only a planar interface, γ is the interfacial tension, V_m is the molar volume of the dispersed phase, R is the ideal gas constant and T is the temperature. As a result of its enhanced solubility, the material contained within small emulsion drops tends to dissolve and diffuse through the continuous phase and recondense onto larger emulsion drops.[59]

1.5 Aims of current research

The aim of the research presented in this thesis is to explore if polyelectrolyte complexes formed in aqueous solution from non-surface-active anionic and cationic synthetic polymers attain sufficient surface activity to adsorb at the oil-water interface of emulsion drops after addition of oil. To the best of our knowledge, this is the first such use of PEC as soft interfacial particles enabling emulsion stabilisation. As explained in section 1.4.1.4, despite numerous examples of emulsions stabilised by protein-polysaccharide mixtures are encountered in the literature, in all cases the protein acts as a good emulsifier alone, *i.e.* is surface-active, and in some cases so does the polysaccharide.

This research project was funded by Shiseido (Japan), whose interest lies in understanding emulsions stabilised by polyelectrolyte complexes to elucidate a general rule that could predict the best polyelectrolyte combination to prepare stable emulsions. Cosmetic products contain surfactants in their formulation, which can cause irritation or burning sensations of the skin. Therefore, the introduction of PEC in the development of future formulations could be of great interest.

A systematic and thoughtful study has been carried out for four PEL combinations of synthetic polyelectrolytes to start to build up an understanding in this area. The complexes (precipitates and coacervates) prepared in water have been characterised visually, *via* dynamic light scattering and microscopy. Emulsions are then prepared from aqueous polymer mixtures and oil, and their stability, drop sizes and arrangement of PEC particles around drops is evaluated.

1.6 Presentation of thesis

Following up a general introduction describing the types of phase separation in polymer mixtures, a brief insight on polyelectrolyte complexes and an overview of emulsion science, Chapter 2 presents all the materials and experimental techniques used throughout this study.

The experimental results are included in Chapters 3 to 6. Each of these summarise the results regarding the characterisation of complexes prepared in water and emulsions stabilised with them for different polyelectrolyte combinations. Moreover, Chapter 4 includes a brief description regarding the use of complex coacervation in microencapsulation and the calculation of spreading coefficients to determine the possible configurations between the three phases involved (oil, water and coacervate phase). The polyelectrolyte systems studied here comprise all the possible combinations that arise from the interaction between two cationic (PDADMAC and PAH, strong and weak, respectively) and two anionic (PSSNa and PAANa, strong and weak, respectively) synthetic polyelectrolytes. The four PEL combinations, together with the chapter in which they are discussed, are shown in Figure 1.16. For aqueous PEC dispersions, the type of associative phase separation is identified and the influence of parameters such as the mole fraction of the anionic polyelectrolyte, [PEL], pH and salt content are evaluated on the complexation process. For emulsions, the same parameters as the ones studied for aqueous PEC dispersions are considered, together with the oil volume fraction.

Finally, Chapter 7 includes a summary of conclusions and suggestions for future work, alongside some preliminary experiments and results.

Figure 1.16. Chart showing the four PEL combinations studied throughout this thesis and the chapter in which they are discussed.

STRONG PEL

PDADMAC

Chapter 3

STRONG PEL

PSSNa

Chapter 4

Chapter 5

WEAK PEL

PAANa

Chapter 6

WEAK PEL

PAH
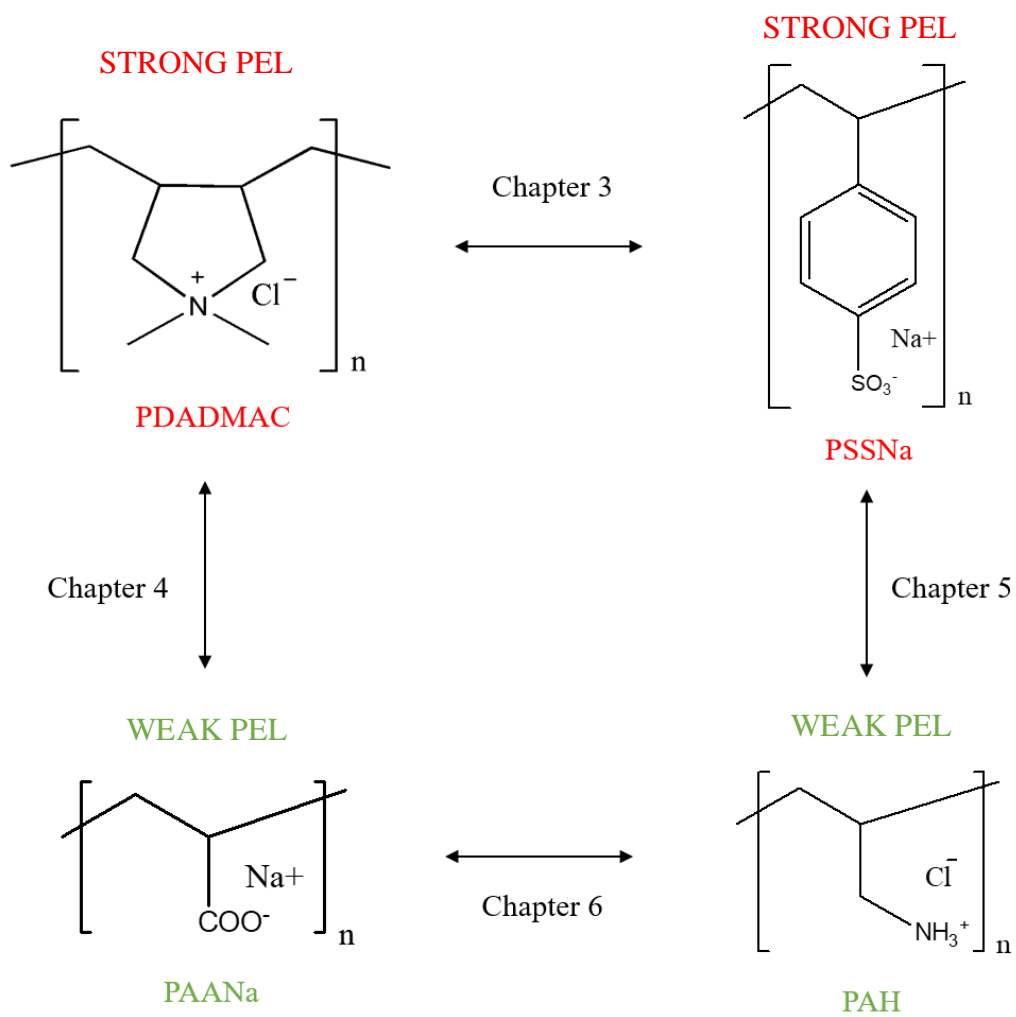
1.7 References

1. P.A. Albertsson, *Partition of Cell Particles and Macromolecules*, Wiley-Interscience, New York, 1971, pp. 18-21.

2. P.J. Flory, *J. Chem. Phys.*, 1941, **9**, 660-661.

3. M.L. Huggins, *J. Chem. Phys.*, 1941, **9**, 440.

4. P.J. Flory, *J. Chem. Phys.*, 1942, **10**, 51-61.

5. M.L. Huggins, *Ann. N. Y. Acad. Sci.*, 1942, **41**, 1-32.

6. P.J. Flory, *Principles of Polymer Chemistry*, Cornell University Press, Ithaca, New York, 1953, ch. 12.

7. M. Taimoori, H. Modarress, A.A. Saboury and A.A. Moosavi-Movahedi *Polym. Eng. Sci.*, 2001, **41**, 867-872.

8. L.M. Robeson, *Polymer Blends: a comprehensive review*, Carl Hanser Verlag, Munich, 2007, p. 15.

9. J.S. Higgins, J.E.G. Lipson and R.P. White, *Phil. Trans. R. Soc. A*, 2010, **368**, 1009-1025.

10. O. Olabisi, L.M. Robeson and M.T. Shaw, *Polymer-Polymer Miscibility*, Academic Press INC., New York, 1979, p. 4.

11. F. Comert, A.J. Malanowski, F. Azarikia and P.L. Dubin, *Soft Matter*, 2016, **12**, 4154-4161.

12. X. Liu, M. Haddou, I. Grillo, Z. Mana, J.-P. Chapel and C. Schatz, *Soft Matter*, 2016, **12**, 9030-9038.

13. J. Koetz and S. Kosmella, *Polyelectrolytes and Nanoparticles*, Springer-Verlag Berlin Heidelberg, New York, 2007, pp. 1-2, 12, 36-37.

14. *Physical Chemistry of Polyelectrolytes*, ed. T. Radeva, Surfactant Science Series, vol. 99, Marcel Dekker, New York, 2001, preface and ch. 20.

15. *Polyelectrolytes. Thermodynamics and Rheology*, ed. P.M. Visakh, O. Bayraktar, G. Picó, Springer International Publishing, Switzerland, 2014, p. 1.

16. R.S. Farinato, in *Polyelectrolytes and Polyzwitterions. Synthesis, properties and applications*, ed. A.B. Lowe and C.L. McCormick, American Chemical Society, Washington DC, 2006, ch. 9, p. 157.

17. A.V. Dobrynin and M. Rubinstein, *Prog. Polym. Sci.*, 2005, **30**, 1049-1118.

18. G.S. Manning, *J. Chem. Phys.*, 1969, **51**, 924-933.

19. M. Müller, *Adv. Polym. Sci.*, 2014, **256**, 197-260.

20. V. Starchenko, M. Müller and N. Lebovka, *J. Phys. Chem. C*, 2008, **112**, 8863-8869.

21. W. Ostwald. *Z. Phys. Chem.*, 1897, **22**, 289.

22. B. Derjaguin and L. Landau, *Acta Physicochim. URSS*, 1941, **14**, 633-662.

23. E.J.W. Verwey and J.T.G. Overbeek, *Theory of the Stability of Lyophobic Colloids*, Elsevier, New York, 1948.

24. R.J. Hunter, *Introduction to Modern Colloid Science*, Oxford University Press, Oxford, 1993.

25. J.T.G. Overbeek and M.J. Voorn, *J. Cell. Comp. Physiol.*, 1957, **49**, 7-26.

26. S. Lindhoud and M.A.C. Stuart, in *Polyelectrolyte Complexes in the Dispersed and Solid State I. Principles and Theory*, ed. M. Müller, Springer-Verlag, Berlin, 2014, p. 142.

27. A. Kossel, *Z. Physiol. Chem.*, 1896, **22**, 176-187.

28. A.S. Michaels, L. Mir, and N.S. Schneider, *J. Phys. Chem.*, 1965, **69**, 1447-1455.

29. A.S. Michaels and R.G. Miekka, *J. Phys. Chem*, 1961, **65**, 1765-1773.

30. E. Tsuchida, Y. Osada and K. Sanada, *J. Polym. Sci.*, 1972, **10**, 3397-3404.

31. A. Kabanov, T. Bronich, V. Kabanov, K. Yu and A. Eisenberg, *Macromolecules*, 1996, **29**, 6797-6802.

32. V.A. Kabanov, in *Macromolecular Complexes in Chemistry and Biology*, ed. P. Dubin, J. Bock, R.M. Davies, D.N. Schulz and C. Thies, Springer-Verlag, Berlin, 1994, ch. 10.

33. V.A. Izumrudov, T.K. Bronich, A.B. Zezin and V.A. Kabanov, *J. Polym. Sci., Part C: Polym. Lett*., 1985, **23**, 439-444.

34. H.V. Sæther, H.K. Holme, G. Maurstad, O. Smidsrød and B.T. Stokke, *Carbohydr. Polym.*, 2008, **74**, 813-821.

35. C. Schatz, A. Domard, C. Viton, C. Pichot and T. Delair, *Biomacromolecules*, 2004, **5**, 1882-1892.

36. C. Schatz, J.M. Lucas, C. Viton, A. Domard, C. Pichot, and T. Delair, *Langmuir*, 2004, **20**, 7766-7778.

37. A. Drogoz, L. David, C. Rochas, A. Domard, and T. Delair, *Langmuir*, 2007, **23**, 10950-10958.

38. F.W. Tiebackx, *Z. Chem. Ind. Kolloide*, 1911, **8**, 198.

39. H.G. Bungenberg de Jong and H.R. Kruyt, *Proc. koninkl. Med. Akad. Wetershap.*, 1929, **32**, 849-856.

40. A.I. Oparin, K.L. Gladilin, D.B. Kirpotin, G.V. Chertibrim, A.F. Orlovsky, *Dokl. Acad. Nauk. SSSR*, 1977, **232**, 485.

41. E. Kizilay, A.B. Kayitmazer and P.L. Dubin, *Adv. Colloid Interface Sci.*, 2011, **167**, 24-37.

42. P.K. Jha, P.S. Desai, J. Li and R.G. Larson, *Polymers*, 2014, **6**, 1414-1436.

43. E. Spruijt, J. Sprakel, M.A. Cohen Stuart and J. van der Gucht, *Soft Matter*, 2010, **6**, 172-178.

44. D. Priftis, R. Farina and M. Tirrell, *Langmuir*, 2012, **28**, 8721-8729.

45. J. Quin, D. Priftis, R. Farina, S.L. Perry, L. Leon, J. Whitmer, K. Hoffmann, M. Tirrell and J.J de Pablo, *ACS Macro Lett.*, 2014, **3**, 565-568.

46. L. de Ruiter and H.G. Bungenberg de Jong, *Proc. KNAW*, 1947, **50**, 836-848.

47. V.S. Meka, M.K.G. Sing, M.R. Pichika, S.R. Nali, V.R.M. Kolapalli and P. Kesharwani, *Drug Discovery Today*, 2017, **22**, 1697-1706.

48. H. Dautzenberg and N. Karibyants, *Macromol. Chem. Phys.*, 1999, **200**, 118-125.

49. Y. Zhang, E. Yildirim, H.S. Antila, L.D. Valenzuela, M. Sammalkorpi and J.L. Lutkenhaus, *Soft Matter*, 2015, **11**, 7392-7401.

50. A.S. Michaels, L. Mir, and N.S. Schneider, *J. Phys. Chem.*, 1965, **69**, 1447-1455.

51. B.K. Johnson and R.K. Prud'homme, *AICHE J.*, 2003, **49**, 2264-2282.

52. C. Ankerfors, S. Ondaral, L. Wågberg and L. Ödberg, *J. Colloid Interface Sci.*, 2010, **351**, 88-95.

53. M.A. Wolfert and L.W. Seymour, *Gene Ther.*, 1996, **3**, 269-273.

54. Y. Hu, T. Yang and X. Hu, *Polym. Bull.*, 2012, **68**, 1183-1199.

55. A.S. Michaels, *Ind. Eng. Chem.*, 1965, **57**, 32-40.

56. Y.A. Shchipunov and I.V. Postnova, *Polym. Sci. Ser. A*, 2006, **48**, 171-176.

57. M. Jonsson and P. Linse, *J. Chem. Phys.*, 2001, **115**, 10975-10985.

58. B. Philipp, H. Dautzenberg, K.-J. Linow, J. Kötz and W. Dawydoff, *Prog. Polym. Sci.*, 1989, **14**, 91-172.

59. B.P. Binks, *Modern Aspects of Emulsion Science*, Royal Society of Chemistry, Cambridge, 1998, ch. 1, pp. 1-48.

60. I.D. Morrison and S. Ross, *Colloidal Dispersions. Suspensions, Emulsions, and Foams*, Wiley, New York, 2002, pp. 420-423.

61. G.T. Barnes and I.R. Gentle, *Interfacial Science: An introduction*, Oxford University Press Inc., New York, 2nd edn., 2011, pp. 152,154.

62. P. Becher, *Encyclopedia of Emulsion Technology*, Marcel Dekker, New York, 1996, vol. 4, pp. 1-37.

63. T.F. Tadros, *Emulsion Formation, Stability, and Rheology*, Wiley-VCH, Weinheim, 2013, pp. 1-47.

64. D. Myers, *Surfaces, Interfaces and Colloids: Principles and Applications*, 2nd edn., Wiley-VCH, New York, 1999.

65. W.D. Bancroft, *J. Phys. Chem.*, 1912, **17**, 501-519.

66. W.C. Griffin, *J. Soc. Cosmet. Chem.*, 1949, **1**, 311-326.

67. C. Wollenweber, A.V. Makievski, R. Miller and R. Daniels, *Colloids Surf. A*, 2000, **172**, 91-101.

68. K. Gosa and V. Uricanu, *Colloids Surf. A*, 2002, **197**, 257-269.

69. *Protein-based surfactants. Synthesis, physicochemical properties and applications*, ed. I.A. Nnanna and J. Xia, Surfactant Science Series, Marcel Dekker, New York, 2011, vol. 101.

70. R.S.H. Lam and M.T. Nickerson, *Food Chem.*, 2013, **141**, 975-984.

71. C.J. Beverung, C.J. Radke and H.W. Blanch, *Biophys. Chem.*, 1999, **81**, 59-80.

72. M. Hu, D.J. McClements and E.A. Decker, *J. Agric. Food Chem.*, 2003, **51**, 1696-1700.

73. D.M. Mulvihill and P.C. Murphy, *Int. Dairy J.*, 1991, **1**, 13-37.

74. J. Li, Y. Cheng, P. Wang, W. Zhao, L. Yin and M. Saito, *Food Hydrocolloids*, 2012, **26**, 448-455.

75. A. Ye and H. Singh, *Food Hydrocolloids*, 2006, **20**, 269-276.

76. Y. Mine, T. Noutomi and N. Haga, *J. Agric. Food Chem.*, 1991, **39**, 443-446.

77. C. Castelain and C. Genot, *J. Agric. Food Chem.*, 1996, **44**, 1635-1640.

78. N. Garti, *J. Disp. Sci. Technol.*, 1999, **20**, 327-355.

79. N. Garti and M.E. Leser, *Polym. Adv. Technol.*, 2001, **12**, 123-135.

80. E. Dickinson, in *Gums and Stabilisers for the Food Industry*, ed. G.O. Phillips, D.J. Wedlock and P.A. Williams, IRL Press, Oxford, 1988, vol. 4, pp. 249-263.

81. S.U. Pickering, *J. Chem. Soc. Trans.*, 1907, **91**, 2001-2021.

82. B.P. Binks and S.O. Lumsdon, *Langmuir*, 2000, **16**, 8622-8631.

83. W. Ramsden, *Proc. R. Soc. Lond.*, 1903, **72**, 156-164.

84. P. Finkle, H.D. Draper and J.H. Hildebrand, *J. Am. Chem. Soc.*, 1923, **45**, 2780-2788.

85. J.H. Schulman and J. Leja, *Trans Faraday Soc.*, 1954, **50**, 598-605.

86. B.P. Binks, *Curr. Opin. Colloid Interface Sci.*, 2002, **7**, 21-41.

87. B.P. Binks and M. Kirkland, *Phys. Chem. Chem. Phys.*, 2002, **4**, 3727-3733.

88. B.R. Midmore, *Colloids Surf. A*, 1998, **132**, 257-265.

89. E. Vignati, R. Piazza and T.P. Lockhart, *Langmuir*, 2003, **19**, 6650-6656.

90. T.S. Horozov and B.P. Binks, *Angew. Chem. Int. Ed.*, 2006, **45**, 773-776.

91. J. Thieme, S. Abend and G. Lagaly, *Colloid Polym. Sci.*, 1999, **277**, 257-260.

92. B.P. Binks and T.S. Horozov, in *Colloidal Particles at Liquid Interfaces*, ed. B.P. Binks and T.S. Horozov, Cambridge University Press, Cambridge, 2006, p. 6.

93. R. Aveyard, B.P. Binks and J.H. Clint, *Adv. Colloid Interface Sci.*, 2003, **100-102**, 503-546.

94. P.S. Clegg, E.M. Herzig, A.B. Schofield, T.S. Horozov, B.P. Binks, M.E. Cates and W.C.K. Poon, *J. Phys.: Condens. Matter*, 2005, **17**, S3433-S3438.

95. N. Yan, M.R. Gray and J.H. Masliyah, *Colloids Surf. A*, 2001, **193**, 97-107.

96. B. Braisch, K. Köhler, H.P. Schuchmann and B. Wolf, *Chem. Eng. Technol.*, 2009, **32**, 1107-1112.

97. J. Zhou, X. Qiao, B.P. Binks, K. Sun, M. Bai, Y. Li and Y. Liu, *Langmuir*, 2011, **27**, 3308-3316.

98. H. Duan, D. Wang, N.S. Sobal, M. Giersig, D.G. Kurth and H. Möhwald, *Nano Lett.*, 2005, **5**, 949-952.

99. J. Kim, L.J. Cote, F. Kim, W. Yuan, K.R. Shull and J. Huang, *J. Am. Chem. Soc.*, 2010, **132**, 8180-8186.

100. H. Katepalli, V.T. John and A. Bose, *Langmuir*, 2013, **29**, 6790-6797.

101. N. Briggs, A.K.Y. Raman, L. Barrett, C. Brown, B. Li, D. Leavitt, C.P. Aichele and S. Crossley, *Colloids Surf. A*, 2018, **537**, 227-235.

102. S. Abend, N. Bonnke, U. Gutschner and G. Lagaly, *Colloid Polym. Sci.*, 1998, **276**, 730-737.

103. B.P. Binks, J.H. Clint and C.P. Whitby, *Langmuir*, 2005, **21**, 5307-5316.

104. J. Dong, A.J. Worthen, L.M. Foster, Y. Chen, K.A. Cornell, S.L. Bryant, T.M. Truskett, C.W. Bielawski and K.P. Johnston, *ACS Appl. Mater. Interfaces*, 2014, **6**, 11502-11513.

105. B. Jiao, A. Shi, Q. Wang and B.P. Binks, *Angew. Chem. Int. Ed.*, 2018, **57**, 9274-9278.

106. *Microgel Suspensions: Fundamentals and Applications*, ed. A. Fernandez-Nieves, H. Wyss, J. Mattsson and D.A. Weitz, Wiley-VCH, New York, 2011, pp. 3-4.

107. R.W. Style, L. Isa and E.R. Dufresne, *Soft Matter*, 2015, **11**, 7412-7419.

108. W. Richtering, *Langmuir*, 2012, **28**, 17218-17229.

109. B. Brugger, B.A. Rosen and W. Richtering, *Langmuir*, 2008, **24**, 12202-12208.

110. B. Brugger and W. Richtering, *Langmuir*, 2008, **24**, 7769-7777.

111. B. Brugger, S. Rutten, K. Phan, M. Möller and W. Richtering, *Angew. Chem., Int. Ed.*, 2009, **48**, 3978-3981.

112. M. Destribats, M. Rouvet, C. Gehin-Delval, C. Schmitt and B.P. Binks, *Soft Matter*, 2014, **10**, 6941-6954.

113. M. Destribats, M. Wolfs, F. Pinaud, V. Lapeyre, E. Sellier, V. Schmitt and V. Ravaine, *Langmuir*, 2013, **29**, 12367-12374.

114. M. Destribats, V. Lapere, E. Sellier, F. Leal-Calderon, V. Schmitt and V. Ravaine, *Langmuir*, 2011, **27**, 14096-14107.

115. M. Destribats, M. Eyharts, V. Lapeyre, E. Sellier, I. Varga, V. Ravaine and V. Schmitt, *Langmuir*, 2014, **30**, 1768-1777.

116. B.P. Binks, W. Liu and J.A. Rodrigues, *Langmuir*, 2008, **24**, 4443-4446.

117. T. Nallamilli, E. Mani and M.G. Basavaraj, *Langmuir*, 2014, **30**, 9336-9345.

118. T. Nallamilli, B.P. Binks, E. Mani and M.G. Basavaraj, *Langmuir*, 2015, **31**, 11200-11208.

119. M. Evans, I. Ratcliffe and P.A. Williams, *Curr. Opin. Colloid Interface Sci.*, 2013, **18**, 272-282.

120. L. Jourdain, M.E. Leser, C. Schmitt, M. Michel and E. Dickinson, *Food Hydrocolloids*, 2008, **22**, 647-659.

121. A.K. Stone and M.T. Nickerson, *Food Hydrocolloids*, 2012, **27**, 271-277.

122. K.G. Zinoviadou, E. Scholten, T. Moschakis and C.G. Biliaderis, *Int. Dairy J.*, 2012, **26**, 94-101.

123. X. Li and R. de Vries, *Curr. Opin. Food Sci.*, 2018, **21**, 51-56.

124. A. Benichou, A. Aserin and N. Garti, *J. Disp. Sci. Technol.*, 2002, **23**, 93-123.

125. G.G. Stokes, *Philos. Mag.*, 1851, **1**, 337.

126. W. Thompson (Lord Kelvin), *Proc. R. Soc. Edinburgh,* 1871, **7**, 63.

CHAPTER 2 – EXPERIMENTAL

2.1 Materials
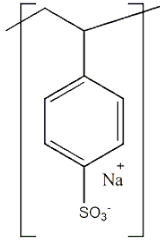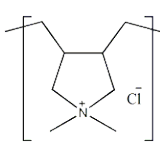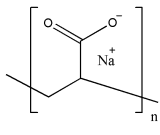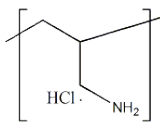
2.1.1   Water

Water was purified by first passing through an Elgastat Prima reverse osmosis unit followed by a Millipore Milli-Q reagent water system equipped with one carbon filter and two ion-exchange filters. After treatment, its resistivity was ~ 18 MΩ cm and the surface tension measured with a Krüss K11 tensiometer and the Wilhelmy plate method was 71.9 ± 0.2 mN m^{-1} at 25 °C, in good agreement with the literature value (72.75 mN m^{-1} at 20 °C).[1]

2.1.2   Polyelectrolytes

Poly(4-styrene sulfonate) sodium salt (PSSNa) and poly(diallyldimethylammonium chloride) (PDADMAC) were selected as strong polyelectrolytes, anionic and cationic, respectively. Poly(acrylic acid) sodium salt (PAANa) and poly(allylamine hydrochloride) (PAH) were selected as weak polyelectrolytes, anionic and cationic, respectively. Pure standards of PSSNa, PDADMAC and PAANa with a relatively low polydispersity index (PDI) and different molecular characteristics were purchased from Polymer Standard Services (PSS, Mainz). Pure standards of PAH and PSSNa ($M_w = 75{,}000$ g mol^{-1}) were purchased from Alfa Aesar. The chemical structures and other characteristics given by the supplier are shown in Table 2.1. All polyelectrolytes were used as received.

Table 2.1. Chemical structures and molecular characteristics of polyelectrolytes (PEL) used. Values taken from the certificate of analysis.
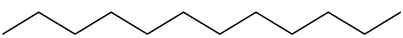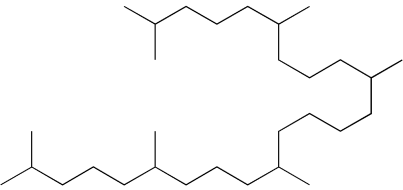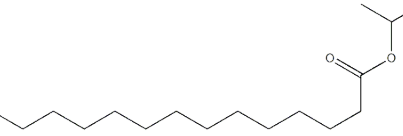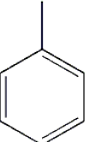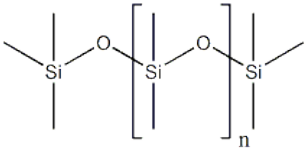
PEL	Repeat unit	Molar mass per charged unit/g mol^{-1}	M_w^a/ g mol^{-1}	M_n^b/ g mol^{-1}	M_p^c/ g mol^{-1}	PDI^d
PSSNa		206.19	148,000	-	152,000	< 1.20
			976,000	-	976,000	< 1.20
			75,000	-	-	-
PDADMAC		161.67	160,000	101,000	-	1.58
			159,000	82,900	-	1.91
			174,000	85,400	-	2.04
PAANa		94.04	131,200	78,400	115,000	1.67
PAH		93.55	120,000 to 200,000	-	-	-

$^a M_w$: Weight average molecular weight; $^b M_n$: Number average molecular weight; $^c M_p$: Molar mass at the peak maximum; ^{d}PDI: Polydispersity index (M_w/M_n).

2.1.3 Oils

For emulsion preparation, five oils were selected (Table 2.2). They include non-polar alkanes, a monoester, an aromatic oil and a silicone oil. Prior to use, all the oils were columned twice through basic chromatographic aluminium oxide (particle size: 0.063-0.200 mm, Merck kGaA) to remove polar impurities.

Table 2.2. Structure, source, purity and density (20 °C) of the oils used.

Name	Structure	Supplier	Purity /%	Density /g cm^{-3}
n-dodecane		Alfa Aesar	> 99	0.796
Squalane		Aldrich	≥ 99	0.818
*Iso*propyl myristate		Aldrich	> 98	0.859
Toluene		Analar Normapur	100	0.866
50 cS polydimethyl siloxane (PDMS)		Dow Corning	100	0.964
Paraffin oil	Mixture of hydrocarbons from petroleum	Sigma-Aldrich	-	0.869

2.1.4 Other materials

Throughout this work, materials other than those already detailed in the previous sections were used as received. They are listed in Table 2.3 alongside with their supplier and purity.

Table 2.3. Use, supplier and purity of other chemicals used throughout this study.

Chemical	Use	Supplier and purity
Sodium chloride (NaCl)	Study influence of salt on complexation	Fisher Chemical, 99.9%
Hydrochloric acid (HCl) aqueous solution (37%)	Reducing solution pH	Fisher Scientific, ~37 wt.% HCl in water
Sodium hydroxide (NaOH)	Increasing solution pH	Fisher Scientific, > 97%
Glycerol	Estimation of the surface energy of a dry coacervate phase from contact angle measurements	VWR Chemicals, 98%
Formamide		VWR Chemicals, > 99%
α-bromonaphthalene		VWR Chemicals, 97%
n-hexadecane		Sigma-Aldrich, 99%
Ethanol absolute	Washing of glassware and other tools	VWR Chemicals, 100%

2.2 Methods

2.2.1 Potentiometric titration of weak polyelectrolytes

Potentiometric titrations were carried out for weak polyelectrolytes (PAANa and PAH) with a pH meter (3510, Jenway) equipped with an InLab Flex-Micro electrode (Mettler Toledo) to determine the degree of ionisation as a function of pH. Prior to use, the pH meter was calibrated with buffer solutions of pH = 4, 7 and 10. The pH of a 1 g L^{-1} PEL solution was first adjusted to pH 12 (PAANa) or 2.5 (PAH) in order to evaluate the full pH range. After that, the titration was performed with a 0.1 M HCl solution (PAANa) or a 0.1 M NaOH solution (PAH).

2.2.2 Preparation of aqueous PEC dispersions

Individual polyelectrolyte solutions of different concentrations (0.01-50 g L^{-1}) were prepared by weighing the corresponding amount of each PEL and dissolving them in Milli-Q water. PEL solutions were either adjusted to the desired pH with NaOH and HCl solutions of various concentrations, or prepared at their natural pH. Aqueous PEC

dispersions of different mole fractions of the anionic polyelectrolyte (x_{PSSNa} or x_{PAANa}) were obtained by mixing known volumes of each individual polyelectrolyte solution of a fixed concentration and pH with a magnetic stirrer (VWR VMS-C7, stirrer speed = 3) at room temperature. Here, x refers to the mole fraction calculated with the values of M_w given in Table 2.1 and the initial pH before mixing is quoted in all cases. All solutions were prepared in 14 mL screw-cap glass vials (internal diameter = 1.8 cm, height = 7 cm). Due to the influence of the mixing procedure on the characteristics of the resulting PEC structures,[2,3] a fixed method was followed in order to obtain reproducible results. The polycation solution was added sequentially with a micropipette up to the total desired volume into the polyanion solution. This was done to allow the added polyelectrolyte to interact with the oppositely charged species present in the vial. Therefore, as an example, for the dispersion with x_{PSSNa} = 0.83 for the system PAH-PSSNa, 1.5 mL of a PAH solution was added into 3.5 mL of a PSSNa solution. Each PAH addition was of 375 μL. With this protocol, the total mixing time for all the samples was 3 min. After complete addition of the polycation solution, mixing was kept at the same speed for an additional minute.

For the study of the influence of salt concentration on the stability of complexes, aqueous PEC dispersions were prepared as above. Immediately after preparation, stipulated amounts of NaCl crystals were added into each dispersion and dissolved by hand-shaking in order to obtain the desired [NaCl].

2.2.3 Characterisation of aqueous PEC dispersions

2.2.3.1 Average diameter and zeta potential

For aqueous PEC dispersions prepared at low polyelectrolyte concentration (0.1 g L^{-1}), dynamic light scattering (DLS) employing the cumulant method[4] was used to determine the average diameter of the complex present. Measurements were carried out at different mole fractions of the anionic polyelectrolyte and pH in absence of added electrolyte at 25 °C in a Zetasizer Nanoseries NanoZS (ZEN3600, Malvern Instruments). Samples were placed in a plastic disposal cuvette of 1 cm path length and the results are given as the average of three measurements.

Particles in suspension are constantly moving due to Brownian motion, *i.e.* movement of particles due to the random collision with solvent molecules. Small particles are

more bombarded by solvent molecules than large particles and therefore they move more rapidly. The schematic representation of the DLS system is shown in Figure 2.1(a).

Figure 2.1. Schematic representation of the Zetasizer Nanoseries NanoZS (Malvern instruments) for the measurement of the (a) average diameter and (b) zeta potential. Redrawn from ref. 5.
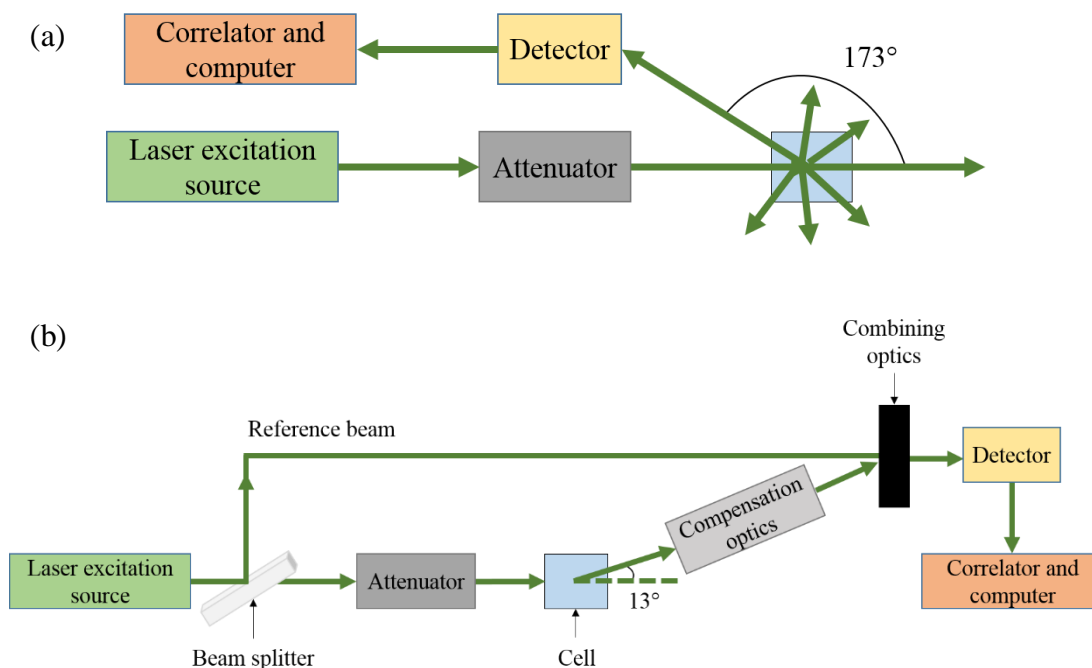
The sample is illuminated with a 4 mW He–Ne laser beam as a light source, operating at $\lambda = 633$ nm. Most of the laser beam passes straight through the sample but some is scattered in all directions by the particles. An attenuator reduces the intensity of the laser and hence the intensity of the scattering in order not to overload the detector, which is placed at 173°. Backscatter detection is used to reduce the effect of multiple scattering. The scattering intensity signal is passed from the detector to a correlator. As particles are in constant motion, the intensity at a particular point appears to fluctuate with time. The correlator compares the scattering intensity at successive time intervals to derive the rate at which the intensity is varying (Figure 2.2). As small particles are moving faster, the correlation of the signal decays more rapidly compared to large particles.

Figure 2.2. Typical correlogram from a sample containing large particles (green) and small particles (red).
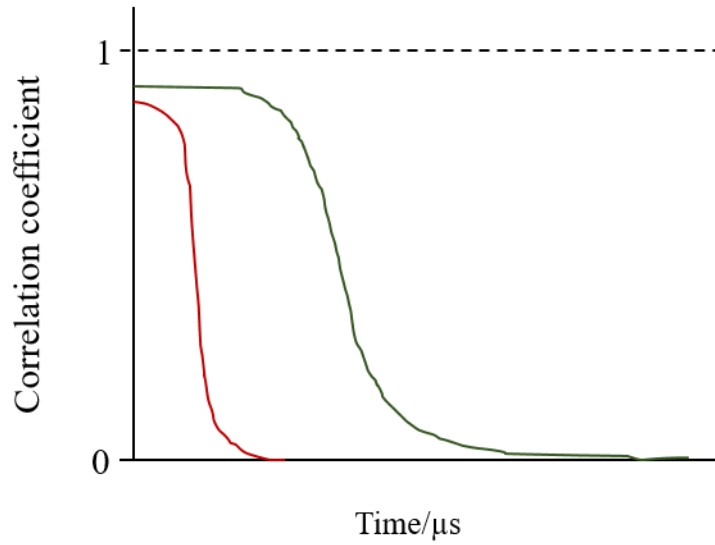
Stokes-Einstein equation relates the size of a particle with its speed due to Brownian motion as shown in equation 2.1,

$$D_H = \frac{kT}{3\pi\eta D} \qquad (2.1)$$

where D_H is the hydrodynamic diameter, k is the Boltzmann constant, T is the absolute temperature, η is the solvent viscosity and D is the translational diffusion coefficient. D can be calculated by fitting the correlation curve to an exponential function of the correlator time delay (τ) as shown in equation 2.2,

$$C(\tau) = A[1 + B\ exp(-2\Gamma\tau)] \qquad (2.2)$$

where A and B are the baseline and the intercept of the correlation function, respectively and Γ is calculated by,

$$\Gamma = Dq^2 \qquad (2.3)$$

$$q = (4\pi n/\lambda)\ sin(\theta/2) \qquad (2.4)$$

where n is the refractive index of the dispersant, λ is the wavelength of the laser and θ is the scattering angle.

The zeta potential was measured at 25 °C by the same instrument. Measurements were made by introducing a universal dip cell (ZEN1002, Malvern Instruments) inside a

59

plastic disposal cuvette containing the dispersion. The schematic representation of the main components is shown in Figure 2.1(b). The setup is similar to that used to measure the average diameter. However, the light source is split in an incident and a reference beam, the scattered light is detected at an angle of 13° and an electric field is applied to the cell. When particles in suspension are charged, the distribution of ions in the surrounding interfacial region is affected. Thus an electrical double layer exists around each particle. For a negatively charged particle, the ionic concentration and the potential difference as a function of the distance from the charged surface is shown in Figure 2.3. In the so-called Stern layer ions are strongly bound to the surface while in the diffuse layer they are less firmly attached. Within the diffuse layer there is a notional boundary (slipping plane) inside which ions and particles form a stable entity. As a result, when a particle moves, ions within this boundary move as well while ions beyond the boundary stay with the bulk dispersant. The zeta potential is the value of the electric potential at the slipping plane.

Figure 2.3. Diagram showing the ionic concentration and potential difference as a function of the distance from the surface of a negatively charged particle suspended in a liquid. Redrawn from ref. 5.
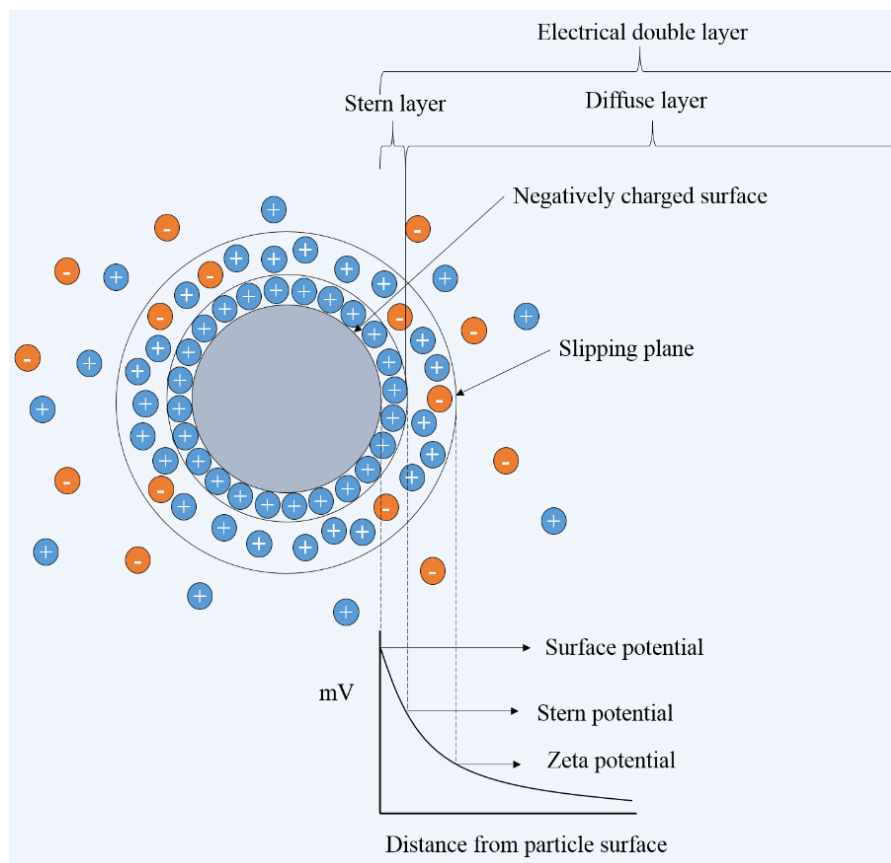
When an electric field is applied, charged particles move towards the electrode of opposite charge. The velocity of the particle in an electric field is known as the electrophoretic mobility (U_E) and can be converted to zeta potential (z) by applying Henry's equation (equation 2.5).

$$U_E = \frac{2\varepsilon z f(ka)}{3\eta} \qquad (2.5)$$

where, ε is the dielectric constant, η is the viscosity and $f(ka)$ is Henry's function. For the experiments reported here, $f(ka)$ equals to 1.5 (Smoluchowski approximation[6]) as the zeta potential is measured in aqueous media and moderate electrolyte concentration.

The Zetasizer measures particle electrophoretic mobility using a combination of laser Doppler velocimetry and Phase Analysis Light Scattering (PALS). A laser beam is passed through a sample undergoing electrophoresis and, as a result, the scattered light from the moving particles is frequency shifted. The frequency shift (Δf) is equal to,

$$\Delta f = 2v \sin(\theta/2)/\lambda \qquad (2.6)$$

where v is the particle velocity, λ is the laser wavelength and θ is the scattering angle. When the particle is not moving, the scattered light has the same frequency as the incident laser. However, when an electric field is applied to the cell, any particles moving through the measurement volume will cause the intensity of light detected to fluctuate with a frequency proportional to the particle speed. Therefore, the scattered light now has greater frequency than the incident laser. By using an interferometric technique (optical mixing), the scattered light from the particles is combined with the reference beam to create intensity variations. The sign of the zeta potential is determined by comparing the beat frequency with that of a reference frequency.

The size distribution of polyelectrolyte complexes prepared at high [PEL] was obtained with a Malvern Mastersizer 2000 (Malvern Instruments) fitted with a small volume sample dispersion unit (model Hydro 2000SM (A)). The bases of this instrument are also substantiated by the light diffraction technique but the size range is higher (micrometer size) than that measured with the Zetasizer Nanoseries NanoZS. About 1250 µL of the dispersion were diluted in 100 mL of Milli-Q water at a specific pH in the dispersion unit, stirred at 2,000 rpm. The particle diameter reported in case

of a monomodal distribution was the mass median diameter ($d(0.5)$), defined as the diameter of particles at which 50% of the sample is smaller and 50% is larger than this diameter. The width of the distribution was given by the span value, calculated as shown in equation 2.7. The smaller the value the narrower the distribution. For multimodal distributions, the size at the peak maximum is reported. In all cases, each value was averaged from three parallel measurements.

$$span = \frac{d(0.9) - d(0.1)}{d(0.5)} \tag{2.7}$$

where $d(0.9)$ gives the diameter of the particle for which 90% of the sample is below this size and $d(0.1)$ is the diameter of the particle for which 10% of the sample is below this size.

The refractive index of water was obtained using a refractometer (M46 313, Hilger) and a sodium lamp ($\lambda = 589$ nm) at 25 °C and was 1.333, in agreement with the literature value (1.33336 at 20 °C).[1] The refractive index of the coacervate phase obtained for the system PDADMAC-PAANa ($x_{PAANa} = 0.5$, [PEL] = 30 g L^{-1}, pH = 10) was measured with the same instrument and it is 1.395.

2.2.3.2 UV-Vis absorption spectroscopy

Transmittance measurements on aqueous PEC dispersions were carried out with a double beam UV-Vis spectrophotometer (Perkin Elmer Lambda 25) equipped with UV WinLab v.6.0.4 software at $\lambda = 400$, 500 and 700 nm. Samples were placed in a quartz cuvette of 1 cm path length with Milli-Q water being used as a reference. Transmittance (%) values are given as the average of three measurements.

2.2.3.3 Determination of unreacted PEL in aqueous PEC dispersions with fluorescence spectroscopy

For the system PAH-PSSNa, the amount of unreacted PAH or PSSNa in selected aqueous PEC dispersions around charge neutrality prepared from 5 g L^{-1} PEL solutions at unmodified pH was assessed. In order to do so, aqueous PEC dispersions at different x_{PSSNa} (0.68, 0.83 and 0.95) were prepared and centrifuged with a minicentrifuge (Minispin plus, Eppendorf) at 10,000 rpm for 10 min to separate the PEC particles from the supernatant. Afterwards, different volumes (0.5, 1 and 2 mL) of PSSNa and PAH solutions of different concentrations (0.1, 1 and 5 g L^{-1}) were added to 5 mL of

the supernatant. The formation of PEC after the addition of PAH or PSSNa indicated the presence in the supernatant of free PSSNa or PAH, respectively.

The amount of unreacted PAH or PSSNa in the supernatant was quantified through fluorescence measurements with a LS55 Fluorescence spectrometer (Perkin Elmer) in a four clear windows quartz cuvette. Standard PSSNa (0.01, 0.025, 0.05, 0.075 and 0.1 g L^{-1}) and PAH (0.5, 1.25, 2.5, 3.75 and 5 g L^{-1}) solutions of different concentrations were prepared and the emission spectra was obtained after exciting the solutions at $\lambda = 300$ nm. The slit width was set to 10 nm in all cases. A calibration curve for each polyelectrolyte was built by plotting the maximum intensity ($\lambda = 382$ nm for PSSNa and $\lambda = 405$ nm for PAH) *versus* the [PEL]. The intensity of emission of the supernatant prepared at different x_{PSSNa} (0.68, 0.83 and 0.95) was recorded and interpolated in the correspondent calibration curve, which allowed the amount of free polyelectrolyte to be quantified. The percentage of free PEL was calculated as the ratio between the concentration of free PEL after complexation over the initial [PEL].

2.2.3.4 Characterisation of the type of associative separation

For aqueous PEC dispersions prepared at high [PEL], the type of associative phase separation (precipitation or complex coacervation) across the mole fraction of anionic polyelectrolyte and pH was assessed by visual inspection and optical microscope images. A drop of an aqueous PEC dispersion was placed on a glass slide (Fisher Scientific) and optical micrographs were taken using an Olympus BX-51 microscope fitted with a DP70 CCD camera. The resolution was 1360 pixels x 1024 pixels. A graticule (Pyser-SGI, PS8, 1 mm/0.01 mm divisions) was used at all magnifications to calibrate the microscope.

For the system PDADMAC-PAANa, the occurrence of both the coacervate phase and the precipitate was further investigated by centrifugation of 1 mL of an aqueous PEC dispersion with a minicentrifuge (Minispin plus, Eppendorf) at 10,000 rpm for different periods of time. Optical microscope images of the different phases separated were also taken. Moreover, the water content in the coacervate phase was determined following the procedure reported in ref. 7 and 8. In order to do so, an aqueous PEC dispersion was prepared from 30 g L^{-1} PEL solutions at pH = 10 ($x_{PAANa} = 0.5$). The coacervate phase so obtained was placed on a clean glass slide and water was allowed

to evaporate in an oven at 100 °C until constant weight. The water content (%) is calculated as in equation 2.8 and it is given as the average of three measurements.

$$water\ content\ (\%) = \frac{w_d}{w_w} \times 100 \qquad (2.8)$$

where w_d and w_w are the weights of the dry and wet coacervate phase, respectively.

2.2.3.5 Scanning electron microscopy (SEM)

Scanning electron microscopy was used to obtain micrographs of polyelectrolyte complexes in order to gain information regarding their shape, size and aggregation state. One drop of an aqueous PEC dispersion prepared with the system PDADMAC-PSSNa ($x_{PSSNa} = 0.56$, [PEL] = 0.1 and 0.5 g L^{-1}, unmodified pH) was applied to a carbon disc and left to evaporate at room temperature for three days. Once dried, the disc was coated with a thermally evaporated carbon film (10 nm thick) using an Edwards high vacuum coating unit. Micrographs were taken with a Zeiss EVO 60 scanning electron microscope at a voltage of 20 kV and a probe current of 70 pA. The average particle diameter was calculated from at least fifty individual entities on SEM images with ImageJ 1.47v software. Energy dispersive X-ray spectra (EDX) were also acquired.

2.2.3.6 Transmission electron microscopy (TEM)

Transmission electron microscope images were taken of an aqueous PEC dispersion prepared with the system PDADMAC-PAANa under the conditions where coacervate droplets were formed ($x_{PSSNa} = 0.5$, [PEL] = 5 g L^{-1}, pH = 10) in order to visualize their interface and interior. Two experimental procedures regarding the sample preparation were carried out. For the unstained case, 5 mL of the aqueous PEC dispersion were placed on a carbon coated copper grid and the sample was air dried. For the stained case, a drop of the sample was placed on parafilm. The grid with the carbon film facing down was placed onto the drop for 2 min. Afterwards, the grid was placed in contact with a drop of Milli-Q water at pH = 10. Then, the grid was left for 1 min in a 1% uranyl acetate solution. The excess of liquid was removed with filter paper after each step. Finally the sample was air dried. TEM images were taken with a JEOL 2010 transmission electron microscope equipped with a Gatan Ultrascan 4000

camera at a voltage of 120 kV. Energy dispersive X-ray Microanalysis (EDX, Oxford Instruments) using INCA Energy software was also conducted.

2.2.3.7 Surface tension

The Wilhelmy plate method was first used by L. Wilhelmy in 1863 and consists of measuring the force acting upon a flat plate immersed through the surface of a liquid (Figure 2.4).[9] If the plate is perfectly wetted by the liquid, a meniscus will form where it passes through the surface with a contact angle (θ) of 0°.

Figure 2.4. Schematic diagram of a Wilhelmy plate in air with liquid meniscus attached to plate.
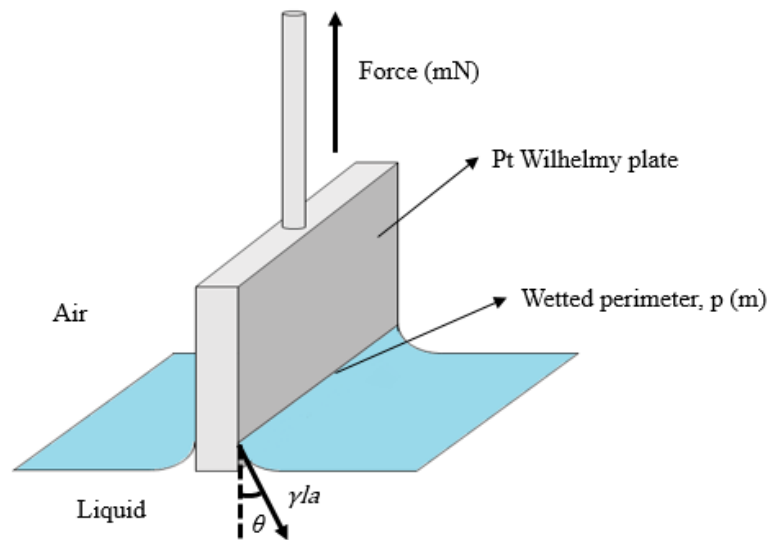
If the plate is hanging vertically, the meniscus will contact the plate along the perimeter, p,

$$p = 2\,(L + b) \tag{2.9}$$

where L and b are the horizontal length and the thickness of the plate, respectively. The surface tension (γ_{la}) can be calculated as,

$$\gamma_{la} = \frac{F}{p\cos\theta} \tag{2.10}$$

where F is the force acting on the plate in mN (measured using a force balance within the tensiometer) and $\cos\theta$ is assumed to be 1.

As shown by Jordan and Lane, despite the complex geometry of the meniscus at the edges of the plate, equation 2.10 still applies.[10] As a result, the only correction needed arises from the buoyancy of the plate. The buoyancy correction depends on the immersion depth and it is equal to zero if the bottom edge of the plate is set level with the flat surface of the liquid.

The surface tension between air and either water, an aqueous PEC dispersion or oil was measured with a Krüss K11 tensiometer and the Wilhelmy plate method at 25 °C (thermostatted by a LTD6G water bath (Grant, UK)). A platinum plate is used due to its high surface free energy resulting in optimal wetting, alongside with it being chemically inert and easy to clean. Surface tensions are given as the average of three independent measurements. After each measurement, the plate was rinsed with ethanol and heated to glowing in a blue Bunsen flame.

2.2.4 Preparation of emulsions

Emulsions composed of either an aqueous PEC dispersion or a PEL solution and oil were prepared in 14 mL screw-cap glass vials. The two phases were emulsified with an Ultra-Turrax homogenizer (IKA T25 digital) having a dispersing element of 8 mm (stator diameter). Mixing was maintained for 2 min at a constant speed of 13,200 rpm. Emulsions were prepared with fresh dispersions and the addition of oil was done in one-shot, unless otherwise stated. Different sets of emulsions were systematically prepared by varying one of the following parameters each time: concentration and pH of the starting PEL solutions, mole fraction of the polyanion and oil volume fraction (ϕ_o).

2.2.5 Characterisation of emulsions

2.2.5.1 Drop test

The emulsion type was inferred from the drop test. This consist of checking whether a drop of an emulsion disperses or not when added to either pure oil or pure water.[11] If the continuous phase of the emulsion is water (o/w emulsion), the emulsion drop will disperse in water and remain as a drop in oil while a w/o emulsion mixes readily with oil and not with water. Drop tests were taken shortly after emulsion preparation.

2.2.5.2 Stability measurements and optical microscopy

Photos and optical microscope images of emulsions were taken after preparation and as a function of time. Emulsions were stored at room temperature. Micrographs of emulsions without dilution were obtained on a dimple glass slide (Fisher Scientific) with a cover slip (Scientific Laboratory Supplies LTD) using an Olympus BX-51 microscope fitted with a DP70 CCD camera. The mean droplet diameter of the emulsion was calculated from at least fifty individual droplets on digital micrographs with ImageJ 1.47v software. The stability of emulsions to coalescence was assessed by monitoring the amount of oil released from the emulsion as a function of time. As the amount of coalescence was relatively low, the oil was carefully removed from above the emulsion with a Pasteur pipette and weighed. The stability of emulsions to creaming was monitored by measuring the height of the aqueous phase resolved after a period of time as shown in Figure 2.5. The fraction of oil (f_o) and water (f_w) was calculated as the ratio between the amount of oil or aqueous phase released after a period of time over the initial amount of oil or aqueous phase added, as shown in equations 2.11 and 2.12, respectively.

$$f_o = \frac{w_t}{w_0} \tag{2.11}$$

$$f_w = \frac{h_t}{h_0} \tag{2.12}$$

where w_t and h_t are the weight of oil and the height of aqueous phase separated after some time, and w_0 and h_0 are the weight of oil and the height of aqueous phase used to prepare the emulsion. According to this, the values of (f_o) and (f_w) span from 0 (stable emulsions) to 1 (unstable emulsions).

Figure 2.5. Determination of the fraction of water resolved from an emulsion.
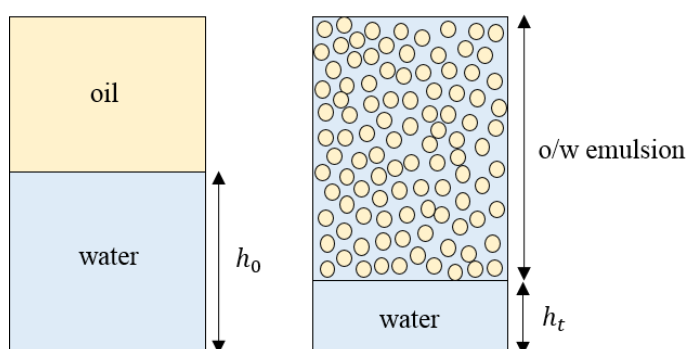
2.2.5.3 Cryogenic scanning electron microscopy (cryo-SEM)

Selected emulsions with different oil volume fractions were imaged with cryo-scanning electron microscopy. A small volume of emulsion was mounted on an aluminium sample holder (diameter ~ 10 mm) with a spatula. The sample was plunged into liquid nitrogen turned into a slush, which minimizes boiling and the Leidenfrost effect upon sample freezing.[12] This nitrogen slush (~ -210 °C) was generated by applying vacuum to liquid nitrogen of temperature around -196 °C. The frozen sample was placed inside the cryo-preparation chamber (PP3010T, Quorum Technologies Ltd) where it was fractured with a sharp knife at -140 °C under high vacuum to expose the internal droplet structure. The anti-contaminator in the preparation chamber was held at -170 °C. Sublimation of the surface water (ice) was performed inside the Zeiss EVO 60 SEM chamber at -75 °C for 10 min to obtain a clearer image of the droplet interface. Afterwards, the sample was coated with platinum to a thickness of ~ 2 nm in the preparation chamber. Finally, it was transferred back to the SEM chamber for imaging at a voltage of 15 kV and a probe current of 30 pA.

2.2.5.4 Confocal laser scanning microscopy (CLSM)

Confocal micrographs of aqueous PEC dispersions and emulsions were taken with a confocal laser scanning microscope (LSM 710, Carl Zeiss, Germany) equipped with a 30 mW Diode 405 laser. Confocal laser scanning microscopy is an optical imaging technique for increasing optical resolution and contrast of a micrograph by means of using a spatial pinhole to block out-of-focus light in image formation. The schematic diagram is shown in Figure 2.6. A point in the sample being analysed is illuminated with one or more focused laser beams. The point of light is reflected by a dichroic mirror and it is focused by an objective lens at the desired focal plane in the sample. Fluorescence emission photons travelling from the sample towards the detector are transmitted by the dichromatic mirror, while excitation light reflected back from the sample is diverted out of the detection light path. The fluorescence barrier filter blocks unwanted spectral components of the emitted fluorescence as well as any residual excitation light. Therefore, only the fluorescence that originates in the plane of focus (in-focus plane) reaches a second pinhole and goes to the photomultiplier, which generates a signal that is related to the brightness of the light from the sample.

Figure 2.6. Schematic diagram of the confocal laser scanning microscope (CLSM). Redrawn from ref. 13.
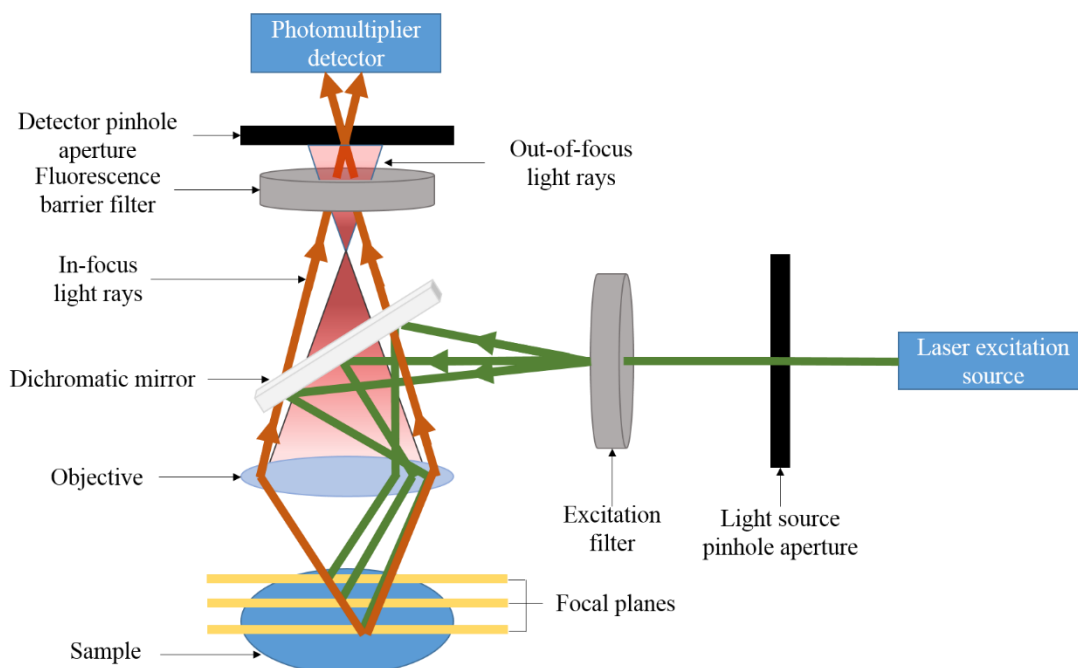
A two-dimensional image is obtained by carrying out measurements at the x-y plane and by combining the measurements from each individual point. Finally, by capturing multiple two-dimensional images at different depths, three dimensional structures can be reconstructed.

Samples were placed in a dimple glass slide with a cover slip. Images were acquired with EC Plan-Neofluar 10x/0.30 and 20x/0.5 and Plan-Apocromat 63x/1.40 oil DIC M27 objectives. For selected emulsions, scans were performed along the z-axis and a 3D image was built with the ZEN 2010 software (Carl Zeiss).

Fluorescence measurements of 5 g L^{-1} PEL solutions (PSSNa, PAH and PAANa) were previously carried out with a LS55 Fluorescence spectrometer (Perkin Elmer) at a λ_{ex} = 405 nm. This was done to ensure that PEL were fluorescent after being excited at the wavelength of the laser in the CLSM.

2.2.5.5 Rheology

Rheological measurements of emulsions prepared at different oil volume fractions were carried out at 25 °C with a Bohlin CV 120 rheometer (Bohlin Instruments) using a 20 mm diameter parallel plate geometry. Temperature control was done with a

Peltier plate. The gap between the two plates was set to 500 μm for all emulsions. Measurements were done at controlled shear stress (from 0.18 to 100 Pa). Freshly prepared emulsions were carefully placed on the lower plate of the rheometer. The upper plate was slowly lowered onto the sample until the pre-set gap size was reached. Any excess of emulsion was gently removed with a tissue.

2.2.6 Interfacial tension

The du Noüy[14] ring is a variant of the Wilhelmy plate in which a horizontal ring is used instead of a vertical plate (Figure 2.7). It is used for the determination of surface and interfacial tensions.

Figure 2.7. Schematic diagram of a du Noüy ring (side-view) in air with liquid meniscus attached to ring.
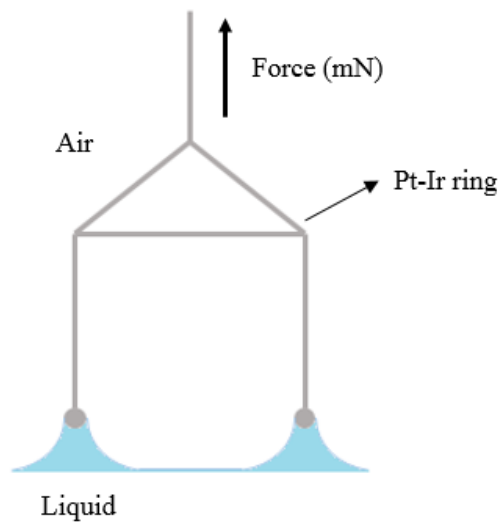
When the ring is raised from the liquid surface, the maximum force required to pull the meniscus from the surface is related to the surface tension of the liquid. When the ring is completely wetted, the wetted perimeter (p) is equal to $2\pi(R - r) + 2\pi(R + r)$, where R is the radius of the ring measured from the center of the ring to the center of the wire and r is the radius of the wire. Usually $R \gg r$ so p can be written as,

$$p = 4\pi R \qquad (2.13)$$

Harkins and Jordan[15] showed that the surface tension (γ) of a liquid is given by,

$$\gamma = \frac{mgf}{p} \tag{2.14}$$

where m is the weight of the liquid raised by the ring and g is the acceleration due to gravity. Due to the complex geometry, a correction factor (f) must be applied. It depends on two dimensionless ratios, R^3/V and R/r, where V is the volume of the liquid pulled from the surface.

The interfacial tension between oil and water or an aqueous PEC dispersion was measured with a Krüss K11 tensiometer and the du Noüy ring method (Pt-Ir) at 25 °C. The du Noüy ring started off in the denser phase (aqueous phase) and it was pulled up through the less dense phase (oil) forming a meniscus around the ring. The radius of the ring was 9.545 mm and the wire diameter was 0.37 mm. The density of the two phases was inputted in the software. The applied correction method was that of Harkins and Jordan.[15] The results of three separate measurements were averaged. After each measurement, the ring was rinsed with ethanol and heated to glowing in a blue Bunsen flame.

2.2.7 Contact angle determination

When a drop of liquid is placed on a solid surface in the presence of another fluid (gas or liquid) (Figure 2.8), the equilibrium three phase contact angle (θ) that arise is determined as a function of three interfacial tensions as stated by Young's equation (equation 2.15).

Figure 2.8. Schematic representation of the contact angle of a liquid drop on a solid surface in air.
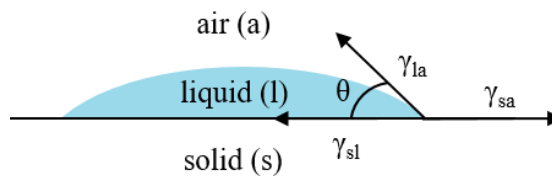
$$\cos\theta = \frac{\gamma_{sa} - \gamma_{sl}}{\gamma_{la}} \tag{2.15}$$

where γ_{sa}, γ_{sl} and γ_{la} represent the solid-air, solid-liquid and liquid-air interfacial tensions, respectively.

The values of the contact angles of five probe liquids in air were measured with a Krüss DSA Mk 10 apparatus with the static sessile drop method, by obtaining the profile of a liquid droplet on a coated glass slide with the coacervate phase. In order to do so, the coacervate phase obtained after mixing 30 g L^{-1} PDADMAC and PAANa solutions ($x_{PAANa} = 0.5$) at pH = 10 was spread carefully on a clean glass slide and water was allowed to evaporate completely in an oven at 100 °C. After that, between 4 and 10 μL of the test liquids were placed on the slide with a micro-syringe. The circle method was used to measure contact angles below 20° while the Young-Laplace fitting was applied for contact angles above 20°. When the contact angle between the liquid and the coacervate coated surface was too low to be measured accurately, it was taken to be < 5°. The contact angle values are given as the average of three independent measurements.

Disks (diameter, 13 mm; thickness, < 3 mm) for contact angle measurements were obtained by compressing 200 mg of PEC particles in a steel die using a hydraulic press (Specac, UK) with 10^{10} tones. Aqueous PEC dispersions were prepared from the system PAH-PSSNa ($x_{PSSNa} = 0.68$ and 0.83, [PEL] = 5 g L^{-1}, pH = unmodified) and were filtered under gravity through a filter paper (Sartorius). PEC particles collected in the filter paper were air dried at room temperature for four days. After that, and before the compression step, particles were grinded with a ceramic mortar and a pestle until a fine powder was obtained.

2.3 References

1. *CRC Handbook of Chemistry and Physics*, ed. D.R. Lide, CRC Press, Boca Raton, 83rd edn., 2002.
2. M. Müller, *Adv. Polym. Sci.*, 2014, **256**, 197-260.
3. C. Schatz, A. Domard, C. Viton, C. Pichot and T. Delair, *Biomacromolecules*, 2004, **5**, 1882-1892.
4. D.E. Koppel, *J. Chem. Phys.*, 1972, **57**, 4814-4820.
5. User manual Zetasizer nano series, Malvern instruments, 2009.
6. M. Smoluchowski, *Handbuch der Electrizität und des Magnetismus*, Leipzig, 1921, vol. 2, 366.
7. P.K. Jha, P.S. Desai, J. Li and R.G. Larson, *Polymers*, 2014, **6**, 1414-1436.
8. E. Spruijt, A.H. Westphal, J.W. Borst, M.A. Cohen Stuart and J. van der Gucht, *Macromolecules*, 2010, **43**, 6476-6484.
9. L. Wilhelmy, *Ann. Phys.*, 1863, **195**, 177-217.
10. D.O. Jordan and J.E. Lane, *Aust. J. Chem.*, 1964, **17**, 7-15.
11. I.D. Morrison and S. Ross, *Colloidal Dispersions: Suspensions, Emulsions and Foams*, Wiley-Interscience, New York, 2002, pp. 420-423.
12. M. Sansinena, M.V. Santos, N. Zaritzky and J. Chirife, *Theriogenology*, 2012, **77**, 1717-1721.
13. http://www.olympusconfocal.com. Accessed 18 Mar 2018.
14. P.L. du Noüy, *J. Gen. Physiol.*, 1919, **1**, 521-524.
15. W.D. Harkins and H.F. Jordan, *J. Am. Chem. Soc.*, 1930, **52**, 1751-1772.

CHAPTER 3 – MIXTURE OF STRONG CATIONIC, PDADMAC, AND STRONG ANIONIC, PSSNa, POLYELECTROLYTES

3.1 Introduction

As mentioned in the aims, with this work the concept of a novel particle stabiliser of oil-water emulsions is put forward, being the polyelectrolyte complex (PEC) formed between oppositely charged water-soluble polymers in cases where both polymers alone are incapable of stabilising an emulsion.

To the best of our knowledge, this is the first such use of PEC as soft interfacial particles enabling emulsion stabilisation. It is worth mentioning, however the literature on protein-polysaccharide mixtures, whose interactions have been studied since 1896 following the pioneering work of Beijerinck.[1] Complex formation is mainly due to electrostatic interactions between oppositely charged domains of each individual biopolymer.[2] The complex at the emulsion droplet surface can enhance emulsion stability compared with emulsions of protein alone by the formation of a thick layer around the droplets that improves the steric stabilisation. The presence of the polysaccharide during the emulsification process leads to a reduction of the droplet size, which causes a decrease in the rate of creaming.[3]

Despite the many examples of emulsions stabilised by protein-polysaccharide mixtures in the literature,[4-6] all of them refer to systems in which the protein alone is an emulsifier, unlike in the system reported here. In this chapter, two strong polyelectrolytes of low polydispersity and similar molecular weight (M_w), poly(4-styrene sulfonate) sodium salt, PSSNa, and poly(diallyldimethylammonium chloride), PDADMAC, have been used to correlate the behaviour of their mixtures in water with that of emulsions after addition of oil.

Before studying the behaviour of emulsions stabilized by polyelectrolyte complexes, a comprehensive study on PEC characterisation was carried out. To gain a deep insight into their formation and properties, aqueous PEC dispersions were first characterised in terms of average diameter and zeta potential, investigating the influence of parameters such as the mixing ratio, polyelectrolyte concentration, order of addition upon mixing and the polyelectrolyte M_w. Spherical particles of diameters between 100 and 200 nm are formed through electrostatic interactions between charged polymer

chains and around equal mole fractions of the two polymers the zeta potential of the particles reverses in sign. Emulsions are then prepared from the aqueous polymer mixtures and oil, and their stability, drop sizes and arrangement of PEC particles around drops is evaluated. The effects of PEL and PEC concentration, salt concentration, oil volume fraction and oil type are investigated. Oil-in-water (o/w) emulsions are obtained, being those prepared with aqueous PEC dispersions close to charge neutrality the most stable to coalescence and creaming. The effects of PEC concentration and the oil:water ratio have been examined. Stability is achieved by close-packed particle layers at drop interfaces and particle aggregation in the continuous phase. Increasing the salt concentration initially causes destabilisation of the aqueous particle dispersion due to particle aggregation followed by dissolution of particles at high concentration; the corresponding emulsions change from being stable to completely unstable and are then re-stabilised due to adsorption of uncharged individual polymer molecules. Air-water and oil-water interfacial tensions of planar interfaces are also monitored but no reduction of the tensions with PEC particles is detected compared to the bare interfaces.

3.2 Characterisation of aqueous PEC dispersions

3.2.1 Dispersions at low PEL concentration

3.2.1.1 Effect of mole fraction of anionic polyelectrolyte

The appearance of aqueous PEC dispersions prepared from 0.1 g L^{-1} individual PEL solutions at different x_{PSSNa} is shown in Figure 3.1, where x refers to mole fraction using the values of M_w given in Table 2.1 (148 kDa PSSNa and 160 kDa PDADMAC). When either PDADMAC or PSSNa is in excess (low and high x_{PSSNa}, respectively), solutions are transparent. However, around the point where all the charges are expected to be neutralised, $x_{PSSNa} = 0.56$, the dispersion appears slightly opalescent.

Figure 3.1. Appearance of freshly prepared aqueous PEC dispersions prepared from 0.1 g L^{-1} individual PEL solutions at different x_{PSSNa} (given). Scale bar = 1 cm.
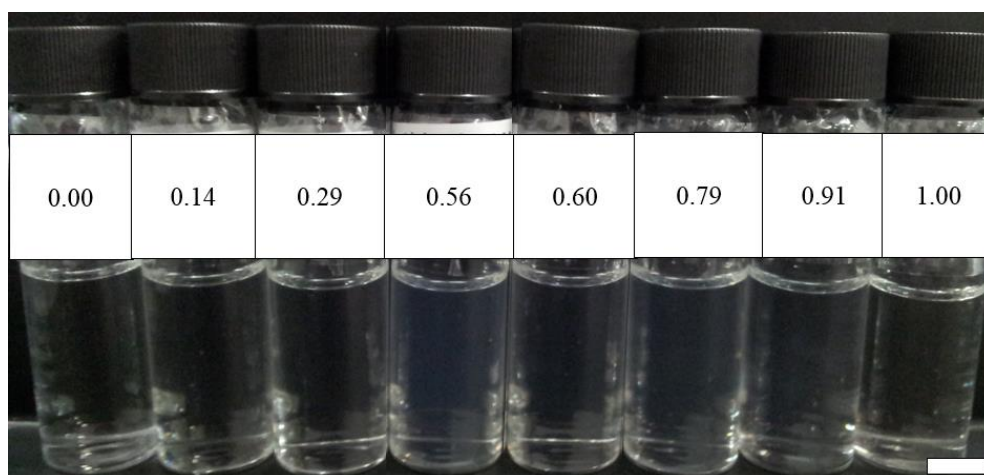

Figure 3.2(a) shows the average diameter of the polyelectrolyte complexes present in the above dispersions as a function of x_{PSSNa}. The results for freshly prepared dispersions and for the same twenty days after preparation are included.

Figure 3.2. (a) Average particle diameter and (b) PDI in size for aqueous PEC dispersions prepared from 0.1 g L^{-1} individual PEL solutions *versus* x_{PSSNa} for freshly prepared dispersions (circles) and 20 days after preparation (triangles).
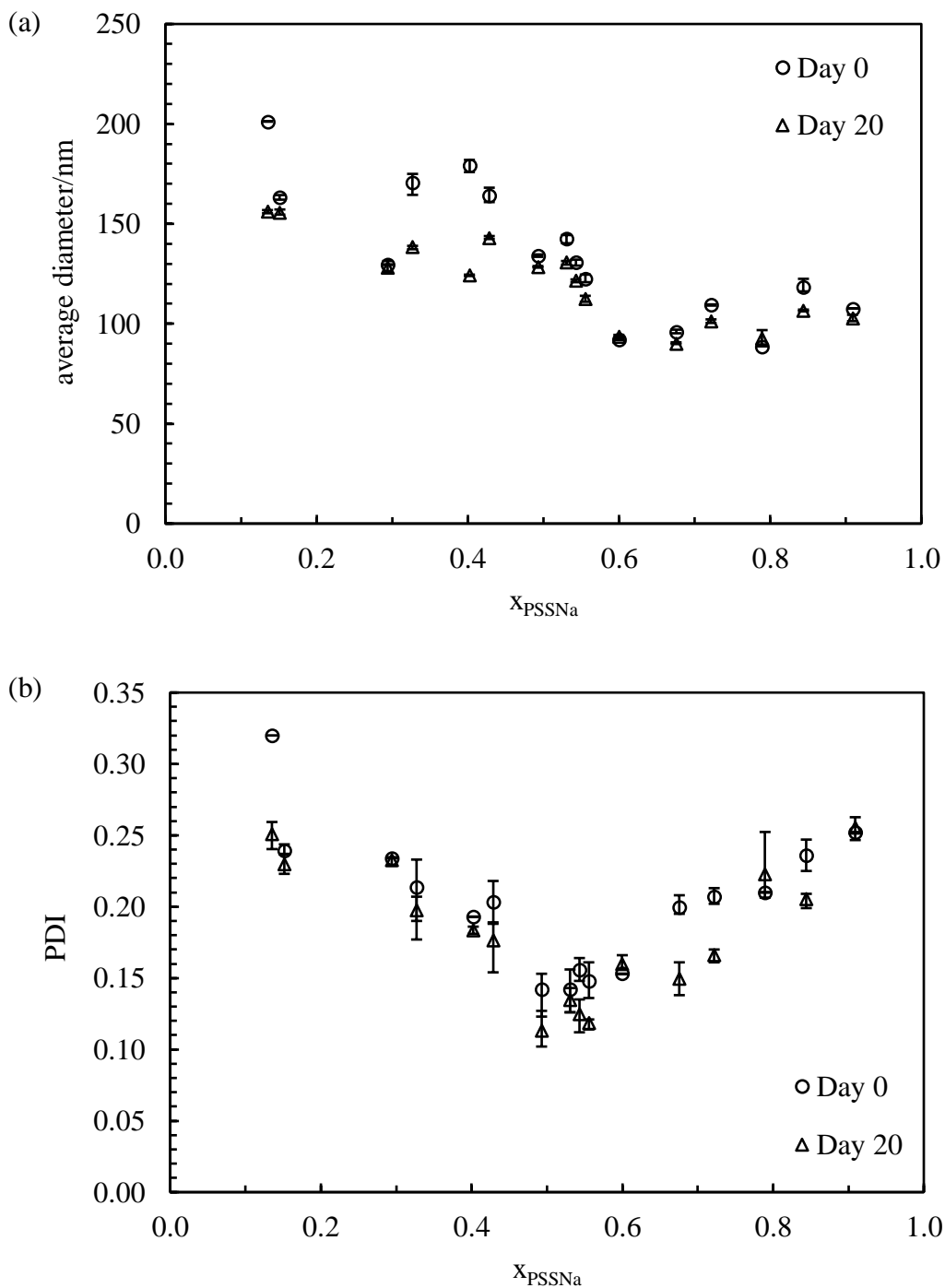

As shown in the plots above, the particle diameter varies from 100 to 200 nm depending on x_{PSSNa}. On the basis of these results, PEC obtained when PDADMAC is in excess (low x_{PSSNa}) seem to be slightly larger and, as soon as the mole fraction of

the anionic polyelectrolyte increases, the particles become smaller. When PSSNa is in excess ($x_{PSSNa} > 0.5$) the particle diameter remains constant at around 100 nm. These results are in agreement with those obtained by Mende *et al.*[7] with the same polyelectrolyte system (PSSNa-70 kDa and 1000 kDa, PDADMAC-5 kDa and 290 kDa) who found that the particle diameter does not vary significantly when PSSNa is in excess. The PSSNa-PDADMAC system was also studied by Dautzenberg (PSSNa-66 kDa, PDADMAC-250 kDa).[8] He reported that the size of PEC particles decreases upon approaching charge neutrality, again consistent with our results. Nevertheless, in the literature there is not full agreement about the dependence of the particle size on the mixing ratio. Depending on the polyelectrolytes used and their concentrations, different tendencies have been reported. While in some cases[8-10] particles with the smallest size are obtained around the point of charge neutralization and the size tends to increase as soon as one of the components is in excess (displaying a minimum), other authors[11,12] show that particles are smaller when one of the components is in excess and the largest size is obtained at the point where all the charges are compensated.

The corresponding plot of the PDI of particles *versus* x_{PSSNa} is given in Figure 3.2(b). Interestingly, the polydispersity in size is least when the proportion of both polyelectrolytes is about the same. When one of the components is in excess, the PDI increases revealing a minimum. This is consistent with the results obtained earlier.[7,8,12] In general, the values of the average diameter and PDI do not change significantly with time.

Zeta potentials were determined for freshly prepared dispersions and for those twenty days after preparation. As shown in Figure 3.3, when PDADMAC is in excess ($x_{PSSNa} < 0.54$), the zeta potential is positive since the positively charged polyelectrolyte in excess surrounds the particles. This value decreases slightly as the PDADMAC proportion decreases. On the other hand, when PSSNa is in excess, the zeta potential is negative and increases slightly in magnitude with increasing x_{PSSNa}. These results are in line with the ones obtained by other authors.[10,12] There is a dramatic change in both the sign and value of the zeta potential at x_{PSSNa} between 0.54 and 0.56. This region refers to complete charge neutralisation and fits with the PDI plot, where the particles are least polydisperse.

Figure 3.3. Variation of zeta potential with x_{PSSNa} for aqueous PEC dispersions prepared from 0.1 g L^{-1} individual PEL solutions for freshly prepared dispersions (circles) and 20 days after preparation (triangles).
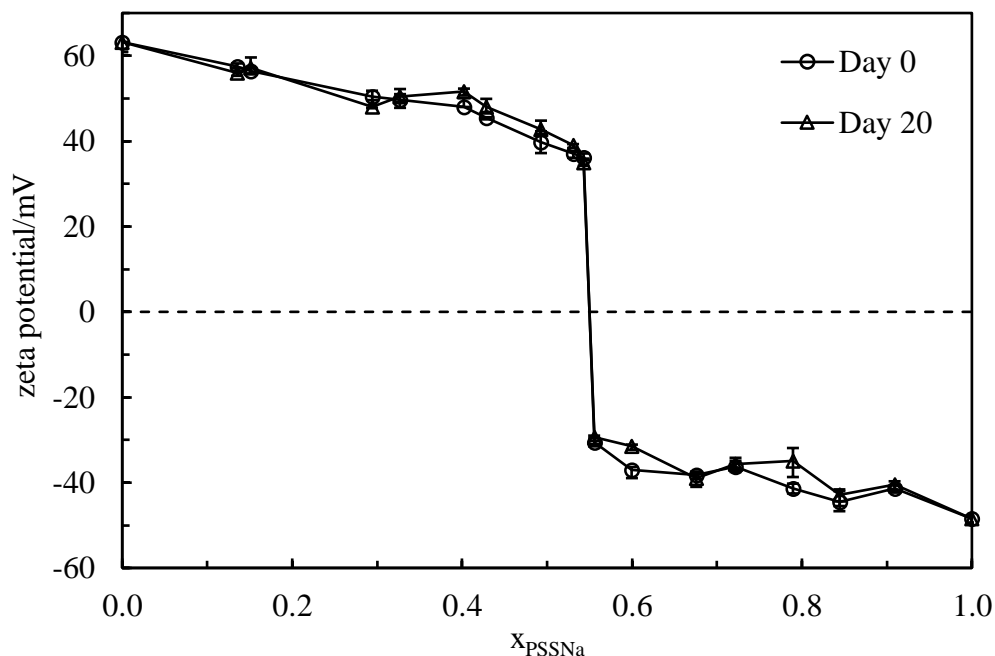

3.2.1.2 Effect of mixing procedure

The formation of more compact structures for $x_{PSSNa} > 0.5$ shown in Figure 3.2 could be linked to the sample preparation. As described in the experimental section, the polycation solution (PDADMAC) was added in different amounts into the polyanion solution (PSSNa). Therefore, on the left hand side of the plot, the major component was added to the minor while for $x_{PSSNa} > 0.5$, the minor component was added into the major. According to Müller,[13] for the minor-to-major scenario, more equilibrated smaller PEC particles were achieved as the charge sign is never reversed. Applied to our system, for $x_{PSSNa} > 0.5$, a small volume of PDADMAC solution is dosed into a big volume of PSSNa solution. Consequently, particles are electrostatically stabilised by the excess like-charged component. However, for the major-to-minor case, immediately after exceeding the critical 1:1 stoichiometry the excess oppositely charged component can "cross-link" the secondary particles to form colloidal networks with lower structural density.[13] Similar trends were reported by Schatz *et al.*[14]

In order to evaluate the effect of the order of addition on the complex size and charge, aqueous PEC dispersions were prepared by adding the PSSNa solution into the PDADMAC solution. In Figure 3.4, the average diameter *versus* x_{PSSNa} for the two mixing procedures is shown.

Figure 3.4. Average diameter *versus* x_{PSSNa} for two sets of aqueous PEC dispersions prepared by varying the order of the PEL addition: PDADMAC to PSSNa (circles) and PSSNa to PDADMAC (triangles). Aqueous PEC dispersions are prepared from 0.1 g L^{-1} individual PEL solutions.
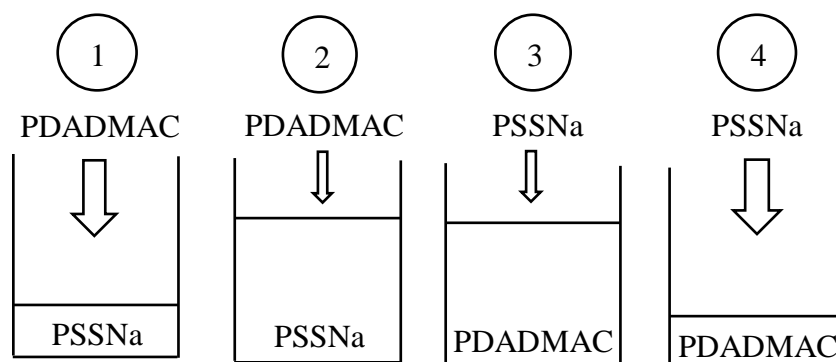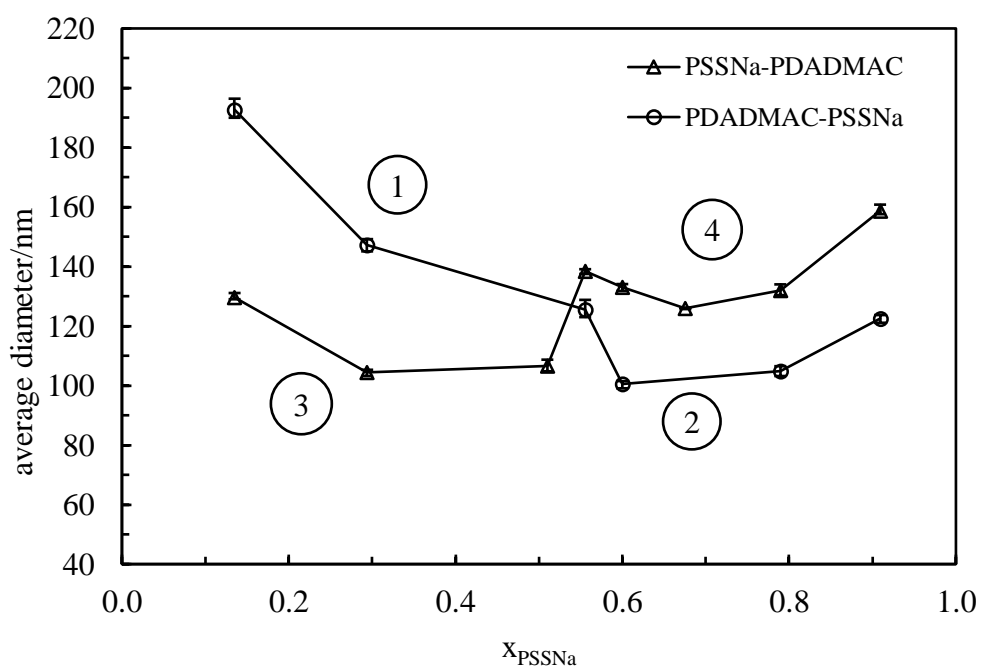
As expected, for the addition of PSSNa into the PDADMAC solution, more compact structures are obtained when the minor component is added to the major (case 3). On the other hand, the mixing procedure does not seem to affect the zeta potential as the two curves overlay (Figure 3.5).

Figure 3.5. Zeta potential *versus* x_{PSSNa} for two sets of aqueous PEC dispersions prepared by varying the order of PEL addition: PDADMAC to PSSNa (circles) and PSSNa to PDADMAC (triangles). Aqueous PEC dispersions are prepared from 0.1 g L^{-1} individual PEL solutions.
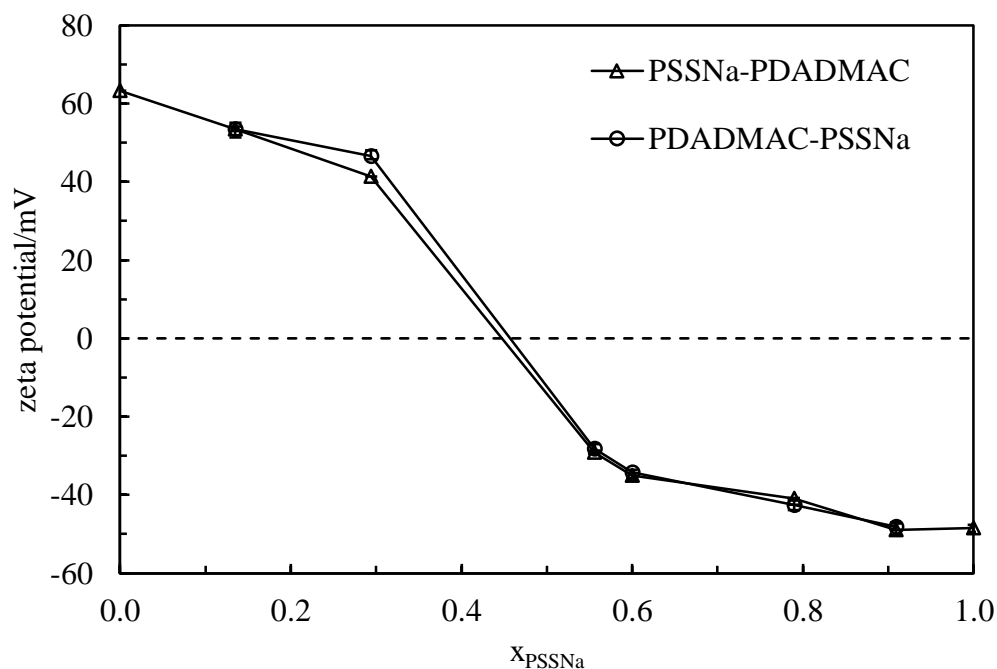
3.2.1.3 Effect of polymer molecular weight

In order to assess the influence of the polymer molecular weight on the structural parameters of the formed PEC, aqueous PEC dispersions at different x_{PSSNa} were prepared from PEL of different molecular weights: PDADMAC (160 kDa) and PSSNa (976 kDa). As shown in Figure 3.6, no remarkable differences in either the particle diameter or PDI are observed in comparison to the previous results where both polymers were of similar M_w (Figure 3.2), although the value of x_{PSSNa} at charge reversal is considerably lower ($x_{PSSNa} = 0.18$) as expected (Figure 3.7). As the M_w of PSSNa is higher than that of PDADMAC and consequently more charged groups are present on the polymer chain, a higher amount of PDADMAC is required to compensate all the negative charges on PSSNa.

Figure 3.6. (a) Average particle diameter and (b) PDI in size *versus* x_{PSSNa} for aqueous PEC dispersions prepared from 0.1 g L^{-1} individual PEL solutions of different molecular weight; $M_{w,PSSNa} = 976$ kDa, $M_{w,PDADMAC} = 160$ kDa. Measurements taken from freshly prepared dispersions.
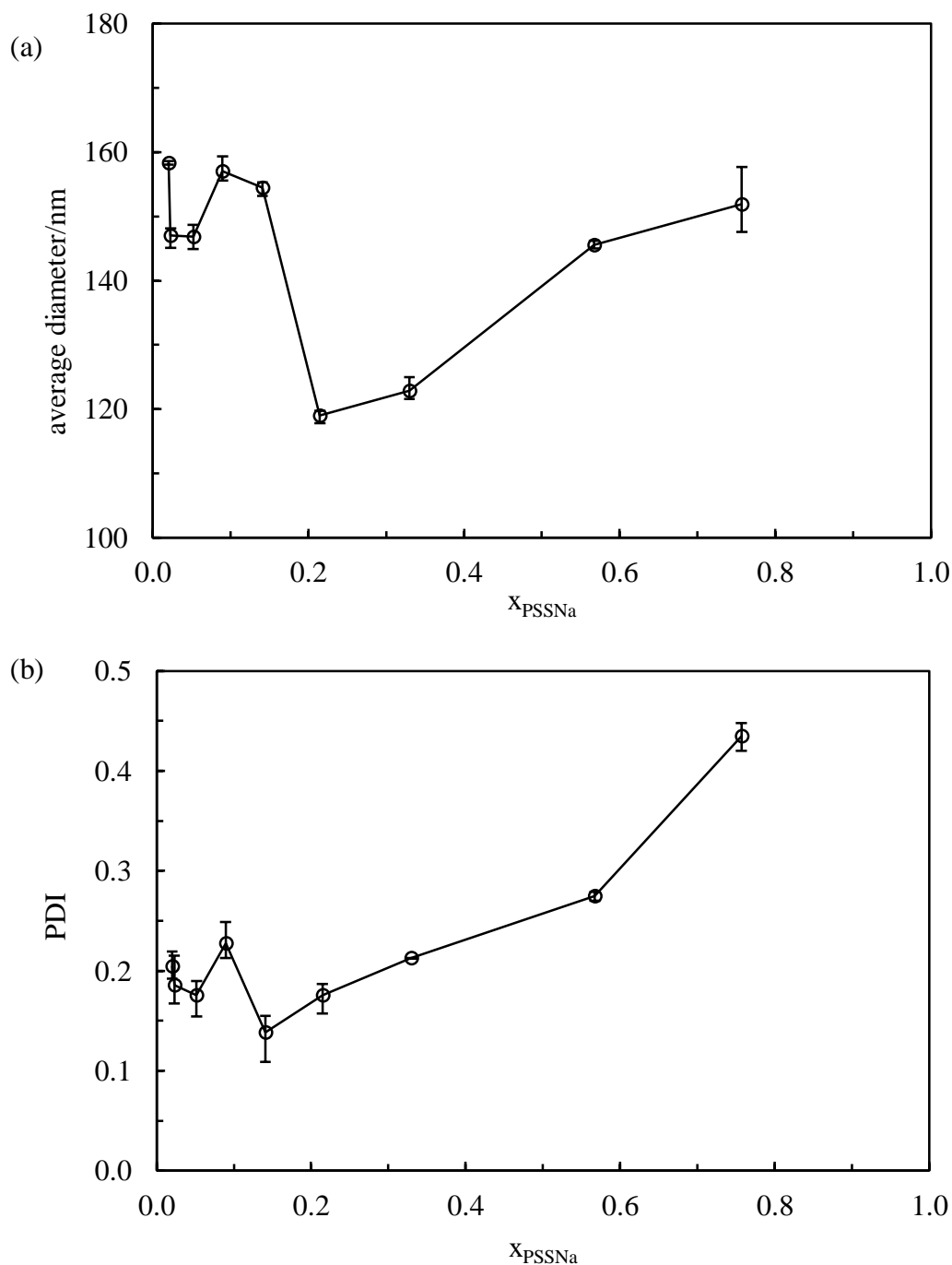

The average diameter for the PEC with $x_{PSSNa} > 0.5$ is approx. 40 nm larger than that for particles prepared from PEL of similar M_w. Generally, small complexes are formed by small polyelectrolytes, while larger polyelectrolytes give larger complexes.[15,16] Ankerfors *et al.*[17] related this tendency to the diffusion-controlled formation of "pre-

complexes". While low M_w polymers form stable complexes quickly, larger polyelectrolytes are more prone to aggregation due to longer diffusion times. Moreover, as pointed out by Starchenko *et al.*, the increase in the PEC particle radii reflects the general trend of polymers in solution as their size parameters increase with increasing the degree of polymerisation, *N*, according to Flory theory.[18] Starchenko *et al.* measured the mean particle radius of PEC prepared with the system PDADMAC-PSSNa. Increasing PSSNa M_w from 4,600 to 1,117,000 g mol^{-1} resulted in an increase of the mean particle radius of ~ 44 nm for a [PEL] of 0.02 M.[18] Finally, Dautzenberg studied the same system and by varying the M_w of PSSNa from 8 to 1,000 kg mol^{-1} no systematic change on the structural parameters was found.[19] He attributed this result to the kinetics of the process of PEC formation that prevails and supresses the effect of the molecular weight on the resulting structures.[19]

From the zeta potential data given in Figure 3.7, slightly higher negative values were achieved when PSSNa is in excess compared to the results from polymer mixtures of the same M_w. This can be attributed to the increase in the amount of negatively charged groups on each PSSNa chain.

Figure 3.7. Variation of zeta potential with x_{PSSNa} for aqueous PEC dispersions prepared from 0.1 g L^{-1} individual PEL solutions of different molecular weight; $M_{w,PSSNa}$ = 976 kDa, $M_{w,PDADMAC}$ = 160 kDa. Measurements taken from freshly prepared dispersions.
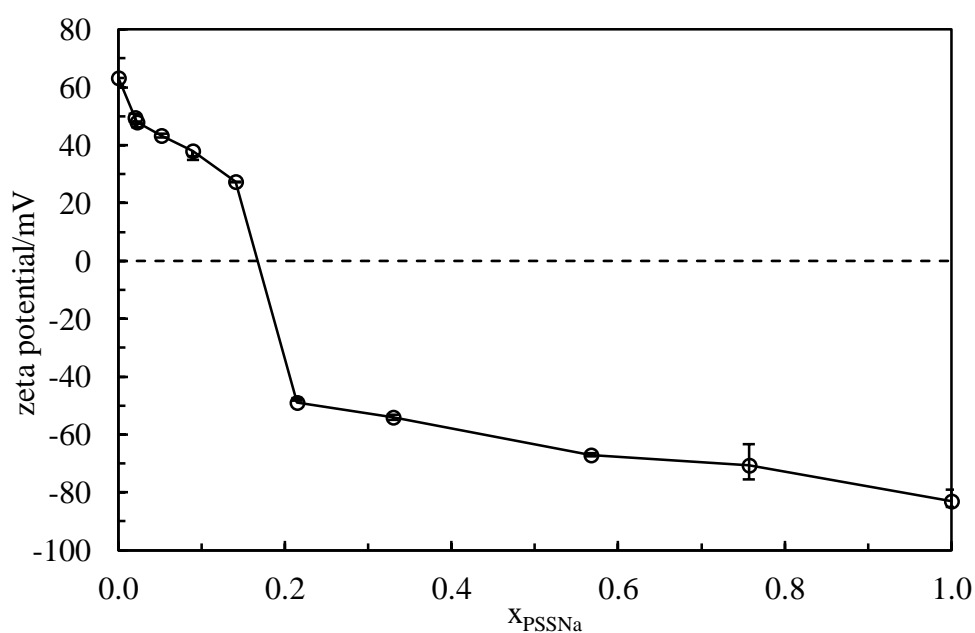
3.2.2 Dispersions at high PEL concentration

3.2.2.1 Effect of mole fraction of anionic polyelectrolyte

The same experimental procedure was followed for aqueous PEC dispersions prepared from the 0.5 g L^{-1} individual PEL solutions at different x_{PSSNa} to corroborate the above tendencies. As depicted in Figure 3.8(a), dispersions become noticeably more turbid as soon as x_{PSSNa} approaches 0.56. The transmittance (at $\lambda = 400$ nm) of these dispersions is given in Figure 3.8(b). The individual PEL do not absorb light in the range from 400 to 800 nm. The increase in turbidity around the charge neutralisation point may be attributed to an increase in the overall particle concentration.

Figure 3.8. (a) Appearance of freshly prepared aqueous PEC dispersions prepared from 0.5 g L^{-1} individual PEL solutions at different x_{PSSNa} (given). Scale bar = 1 cm. (b) Transmittance at $\lambda = 400$ nm for the above.
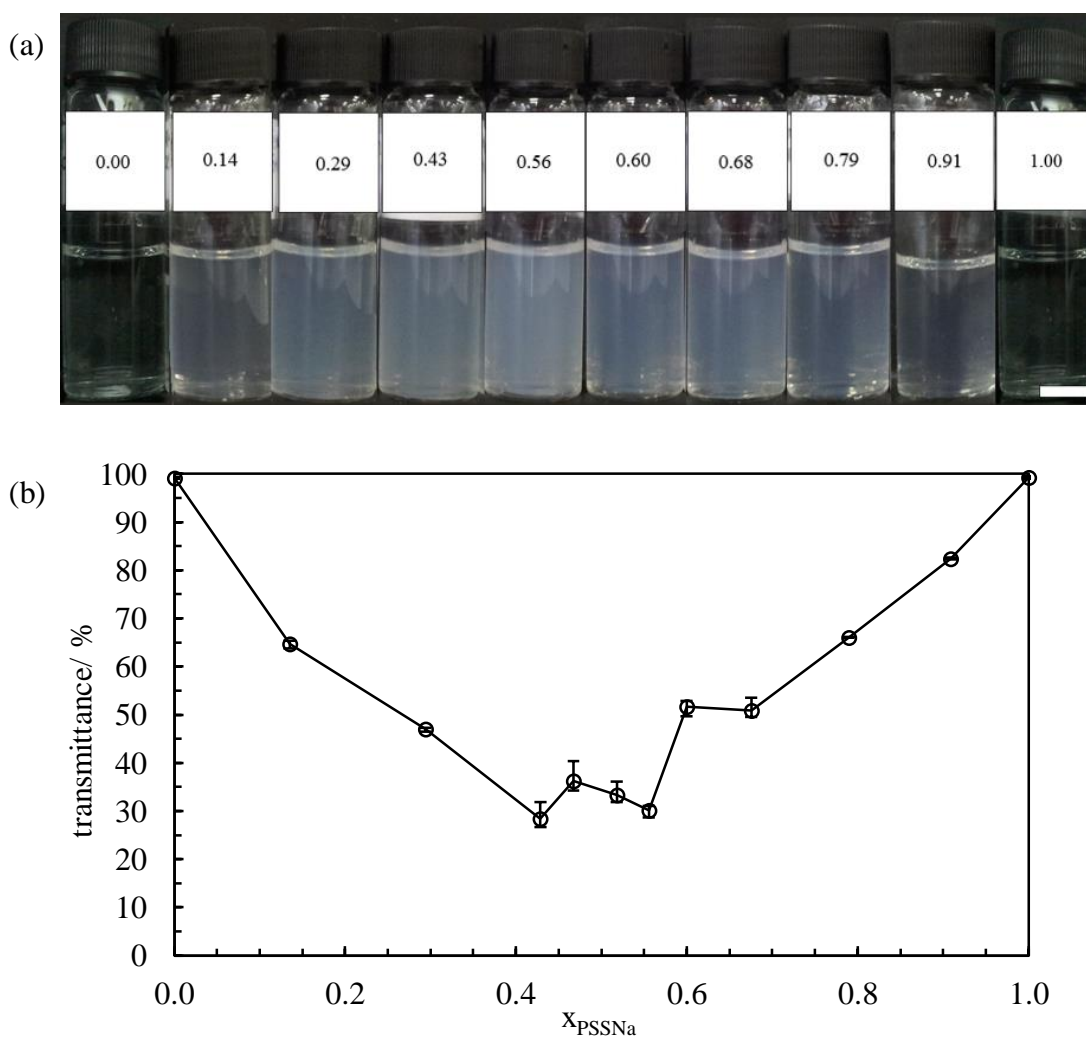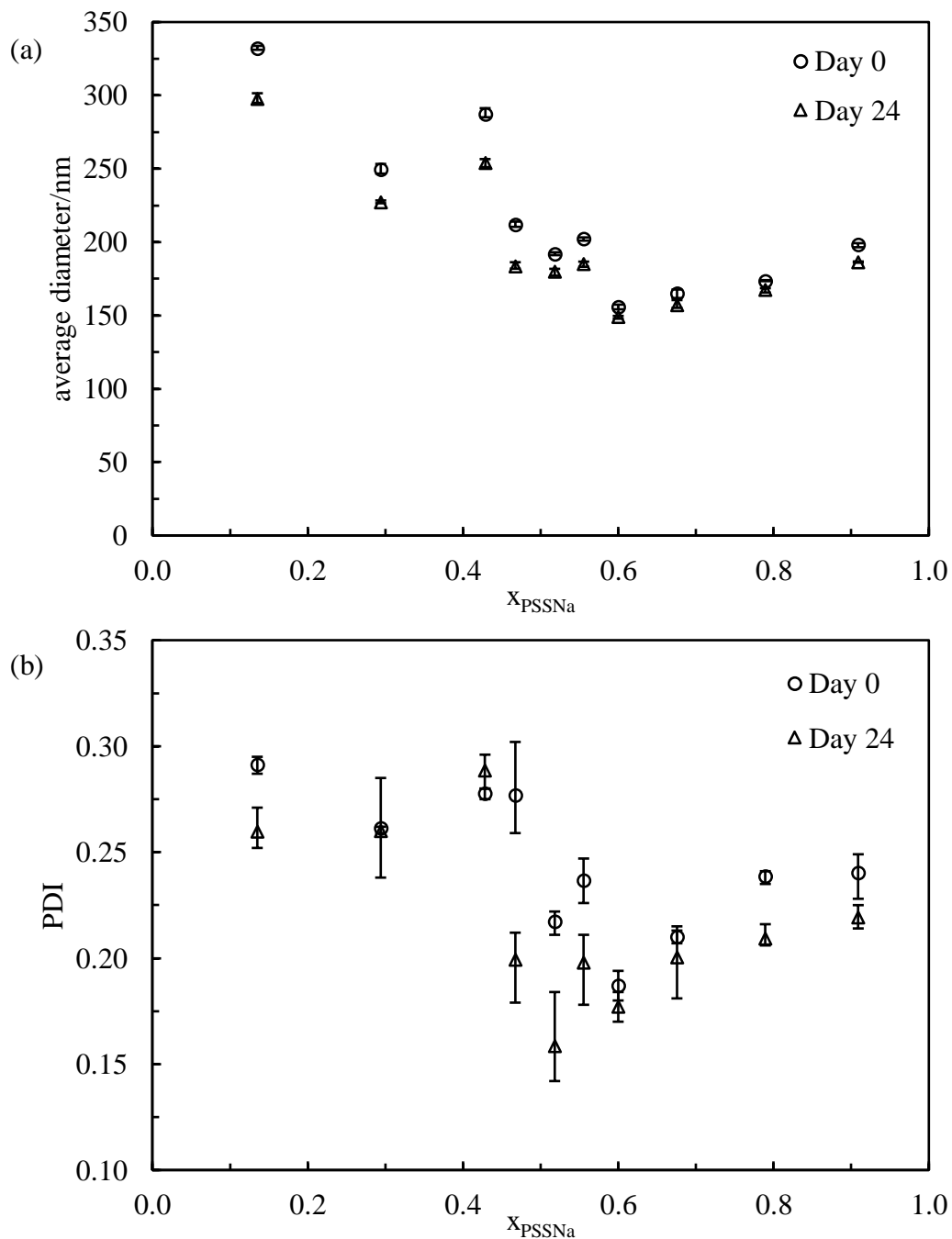
Figure 3.9. (a) Average particle diameter and (b) PDI *versus* x_{PSSNa} for aqueous PEC dispersions prepared from 0.5 g L^{-1} individual PEL solutions for freshly prepared dispersions (circles) and values 24 days after preparation (triangles).

The possibility of particle aggregation at the point of charge neutrality ($x_{PSSNa} \approx 0.5$) was discounted from light scattering measurements as the smallest particles were obtained when both charges were neutralised (Figure 3.9(a)). For this set of aqueous PEC dispersions prepared at a higher concentration, profiles for the average particle diameter, PDI in particle diameter and zeta potential (Figures 3.9 and 3.10) were entirely consistent with the ones obtained at the low concentration range. However, the average diameter is slightly larger compared to that measured from aqueous PEC dispersions prepared from 0.1 g L^{-1} PEL solutions (Figure 3.2(a)).

Figure 3.10. Variation of zeta potential with x_{PSSNa} for aqueous PEC dispersions prepared from 0.5 g L^{-1} individual PEL solutions for freshly prepared dispersions (circles) and values 24 days after preparation (triangles).
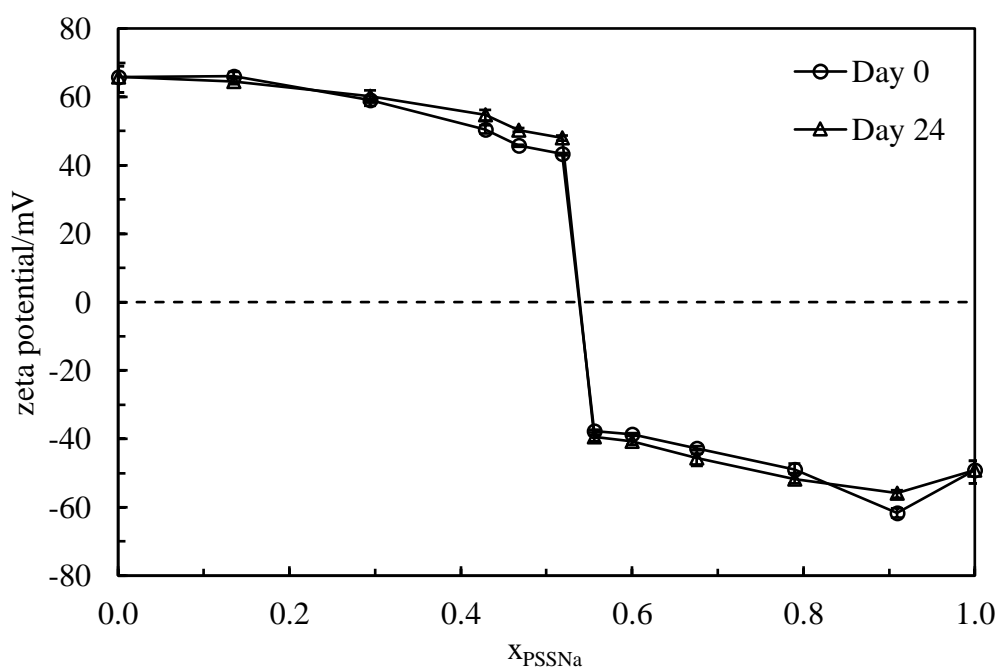
Finally, to evaluate the influence of the PEL concentration on the structural parameters of the obtained particles, solutions at higher concentrations were prepared at a constant $x_{PSSNa} \approx 0.54$. As shown in Figure 3.11(a), the higher the initial PEL concentration, the more turbid the dispersion is as seen from the decrease in the transmittance value (Figure 3.11(b)).

Figure 3.11. (a) Appearance of aqueous PEC dispersions ($x_{PSSNa} \approx 0.54$) obtained from individual PEL solutions of the given concentrations. Scale bar = 1 cm. (b) Variation of the transmittance at $\lambda = 500$ nm for aqueous PEC dispersions prepared at $x_{PSSNa} \approx 0.54$ with concentration of PSSNa.
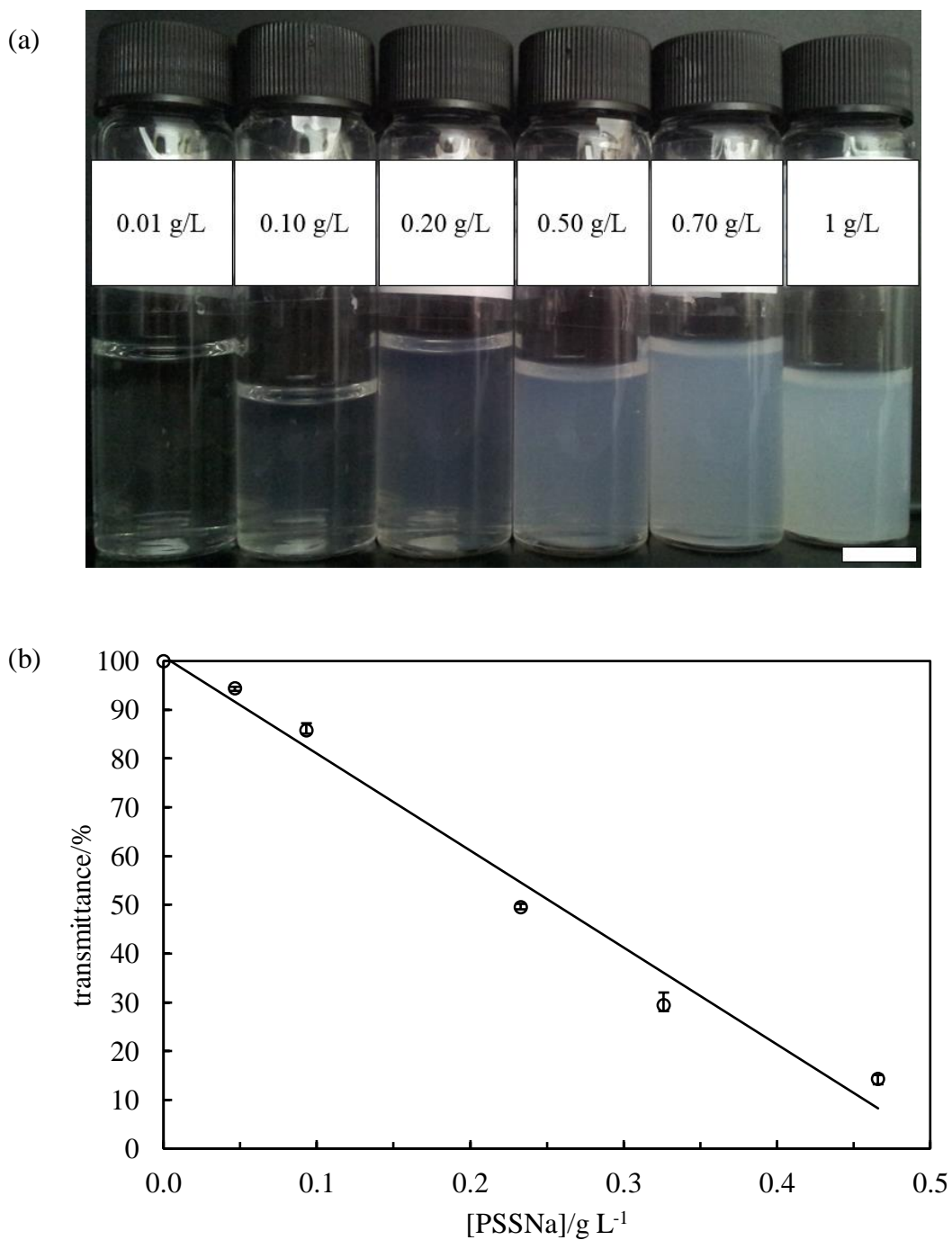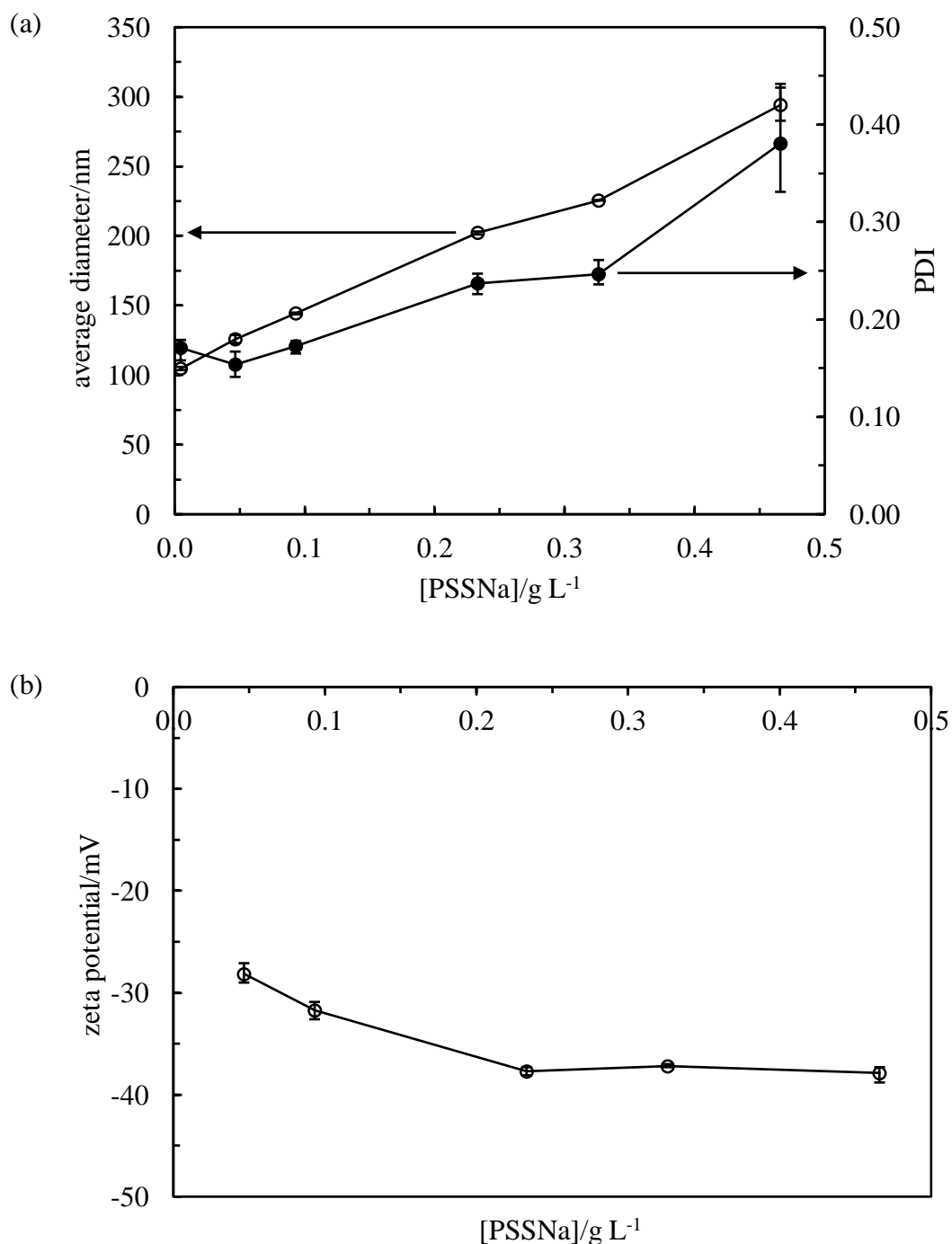
Figure 3.12. Plots for (a) average particle diameter (unfilled circles) and PDI in size (filled circles) and (b) zeta potential *versus* [PSSNa] in the dispersion for aqueous PEC dispersions ($x_{PSSNa} \approx 0.54$) obtained from individual PEL solutions of different concentrations.


From dynamic light scattering measurements, Figure 3.12(a), it can be concluded that particles seem to aggregate as both the average diameter and the PDI increase with the polyelectrolyte concentration. This can be gleaned from the results of Starchenko *et*

al.[18] for the same polyelectrolyte system. By increasing the PEL concentration, and consequently the concentration of primary particles, it accelerates the aggregation and increases the size of the secondary particles.[18] The zeta potential of the particles appears to increase slightly with the polyelectrolyte concentration until it reaches a plateau around -38 mV (Figure 3.12(b)).

3.2.2.2 Effect of salt concentration

One important parameter that influences PEC formation and their final structure is the concentration of salt as its ions interact with the charges on the oppositely charged polyelectrolytes. For this reason, its influence on aqueous PEC dispersions was evaluated. Salt was added after PEC formation. The appearance of aqueous PEC dispersions prepared at different NaCl concentrations (from 0 to 5 M) from the 1 g L^{-1} PEL solutions at $x_{PSSNa} = 0.52$ is shown in Figure 3.13.

Figure 3.13. Appearance of aqueous PEC dispersions prepared from 1 g L^{-1} individual PEL solutions and $x_{PSSNa} = 0.52$ at different concentrations of NaCl (given) after preparation. Scale bar = 1 cm.
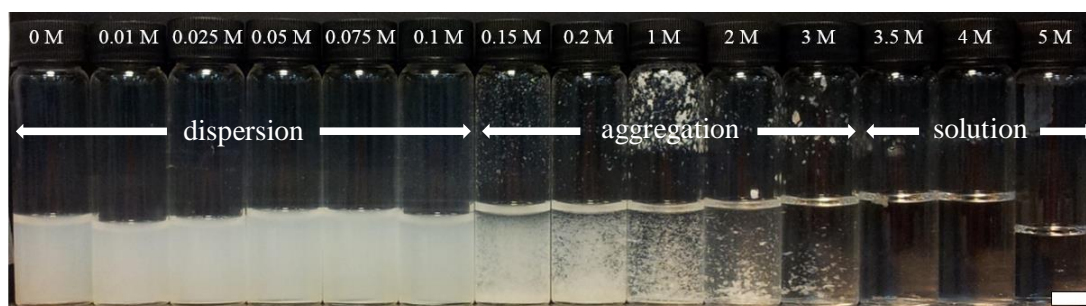
Three different regions can be distinguished. Between 0 and 0.1 M NaCl, turbid stable dispersions are obtained. The transmittance at 700 nm decreased from 39% (no added salt) to 13% (in 0.1 M NaCl). The average diameter of PEC particles was 294 nm without salt and 873 nm in the presence of 0.1 M NaCl, with a broad size distribution in both cases (PDI > 0.3). Moreover, after allowing the dispersions to stand for a couple of days, precipitation of white PEC aggregates was visible at the bottom of the vessels with a [NaCl] = 0.075 and 0.1 M. Taken together, the evidence suggests that colloidally stable particles without salt begin to aggregate due to the screening effect of the counterions (Na$^+$ and Cl$^-$). The second region, between 0.15 M and 3 M NaCl, is where flocs of PEC aggregates of several hundred microns appear. Within this range,

the floc concentration decreases with salt concentration. Finally, for aqueous PEC dispersions prepared at [NaCl] $\geq$ 3.5 M, they were completely transparent. However, immediately after salt addition, white flocs were obtained which rapidly dissolved with time. The absence of colloidal particles in these solutions was confirmed through dynamic light scattering. At such high ionic strength conditions, electrostatic interactions between the PEL no longer exists because of the high screening effect of the counterions. Therefore, PEC particles dissolve liberating the initial soluble chains of both polyelectrolytes which remain unchanged for over 3 months. Our findings are in good agreement with those from Zhang et $al.$[20] for the same pair of polyelectrolytes but of higher polydispersity. Without added salt, neutral small size primary particles surrounded by excess polyelectrolyte were formed (stable PEC). At intermediate salt concentration, small counterions screened the PEC leading to aggregation in large secondary particles that eventually precipitated (unstable PEC). At even higher salt concentrations, dissolution of PEC into the individual chains occurred.[20]

3.2.3   SEM images of PEC

SEM images of PEC were carried out to compare the complex sizes to those obtained by dynamic light scattering. Figure 3.14(a) shows an SEM image of an aqueous PEC dispersion prepared from 0.1 g L^{-1} individual PEL solutions at x_{PSSNa} = 0.56. In general, particles can be considered quasi-spherical despite some aggregation also being detected. The average particle diameter measured from the micrograph of approx. 100 nm is in good agreement with the one acquired by light scattering.

The SEM image of the aqueous PEC dispersion (x_{PSSNa} = 0.56) from the 0.5 g L^{-1} individual PEL solutions is shown in Figure 3.14(b). Here, the concentration of particles is seen to be higher than in the previous case. It is likely however that the film of aggregated particles observed is formed during the slow evaporation process during sample preparation. At higher [PEL], 1 g L^{-1}, this effect is even more pronounced as seen in Figure 3.15(a). The EDX spectra of the particles verified the presence of sulphur, which is present in PSSNa (Figure 3.15(b), right).

Figure 3.14. SEM images at different magnifications of freshly prepared aqueous PEC dispersions (x_{PSSNa} = 0.56) from (a) 0.1 g L^{-1} and (b) 0.5 g L^{-1} individual PEL solutions.
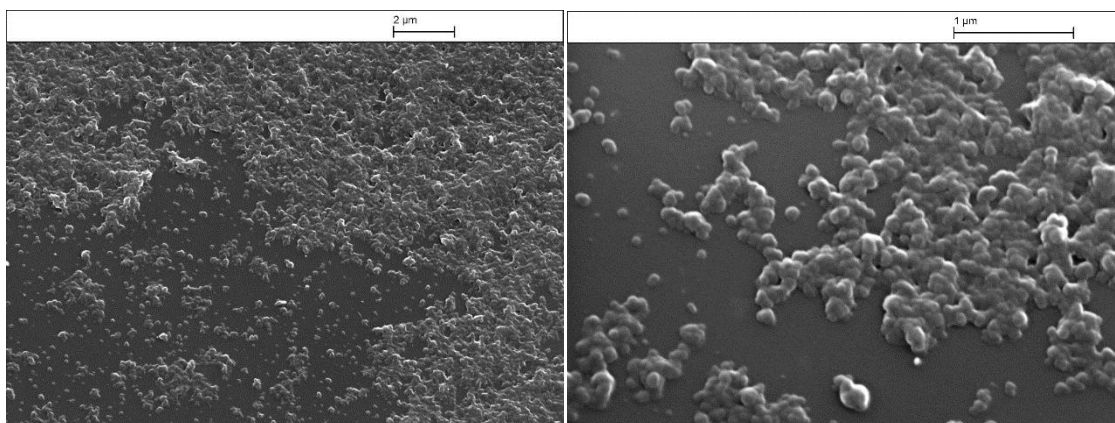
(a)
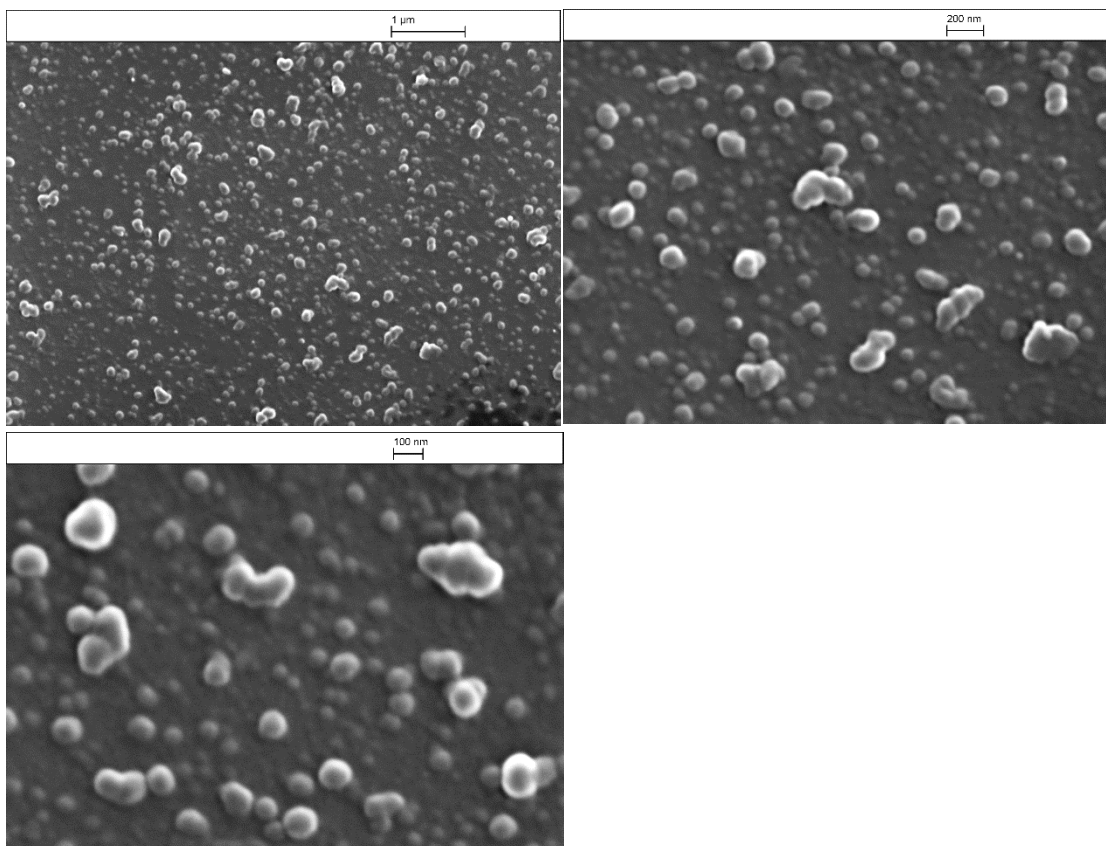
(b)

Figure 3.15. (a) SEM images at different magnifications of a freshly prepared aqueous PEC dispersion ($x_{PSSNa} = 0.56$) from 1 g L^{-1} PEL solutions. (b) EDX spectra of a bare carbon coated coverslip (left) and a carbon coated coverslip containing the PEC.

(a)

(b)
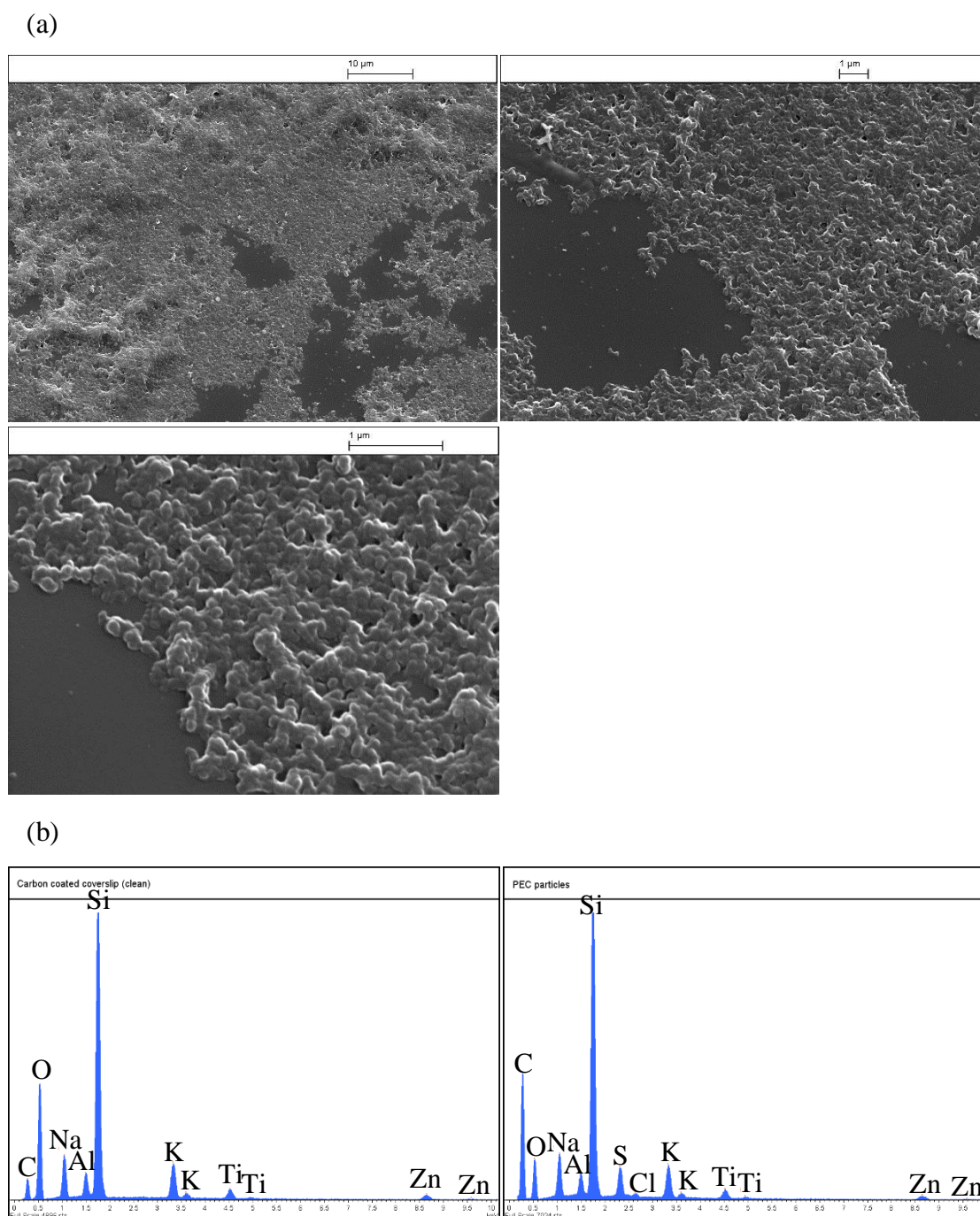
3.2.4 Summary of aqueous PEC dispersions

From the results obtained from the characterisation of aqueous PEC dispersions, the following conclusions can be taken. PEC particles are obtained across the mole fraction range as a result of a strong electrostatic interaction and the highest amount

of entities is obtained around charge neutrality. By increasing the [PEL] upon the preparation of aqueous dispersions, both aggregation of primary particles and an increase in the number of PEC was achieved. Salt has a significant effect on the stability of the aqueous dispersions. By increasing the salt concentration, the transition: stable dispersions – aggregated and unstable dispersions – solutions of individual polymer molecules is found.

3.3 Oil-in-water emulsions prepared from polymer mixtures

Our interest here is whether PEC particles prepared in water are surface-active enough to adsorb to an oil-water interface created on emulsifying the aqueous phase with a non-polar alkane. After a detailed study on the characterisation of aqueous PEC dispersions, the effect of three parameters on the emulsion behaviour are evaluated, being the x_{PSSNa}, [PEL] and the oil volume fraction (ϕ_o). Finally the effect of salt concentration on emulsion stability will be assessed, as well as the oil type.

3.3.1 *Effect of mole fraction of anionic polyelectrolyte on emulsion stability*

Emulsions of *n*-dodecane ($\phi_o = 0.2$) and an aqueous PEC dispersion from the 20 g L^{-1} individual PEL solutions were prepared for different values of x_{PSSNa} from 0 to 1. From Figure 3.16(a), it can be seen that oil-in-water (o/w) emulsions prepared with the polyelectrolytes alone ($x_{PSSNa} = 0$ and 1) are extremely unstable and phase separate completely immediately after preparation; *i.e.* the polymers are not surface-active. This finding contrasts that in the field of emulsions stabilized by protein-polysaccharide complexes, for example, where one or both components stabilize the emulsion alone.[4-6] However, once PEC are present in the aqueous phase, long-term stable o/w emulsions are achieved, implying that PEC particles are the stabilizing emulsifier. These emulsions cream with time with water separating below the cream, apart from the emulsion prepared close to charge neutralization ($x_{PSSNa} = 0.52$) which is stable.

The fractions of water (due to creaming) and oil (due to coalescence) released one week after preparation are plotted in Figure 3.16(b). In both cases, a minimum is achieved for x_{PSSNa} around 0.5, and the extent of coalescence is extremely small (< 0.05) for all polymer mixtures. The average droplet diameter of emulsions immediately after preparation is given in Figure 3.16(c) and passes through a shallow

minimum value of *ca*. 15 μm for x_{PSSNa} around 0.5, consistent with the inhibition of creaming at this condition. Optical micrographs of selected emulsions are shown in Figure 3.17 where all droplets are spherical. It thus appears that, by reducing the overall charge of PEC particles in mixtures of polymers, their hydrophobicity is increased to such an extent that they prefer to adsorb to the oil-water interface during mixing. This argument was used to explain the stabilization of emulsions at optimum ratios of anionic and cationic solid particles.[21,22]

Figure 3.16. (a) Appearance of dodecane-in-water emulsions ($\phi_o = 0.2$) stabilised by PEC particles prepared from 20 g L^{-1} individual PEL solutions at different x_{PSSNa} given. Scale bar = 1 cm. (b) Fraction of water (filled points) and fraction of oil (unfilled points) released from emulsions after 1 week *versus* x_{PSSNa}. (c) Average droplet diameter of above emulsions after preparation *versus* x_{PSSNa}.
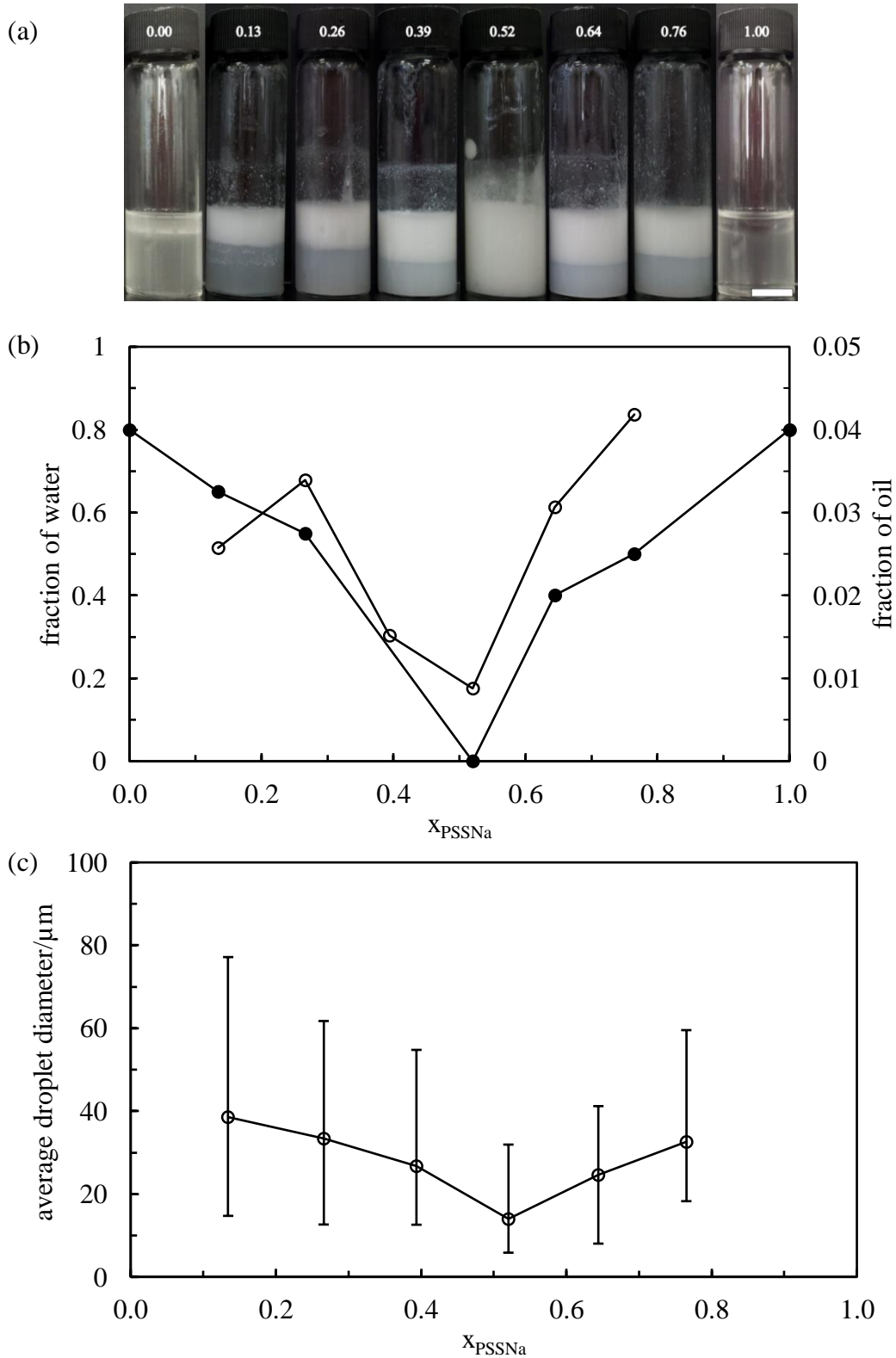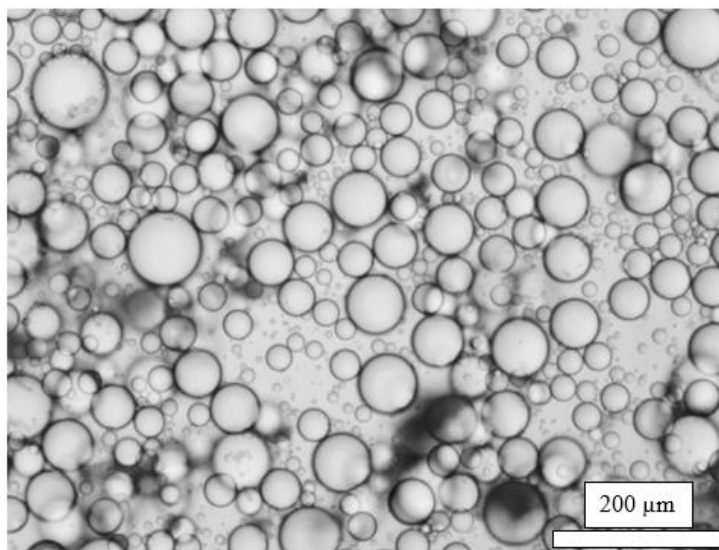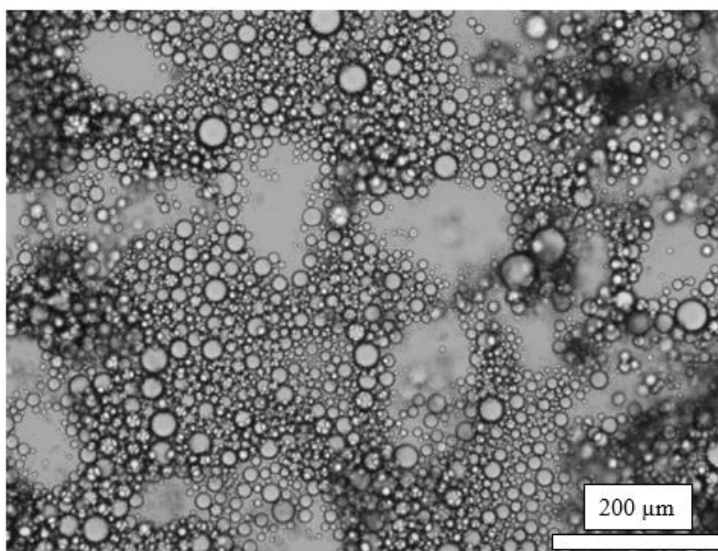
Figure 3.17. Optical microscope images of selected emulsions in Figure 3.16 at x_{PSSNa} of (a) 0.13, (b) 0.52 and (c) 0.64. The bare patches in (b) correspond to the glass slide.
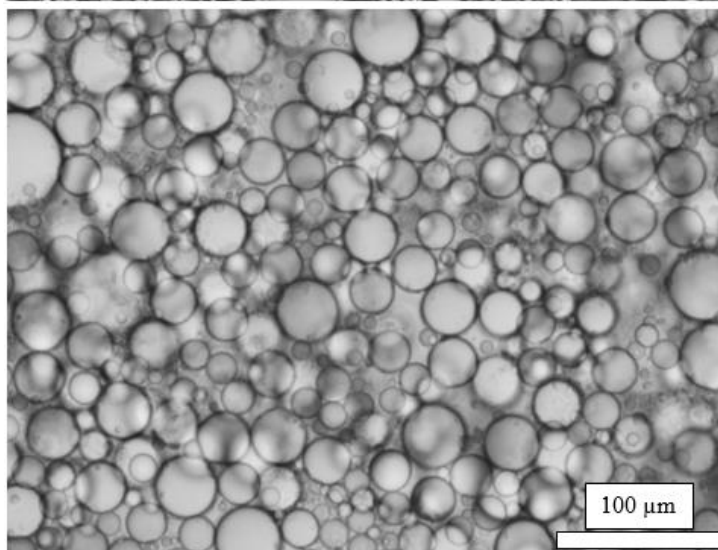
(a)

(b)

(c)

3.3.2   *Effect of PEL concentration on emulsion stability*

3.3.2.1 Comparison with the limited coalescence model

Depending on the initial emulsifier concentration, two main régimes are distinguished with respect to emulsion formation in particle-stabilised emulsions.[23] When the system is emulsified at low concentration of stabilizer, known as the emulsifier-poor régime, droplets are partially covered with the emulsifier. Therefore, once the agitation is stopped, droplets coalesce to a limited extent. The degree of interface coverage by particles increases leading to a reduction of the total interfacial area between oil and water. This prevents further coalescence events.[24] In this régime, the mean drop size decreases with increasing emulsifier concentration. In contrast, at high emulsifier concentrations (emulsifier-rich régime) the interfaces are sufficiently covered by particles and the average drop size is practically independent of the stabilizer concentration. For emulsions experiencing limited coalescence, the following equation can be written, considering complete adsorption of spherical particles at the interface,[25]

$$\frac{1}{D_{[3,2]}} = \frac{1-\phi_o}{6\phi_o\tau}c \tag{3.1}$$

where ϕ_o is the volume fraction of the dispersed phase, c is the initial emulsifier concentration, τ is the stabilizer adsorption density and $D_{[3,2]}$ is the Sauter mean diameter obtained from,

$$D_{[3,2]} = \frac{\sum_i N_i D_i^3}{\sum_i N_i D_i^2} \tag{3.2}$$

where N_i is the total number of droplets with diameter D_i. The Sauter mean diameter expresses the mean diameter of particular matter by taking into account the volume-to-surface area ratio and it is especially important in cases where the active surface area is important, as in this case for the determination of the stabilizer adsorption density.[26]

By plotting the inverse of the mean drop diameter *versus* the concentration of the emulsifier, a straight line is expected to be obtained. From the slope, the stabilizer adsorption density can be calculated. For that purpose, a series of emulsions of dodecane-in-water *($\phi_o = 0.2$)* were prepared from aqueous PEC dispersions at $x_{PSSNa} \approx$

0.5 from the individual PEL solutions at different concentrations. The appearance of selected emulsions can be seen in Figure 3.18(a).

Figure 3.18. (a) Appearance of dodecane-in-water emulsions ($\phi_o = 0.2$) stabilised by PEC particles ($x_{PSSNa} \approx 0.50$) prepared from the individual PEL solutions of the given concentrations immediately after preparation. Scale bar = 1 cm. (b) Average droplet diameter *versus* initial [PSSNa] in the dispersion for the above emulsions. Inset - inverse of average droplet diameter as a function of initial [PSSNa] in the dispersion.
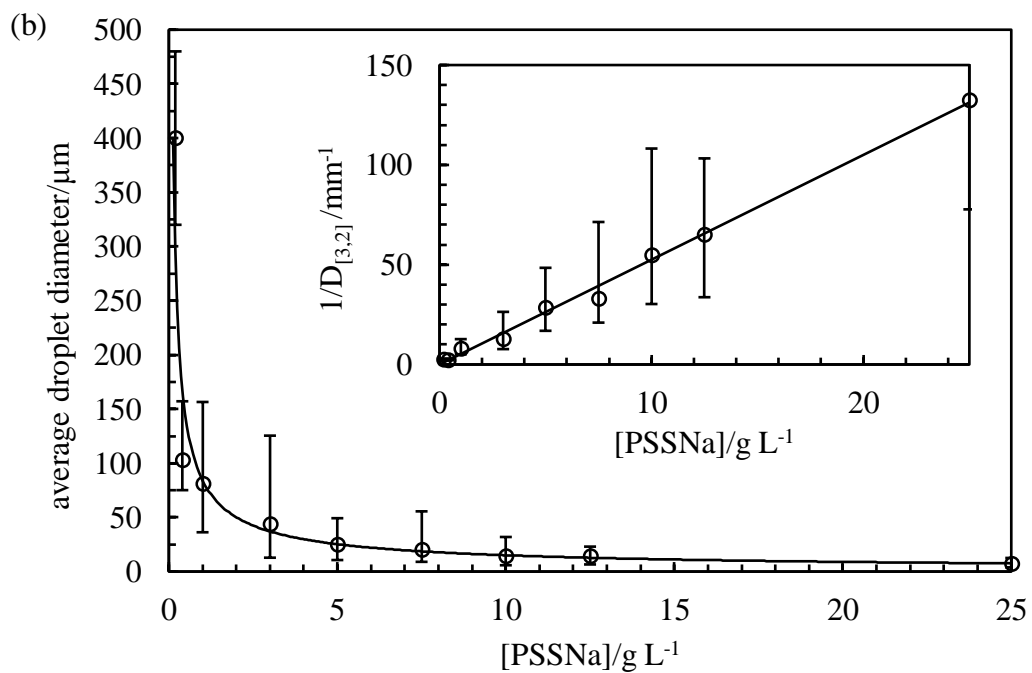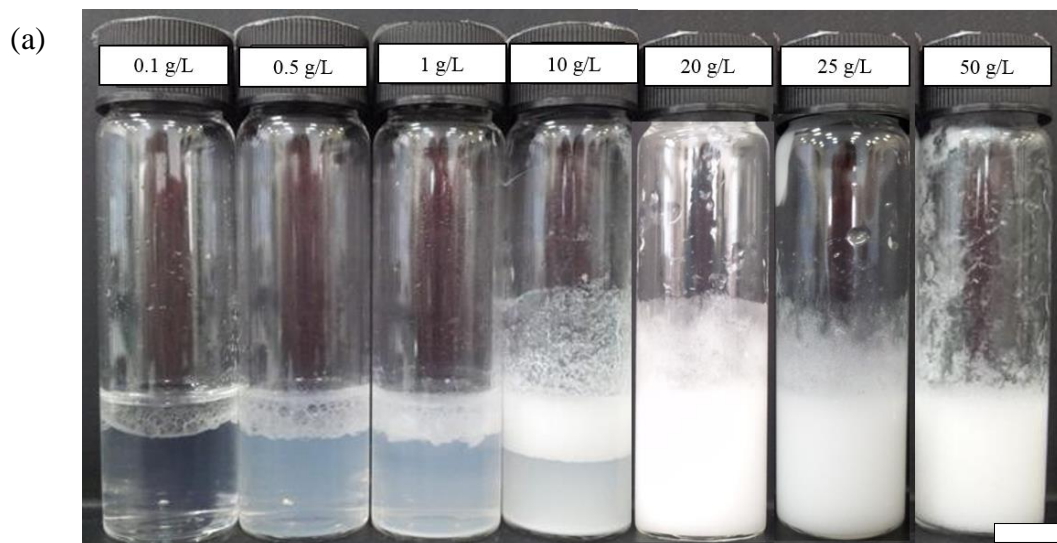
At low concentrations (< 0.1 g L^{-1}) no stable emulsions were achieved. However, as soon as the starting PEL concentration increased, emulsions stable to coalescence were formed. For emulsions prepared with a [PEL] ≥ 20 g L^{-1} no sign of creaming was shown and their viscosity increased considerably. Droplet diameters of stable emulsions were determined directly from optical micrographs and are plotted as a function of the polyelectrolyte concentration in the aqueous phase in Figure 3.18(b). In the inset, the plot corresponding to equation 3.1 is also given. The linear relationship confirms that these emulsions experience limited coalescence in the emulsifier-poor régime. For the explored concentration range, the transition towards the emulsifier-rich régime was not reached and droplets with average diameter as low as 8 μm are formed.

From the slope of the graph, the calculated adsorption density by particles is 0.127 ± 0.003 g m^{-2}. For this calculation, it has been assumed that at this concentration range all the emulsifier adsorbs at the drop interfaces. However, as it will be seen from cryo-SEM images (section 3.3.2.2), at high [PEL] particles are both at the interface and in the continuous aqueous phase. Destribats *et al.* obtained the interfacial adsorption density (τ) for emulsions prepared with covalently cross-linked whey protein microgel particles (WPM).[25] Formulations were carried out at different pH and two salt concentrations and for emulsions prepared with no added salt, τ spans between 18 to 38 mg m^{-2} (*i.e.* 10 times smaller than the value reported here).[25] They compared these experimental values with those of ideal WPM monolayers at the interface, based on hexagonal close packing of monodisperse, spherical particles with only 90% of the interfacial area being covered.[25] These estimations were done prior requirement of the particle diameter and density and interfacial densities corresponded closely to those of a monolayer or 1.5 monolayers depending on the pH.[25] In our case, without knowing the particle density, it is difficult to compare this value with that expected for close packing of monodisperse particles. Arditty *et al.* used a modified equation to measure s$_f$, defined as the asymptotic limit of the specific surface area at infinite time, for emulsions stabilized by silica particles.[24] The value reported for s$_f$ (3.1 m^2 g^{-1}) was 10 times larger than the one expected for a monolayer of hexagonally closed-packed spherical particles at the interface (30-40 m^2 g^{-1}). This discrepancy was explained by the fact that as initially particles are forming aggregates in the continuous phase, the adsorption cannot be considered at the level of primary particles but at the scale of

aggregates or clusters.[24] Joseph *et al.* calculated the specific surface area (s_f) of particles for emulsions stabilized by cocoa powder, which was ~16 m^2 g^{-1}. They compared their s_f value to that for proteins, which is in the order of several thousand m^2 g^{-1}. This suggested that, per unit mass of stabilising material, proteins have higher amounts of available sites for adsorption.[27]

3.3.2.2 Cryo-SEM images

Cryo-SEM analysis was attempted with several o/w emulsions around the composition $x_{PSSNa} \approx 0.5$. At a relatively low initial PEL concentration (1 g L^{-1}), Figure 3.19 shows two different areas of the sample (a and b) at different magnifications. In some cases, the frozen oil was removed allowing visualization of the interface, which appeared to be partly covered by discrete PEC particles. The particle diameter estimated from the image (230 nm) is comparable to that measured for particles in water with dynamic light scattering (250 nm).

In Figure 3.20, emulsion droplets obtained from the aqueous PEC dispersion prepared from 25 g L^{-1} PEL solutions are shown at different magnifications. In this case, the frozen water has been sublimed to better visualize the particles. Polyelectrolyte complexes are seen to be densely packed at the oil-water interface and excess particles form a network in the continuous aqueous phase. This dual location of particles explains the excellent stability of emulsions to both coalescence and creaming. Closer inspection of images at high magnification in Figure 3.20(a) and (b) may indicate that more than one particle layer exists at the droplet interface; however it may be that these thicker layers are those responsible for the bridging between neighboring droplets. The diameter of polyelectrolyte complexes is in the nanometer range.

Figure 3.19. Cryo-SEM images of a dodecane-in-water emulsion ($\phi_o = 0.2$) prepared with an aqueous PEC dispersion ($x_{PSSNa} = 0.47$) from 1 g L^{-1} individual PEL solutions. Columns (a) and (b) show two different areas of the sample at increasing magnifications.

(a)   (b)
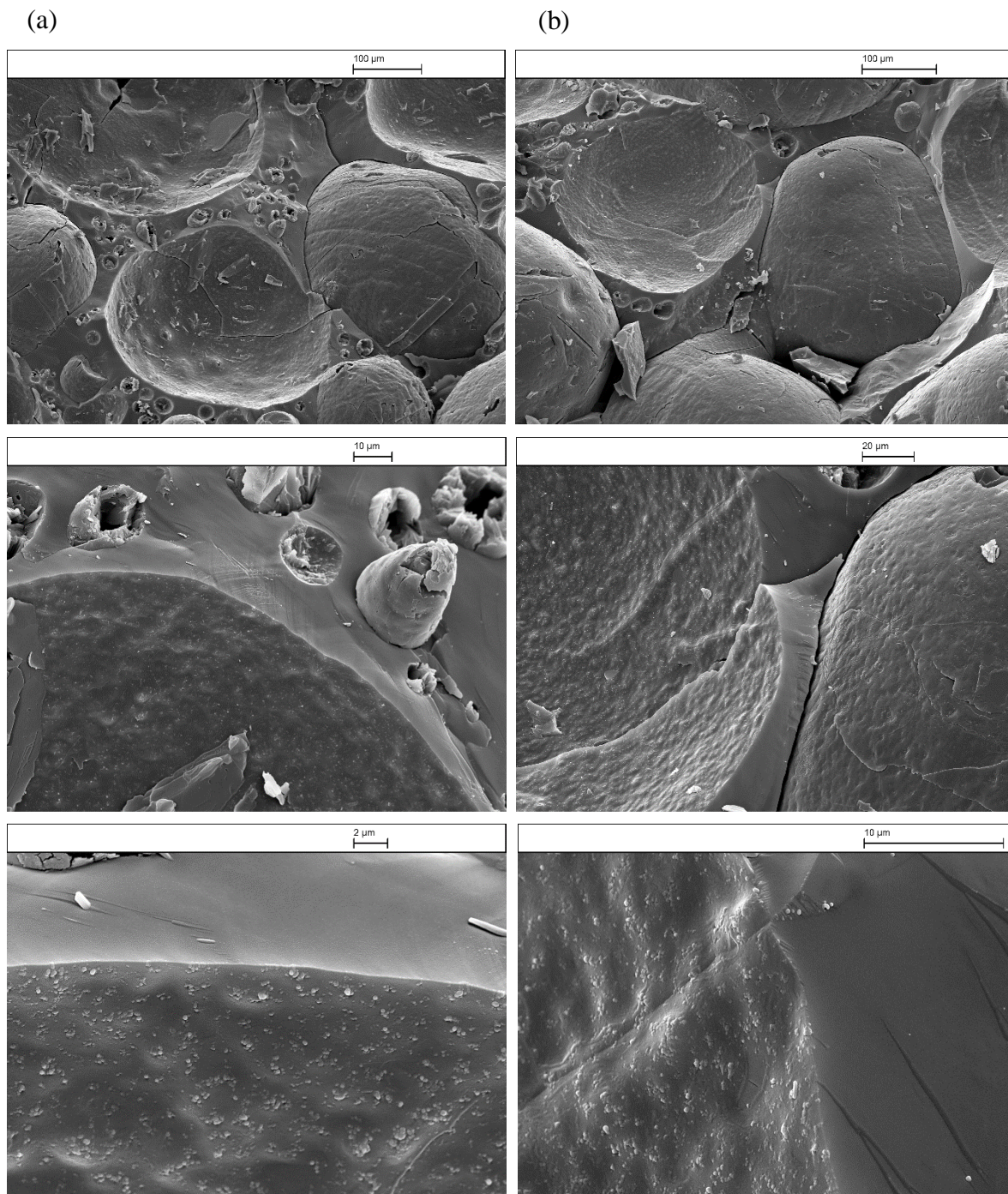
Figure 3.20. Cryo-SEM images of a dodecane-in-water emulsion ($\phi_o = 0.2$) prepared with an aqueous PEC dispersion ($x_{PSSNa} = 0.52$) from 25 g L^{-1} individual PEL solutions. (a) and (b) show a series of images taken from the same area at different magnifications. (c) Detail of the interface of an oil drop in (a) at higher magnification.

(a)

More than one particle layer at the droplet interface
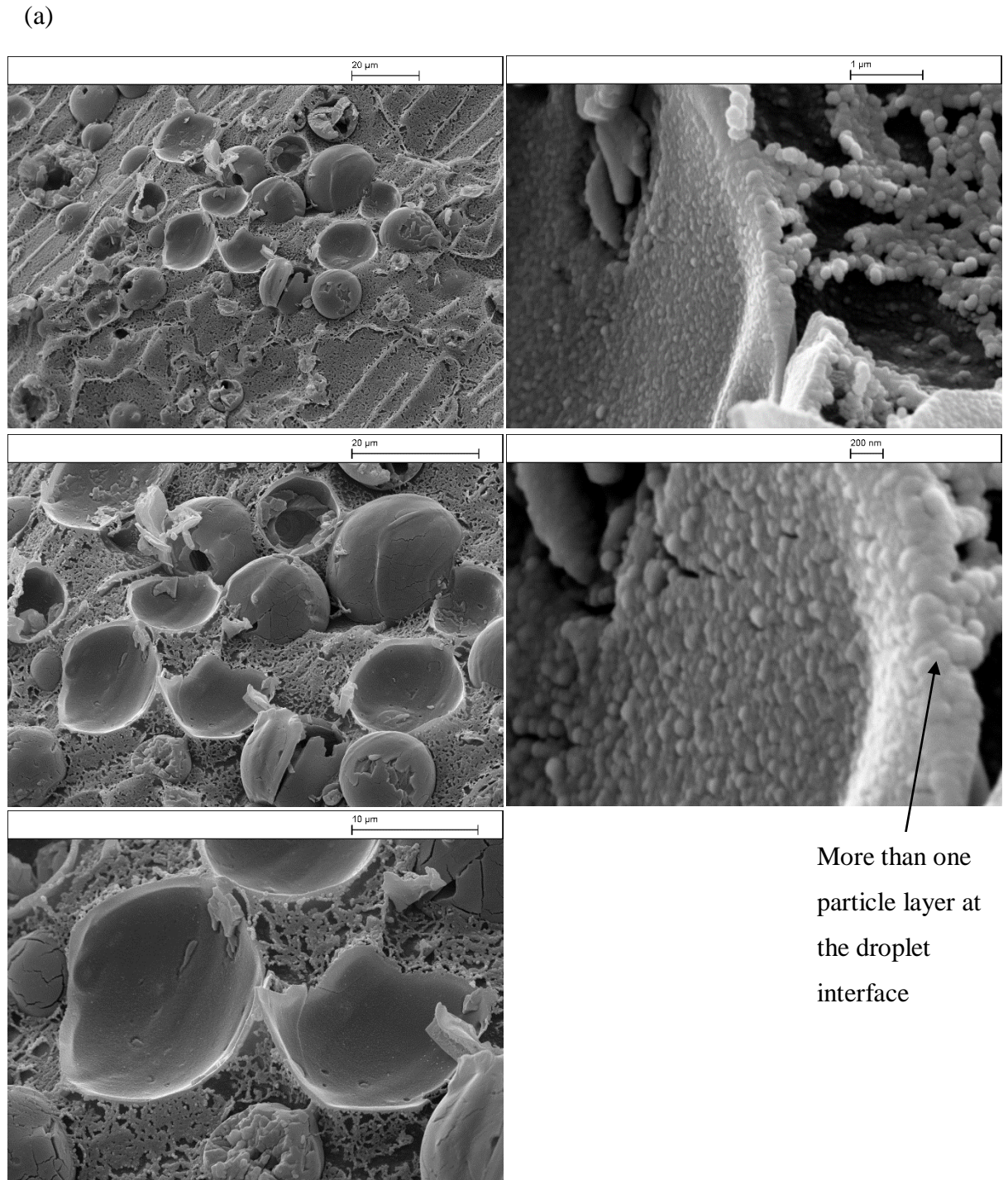
(b)
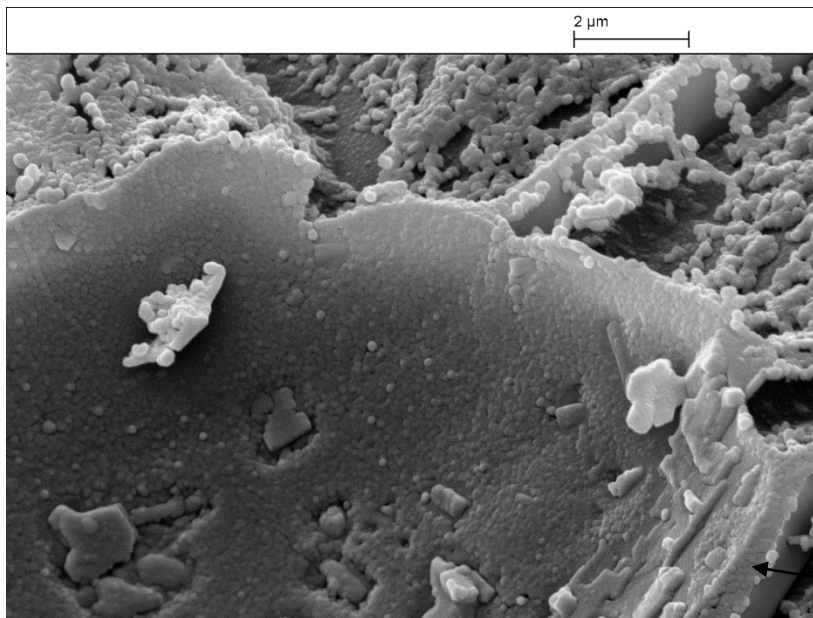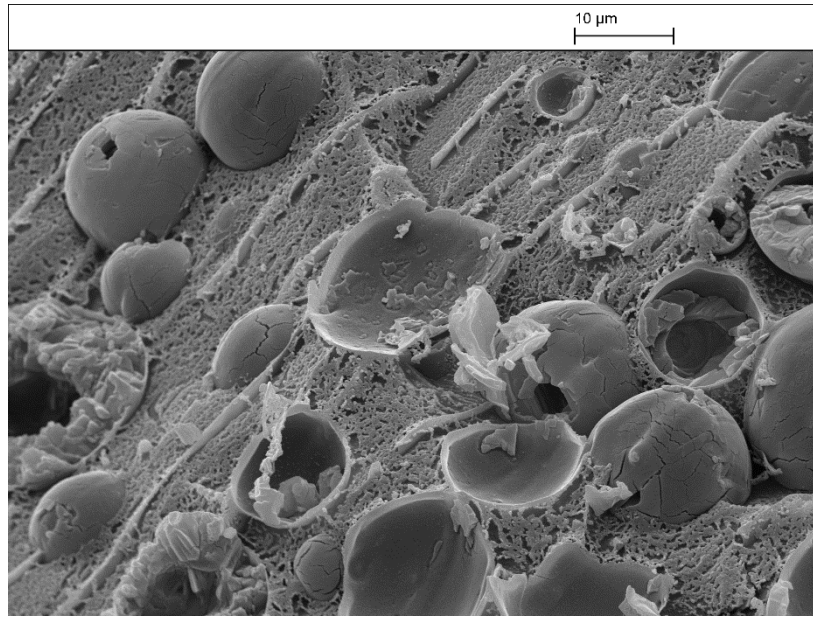
(c)
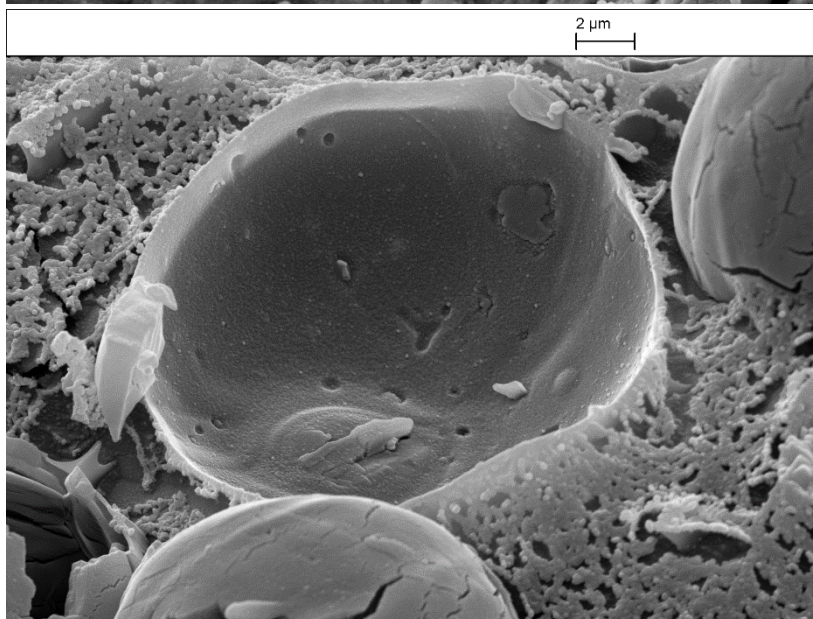
More than one
particle layer at
the droplet
interface

3.3.3 Effect of oil volume fraction on emulsion stability

Catastrophic phase inversion occurs when the emulsion type changes (o/w to w/o or *vice versa*) by varying the oil:water ratio. In order to establish whether catastrophic phase inversion is achievable in this system, the influence of the oil volume fraction (ϕ_o) was studied by fixing both the polyelectrolyte concentration in the final emulsion (8 g L^{-1}) and the value of x_{PSSNa} (0.54).

The appearance of emulsions at ϕ_o between 0.1 and 0.8 is shown in Figure 3.21. Upon increasing ϕ_o, all emulsions are o/w in which the volume of emulsion prepared also increases until all the oil and water mixture becomes emulsified at $\phi_o \geq 0.5$. Emulsions at higher oil fractions ($\phi_o = 0.5$ and 0.6) were noticeably more viscous but completely stable for at least 6 months. The average droplet diameter determined from optical micrographs decreased from 133 ± 32 µm at $\phi_o = 0.1$ to 10 ± 4 µm at $\phi_o = 0.6$. For emulsions prepared with a $\phi_o = 0.7$ and 0.8, the homogenization step could not be carried out properly as the aqueous PEC dispersion was very concentrated in the polyelectrolyte mixture and hence very viscous. Therefore, for this polymer mixture and oil chosen, catastrophic phase inversion cannot be achieved. The preferred emulsion at $\phi_o = 0.5$ being o/w implies that the PEC particles so formed are only partially hydrophobic.

**Figure 3.21.** Appearance of dodecane-in-water emulsions immediately after preparation for different ϕ_o values (given) prepared with aqueous PEC dispersions. [PSSNa] in each emulsion is 8 g L^{-1} and x_{PSSNa} is 0.54. Scale bar = 1 cm.

3.3.4 Effect of salt concentration on emulsion stability

From the dispersions/solutions shown in Figure 3.13, emulsions containing *n*-dodecane ($\phi_o = 0.2$) were prepared by the standard procedure. Their appearance immediately after homogenisation is shown in Figure 3.22. Three different regions can be identified which correlate with the three regions described above for aqueous PEC dispersions. Emulsions prepared with a salt content between 0 M and 0.1 M were o/w and stable to coalescence. Those prepared at [NaCl] between 0.15 M and 3.0 M exhibited complete phase separation as if no polymer mixture was present. Emulsions prepared at salt concentrations greater than 3.5 M were o/w and stable again.

Figure 3.22. Appearance of dodecane-in-water emulsions ($\phi_o = 0.2$) prepared from the dispersions in Figure 3.13. Scale bar = 1 cm.
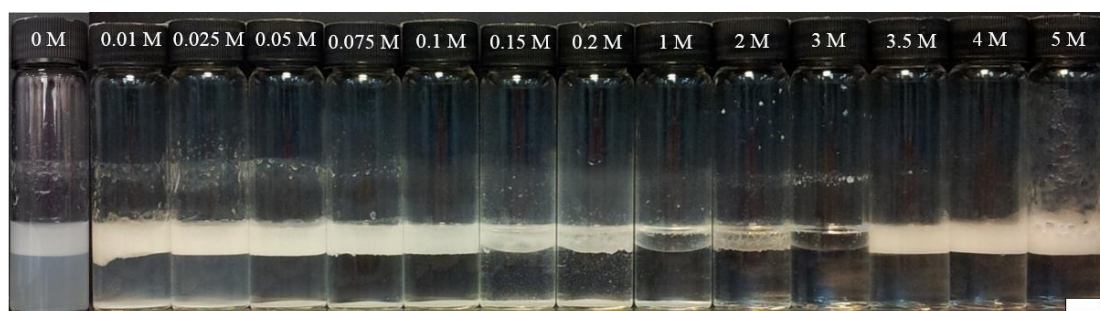
Therefore, emulsions stabilised by PEC particles are stimuli-responsive being destabilised and subsequently re-stabilised by salt addition and their behaviour is closely linked to the properties of the pre-cursor aqueous dispersion/solution. The average droplet diameter was measured from optical micrographs for stable emulsions. By increasing the salt concentration from 0 M to 0.1 M, the droplet diameter increased progressively and at very high ionic strengths the droplet diameter was relatively small as shown in the optical micrographs of Figure 3.23(a). The plot of the average droplet diameter as a function of NaCl concentration is shown in Figure 3.23(b). The increase of the droplet diameter in the first region is related to the aggregation process of particles in water before emulsification. Moreover, the overall PEC concentration decreases due to this aggregation process. In the second region, aggregation levels are exceptionally high. The inability to stabilise any emulsion may be due to a change in the hydrophobicity of the particles following salt addition at this level or to the fact that very large aggregates are easily dislodged from droplet interfaces if they initially adsorb. In the third region, unexpectedly, stable emulsions appear again, this time

stabilised by individual polyelectrolyte molecules. The average droplet diameter for these emulsions (17 µm) was even lower than the one achieved for the initial emulsion with no added salt stabilised by PEC particles (103 µm). Moreover, during emulsification, a volume of foam was created which was not observed for any of the other emulsions. This suggests that polyelectrolyte molecules have become surface-active at this high concentration of salt.

Figure 3.23. (a) Optical microscope images of dodecane-in-water emulsions ($\phi_o = 0.2$) stabilised by PEC particles prepared from 1 g L^{-1} individual PEL solutions at different [NaCl] (from left to right and up to down): 0, 0.025, 0.05, 0.1, 4 and 5 M. (b) Average droplet diameter *versus* [NaCl] for emulsions in Figure 3.22. The curve drawn is only for guidance.

(a)

(b)
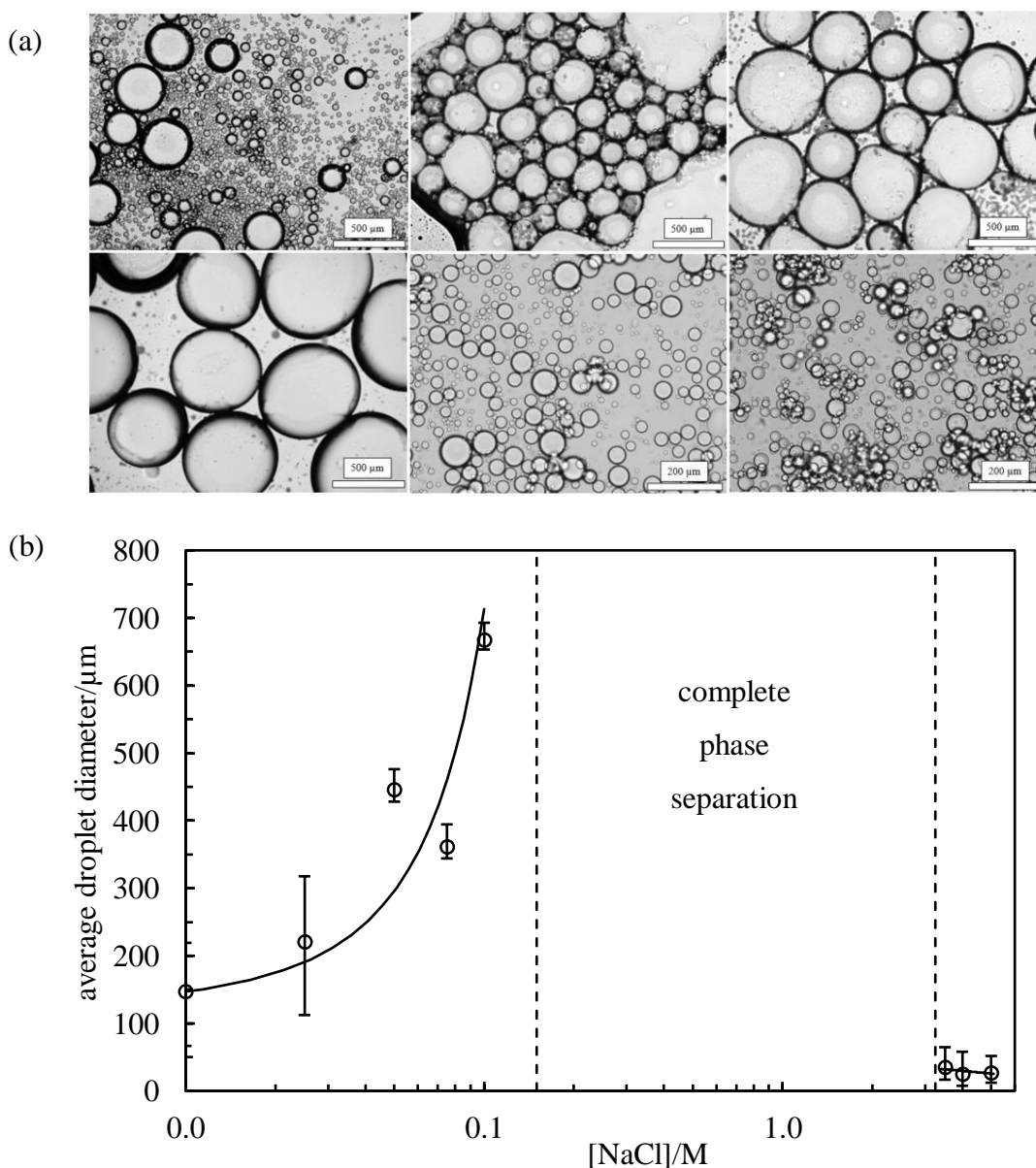
In order to prove this hypothesis, the behaviour of the polyelectrolytes alone dissolved in 5 M NaCl was briefly investigated. In Figure 3.24(a), the appearance of 1 g L^{-1} individual PEL solutions in 5 M NaCl after hand-shaking for 30 s is shown for both polymers. A compact foam was only obtained for PSSNa, implying this polyelectrolyte becomes surface active at the air-water interface. Similarly, the emulsification of both polyelectrolyte solutions with *n*-dodecane ($\phi_o = 0.2$) was attempted with an Ultra-turrax (Figure 3.24(b)). During homogenisation, air bubbles were formed in both cases but were smaller and more compact in the case of PSSNa. For both polymers, a stable o/w emulsion below the foam was formed, confirming their surface activity when alone at the oil-water interface. There is literature reporting that polyelectrolytes at high ionic strength behave as neutral polymers due to the neutralisation of the ionized groups,[28,29] but to the best of our knowledge, no studies are found demonstrating the stabilisation of emulsions in this case.

Figure 3.24. (a) Appearance of 1 g L^{-1} PEL solutions in 5 M NaCl after hand shaking for 30 s for (1) PDADMAC and (2) PSSNa. (b) Appearance of emulsions prepared between *n*-dodecane ($\phi_o = 0.2$) and a 1 g L^{-1} PEL solution after preparation for (1) PDADMAC and (2) PSSNa. Scale bars = 1 cm.
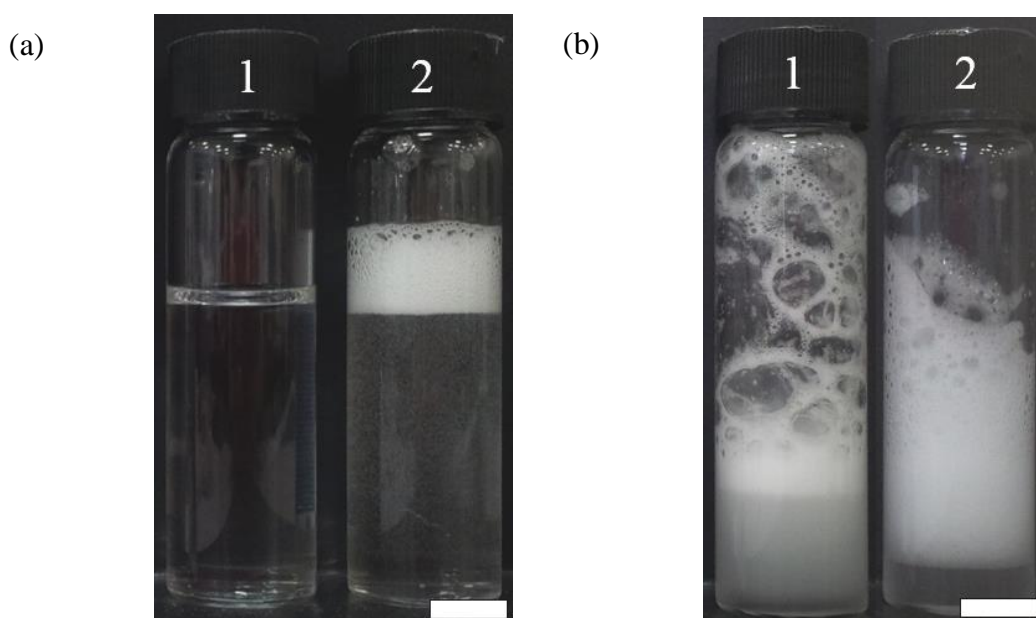
The influence of salt on an already prepared o/w emulsion was also evaluated by adding 1 mL of 5 M NaCl solution to 5 mL of emulsion resulting in an overall salt concentration in the emulsion of 1 M. This final concentration was chosen as complete

phase separation was obtained when salt was added before emulsification. Surprisingly, in this case no phase separation was achieved and the o/w emulsion was stable, although with a larger droplet diameter (163 µm) compared with the emulsion prepared with no added electrolyte (103 µm). The effect of salt is thus not as pronounced if added after emulsification. Here, salt is not only added after PEC formation (compared to earlier) but also after their adsorption to the oil-water interface. It is conceivable that salt ions dissolved outside of droplets may not access all parts of interfacially bound particles but the origin of the difference needs to be probed in a future study.

The influence of pH on both aqueous PEC dispersions and emulsions was also evaluated. Both PSSNa and PDADMAC are strong polyelectrolytes dissociating completely in the entire pH range. The influence of pH would be negligible for each polyelectrolyte alone. However, its influence is very relevant upon complex formation as the ion concentration increases due to addition of HCl or NaOH used to prepare the acid and basic solutions. The behaviour was evaluated at pH 2 and 12 for aqueous PEC dispersions prepared from 1 g L^{-1} individual PEL solutions. Their appearance was similar to those obtained from the polyelectrolyte mixture at unmodified pH (Figure 3.11(a)). The transmittance at $\lambda = 700$ nm decreased from 39.0% for the PEC prepared at natural pH to 26.4% and 32.9% for PEC dispersions prepared at pH 2 and 12, respectively. Therefore, the same effect as the one obtained after salt addition was noticed. Emulsions prepared from these dispersions and *n*-dodecane ($\phi_o = 0.2$) either completely phase separated (pH = 2) or contained much larger droplets (660 µm, pH = 12) compared with that prepared at unmodified pH (103 µm). More work is required to understand the origin of these effects.

3.3.5 *Variation of oil type*

The study until now has been carried out with a non-polar alkane which has no groups to modify the surface properties of PEC particles. In order to establish how generic this novel emulsion stabilisation mechanism is, emulsions were prepared from aqueous PEC dispersions from 50 g L^{-1} individual PEL solutions ($x_{PSSNa} \approx 0.5$) and different oils. Their appearance and optical microscope images are given in Figure 3.25 for a long chain alkane, an ester, an aromatic oil, a silicone oil and a commercial paraffin. In all cases, o/w emulsions stable to coalescence were obtained. The average

drop diameter was approx. 20 µm for all oils except toluene for which it was ≈ 60 µm. It has also been verified that emulsions with the different oils containing each polyelectrolyte alone (10 and 25 g L^{-1}) exhibited complete phase separation, confirming that PEL are not surface-active alone (Figure 3.25(b)).

Figure 3.25. (a) Appearance of o/w emulsions of an aqueous PEC dispersion (x_{PSSNa} ≈ 0.5, [PEL] = 50 g L^{-1}) and different oils (ϕ_o = 0.2) three months after preparation. (1) squalane, (2) isopropyl myristate, (3) toluene, (4) 50 cS PDMS and (5) paraffin oil. (b) Emulsions prepared with 25 g L^{-1} individual PEL solutions (except from those prepared with toluene (10 g L^{-1})). Images taken 1 day after preparation. (c) Corresponding optical micrographs for emulsions in (a).
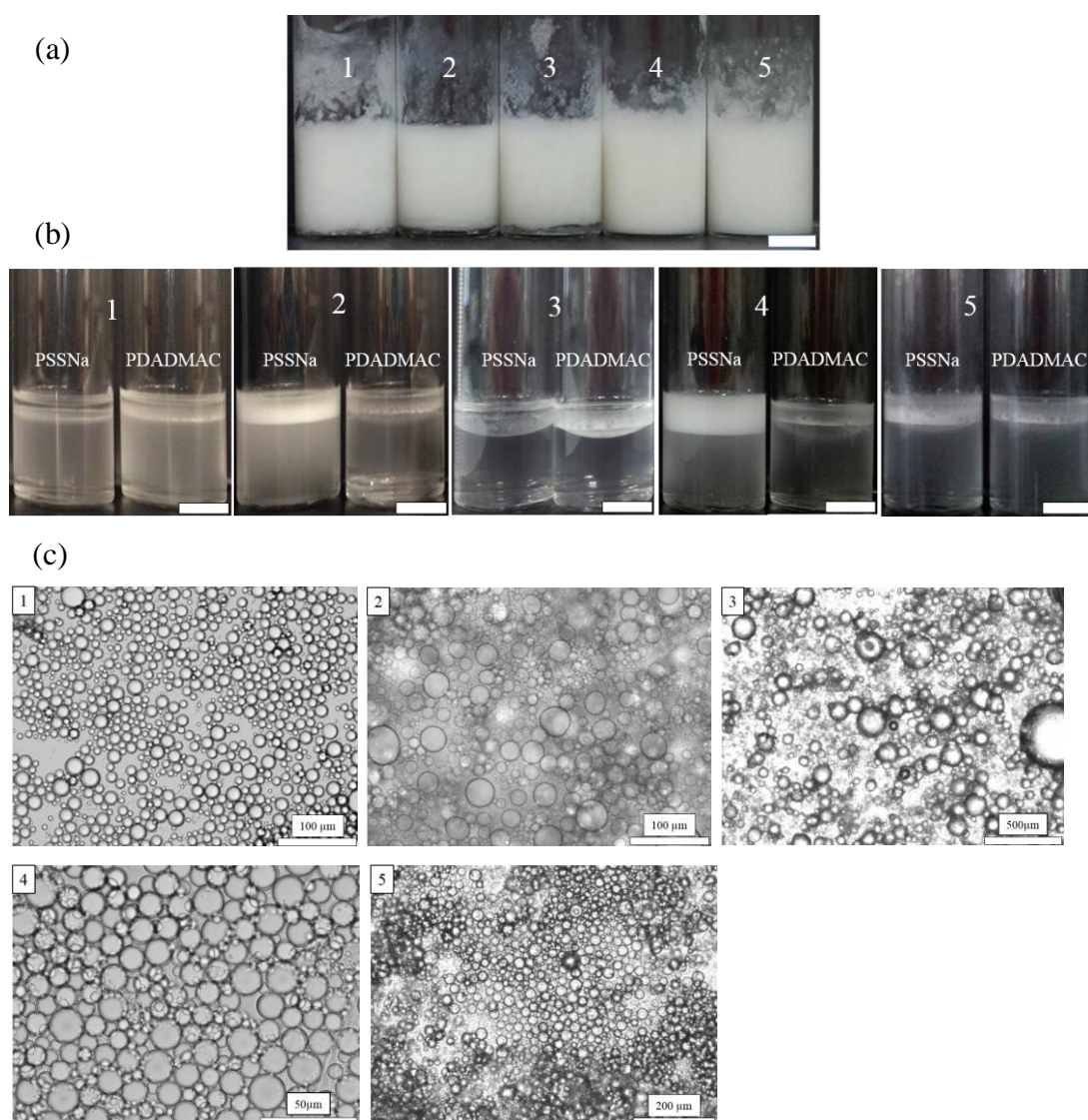
3.3.6 *Behaviour at air-water and oil-water planar interfaces*

Finally, in the light of emulsion stabilisation by PEC particles, their surface activity at planar air-water and oil-water interfaces *via* interfacial tension measurements was investigated.

Aqueous PEC dispersions varying in x_{PSSNa} from 0 to 1 obtained from 0.5 g L^{-1} PEL solutions were prepared. As shown in Figure 3.26(a), the air-water surface tension of all dispersions and solutions, including the ones in which polyelectrolytes alone are present, is 72.0 ± 0.4 mN m^{-1} representing no reduction compared to that for pure water. The surface tension for an aqueous PEC dispersion at higher concentration ($x_{PSSNa} = 0.53$, [PEL] = 1 g L^{-1}) was also 72.0 ± 0.5 mN m^{-1}. The PEL and PEC do not therefore lower the tension of the air-water surface, as shown earlier for sodium polyacrylate.[30]

Likewise, the dodecane-water interfacial tension was measured for aqueous PEC dispersions prepared from 1 g L^{-1} PEL solutions at different x_{PSSNa}, Figure 3.26(b). In the absence of polymer, the interfacial tension of 52.6 ± 0.2 mN m^{-1} is in agreement with the value reported in ref. 31 of 52.5 mN m^{-1} confirming the absence of surface-active impurities. Here however, all polymer-containing dispersions/solutions exhibit a lower tension than the bare interface and the tension passes through a shallow minimum at intermediate values of x_{PSSNa}. The maximum lowering however is only *ca.* 10 mN m^{-1} compared with low molar mass surfactant systems which typically lower interfacial tensions to *ca.* 1-5 mN m^{-1} above their critical micelle concentration.[32]

As with emulsions stabilised by hard particles, the reduction of the interfacial tension is not the operative mechanism. Further, these may not be equilibrium tensions as an energy barrier to adsorption of PEC particles may not be surmounted in the absence of stirring. The findings are in line with those of several authors interested in adsorption of particles from bulk water. Drelich *et al.*[33] found that the paraffin oil-water tension in the presence of hydrophobic fumed silica particles was not significantly different from the value obtained without particles. Similar results were obtained by Vignati *et al.*[34] with silanized silica particles at isooctane or octanol-water interfaces. Even though particles strongly adhered to the interface of emulsion drops, no reduction of the interfacial tension was detected. Aveyard *et al.*[35] found that

polystyrene latex particles spontaneously adhere to the octane-water interface, lowering its tension by approximately 4 mN m^{-1}. Importantly, only when spread monolayers of particles are compressed and particles in close proximity exhibit mutual repulsion, does the interfacial tension reach very low values (< 2 mN m^{-1}). Thus, the modest lowering mentioned above for adsorbed films does not imply that PEC particles are surface-inactive at the oil-water interface.

Figure 3.26. (a) Air-water surface tension *versus* x_{PSSNa} for aqueous PEC dispersions prepared from 0.5 g L^{-1} individual PEL solutions; dashed line is bare surface. (b) Dodecane-water interfacial tension *versus* x_{PSSNa} for aqueous PEC dispersions prepared from 1 g L^{-1} individual PEL solutions; dashed line is bare interface.
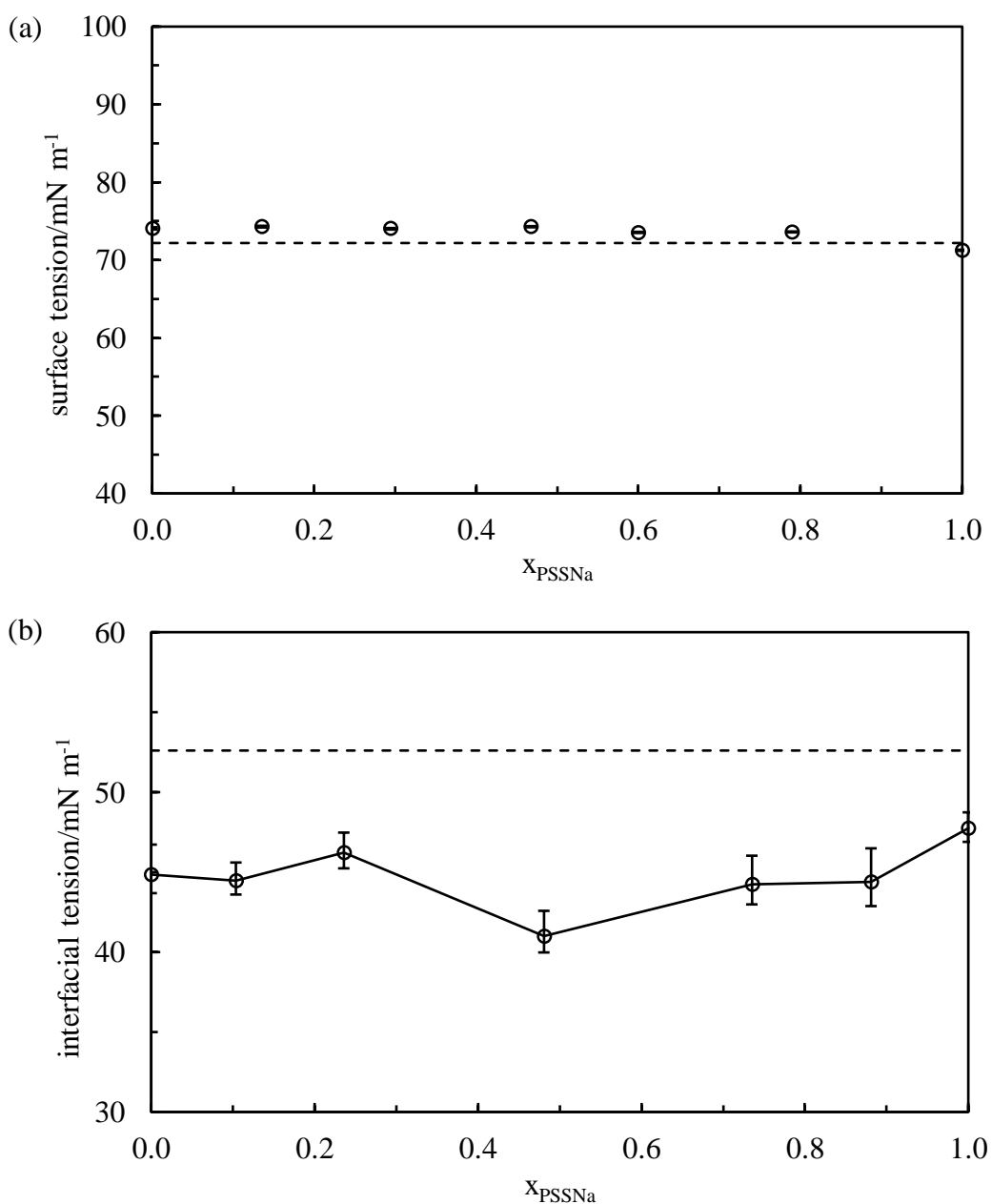
3.4 Conclusions

The use of polyelectrolyte complexes as novel oil-water emulsion stabilisers using relatively monodisperse polyelectrolytes of PSSNa and PDADMAC of similar molecular weight has been demonstrated. The anionic and cationic polyelectrolytes alone are not emulsifiers as complete phase separation occurred immediately after mixing. The polyelectrolyte complex formed in mixtures through electrostatic interactions yields particles of between 100 and 200 nm in diameter depending on the ratio of polymers.

Oil-in-water emulsions for a range of oils at different oil:water ratios can be prepared exhibiting exceptional resistance to coalescence. The most stable emulsion to both creaming and coalescence is formed at around equal mole fraction of the two polymers, and it possesses the smallest drop diameter. The average drop diameter could be tuned depending on the initial polyelectrolyte concentrations used to prepare aqueous PEC dispersions. From cryo-SEM images particles are found to be located at the oil-water interface of emulsion drops. Their distribution is not uniform at low polyelectrolyte concentrations, whereas at high concentrations a close-packed layer of particles covers the interfaces and excess particles aggregate in water enhancing emulsion stability.

The addition of increasing concentrations of salt to aqueous particle dispersions causes a transition from stable dispersions to aggregated and unstable dispersions and finally to dissolution of the particles of complex yielding solutions of individual polymer molecules. The corresponding emulsions are initially destabilized completely at intermediate salt concentrations but, at high salt concentrations, emulsions are re-stabilised in this case by adsorbed polymer molecules.

Reduction of the oil-water interfacial tension with PEC has not been detected *via* interfacial tension measurements, which implies that the homogenization step is essential to promote the particles to the interface.

3.5 References

1. M.W. Beijerinck, *Zentbl. Bakteriolog. P.*, 1896, **2**, 697-699.

2. A.K. Ghosh and P. Bandyopadhyay, in *The Complex World of Polysaccharides*, ed. D.N. Karunaratne, InTech, Rijeka, 2012, pp. 395-408.

3. A. Benichou, A. Aserin and N. Garti, *J. Dispersion Sci. Technol.*, 2002, **23**, 93-123.

4. L. Jourdain, M.E. Leser, C. Schmitt, M. Michel and E. Dickinson, *Food Hydrocolloids*, 2008, **22**, 647-659.

5. A.K. Stone and M.T. Nickerson, *Food Hydrocolloids*, 2012, **27**, 271-277.

6. K.G. Zinoviadou, E. Scholten, T. Moschakis and C.G. Biliaderis, *Int. Dairy J.*, 2012, **26**, 94-101.

7. M. Mende, H. Buchhammer, S. Schwarz, G. Petzold and W. Jaeger, *Macromol. Symp.*, 2004, **211**, 121-133.

8. H. Dautzenberg. *Macromolecules,* 1997, **30**, 7810-7815.

9. M. Sotiropoulou, C. Cincu, G. Bokias and G. Staikos, *Polymer*, 2004, **45**, 1563-1568.

10. A. Matralis, M. Sotiropoulou, G. Bokias and G. Staikos, *Macromol. Chem. Phys.*, 2006, **207**, 1018-1025.

11. L. Gärdlund, L. Wågberg and M. Norgren, *J. Colloid Interface Sci.*, 2007, **312,** 237-246.

12. M. Mende, G. Petzold and H. Buchhammer, *Colloid Polym. Sci.*, 2002, **280**, 342-351.

13. M. Müller, *Adv. Polym. Sci.*, 2014, **256**, 197-260.

14. C. Schatz, A. Domard, C. Viton, C. Pichot and T. Delair, *Biomacromolecules*, 2004, **5**, 1882-1892.

15. M.A. Wolfert and L.W. Seymour, *Gene Ther.*, 1996, **3**, 269-273.

16. Y. Hu, T. Yang and X. Hu, *Polym. Bull.*, 2012, **68**, 1183-1199.

17. C. Ankerfors, S. Ondaral, L. Wågberg and L. Ödberg, *J. Colloid Interface Sci.*, 2010, **351**, 88-95.

18. V. Starchenko, M. Müller and N. Lebovka, *J. Phys. Chem. B*, 2012, **116**, 14961-14967.

19. H. Dautzenberg, in *Physical Chemistry of Polyelectrolytes*, ed. T. Radeva, Vol. 99, Surfactant science series, Marcel Dekker, New York, 2001.

20. Y. Zhang, E. Yildirim, H.S. Antila, L.D. Valenzuela, M. Sammalkorpi and J.L. Lutkenhaus, *Soft Matter*, 2015, **11**, 7392-7401.

21. B.P. Binks, W. Liu and J.A. Rodrigues, *Langmuir*, 2008, **24**, 4443-4446.

22. T. Nallamilli, B.P. Binks, E. Mani and M.G. Basavaraj, *Langmuir*, 2015, **31**, 11200-11208.

23. S. Tcholakova, N.D. Denkov and A. Lips, *Phys. Chem. Chem. Phys.*, 2008, **10**, 1608-1627.

24. S. Arditty, C.P. Whitby, B.P. Binks, V. Schmitt and F. Leal-Calderon, *Eur. Phys. J. E*, 2003, **11**, 273-281.

25. M. Destribats, M. Rouvet, C. Gehin-Delval, C. Schmitt and B.P. Binks, *Soft Matter*, 2014, **10**, 6941-6954.

26. P.B. Kowalczuk, J. Drzymala, *Part. Sci. Technol.*, 2016, **34**, 645-647.

27. C. Joseph, R. Savoire, C. Harscoat-Schiavo, D. Pintori, J. Monteil, F. Leal-Calderon and C. Faure, *Food Res. Int.*, 2018, in press.

28. P. Walstra, *Physical Chemistry of Foods*, Marcel Dekker, 2001, New York, p. 178.

29. *Polysaccharides. Structural Diversity and Functional Versatility*, ed. S. Dumitriu, 2nd edn., Marcel Dekker, 2004, New York.

30. T. Okubo, *J. Colloid Interface Sci.*, 1988, **125**, 386-398.

31. S. Zeppieri, J. Rodríguez, and A.L. López de Ramos, *J. Chem. Eng. Data*, 2001, **46**, 1086-1088.

32. R. Aveyard, B.P. Binks and J. Mead, *J. Chem. Soc., Faraday Trans. 1*, 1987, **83**, 2347-2357.

33. A. Drelich, F. Gomez, D. Clausse and I. Pezron, *Colloids Surf. A*, 2010, **365**, 171-177.

34. E. Vignati, R. Piazza and T.P. Lockhart, *Langmuir*, 2003, **19**, 6650-6656.

35. R. Aveyard, J.H. Clint, D. Nees and N. Quirke, *Langmuir*, 2000, **16**, 8820-8828.

CHAPTER 4 – MIXTURE OF STRONG CATIONIC, PDADMAC, AND WEAK ANIONIC, PAANa, POLYELECTROLYTES

4.1 Introduction

In this chapter, both aqueous PEC dispersions and emulsion stabilisation with a different system of water-soluble polymers constituted by a strong (PDADMAC) and a weak (PAANa) polyelectrolyte are studied in detail in an attempt to establish the general pattern of behaviour. For this system, unlike the one discussed in Chapter 3, the effect of pH is an important consideration as PAANa will be uncharged at low pH and fully charged at high pH. As a result, this will have an impact on the strength of the interaction with the oppositely charged polymer.

The behaviour of aqueous mixtures of the two polymers at different pH and mole fraction of the anionic polyelectrolyte was first investigated. There is no other study in the literature reporting the behaviour over a wide range of pH (2-10). The size and charge of the obtained complexes are measured and the type of associative phase separation (precipitation and complex coacervation) is carefully appraised. Both solid precipitates and coacervate droplets form along the studied pH range, while for the case of two strong PEL (Chapter 3) only precipitates were detected. Moreover, despite expecting this system at high pH to behave like that of two strong PEL, coacervate droplets are preferred instead of precipitates.

Emulsions stabilised by coacervate droplets are then prepared from aqueous polymer mixtures at pH = 10 and oil and their stability and the arrangement of the complexes around drops is evaluated. Emulsions prepared with PEC precipitates are not stable however probably due to their large size, their relatively low amount or their inherent hydrophilicity. Finally, a method to determine the surface energy of the coacervate phase is described. To conclude, calculations of the three spreading coefficients for systems containing water, coacervate and various oils requiring measurement of the interfacial tension between the coacervate phase and water are given to predict the equilibrium configuration between the three phases. These are compared with the configuration established by experiment.

4.2 Microencapsulation with complex coacervation

4.2.1 Determination of spreading coefficients

One of the most important applications of complex coacervation is in microencapsulation.[1] In this process, a substance (also called core material) which can be liquid or solid in nature, is encapsulated within a layer of coacervate phase.[2] Thus, oil drops or solid particles in water may be coated with this phase. For the encapsulation to be successful the adsorption of the complex onto the core material and its wettability are key parameters to consider.[3] The complex coacervate has to spread spontaneously over the surface of dispersed liquid droplets or particles and coat them to form a capsule.[4] This ability can be assessed by consideration of the relevant spreading coefficients (S). The spreading coefficient measures the ability of one liquid to spontaneously spread across another and it is defined as the difference between the surface energy (per unit area) before and after spreading occurs.[5] At the same time the surface tension is the energy required to create unit area of surface. Therefore, for the three-phase system under study (oil, water, coacervate phase) depicted in Figure 4.1, three spreading coefficients can be defined by determining the interfacial tensions between different pairs of the three phases involved.

Figure 4.1. Schematic representation of the three-phase system: oil (o), water (w) and coacervate phase (c).
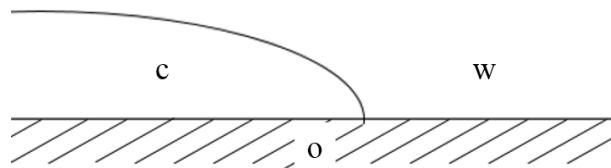
As a result, the spreading of the coacervate phase onto the oil phase in water can be written as,

$$S_c = \gamma_{ow} - (\gamma_{oc} + \gamma_{wc}) \tag{4.1}$$

The first term in equation 4.1 (γ_{ow}) represents the energy per unit area of the original system, prior to the spreading of the coacervate phase. The negative term ($\gamma_{oc} + \gamma_{wc}$) denotes the energy per unit area of the new system, where two new interfaces have been created. Therefore, if $S < 0$, the new surface energy is higher than the initial one

and partial wetting occurs. On the other hand, if $S > 0$, the coacervate covers the total surface forming a film (total wetting).

As it is a three-phase system, the spreading of the other phases must also be considered. Hence, for the system under study three spreading coefficients can be defined,

$$S_o = \gamma_{wc} - (\gamma_{ow} + \gamma_{oc}) \tag{4.2}$$

$$S_w = \gamma_{oc} - (\gamma_{ow} + \gamma_{wc}) \tag{4.3}$$

$$S_c = \gamma_{ow} - (\gamma_{oc} + \gamma_{wc}) \tag{4.4}$$

Low interfacial tensions between the coacervate phase and the coexisting supernatant phase are reported in the literature.[6-8] Therefore, if we assume that $\gamma_{wc} < \gamma_{ow}$, then S_o is always negative and only three possible combinations of the spreading coefficients arise depending on the relative magnitudes of S_w and S_c.[9] As a result, different equilibrium morphologies (complete engulfing, partial engulfing or non-engulfing) can be predicted, as first described by Torza and Mason and represented in Figure 4.2.[9]

Figure 4.2. Schematic diagram showing the three possible configurations: (a) complete engulfing, (b) partial engulfing and (c) non-engulfing, corresponding to the three sets of relations for S (given). o, w and c represents the oil, water and coacervate phase, respectively. Redrawn from ref. 9.

(a) Complete engulfing	(b) Partial engulfing	(c) Non-engulfing
$S_o < 0, \ S_w < 0, \ S_c > 0$	$S_o < 0, \ S_w < 0, \ S_c < 0$	$S_o < 0, \ S_w > 0, \ S_c < 0$
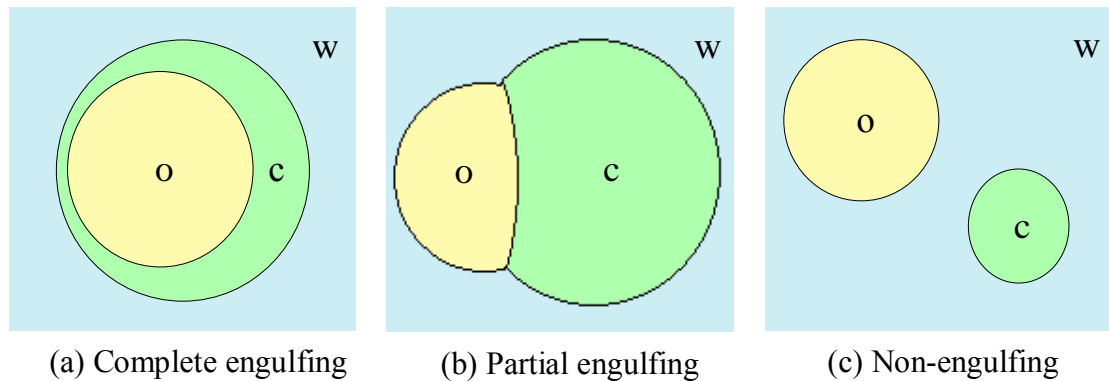
Several studies have determined the various spreading coefficients to evaluate the different capsule morphologies.[10,11] Loxley and Vincent worked with a three-phase system composed by oil, water and poly(methylmethacrylate) and spreading coefficients were calculated to account for the morphologies observed.[10] They

117

measured interfacial tensions between core oils and aqueous solutions with a tensiometer and the du Noüy ring method. Interfacial tensions between the polymer and the different liquid phases (oil and aqueous solutions) were measured from the contact angle that each liquid made against a dry film of the polymer deposited on a clean glass slide. Then, from those values the three spreading coefficients were calculated.[10] This procedure can be applied to our three-phase system (oil, water, coacervate phase) depicted in Figure 4.1. γ_{ow} can be measured with the tensiometer and the du Noüy ring method while γ_{oc} and γ_{wc} can be found by applying Young's equation with previous knowledge of the contact angle that each liquid (oil and water) makes against a dry film of the coacervate phase deposited on a glass slide. To fully understand the role of Young's equation in order to elucidate the unknown interfacial tensions (γ_{oc} and γ_{wc}), a brief explanation is given below.

When a drop of liquid is placed on a solid surface in the presence of another fluid (gas or liquid) (Figure 4.3), the equilibrium three-phase contact angle that arises (θ) is determined as a function of the three interfacial tensions as stated by Young's equation,

$$\gamma_{SG} = \gamma_{SL} + \gamma_{LG} \cos \theta \qquad (4.5)$$

where γ is the interfacial tension and the subscripts S, G and L refer to the solid, gas and liquid phase, respectively. The contact angle (θ) is the angle formed between the solid surface and the tangent to the liquid surface at the line of contact with the solid. This equation is valid only for smooth, chemically homogeneous, impermeable and non-deformable surfaces.[5]

Figure 4.3. Three-phase contact line of a drop of liquid wetted to a solid surface in a gas phase.
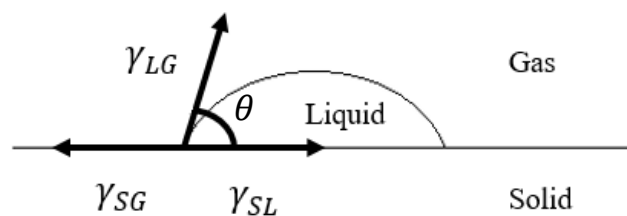
Therefore, for our three-phase system, the phases in Figure 4.3 can be relabelled (Figure 4.4). The adapted Young's equations for each system, (a) and (b), are shown in equations 4.6 and 4.7, respectively.

Figure 4.4. Three-phase contact angle of the system (a) air-water-coacervate and (b) air-oil-coacervate.
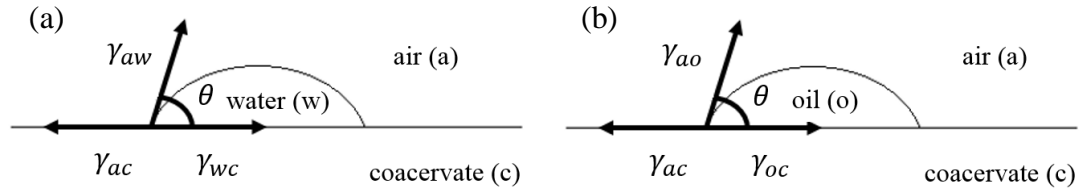
From equations 4.6 and 4.7, γ_{wc} and γ_{oc} are the unknowns. γ_{aw} and γ_{ao} are the water and the oil surface tensions, respectively, which can be measured with the tensiometer and the du Noüy ring method. The contact angles θ_{aw} and θ_{ao} are measured by placing a drop of water or oil in air onto a glass slide coated by the coacervate phase. Finally, γ_{ac} is the surface energy of the coacervate and can be found in the literature for specific systems. Otherwise, it can be estimated by indirect methods which are based on the nature of the interaction between the liquids and the solid surface. The surface energy (γ) is commonly decomposed into its polar (γ^p) and dispersive (γ^d) components (equation 4.8).[12-14] The polar component comprises interactions such as hydrogen bonding whilst the dispersive component comes from van der Waals forces between the molecules of the material.

$$\gamma = \gamma^p + \gamma^d \tag{4.8}$$

The interfacial tension between a solid and a liquid phase (γ_{SL}) can be expressed in terms of the two components (dispersive and polar) for each phase as given by equation 4.9,[15]

$$\gamma_{SL} = \gamma_{SG} + \gamma_{LG} - 2\left(\sqrt{\gamma_{SG}^d \gamma_{LG}^d} + \sqrt{\gamma_{SG}^p \gamma_{LG}^p}\right) \tag{4.9}$$

By combining equation 4.9 with Young's equation (equation 4.5), the following relationship is encountered,

$$\gamma_{SG} - \gamma_{LG} \cos \theta_{LG} = \gamma_{SG} + \gamma_{LG} - 2\left(\sqrt{\gamma_{SG}^d \gamma_{LG}^d} + \sqrt{\gamma_{SG}^p \gamma_{LG}^p}\right) \tag{4.10}$$

After rearranging equation 4.10, a final expression is found,

$$\frac{1}{2}\gamma_{LG}(1 + \cos\theta_{LG}) = \sqrt{\gamma_{SG}^d\gamma_{LG}^d} + \sqrt{\gamma_{SG}^p\gamma_{LG}^p} \tag{4.11}$$

For consistency with the nomenclature of the system under study, the subscripts L, G and S in equation 4.11 are replaced by liquid (l), air (a) and coacervate (c), respectively (equation 4.12),

$$\frac{1}{2}\gamma_{al}(1 + \cos\theta_{al}) = \sqrt{\gamma_{al}^d\gamma_{ac}^d} + \sqrt{\gamma_{al}^p\gamma_{ac}^p} \tag{4.12}$$

The two unknowns in this modified equation are γ_{ac}^d and γ_{ac}^p and can be determined by solving simultaneously two versions of equation 4.12 with two liquids of different polarity. However, it is advisable to consider more than two liquids.[16,17] The values of $\cos\theta_{al}$ of the probe liquids can be measured with a drop shape analysis (DSA) apparatus by obtaining the profile of a liquid droplet on a coated glass slide with the coacervate phase. Values of γ_{al}^d and γ_{al}^p for the different test liquids can be easily found in the literature. After solving the equation for all the possible combinations of probe liquids, a least-squares calculation is carried out to determine the best combination of γ_{ac}^d and γ_{ac}^p that fit all the oils simultaneously. A 3-D surface energy diagram can be obtained by plotting the goodness of fit to contact angle against a set of possible values of γ_{ac}^d and γ_{ac}^p. From the coordinates that define the position of the peak in the chart, the values of γ_{ac}^d and γ_{ac}^p that best fit all the contact angles can be read.[16,17] As a result the value of γ_{ac} can be obtained and therefore the values of γ_{wc} and γ_{oc} in equations 4.6 and 4.7. With all these tensions, spreading coefficients in equations 4.2 to 4.4 can be calculated.

4.3 Potentiometric titration of PAANa and degree of ionisation

Since PDADMAC is a strong polybase, it is fully ionised at all pH. On the contrary, PAANa is a weak polyacid. Therefore, its degree of ionisation varies with pH. A potentiometric titration of a 1 g L^{-1} PAANa solution was carried out in triplicate to determine the degree of ionisation as a function of pH and consequently the pK_a of the polyacid (Figure 4.5). The black line that connects the filled points corresponds to the derivative of the pH as a function of the volume of titrating agent (dpH/dV). In this case, two jumps were observed during the titration, in agreement with the data reported in the literature.[18,19] The one at low pH corresponds to the titration of the hydroxide ions coming from the NaOH used to increase the pH of the solution (the natural pH of the solution at the concentration stated above was 9.7). The distance between the two maxima corresponds to the titration of the polyacid. The inset plot in Figure 4.5 displays the curve of the degree of ionisation against the pH and it is obtained from the data of the titration curve. In order to do so, PAA is considered to be fully ionised (degree of ionisation = 100%) at pH = 9.80 and fully protonated (degree of ionisation = 0%) at pH = 4.25. These two values correspond to the pH where the inflection points take place. Intermediate points at different degrees of ionisation were selected and interpolated in the titration curve to build the full ionisation curve.

The pK_a value for this sample of PAANa was found to be 6.6, in reasonable agreement with the literature whose values range from 5.5 to 6.8.[20,21] It is worth noting the increased pK_a of a polyacid compared to the value of a low molecular weight analogue (pK_a = 4.2). The behaviour of weak polyelectrolytes upon increasing or decreasing the charge density is not equivalent to the case of low molecular weight electrolytes. In a polyelectrolyte, not all the counterions will dissociate from the polymer chain. In fact, as the magnitude of the charge on the chain increases (by dissociation), it becomes progressively more difficult to remove the next proton due to the close proximity of charged groups.[22] When the polyelectrolyte is strongly charged, some of the counterions remain bound to the polymer chain due to the large electrostatic potential on the chain, thereby reducing the effective charge of the polyion. This is known as counterion condensation and is described by Manning's theory.[23]

Figure 4.5. Potentiometric titration of a 1 g L^{-1} PAANa solution against 0.1 M HCl solution (open points). The pH of the initial PAANa solution was increased to ≈ 11.5 with NaOH to evaluate the full pH range. The curve that connects the filled points corresponds to the derivative of the pH as a function of the volume of titrating agent (dpH/dV). Inset plot: degree of ionisation *versus* pH obtained from the titration curve.
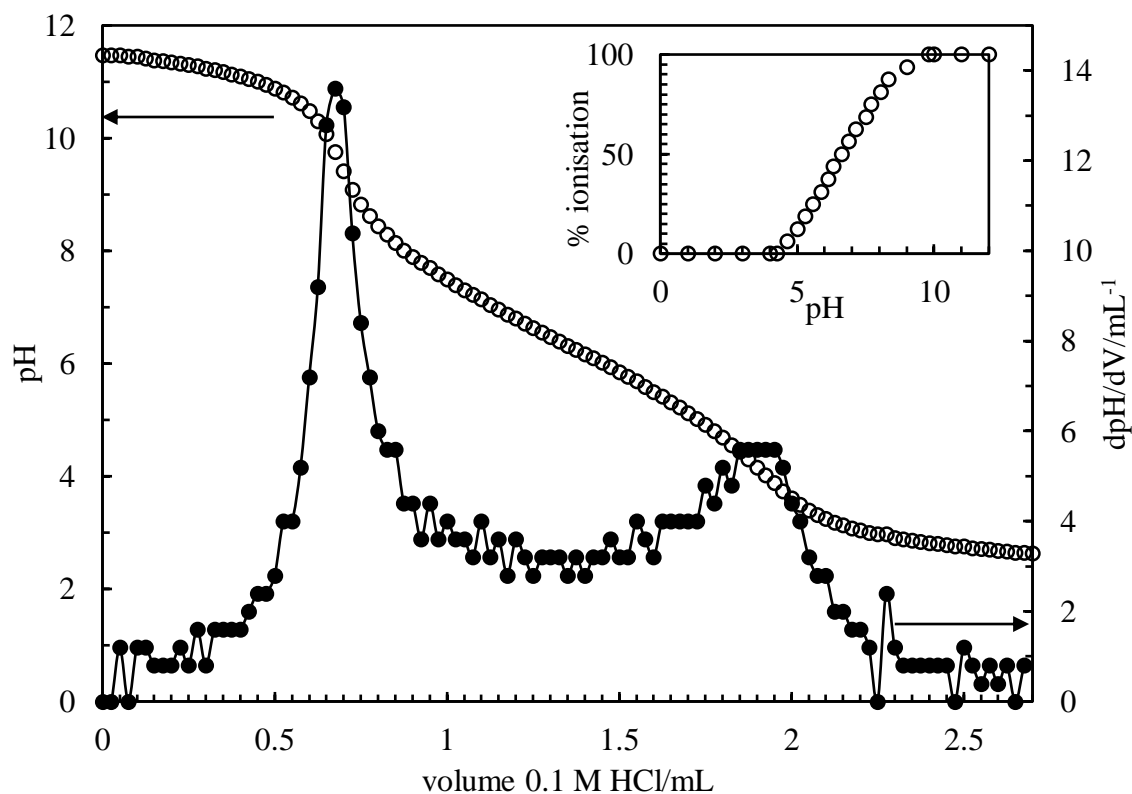

4.4 Characterisation of aqueous PEC dispersions at different pH

4.4.1 Dispersions at low PEL concentration

As shown above, the pH is a key parameter to consider in the study of PEC formation in this polyelectrolyte mixture. Aqueous PEC dispersions at low concentration were first characterised in terms of their average diameter and zeta potential. The appearance of aqueous PEC dispersions prepared from 0.1 g L^{-1} PEL solutions at different x_{PAANa} and pH is shown in Figure 4.6. Here, x refers to the mole fraction using the values of M_w given in Table 2.1 (131.2 kDa for PAANa and 174 kDa for PDADMAC). In general, all aqueous PEC dispersions and solutions of the neat polymers are transparent and colourless. However, some mixtures at specific x_{PAANa} are bluish or show signs of precipitation.

Figure 4.6. Appearance of freshly prepared aqueous PEC dispersions from 0.1 g L^{-1} individual PEL solutions at different x_{PAANa} (given) and pH. Scale bar = 1 cm.
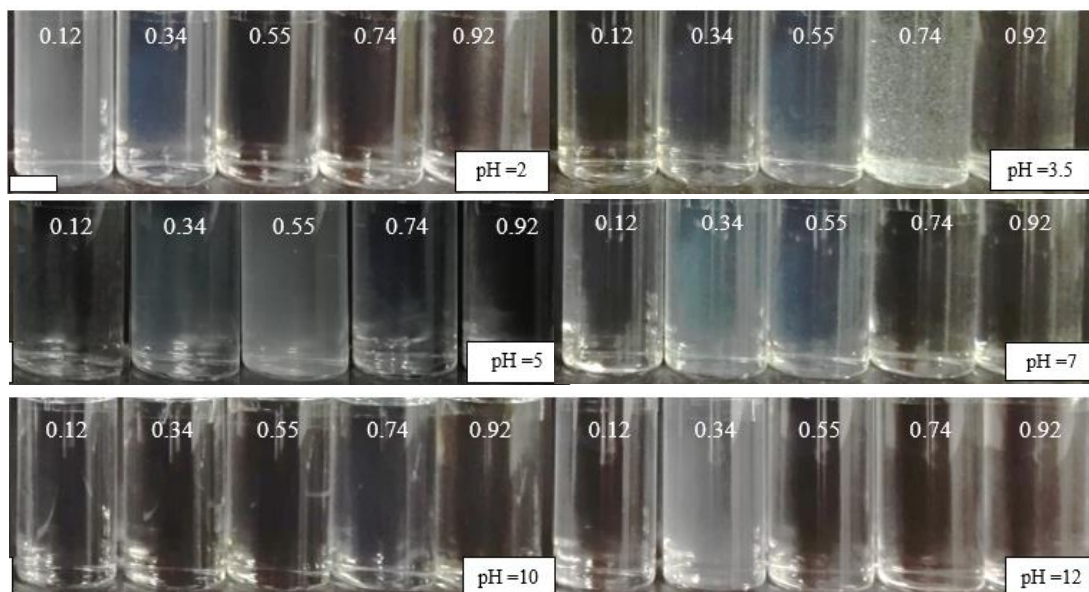
The average diameter of the entities obtained after mixing the polyelectrolyte solutions at selected pH was measured and is shown in Figure 4.7. Despite the occasional high values (which match with samples that are more hazy), there is a tendency for the average diameter of the complex to decrease upon increasing x_{PAANa} from around 120 nm to around 60 nm. At pH = 2 (not shown), despite not expecting complexes to be formed through electrostatic interactions as PAANa is fully protonated, monomodal distributions centred around 100 nm at $x_{PAANa} < 0.64$ were present. At pH = 12 one would expect to obtain complexes through electrostatic interactions as both polyelectrolytes are fully charged. Monomodal distributions were only obtained however for the samples prepared with $x_{PAANa} = 0.34$ and 0.55 (diameters 382 nm and 74 nm, respectively). At the other mole fractions, samples were too polydisperse for cumulant analysis and in some cases the size distribution showed more than one peak.

Figure 4.7. Variation of the average particle diameter with x_{PAANa} for aqueous PEC dispersions prepared from 0.1 g L^{-1} individual PEL solutions at different pH.
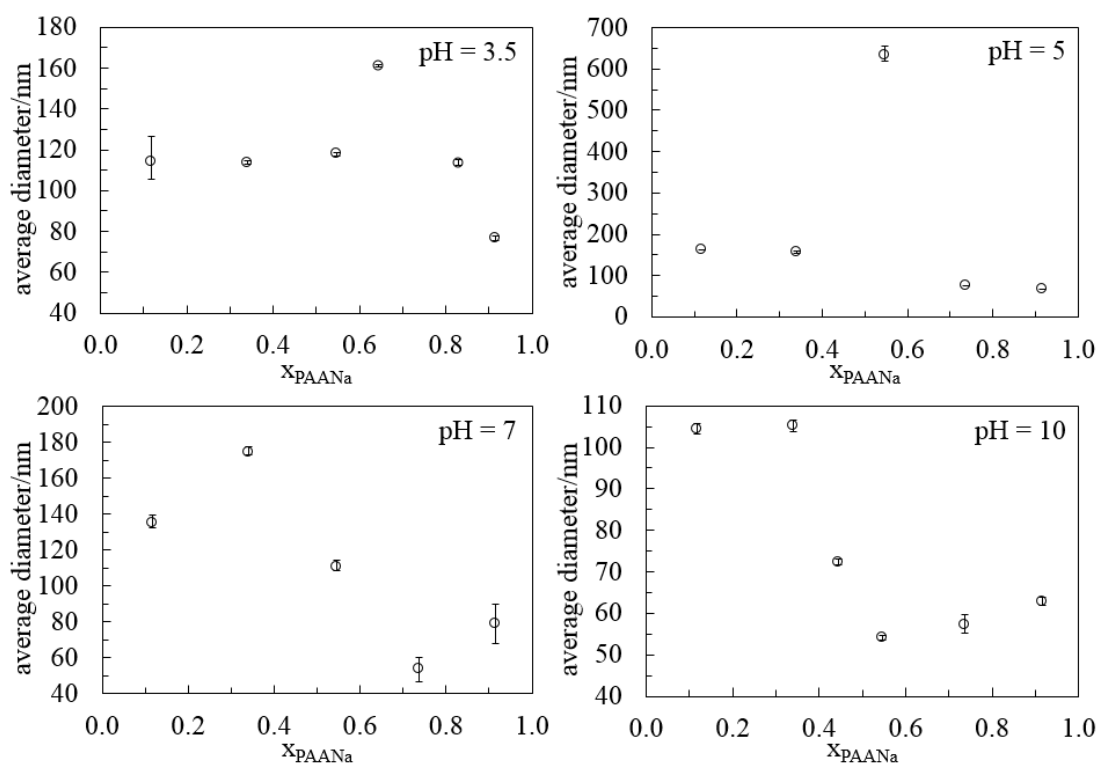

Therefore, from the results obtained at extreme pH values, one can state that the interactions in the system PDADMAC-PAANa cannot be ruled by electrostatics alone. This associative phase separation has to be also mediated through additional inter-molecular interactions, such as van der Waals, hydrogen bonding or hydrophobic and dipole interactions.[24] This agrees with previous work from Alonso *et al*.[25] They detected aggregates at pH = 3 where PAA is not ionised. Their occurrence was explained by the formation of H-bonds between different chains of PAA.[25] The carboxylic acid moiety is a highly polar functional group due to the strongly polarized carbonyl and hydroxyl groups which can interact through hydrogen bonding with other carboxylic acids or water molecules.[25] At low pH, the authors also pointed out the possibility that PDADMAC could form complexes with single chains or small aggregates of PAA. On the other hand, they found that no complex was detected at pH = 13. By increasing the pH, the charge density of PAA increases. As a result, there is an increase in the amount of water linked to the polymer through hydrogen bonding.[25] Conversely, the charges in PDADMAC are given by a quaternary amine surrounded by an organic environment, which makes it less favourable for structured water.[25] At intermediate pH these quaternary amines can destroy the water shell that surrounds

the carboxylic acid groups of PAA and electrostatic interaction takes place.[25] However, with increasing pH, the number of water molecules associated with the carboxylate group increases and the breaking of the water shell by the quaternary amines becomes less likely.[25] As a result, no complexation is achieved. Alonso *et al.* proved the hindering effect of water molecules since, after the addition of a hydrogen bonding breaker, the complexation at high pH took place.[25] However, it is worth mentioning that other parameters such as the chain rigidity and the ionic strength can also affect the strength of the interaction between charged polymers.[26-28]

The zeta potential of each mixture at various pH was also measured (Figure 4.8). At pH = 2 all the dispersions exhibited a positive value of zeta potential. As PAANa is fully protonated, the positive charge is given by the quaternary nitrogen groups in PDADMAC. For the other pH values, the curve is sigmoidal in shape in which the zeta potential changes from positive values to negative ones on increasing x_{PAANa}.

Figure 4.8. Variation of the zeta potential with x_{PAANa} for aqueous PEC dispersions prepared from 0.1 g L^{-1} individual PEL solutions at different pH where PAANa is (a) uncharged, (b) progressively charged and (c) fully charged.
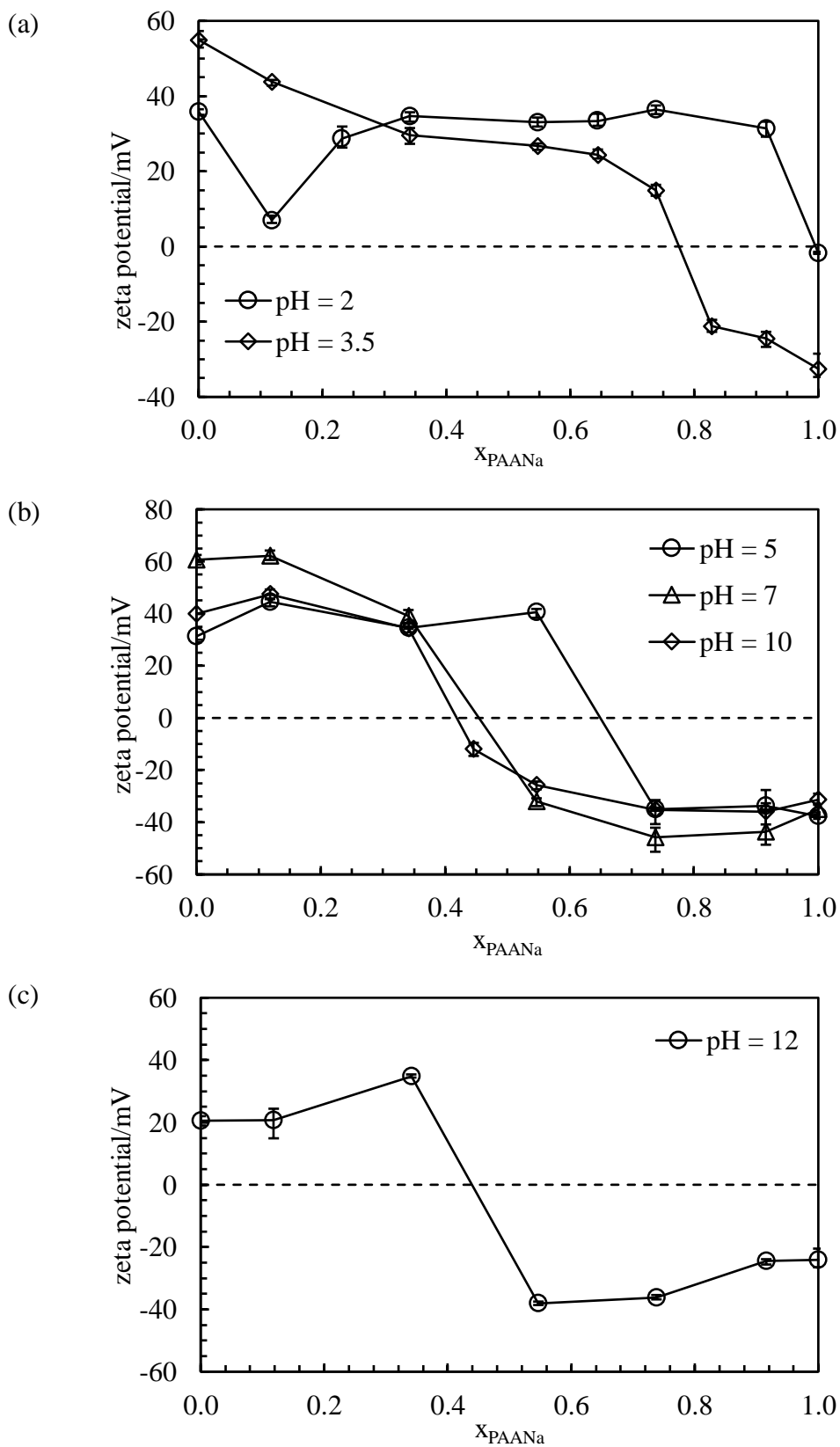
As shown in Figure 4.9, the value of x_{PAANa} at sign reversal is lower at higher pH. At low pH values, only a small fraction of PAANa groups is ionised. Therefore, a higher fraction of PAANa chains is required to fully neutralise the PDADMAC charges. As the pH increases, the change in the sign of the zeta potential occurs at lower x_{PAANa}. From a pH equal to the pK_a onwards, the x_{PAANa} of zero zeta potential reaches a plateau, as expected.

Figure 4.9. Variation of x_{PAANa} at zeta potential $= 0$ with pH for aqueous PEC dispersions prepared from 0.1 g L^{-1} individual PEL solutions.
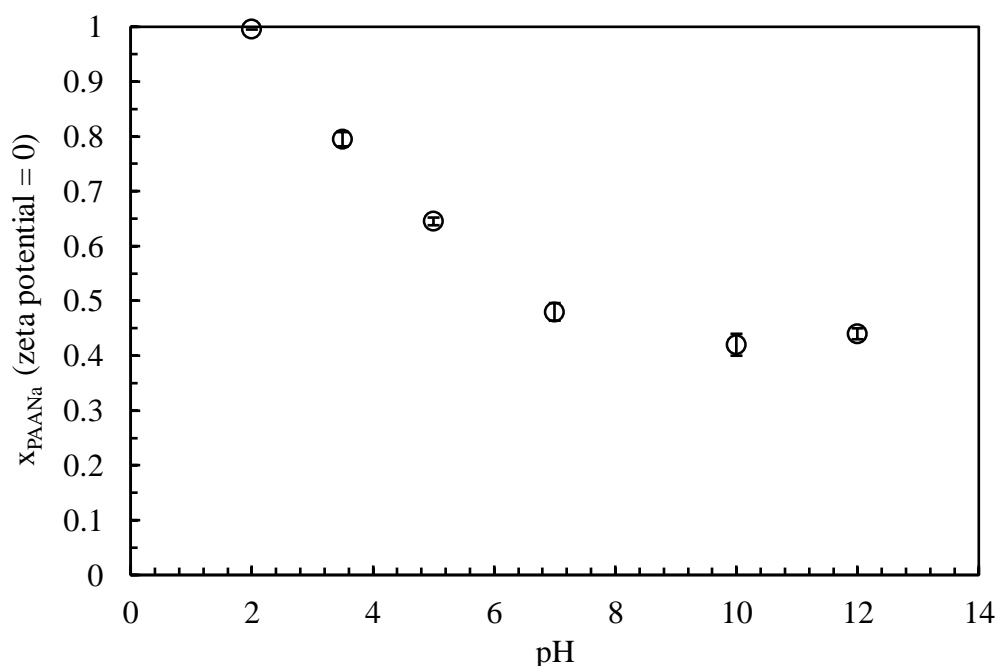
Vitorazi et al.[18] performed an extensive study for the same PEL system by using a combination of titration calorimetry, light scattering and electrophoresis. They studied the influence of [PEL], pH (7 and 10), molecular weight and mixing protocol (direct or stepwise). Our results regarding the size and charge of the obtained entities are in line with their findings. Dispersions of higher turbidity occurred around charge neutrality and the charge of the complexes is governed by the polyelectrolyte in excess.

4.4.2.1 Effect of pH on the type of associative phase separation

In terms of visual inspection at this low concentration, this system is comparable to the system containing PDADMAC-PSSNa (two strong polyelectrolytes) reported in Chapter 3. However, the appearance of the dispersions change upon increasing the concentration of the initial PEL solutions. This study was completed at four different pH values covering the entire range, *i.e.* pH = 2, 4, 6 and 10. Figure 4.10 shows the appearance of dispersions prepared at pH = 4 and 10 at different x_{PAANa} from 5 g L^{-1} PEL solutions.

Figure 4.10. Appearance of fresh aqueous PEC dispersions prepared from 5 g L^{-1} PEL solutions at (a) pH = 4 and (b) pH = 10 at different x_{PAANa} (given). Scale bars = 1 cm. Optical microscope image of a drop of the dispersion at (c) pH = 4, x_{PAANa} = 0.13 and (d) pH = 10, x_{PAANa} = 0.57.
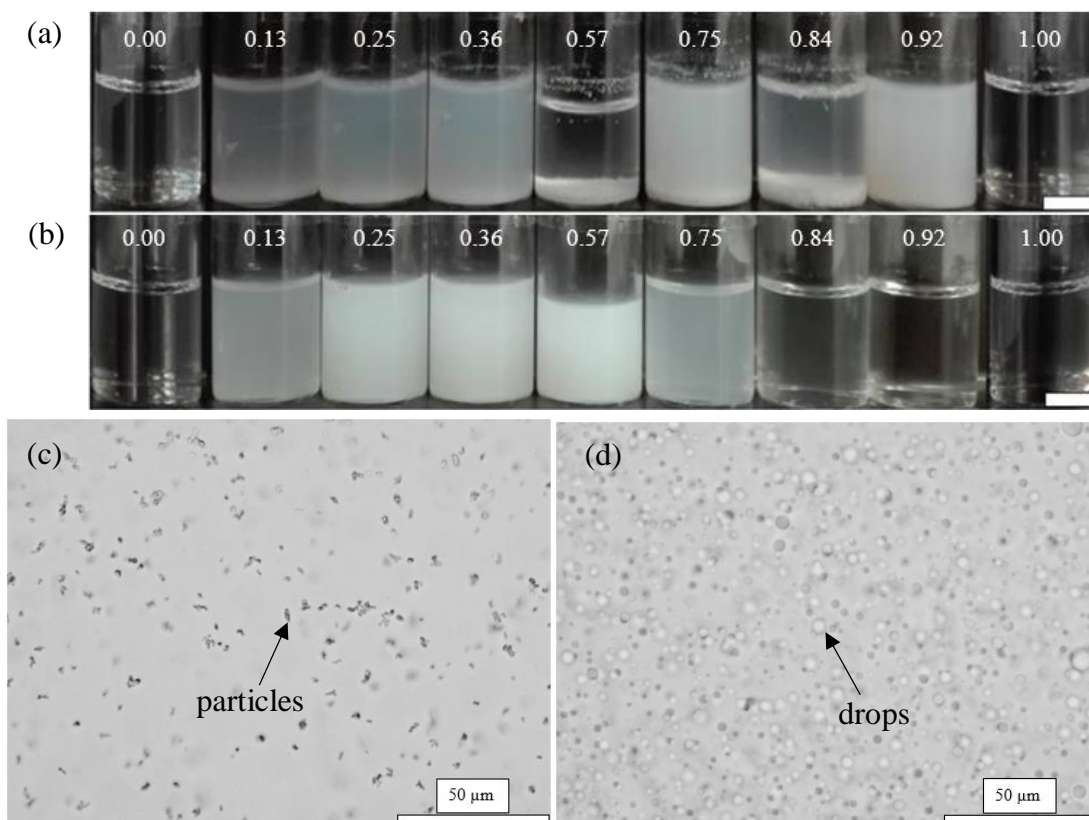
At pH = 4 precipitation in mixtures is observed at all values of x_{PAANa} (*i.e.* particles form) while at pH = 10 no complex precipitated from solution despite the fact that

dispersions were whitish at low and intermediate values of x_{PAANa}. A close inspection of a drop of the dispersion at pH = 10 using optical microscopy reveals the presence of coacervate droplets several microns in size in contrast to solid particles formed at pH = 4 (Figure 4.10 (d) and (c), respectively). Both kinds of dispersed phase can be distinguished quite easily as coacervate droplets are fluid spherical entities whereas particles are less spherical and solid in nature. The appearance of aqueous PEC dispersions at pH = 2 and 6 are included in Figure 4.11 together with selected optical microscope images of the resulting mixtures.

Figure 4.11. Appearance of fresh aqueous PEC dispersions prepared from 5 g L^{-1} PEL solutions at (a) pH = 2 and (b) pH = 6 at different x_{PAANa} (given). Scale bars = 1 cm. Optical microscope image of a drop of the dispersion at (c) pH = 2, x_{PAANa} = 0.57 and (d) pH = 6, x_{PAANa} = 0.57.
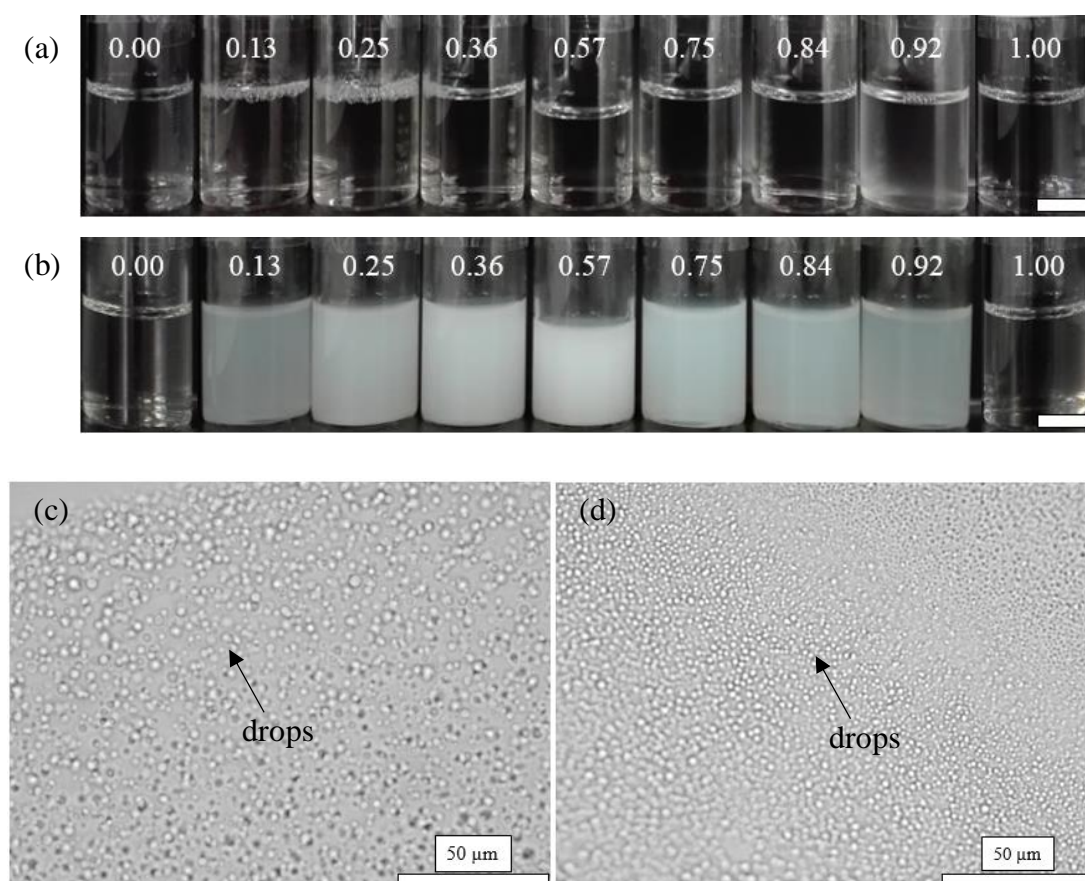
At pH = 2 all the dispersions were transparent, apart from the one at x_{PAANa} = 0.92 which was slightly hazy. At pH = 6 all the dispersions were turbid with that of highest turbidity around charge neutralisation. Coacervate droplets were observed in all the mixtures at these two pH values. Therefore, the transition coacervate-precipitate-

coacervate can be observed by increasing the pH. A transition from precipitate to coacervate by increasing the pH from 4 to 7 was also reported by Jha and co-workers for the same polyelectrolyte system.[29] However, in the literature regarding the characterisation of PEC in aqueous media, apart from ref. 29 no systematic study describing the type of associative phase separation across all the pH range exists. Instead, investigations have mainly been focused at a specific pH[27] or at two pH values.[18]

By increasing the concentration of PEL, several different scenarios can occur. The number of complexes could increase at constant size or complexes of larger size may form at constant number or a combination of both could ensue. There is evidence that the size of the PEC (particles or coacervate droplets) increases with PEL concentration at all pH values. From light scattering measurements at a $[PEL] = 0.1$ g L^{-1} the entities had a diameter centred on 100 nm. However, as seen from the optical microscope images in Figures 4.10 and 4.11 at this higher [PEL], the size of some of the complexes is in the micron range. As gleaned from the results of Starchenko *et al*. for the system PDADMAC-PSSNa[30] and from the results presented in Chapter 3, upon increasing the PEL concentration the aggregation of primary particles is accelerated and this leads to an increase in the size of secondary particles.

In order to further evaluate the difference between these two types of associative phase separation (precipitation and coacervation) centrifugation of 1 mL of an aqueous PEC dispersion ($x_{PAANa} = 0.5$) prepared at two different pH was carried out. The initial concentrations of the PEL solutions used were 5 g L^{-1} and 10 g L^{-1} for pH = 4 and 10, respectively. At pH = 4, after centrifugation a white precipitate is collected on the bottom of the Eppendorf tube as seen in Figure 4.12(2), consistent with the solid-liquid type of phase separation. The appearance of the aqueous PEC dispersion at pH = 10 is shown before and after centrifugation in Figure 4.12(1). The dispersion was initially whitish which after centrifugation yields a phase separated system consistent with the liquid-liquid type of phase separation of the complex coacervate. Three different phases were identified and designated supernatant (phase A), interface (phase B) and coacervate phase (phase C). The supernatant was mostly water depleted in coacervate droplets (Figure 4.12(A)). Some spherical entities were still evident around the edges of the drop as soon as the water began to evaporate. However, they were hardly visible at the outset. The interface consisted of an aqueous phase rich in coacervate droplets

(Figure 4.12(B)). Images of the same drop placed on a glass slide were taken at different times. Coalescence of the coacervate droplets occurred as after 17 min a substantial increase in their size was detected. After 22 min droplets were no longer visible as they had coalesced to a bulk film of coacervate phase. Finally, the coacervate phase after centrifugation was a transparent and viscous phase concentrated in both polymers (Figure 4.12(C)). The water content was $63 \pm 3\%$ which is close ($\sim 66\%$) to the value reported for the same system at pH = 7.[29]

Figure 4.12. (1) Appearance of 1 mL of aqueous PEC dispersion ($x_{PAANa} = 0.5$, [PEL] = 10 g L^{-1}, pH = 10) before and after centrifugation. The three different phases separated after centrifugation are supernatant (A), interface (B) and coacervate phase (C). Optical microscope images of the different phases are included. For phase B, images from the same drop are shown at different times. (2) Appearance of 1 mL of aqueous PEC dispersion ($x_{PAANa} = 0.5$, [PEL] = 5 g L^{-1}, pH = 4) after centrifugation.
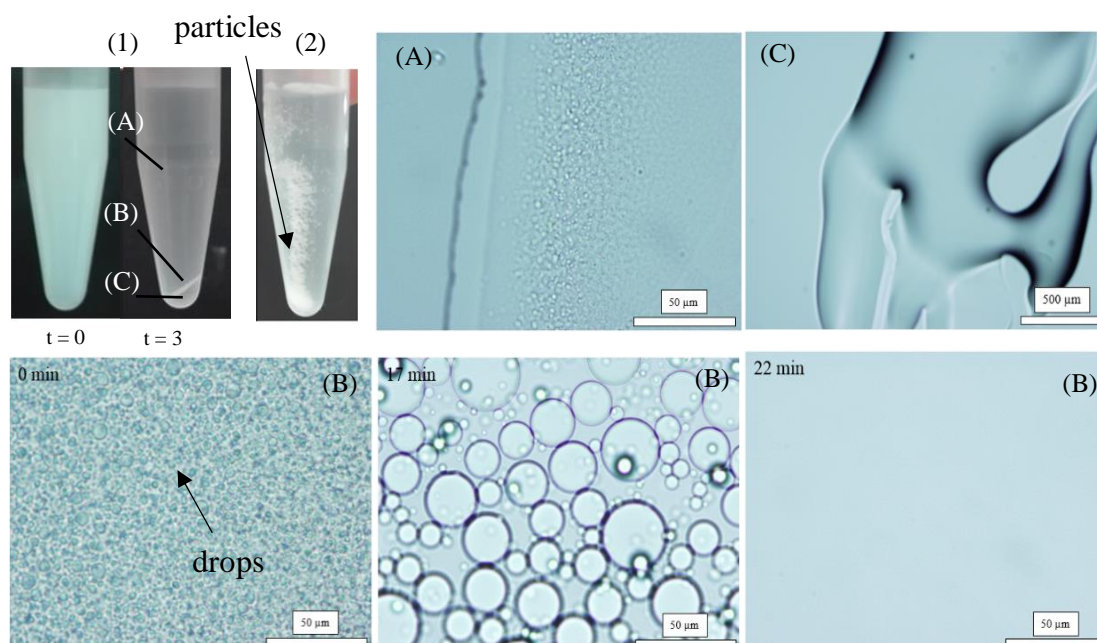
The entire pH range was studied at a high PEL concentration (5 g L^{-1}) for a mixture containing an equal mole fraction of both polymers ($x_{PAANa} = 0.5$). Figure 4.13(a) shows the appearance of the vials at different pH values immediately after preparation and at three subsequent times. The same conclusions regarding the type of associative phase separation arise from this set of experiments as derived from the experiments above.

Figure 4.13. (a) Evolution of the stability of aqueous PEC dispersions prepared from 5 g L^{-1} individual PEL solutions (x_{PAANa} = 0.50) at different pH (given). Scale bar = 1 cm. Optical microscope images of the aqueous PEC dispersion at pH (b) 2, (c) 3, (d) 4 and (e) 6.
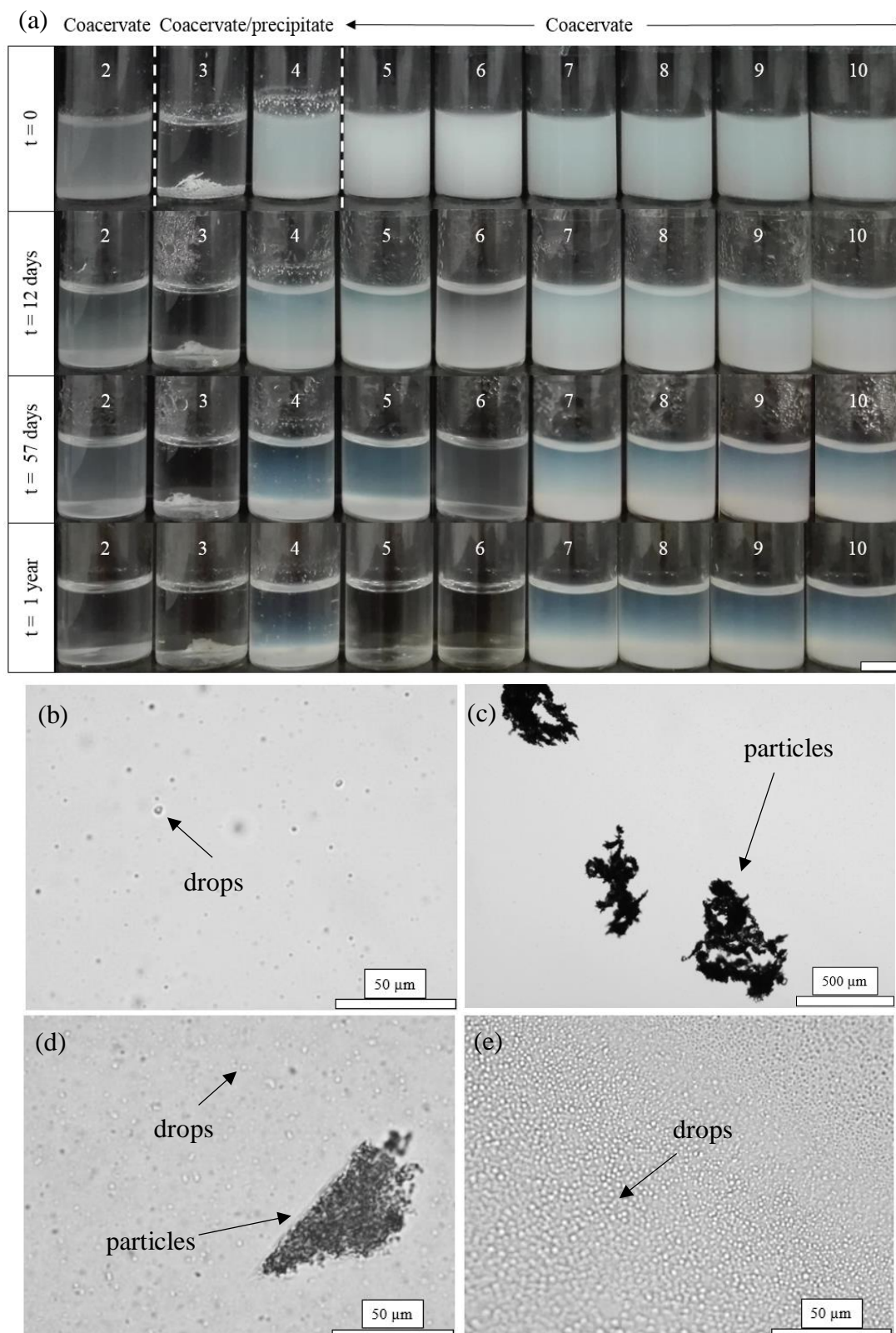
At pH = 2 the sample displays turbidity and coacervate droplets are detected despite the possibility that no electrostatic interaction is expected to occur (Figure 4.13(b)). At pH 3 and 4 both coacervate droplets and solid precipitates coexisted (Figure 4.13(c) and (d)). The size of the solid or liquid particles range between a few microns and several hundred microns as they aggregate quite easily. Co-appearance of both types of phase separation has been reported in the literature for the system under study. Koetz and Kosmella found co-existence of coacervation and particle flocculation at specific polymer M_w's and PEL concentrations.[31]

From pH = 5 onwards, no precipitates are observed either visually or *via* optical microscopy and only coacervate droplets form. As pointed out in Chapter 1, it is generally assumed that precipitation rather than coacervation is obtained for strongly interacting polymer pairs. Therefore, one would expect precipitate formation at high pH values, which is not the case. This may be related to the enhanced ability of PAANa to form hydrogen bonds at high pH, as explained earlier. Due to the dipoles present in the carboxylic acid moieties, water is associated to them through hydrogen bonding leading to partial screening of the negative charge of the ionic groups.[25] Therefore, the electrostatic interaction with PDADMAC is weakened and this results in the formation of a complex coacervate containing water instead of a precipitate. The volume fraction of coacervate droplets is higher at pH 5 and 6 *cf.* higher pH and these samples display maximum turbidity initially (Figure 4.13(a)). One year after preparation the coacervate droplets in these dispersions fully coalesced forming a transparent coacervate phase on the bottom leaving a transparent supernatant solution where few coacervate droplets were still detected. Despite a low interfacial tension between the coacervate droplets and water,[6-8] since the droplets are very small the Laplace pressure is high which is consistent with the occurrence of coalescence at pH = 5 and 6. The Laplace pressure (ΔP) is the pressure difference between the inside and outside of a curved interface. ΔP in the case of spherical droplets is related to the interfacial tension (γ) and the radii of curvature of the droplet (R) as shown in equation 4.13.[32]

$$\Delta P = \gamma \frac{2}{R} \qquad (4.13)$$

From pH = 7 to 10, a white dispersion concentrated in coacervate droplets sediments slowly but complete coalescence is not achieved. Moreover, it easily re-disperses recovering the white dispersion obtained after preparation. Therefore, the stability to

coalescence of the coacervate droplets at high pH is considerably improved. It may be that coacervate droplets at high pH possess excess of charged polymer at their interfaces which act to prevent their coalescence.

4.4.2.2 TEM images of coacervate droplets

As mentioned in the previous section, coacervate droplets prepared at pH = 10 were stable to coalescence. Therefore, TEM images of a dispersion containing coacervate droplets ($x_{PAANa} \approx 0.5$, [PEL] = 5 g L^{-1}, pH = 10) were taken to check whether they are homogenous from their core to the surface or if a distinct surface layer of mixed polymers is formed around the core. Figure 4.14 shows different areas of the unstained sample, whereas Figure 4.15 corresponds to the sample negatively stained with uranyl acetate. The uranyl acetate crystals surround the structures giving a 3D appearance. In all cases, near spherical droplets ranging in diameter between 200 nm and 500 nm are observed, although some are distinctly non-spherical. Since water evaporates from the droplets during preparation, the size of the remaining concentrated polymer droplet will be less than that in the original dispersion (fully hydrated).

The droplets are homogeneous in texture and exhibit no internal ordering. For the unstained case, the droplets appear to be surrounded by very small particulates (black dots in Figure 4.14). For the stained sample, these particulates are not visible as uranyl acetate crystals surround the droplets. Using EDX analysis, no special element was detected. In fact the polyelectrolytes are composed mainly of C and in lower proportion N, O, Na and Cl. Since the TEM grid is carbon coated, carbon was one of the main peaks displayed in the spectra (data not shown). The small particulates have not been identified. Using this technique, it can be concluded that coacervate droplets are homogeneous and do not appear to possess any internal structure or surface shell. However, the reason for their coalescence stability at high pH remains to be established. Few TEM images of the coacervate phase in mixed polymer systems exist in the literature.[33,34] They also display a homogeneous texture without internal ordering or evidence of a surface shell or membrane.

Figure 4.14. TEM images of a fresh aqueous PEC dispersion (x_{PAANa} = 0.5) prepared from 5 g L^{-1} PEL solutions at pH = 10 taken at different regions of the grid, (b) is a higher magnification image of (a). All correspond to the unstained sample.
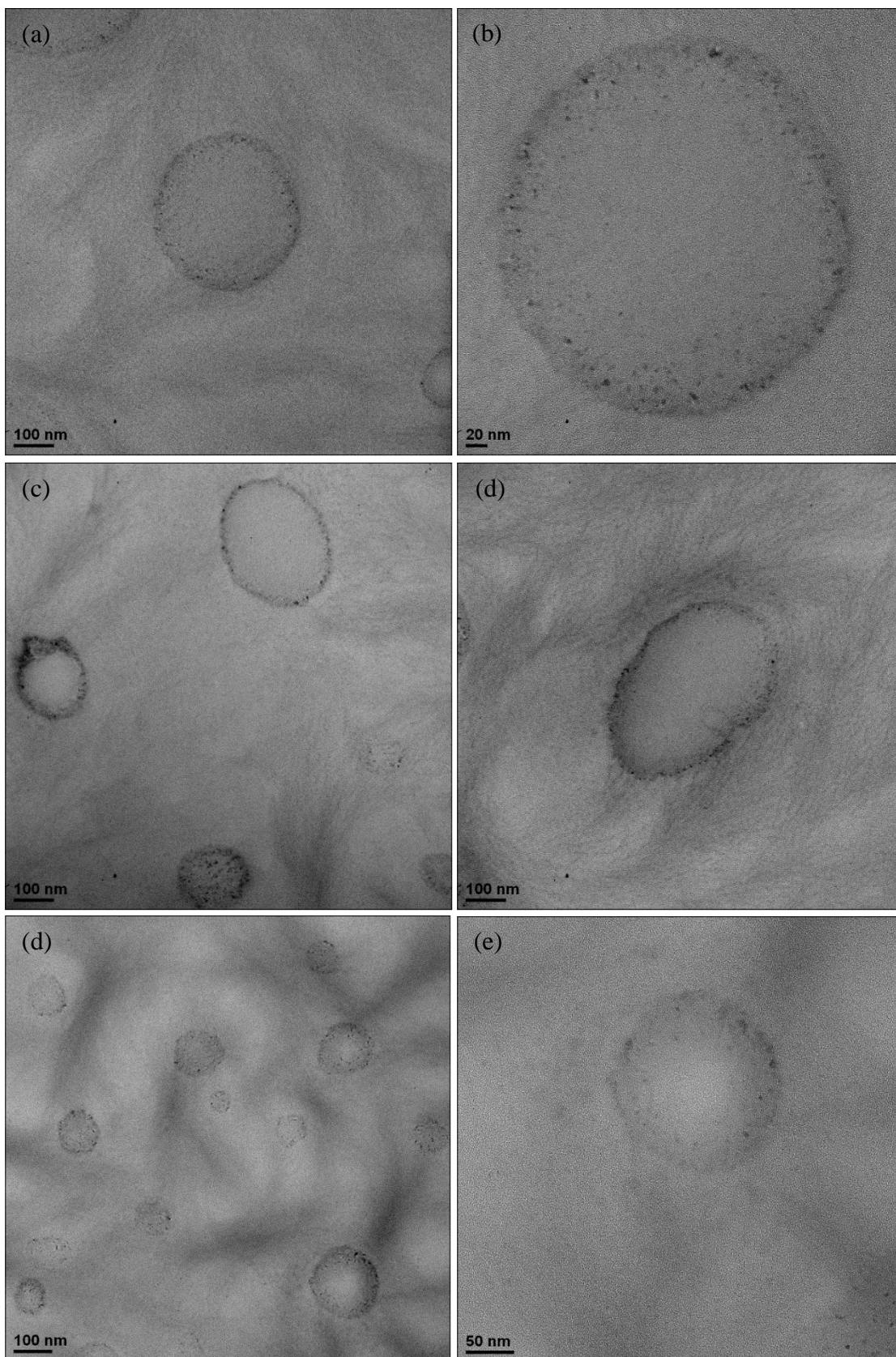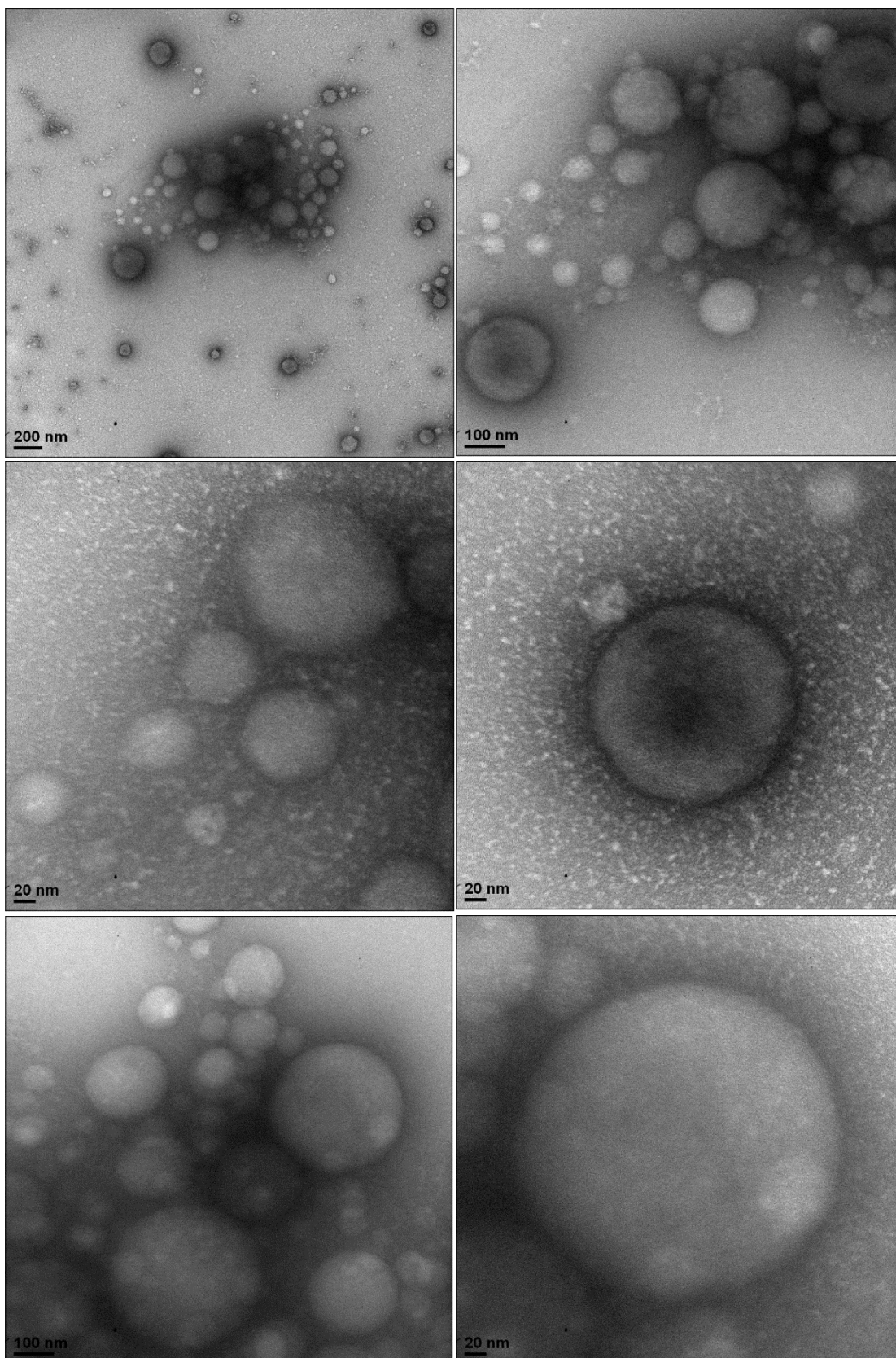
Figure 4.15. TEM images of a freshly prepared aqueous PEC dispersion (x_{PAANa} = 0.5) prepared from 5 g L^{-1} PEL solutions at pH = 10 at different magnifications. The sample was negatively stained with uranyl acetate.

4.4.2.3 Effect of salt concentration on the stability of coacervate droplets

The influence of salt concentration was evaluated for a wide range of [NaCl] (0-4 M) for an aqueous PEC dispersion where only coacervate droplets are formed (x_{PAANa} = 0.5, [PEL] = 5 g L^{-1}, pH = 10). Different amounts of NaCl crystals were added to the above dispersion to achieve the desired [NaCl]. After each addition, the dispersion was hand-shaken, the absorbance at 600 nm was measured and optical microscope images were taken. Figure 4.16(a), shows the appearance of the aqueous PEC dispersion at selected [NaCl].

Figure 4.16. (a) Appearance of an aqueous PEC dispersion (x_{PAANa} = 0.5, [PEL] = 5 g L^{-1}, pH = 10) after the subsequent addition of NaCl (concentration in the dispersion given). Scale bar = 1 cm. (b) Absorbance at λ = 600 nm *versus* [NaCl] for the above aqueous PEC dispersions.
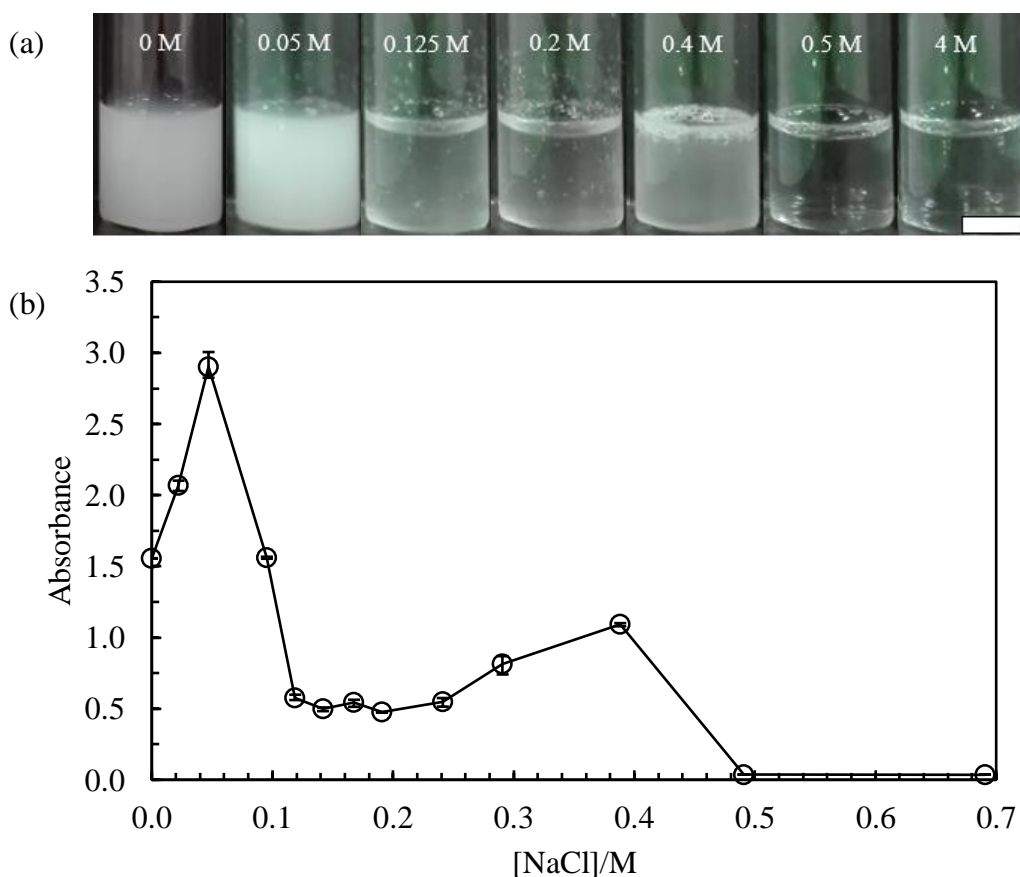
From the plot in Figure 4.16(b), the absorbance first increases displaying an absolute maximum at a [NaCl] = 0.05 M and a relative maximum at a [NaCl] = 0.4 M. From optical microscope images in Figure 4.17 at a [NaCl] = 0 and 0.05 M, coacervate droplets are abound and small in size. When the [NaCl] is between 0.05 M and 0.4 M,

the wall of the vial was covered by a viscous gel (coacervate phase) and the coacervate droplets remaining in dispersion increased in size considerably (Figure 4.17). From [NaCl] = 0.5 M onwards, the solution became completely transparent and the viscous layer around the wall disappeared. Moreover, no evidence of coacervate droplets was detected under the optical microscope (Figure 4.17). For [NaCl] > 0.5 M the absorbance at 600 nm was close to zero. In Chapter 3 a similar study was carried out by adding NaCl to a solution containing PEC particles. The same transition was achieved: solid particles started to aggregate until a critical [NaCl] where the electrostatic interaction between the polyelectrolytes was completely screened and individual polymer chains remained in solution.

Figure 4.17. Optical microscope images of an aqueous PEC dispersion (x_{PAANa} = 0.5, [PEL] = 5 g L^{-1}, pH = 10) at different [NaCl] (given). Drops are detected at [NaCl] < 0.5 M.
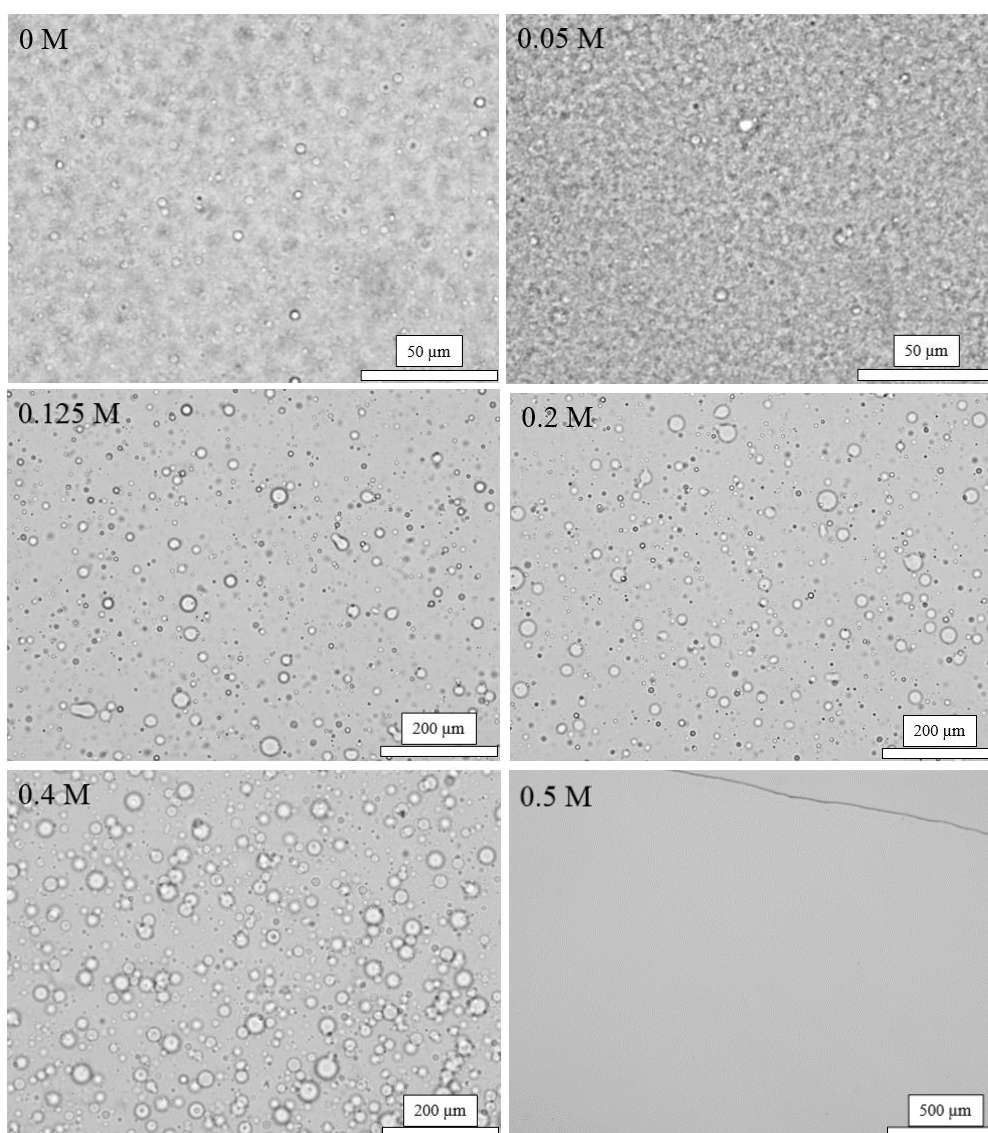
4.4.3 Summary of aqueous PEC dispersions

In aqueous mixtures of this polyelectrolyte combination, both precipitation and complex coacervation occurred as a result of an associative phase separation phenomenon which is dependent on pH. The progression coacervate – precipitate/coacervate – coacervate ensued upon increasing the pH as PAANa becomes ionised. Despite precipitates are expected to be formed at high pH when both polyelectrolytes are fully charged, complex coacervation resulted. TEM images of coacervate droplets revealed the presence of no internal structure. For a dispersion containing coacervate droplets, salt induces first their coalescence, followed by a dissolution of the complex when the salt content is really high.

4.5 Oil-in-water emulsions prepared from polymer mixtures

4.5.1 Effect of pH on emulsion stability

Our interest here is whether the PEC prepared in water are surface-active enough to adsorb to an oil-water interface created on emulsifying the aqueous phase with the non-polar alkane *n*-dodecane. For the system PDADMAC-PSSNa discussed in Chapter 3, emulsion stability was enhanced by increasing the initial concentration of PEL. Moreover, on varying x_{PSSNa}, the emulsion droplet size and the extent of coalescence were reduced upon approaching the conditions leading to charge neutrality. In that case, the oil was added in one step during homogenisation. As mentioned previously, for the system PDADMAC-PAANa, pH has a dramatic influence on the associative phase separation that takes place. Therefore, this parameter will be a key one in the study of emulsion stabilisation. Figure 4.18 shows the appearance of emulsions obtained from aqueous PEC dispersions prepared at pH values from 2 to 6 from 5 g L^{-1} PEL solutions at $x_{PAANa} = 0.5$. At pH = 2 (coacervate), an o/w emulsion was formed after mixing which creamed rapidly and completely phase separated within 11 days after preparation. An air-in-water foam was also formed during mixing which was only stable for a few min. This surface activity is most likely connected with the presence of fully protonated poly(acrylic acid).

Figure 4.18. Appearance of dodecane-in-water emulsions (ϕ_o = 0.20 added in one step) from aqueous PEC dispersions ($x_{PAANa} \approx 0.50$, [PEL] = 5 g L^{-1}) at different pH (given). Appearance of the emulsions 11 days after preparation is also shown. Scale bar = 1 cm.
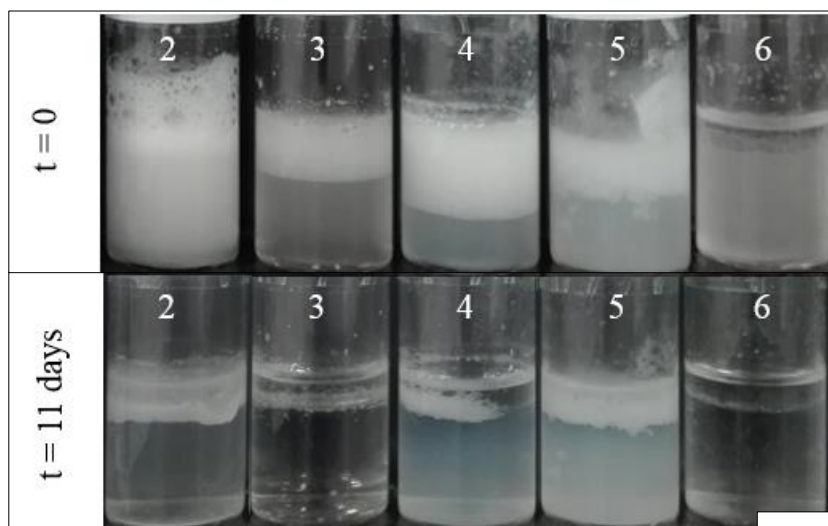
In order to verify this assumption, emulsions containing the individual PEL solutions at the same concentration and pH were prepared with *n*-dodecane. That with PDADMAC coalesced rapidly after preparation until complete phase separation whilst emulsion formation with PAANa produces considerable amount of foam and the emulsion was stable for a longer period of time compared to that formed from the aqueous PEC dispersion (Figure 4.19). This is consistent with the findings of Ishimuro and Ueberreiter[35] who showed that the air-water surface tension was lowered at low pH on adding PAA (uncharged) whereas PAA was not surface-active at higher pH (charged). Further investigation of the ability of the PAANa solution at pH = 2 to stabilise emulsions was carried out. Solutions of PAANa at different concentrations (0.05 to 5 g L^{-1}) were prepared and emulsions were obtained following the standard procedure. As seen in Figure 4.19, o/w emulsions prepared at 0.05 and 0.10 g L^{-1} coalesced completely in less than 10 min after preparation and no air bubbles persisted during high-shear homogenisation. On the other hand, emulsions prepared from solutions at higher concentration (> 0.50 g L^{-1}) generated bubbles while mixing and a stable emulsion cream was achieved for a longer period of time despite some coalescence of oil. Therefore, the concentration of PAANa required to display surface activity must be > 0.10 g L^{-1}.

Figure 4.19. Appearance of dodecane-in-water emulsions ($\phi_o = 0.20$ added in one step) stabilised by PAANa alone at pH = 2 and different concentrations (given in g L^{-1}) at various times. Scale bar = 1 cm.
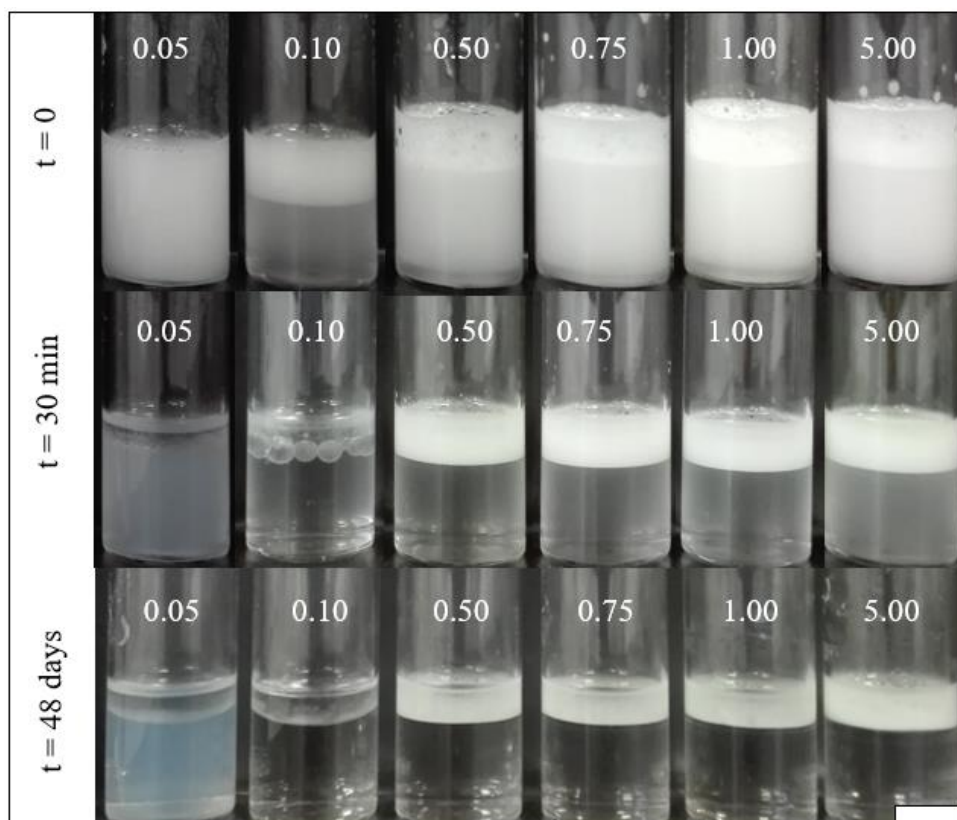

At pH values of 3 and 4, where coacervate droplets and precipitate particles co-exist in water, no stable emulsions were obtained either (Figure 4.18). The reasons may be that the number of particles and coacervate drops is not sufficient for stabilisation or that particles/aggregates are too large to remain attached to droplet interfaces or that they are too hydrophilic in nature. In order to increase the overall particle concentration, aqueous PEC dispersions were prepared from PEL solutions at 10 g L^{-1}. However, this was not sufficient as the emulsion completely coalesced after homogenisation (data not shown). At pH 5 and 6 (coacervate), an unexpected situation was encountered. At these pH aqueous PEC dispersions are the most turbid. However, after homogenisation of oil, the aqueous phase became almost transparent at pH = 6 and no emulsion was obtained. It was noticed that coacervate droplets coalesced on the head of the homogeniser and did not take part in emulsion stabilisation. At pH = 5, an initial viscous emulsion collected on the top of the vial; it was not stable for a long period of time however. In this case, the turbidity of the separated aqueous

solution decreased as well due to the coalescence of some of the coacervate phase on the head of the homogeniser. The highly viscous nature of these particular coacervate systems makes it difficult with respect to emulsification.

For pH values between 7 and 10 (coacervate), the behaviour was similar so the discussion will be focused on the emulsion prepared at pH = 10. Emulsions prepared with the individual PEL at that pH were not stable as complete phase separation was obtained after homogenisation (Figure 4.20).

Figure 4.20. Appearance of emulsions prepared with *n*-dodecane ($\phi_o = 0.20$) and a 5 g L^{-1} individual PEL solution at pH = 10 (PAANa and PDADMAC) after homogenisation. Scale bar = 1 cm.
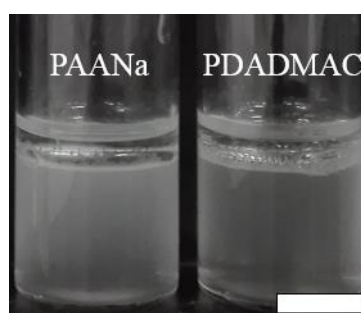
For the PEL mixture, two different preparations were evaluated ($\phi_o = 0.20$): addition of oil in one step and addition of oil stepwise summarised in Figure 4.21. For the emulsion prepared with the addition of oil stepwise, the oil was added in aliquots of 200 μL and homogenised with the Ultra-turrax homogeniser each time. Between each addition, the emulsion was left to stand for a few hours to assess its stability. In the case of the addition of oil in one step, the emulsion was virtually completely phase separated in less than 1 day. The extent of coalescence was high but there was a residual volume of emulsion cream around the walls of the vial. For the emulsion prepared stepwise, the emulsion cream was stable for a longer period of time. The final emulsion containing $\phi_o = 0.20$ liberated around 10% of oil by coalescence but was subsequently stable for at least 6 months (Figure 4.21(b)). The viscosity of the emulsion increased with an increase in ϕ_o as expected. Since the average drop diameter was independent of ϕ_o (between 24 and 28 μm), it implies that the additional oil does not swell existing drops stabilised by coacervate but is used in creating new drops which become stabilised. In order to compare the one step and multi-step protocols more correctly, an extra experiment was performed. Oil was added in one step and

then five homogenisations were carried out leaving the emulsion to stand for 1 h between each step. No stable emulsion could be prepared either with this modified procedure. This highlights the importance of the addition of oil stepwise in obtaining a stable emulsion.

Figure 4.21. Stability with time of dodecane-in-water ($\phi_o = 0.20$) emulsions prepared from aqueous PEC dispersions ($x_{PAANa} = 0.5$, [PEL] = 5 g L^{-1}, pH = 10). (a) Oil added in one step, (b) oil added stepwise; ϕ_o in the overall emulsion after each addition is given. Scale bars = 1 cm.
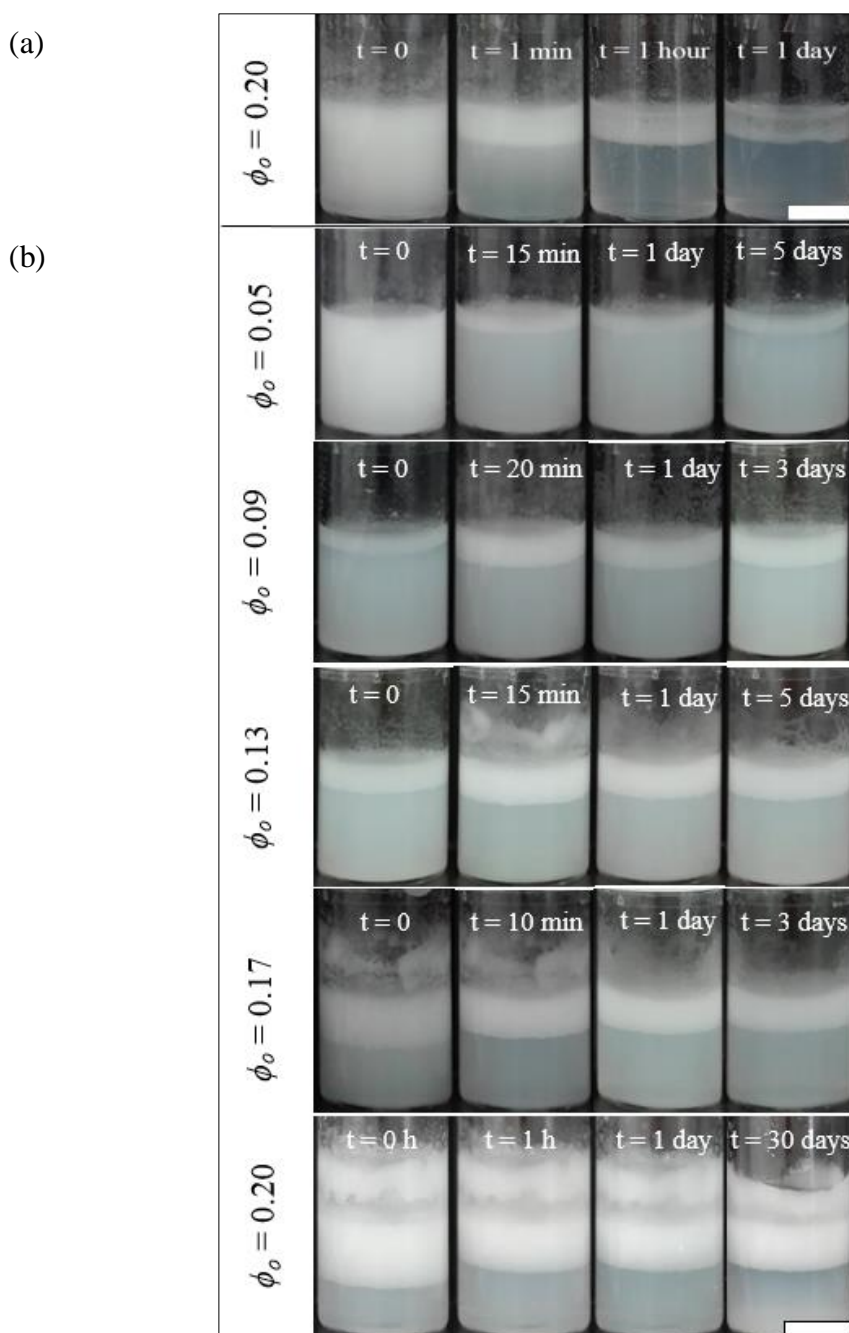
Forgiarini et al.[36] studied the system water / nonionic surfactant / decane to obtain nanoemulsions by three different emulsification methods: (i) stepwise addition of oil to a water-surfactant mixture, (ii) stepwise addition of water to an oil-surfactant mixture and (iii) mixing of all components simultaneously. Although the nature of the emulsifier is different to the one studied here, nanoemulsions with high kinetic stability were only obtained by method (ii). In this case, the reason why a stable emulsion can only be prepared with the addition of oil stepwise is not fully understood. On the one hand, the kinetics of adsorption of the coacervate phase onto the oil-water interface could be relatively slow compared to that of surfactant molecules. Therefore, the subsequent addition of oil followed by homogenisation may enable a more homogeneous coating around oil drops to be formed. In fact, it is common during industrial manufacture of emulsions that the dispersed phase (here oil) is drip fed into the reactor during mixing as this allows good dispersion and stabilisation in a more controlled manner.

Optical microscope images were obtained by placing a sample of fresh emulsion on a glass slide without a coverslip (Figure 4.22(a)). As seen in the left hand image, the central group of droplets are enveloped by a film which is most likely that of coacervate. On the right hand image, concentric spheres are visible and in some cases the inner sphere possesses nodules or horns. These kind of structures were reported in a study of microencapsulation in which oil droplets were surrounded by the coacervate complex prepared between a protein and a polysaccharide.[37] Cryo-SEM images of a selected emulsion (Figure 4.22(b)) show the curvature of the oil-water interface with the interior of the oil droplet on the left and the adjacent continuous phase on the right. Both the interface and the aqueous phase contain frozen, monodisperse spherical entities which are attributed to coacervate droplets of diameter around 150 nm. The different appearance of the interface around oil drops observed *via* optical microscopy and SEM is at first sight puzzling. From optical microscope images, what appears to be a continuous film is observed which may indicate that coacervate droplets coalesce during emulsification. It may be however that sub-micron coacervate droplets do not coalesce but adsorb to drop interfaces and cannot be resolved optically. Cryo-SEM images reveal individual spherical entities which are probably frozen coacervate droplets, *i.e.* implying that intact coacervate droplets aggregate at the oil-water interface in multilayers.

Figure 4.22. (a) Optical microscope images of freshly prepared dodecane-in-water emulsion ($\phi_o = 0.05$) from an aqueous PEC dispersion ($x_{PAANa} = 0.5$, [PEL] = 5 g L^{-1}, pH = 10) at different magnifications (given). (b) Cryo-SEM images of freshly prepared dodecane-in-water emulsion ($\phi_o = 0.20$) from an aqueous PEC dispersion ($x_{PAANa} = 0.5$, [PEL] = 5 g L^{-1}, pH = 10) at different magnifications (given). In both cases, the emulsion was prepared with the addition of oil stepwise.

(a)

(b)
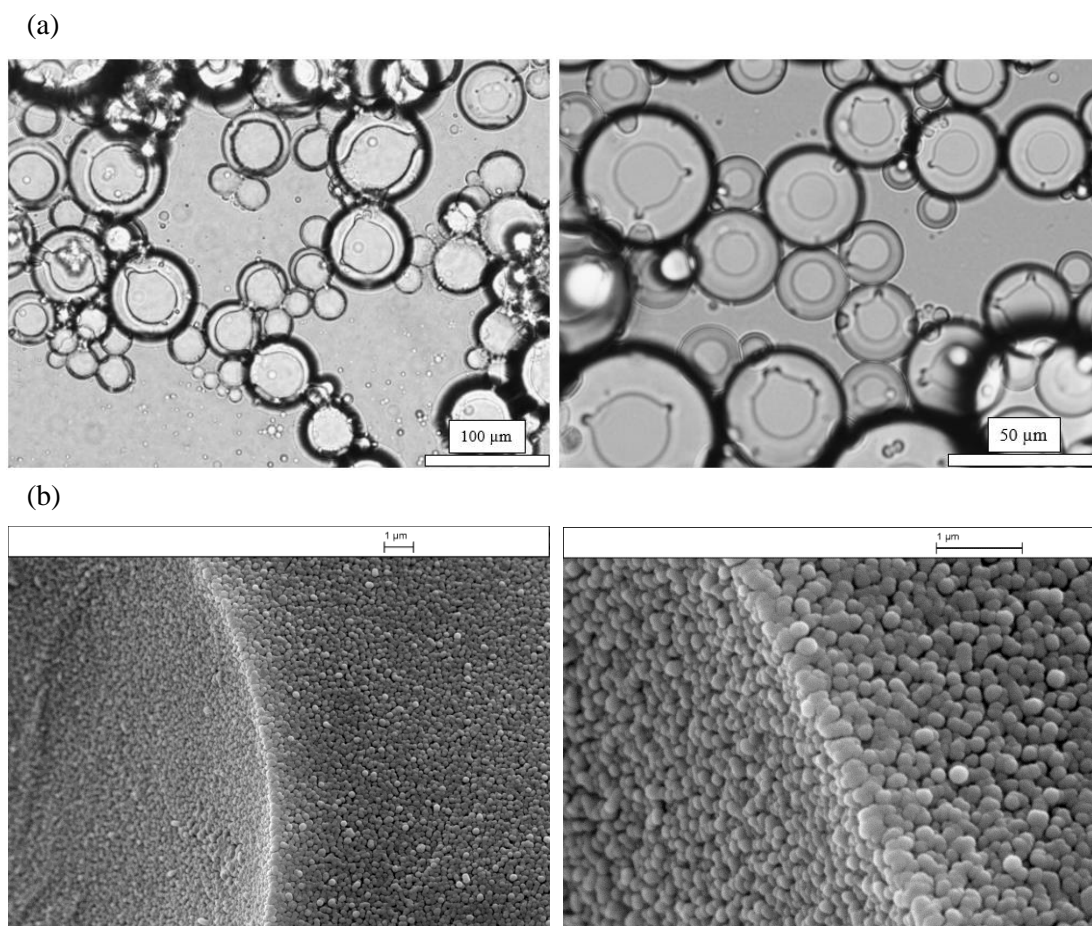
In order to enhance the emulsion stability, an aqueous PEC dispersion prepared from 30 g L^{-1} PEL solutions at pH = 10 was prepared (Figure 4.23(a)). The dispersion exhibits similar turbidity to the one prepared from 5 g L^{-1} PEL solutions. However, a viscous coacervate phase formed on the bottom of the vial, around the walls and on the magnetic stirrer bar as seen in the inverted vial (Figure 4.23(d)). Spherical coacervate droplets were visible in the dispersion (Figure 4.23(c)). However, upon addition of oil and homogenisation, the head of the homogeniser was covered by the viscous coacervate phase and the oil on the top was mixed with it without being emulsified (Figure 4.23(b)). The aqueous phase after homogenisation was significantly depleted of coacervate droplets (Figure 4.23(e)). Therefore, systems

145

exhibiting complex coacervation are very sensitive and the stabilisation of emulsions from them has to be optimised for each individual pair of polyelectrolytes.

Figure 4.23. (a) Appearance of aqueous PEC dispersion prepared from 30 g L^{-1} PEL solutions at pH = 10, x_{PAANa} = 0.5. A white dispersion coexists with a viscous gelatinous phase as seen on the inverted vial. (b) Appearance of dodecane-in-water emulsion immediately after homogenisation (left, ϕ_o = 0.20 in one step); right - corresponds to the same vial after removal of the gelatinous phase on top. Scale bar = 1 cm. Optical microscope image of (c) white dispersion in (a), (d) gelatinous phase in (a) and (e) aqueous dispersion separated after emulsification in (b).
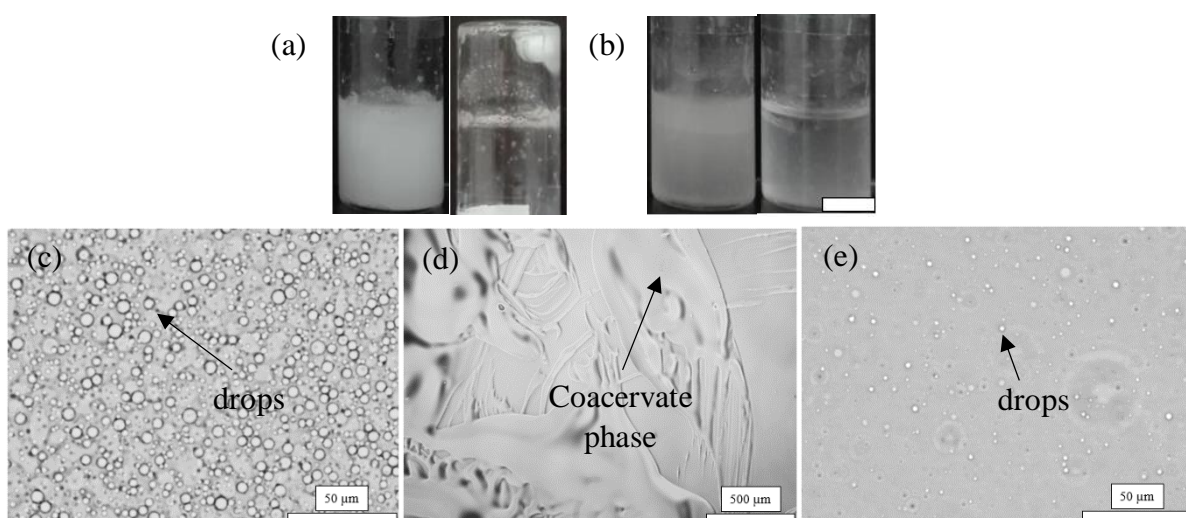
4.5.2   Effect of oil type on coacervate-stabilised emulsions

As the most promising results on emulsion stabilisation were achieved with the aqueous PEC dispersion prepared from 5 g L^{-1} PEL solutions (x_{PAANa} = 0.5) at pH = 10 by stepwise addition of oil, the emulsion stability in the case of different oils was evaluated. Different behaviour was observed depending on the type of oil. Emulsions of squalane and isopropyl myristate completely phase separate in less than 1 h after preparation (Figure 4.24). That of PDMS also coalesces 1 day after preparation but optical microscope images once creaming had halted reveal the same kind of behaviour as with dodecane: oil droplets surrounded by a coacervate phase (Figure 4.25). For these three oils, a viscous phase remained at the oil-water interface and around the walls after the majority of oil had coalesced. For toluene, the emulsion was much more stable to coalescence compared with the other oils and optical microscopy reveals a different morphology of the oil droplets (Figure 4.26). Here, the droplets are

146

more deformed and stretched and a large number of them become encased by the coacervate phase.

Figure 4.24. Appearance of o/w emulsion ($\phi_o = 0.20$, added stepwise) with (a) isopropyl myristate and (b) squalane from an aqueous PEC dispersion ($x_{PAANa} = 0.5$, [PEL] = 5 g L^{-1}, pH = 10) at different times. Scale bars = 1 cm.
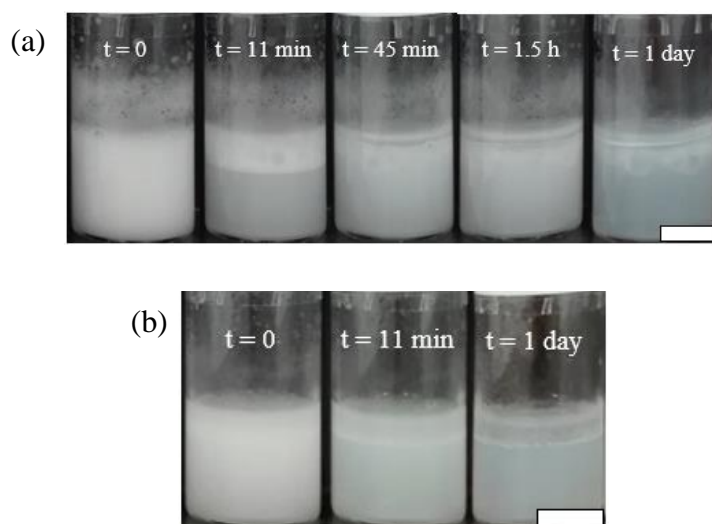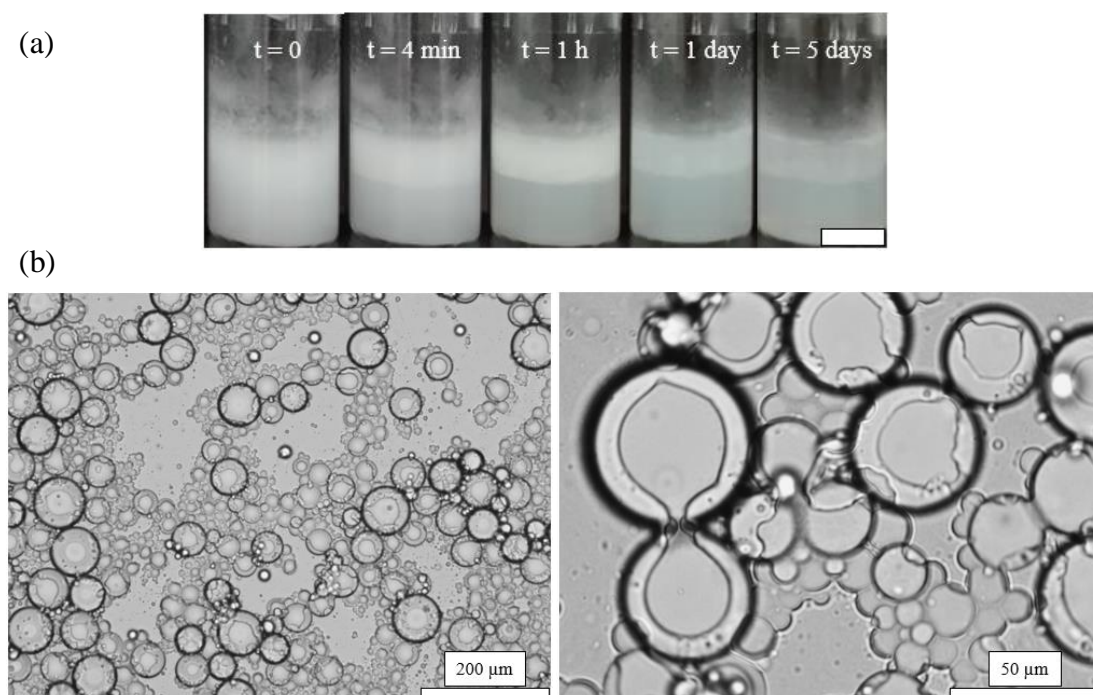

Figure 4.25. (a) Appearance of PDMS-in-water emulsion ($\phi_o = 0.20$, added stepwise) from an aqueous PEC dispersion ($x_{PAANa} = 0.5$, [PEL] = 5 g L^{-1}, pH = 10) with time. Scale bar = 1 cm. (b) Optical microscope images of the above emulsion once creaming halted.
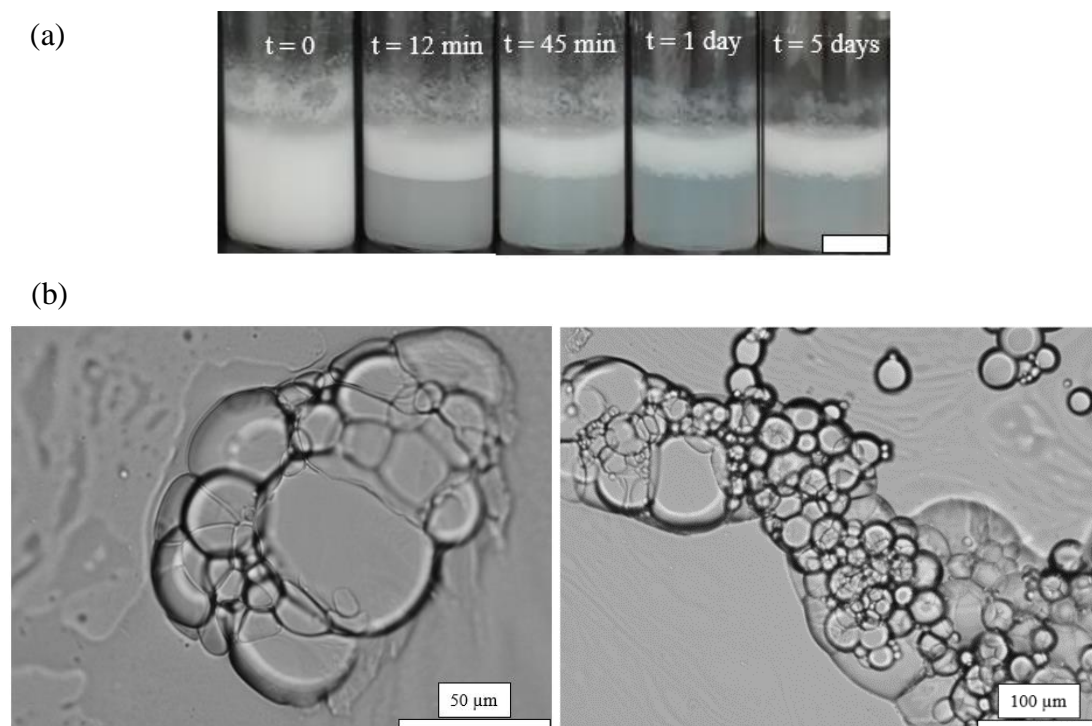
Figure 4.26. (a) Appearance of toluene-in-water emulsion ($\phi_o = 0.20$, added stepwise) from an aqueous PEC dispersion ($x_{PAANa} = 0.5$, [PEL] = 5 g L^{-1}, pH = 10) with time. Scale bar = 1 cm. (b) Optical microscope images of the above emulsion once creaming halted.

(a)

(b)

4.6 Agreement between observed and predicted morphologies *via* determination of spreading coefficients

In microencapsulation, complex coacervates are used to encapsulate hydrophobic core materials (oil drops or solid particles). In order to form core/shell drops (as here), the coacervate phase needs to coat the oil drops resulting in a composite emulsion of oil drops contained within larger coacervate drops. In principle, this coating could occur either by (i) spreading of the coacervate phase at the oil-water interface forming a thin coacervate film with the shell building up by further growth *via* coalescence of additional coacervate droplets or (ii) individual coacervate droplets surround the oil core without spreading such that the shell is formed by sequential wetting with additional coacervate droplets until a shell is obtained.[3] Two immiscible liquid drops (here oil and coacervate) surrounded by a third immiscible liquid (here water) may form a range of equilibrium configurations depending on the various interfacial tensions (γ) and spreading coefficients (S), see equations 4.2 to 4.4.[9] Based on

equilibrium interfacial energy considerations and depending on the sign combinations of the three spreading coefficients, three different scenarios are predicted as depicted in Figure 4.2: complete engulfing, partial engulfing and non-engulfing of the coacervate phase around oil drops in water. At fixed values of γ_{oc} (oil-coacervate) and γ_{wc} (water-coacervate), an increase in γ_{ow} (oil-water) is predicted to promote complete engulfing (from either non- or partial engulfing).

For the oils tested in this study, examples of complete engulfing (dodecane and toluene) and non-engulfing (isopropyl myristate and squalane) have been encountered. However, additional parameters including the viscosity of the coacervate phase affect the kinetics of spreading and, if the shell material possesses shear elasticity, this can actually result in a resistance to spreading. It was further demonstrated that three-phase wetting in coacervate-containing systems depends not only on interfacial energies but on the character of the flow process; a coacervate drop approaching an oil drop in water initially wets and then de-wets the oil-water interface whereas an oil drop in a coacervate phase when released from a needle can penetrate the coacervate-water interface forming a stable compound drop.[3]

In order to evaluate whether the experimental findings are in line with theoretical predictions, S_o, S_w and S_c have been calculated from knowledge of the respective interfacial tensions as explained earlier. For these, γ_{aw} was 71.9 ± 0.2 mN m^{-1} at 25 ºC, in good agreement with the best literature value.[38] The value of γ_{ao} for each oil is shown in Table 4.1. The static contact angles θ_{aw} and θ_{ao} are measured by placing a drop of water or oil in air onto a glass slide coated by the coacervate phase. The film of coacervate phase placed on the glass slide after water removal was completely transparent and homogeneous. For a water drop, θ_{aw} was 49.6º. All the selected oils appeared by eye to spread completely so θ_{ao} is considered to be < 5º. In order to determine γ_{ac}^d and γ_{ac}^p, values of γ_{al}^d and γ_{al}^p for the different test liquids are given in Table 4.2 together with the air-liquid contact angles on a glass slide covered with the coacervate phase.

Table 4.1. Measured surface and interfacial tensions for the different oils (γ_{ao}, γ_{ow}) and calculated surface energy of the oil-coacervate interface, γ_{oc}. Calculated spreading coefficients, S, for the different scenarios together with the predicted and observed morphology of oil droplets in water in the presence of coacervate phase.

Oil	γ_{ow}/mN m^{-1}	γ_{ao}/mN m^{-1}	γ_{oc}/mN m^{-1}	S_o/mN m^{-1}	S_w/mN m^{-1}	S_c/mN m^{-1}	Predicted	Observed
Dodecane	52.5 ± 2.0	24.7 ± 0.3	26.2 ± 0.8	-74.5 ± 6.1	-30.5 ± 2.5	22.8 ± 1.8	Complete engulfing	Complete engulfing
Toluene	36.1 ± 1.4	28.0 ± 0.1	22.9 ± 0.6	-54.8 ± 4.5	-17.4 ± 1.4	9.0 ± 0.7	Complete engulfing	Complete engulfing
Isopropyl myristate	28.8 ± 0.7	28.2 ± 0.1	22.7 ± 0.6	-47.3 ± 3.6	-10.3 ± 0.8	1.89 ± 0.1	Complete engulfing	Non-engulfing
Squalane	52.5 ± 0.6	28.3 ± 0.1	22.6 ± 0.6	-70.9 ± 5.1	-34.1 ± 2.5	25.7 ± 1.9	Complete engulfing	Non-engulfing
PDMS	50.5 ± 0.8	20.4 ± 0.1	30.5 ± 0.8	-76.8 ± 5.6	-24.2 ± 1.7	15.8 ± 1.1	Complete engulfing	Complete engulfing

Table 4.2. Values of dispersion component (γ_{al}^d), polar component (γ_{al}^p) and γ_{al} for the test liquids used at 25 ºC (taken from ref. 16) and three-phase liquid-air contact angles measured through the liquid on the surface of a glass slide covered with coacervate phase.

Liquid	Tension/mN m⁻¹			$\theta_{al}/°$
	γ_{al}^d	γ_{al}^p	γ_{al}	
Water	21.8	51.0	72.8	50 ± 3
Glycerol	34.0	30.0	64.0	55 ± 9
Formamide	39.0	19.0	58.0	38 ± 5
α-Bromonaphthalene	44.4	0.0	44.4	27 ± 3
Hexadecane	27.8	0.0	27.8	< 5

The least squares calculation was carried out to determine the best combination of γ_{ac}^d and γ_{ac}^p that fits all the data simultaneously. The 3-D surface energy diagram so obtained is shown in Figure 4.27. The values that best fit all the contact angles are read from the coordinates of the peak. These values are $\gamma_{ac}^d = 39.3$ mN m⁻¹ and $\gamma_{ac}^p = 11.6$ mN m⁻¹ so that $\gamma_{ac} = 50.9$ mN m⁻¹. In comparison, the surface energy of hydrophilic Crown glass was estimated to be 76 mN m⁻¹,[16,39] whereas that for PTFE was estimated to be 18 mN m⁻¹.[16] Our value for the coacervate phase indicates it is partially hydrophobic originating from its relatively high dispersion component.

Figure 4.27. 3-D surface energy plot for the coacervate phase as a function of the possible values of γ_{ac}^d and γ_{ac}^p. The ordinate represents the goodness of fit to contact angles.
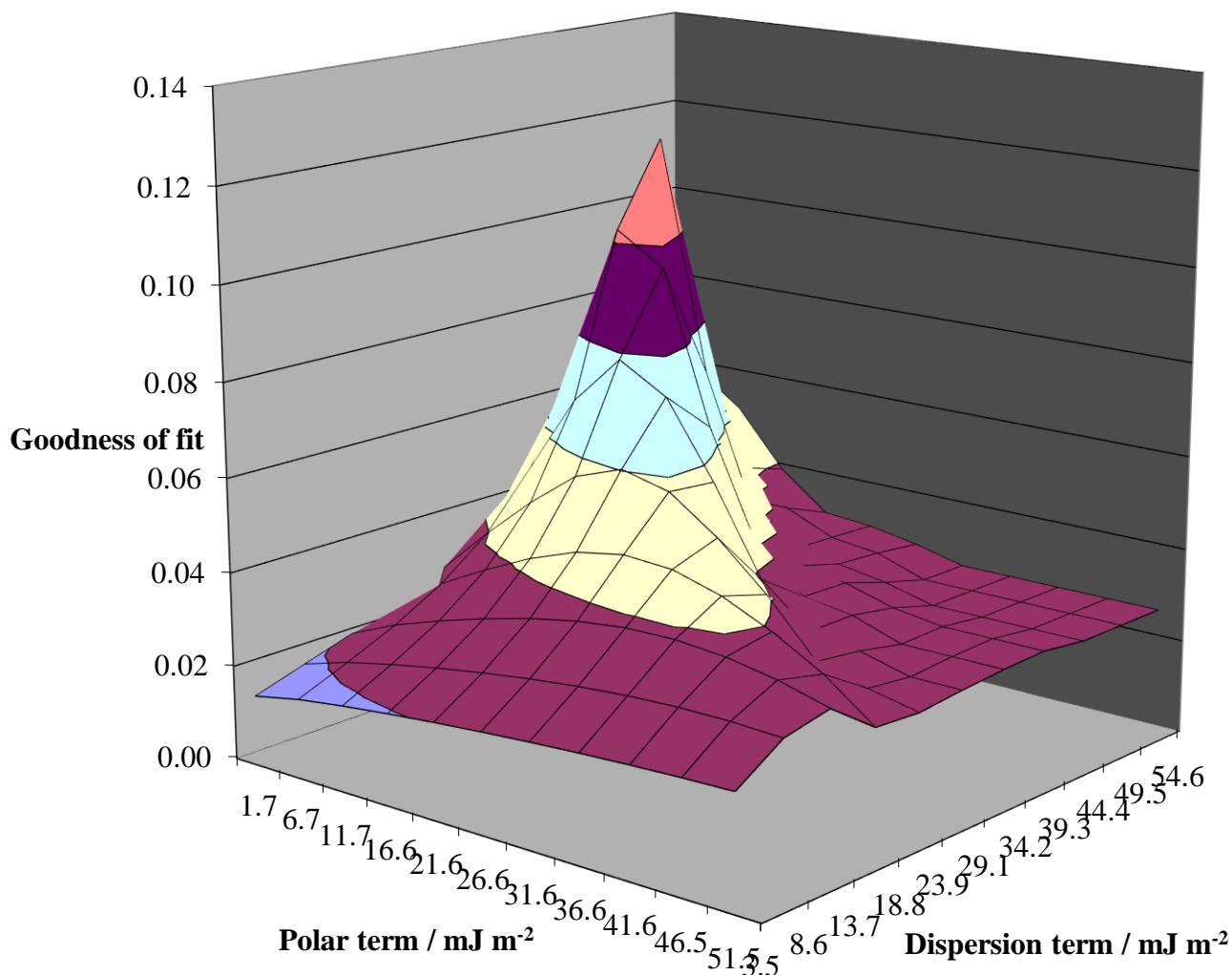
By solving equation 4.9 with the given data, $\gamma_{wc} = 4.2 \pm 0.3$ mN m^{-1}. This is broadly in agreement with the low values for the interfacial tension of the coacervate phase against the continuous aqueous phase in the literature. However, they tend to be smaller.[6-8] With our calculated value of γ_{wc}, the assumption of $\gamma_{wc} < \gamma_{ow}$ stated in the introduction is confirmed. Further, by solving equation 4.10 for each oil, values for γ_{oc} can be calculated (Table 4.1). They are around 25 mN m^{-1} and do not change much with oil type. Finally, by substituting the values of γ_{ow}, γ_{wc} and γ_{oc} into equations 4.2 to 4.4, the values of S_o, S_w and S_c can be calculated for each oil and these are also given in Table 4.1. For dodecane and toluene, the combination of the three spreading coefficients fulfil the condition for complete engulfing observed experimentally.

However, for isopropyl myristate and squalane the predicted morphology is complete engulfing although the emulsion was destabilised in less than 2 h. For PDMS, even if the optical microscope images of the freshly prepared emulsion showed oil droplets surrounded by the coacervate phase, the emulsion was broken 1 day after preparation. In these cases the prediction does not reflect the observed morphology. It is found however, that agreement between predicted and observed morphology is not always fulfilled.[9-11] Torza and Mason[9] found discrepancies in systems when some spreading coefficients were quite small (related to the errors in measuring interfacial tensions). Tasker *et al*.[11] also noted the discrepancy between the predicted and observed morphologies when one of the spreading coefficients was close to 0. It is important to mention that this analysis uses as a substrate a dried coacervate phase which may possess a surface energy different to that of a hydrated one formed *in situ* in water.

4.7 Conclusions

In aqueous mixtures of a strong (PDADMAC) and a weak (PAANa) polyelectrolyte, both precipitation and coacervation occur as a result of associative phase separation which is dependent on pH. The progression coacervate - precipitate/coacervate - coacervate occurs upon increasing the pH as PAANa becomes charged. Although precipitates are expected to be formed when the interactions between the PEL are strong, at high pH when both polymers are fully ionised complex coacervation yielding droplets in water occurs at all mixing ratios. The weak interaction is explained by the formation of hydrogen bonds between water molecules and carboxylate groups in PAANa that weaken the electrostatic interaction with the quaternary amine groups in PDADMAC.

Regarding emulsions prepared from aqueous PEC dispersions, no stable emulsion was possible at low and intermediate pH where coacervate droplets or coacervate droplets and solid particles coexist exhibiting positive values of the zeta potential. This could be a result of their relatively low amount, their considerable size or their intrinsic hydrophilicity. By contrast, at higher pH between 7 and 10, stable dodecane-in-water emulsions could be formed from the coacervate phase of near neutral charge if oil is added sequentially. Oil droplets coated by the coacervate phase are observed. The morphology of the oil droplets coated by the coacervate phase is compared with theoretical predictions using equilibrium spreading coefficients for a range of oils. Despite the agreement for dodecane and toluene (complete engulfing), a discrepancy is found for the other oils. It is suggested that kinetic aspects linked to the viscosity of the coacervate phase play a role in the encapsulation process which are not accounted for in equilibrium spreading coefficients.

4.8 References

1. H.G. Bungenberg de Jong and H.R. Kruyt, *Proc. K. Med. Akad. Wetershap.*, 1929, **32**, 849-856.

2. N. Devi, M. Sarmah, B. Khatun and T.K. Maji, *Adv. Colloid Interface Sci.*, 2017, **239**, 136-145.

3. G. Dardelle and P. Erni, *Adv. Colloid Interface Sci.*, 2014, **206**, 79-91.

4. C. Thies, *Encapsulation and Controlled Release Technologies in Food Systems*, ed. J.M. Lakkis, Wiley Blackwell, Oxford, 2nd edn., 2016, ch. 3.

5. G.T. Barnes and I.R. Gentle, *Interfacial Science: An introduction*, Oxford University Press Inc., New York, 2005, pp. 8-15.

6. E. Spruijt, J. Sprakel, M.A. Cohen Stuart and J. van der Gucht, *Soft Matter*, 2010, **6**, 172-178.

7. D. Priftis, R. Farina and M. Tirrell, *Langmuir*, 2012, **28**, 8721-8729.

8. J. Qin, D. Priftis, R. Farina, S.L. Perry, L. Leon, J. Whitmer, K. Hoffmann, M. Tirrell and J.J. de Pablo, *ACS Macro Lett.*, 2014, **3**, 565-568.

9. S. Torza and S.G. Mason, *J. Colloid Interface Sci.*, 1970, **33**, 67-83.

10. A. Loxley and B. Vincent, *J. Colloid Interface Sci.*, 1998, **208**, 49-62.

11. A.L. Tasker, J.P. Hitchcock, L. He, E.A. Baxter, S. Biggs and O.J. Cayre, *J. Colloid Interface Sci.*, 2016, **484**, 10-16.

12. C.J. Van Oss, *Interfacial Forces in Aqueous Media*, Marcel Dekker, New York, 1994.

13. F.M. Fowkes, *J. Phys. Chem.*, 1963, **67**, 2538-2541.

14. D.K. Owens and R.C. Wendt, *J. Appl. Polym. Sci.*, 1969, **13**, 1741-1747.

15. J.H. Clint, *Curr. Opin. Colloid Interface Sci.*, 2001, **6**, 28-33.

16. J.H. Clint and A.C. Wicks, *Int. J. Adhes. Adhes.*, 2001, **21**, 267-273.

17. B.P. Binks and A.T. Tyowua, *Soft Matter*, 2013, **9**, 834-845.

18. L. Vitorazi, N. Ould-Moussa, S. Sekar, J. Fresnais, W. Loh, J.-P. Chapel and J.-F. Berret, *Soft Matter*, 2014, **10**, 9496-9505.

19. E.A. Litmanovich, E.V. Chernikova, G.V. Stoychev and S.O. Zakharchenko, *Macromolecules*, 2010, **43**, 6871-6876.

20. J. Choi and M.F. Rubner, *Macromolecules*, 2005, **38**, 116-124.

21. S.E. Burke and C.J. Barrett, *Langmuir*, 2003, **19**, 3297-3303.

22. M. Fang, C.H. Kim, G.B. Saupe, H.-N. Kim, C.C. Waraksa, T. Miwa, A. Fujishima and T.E. Mallouk, *Chem. Mater.*, 1999, **11**, 1526-1532.

23. G.S. Manning, *J. Chem. Phys.*, 1969, **51**, 924-933.

24. J. Koetz and S. Kosmella, *Polyelectrolytes and Nanoparticles*, Springer-Verlag, Berlin, 2007, p. 36.

25. T. Alonso, J. Irigoyen, J.J. Iturri, I.L. Iarena and S.E. Moya, *Soft Matter*, 2013, **9**, 1920-1928.

26. F. Comert, A.J. Malanowski, F. Azarikia and P.L. Dubin, *Soft Matter*, 2016, **12**, 4154-4161.

27. X. Liu, M. Haddou, I. Grillo, Z. Mana, J.-P. Chapel and C. Schatz, *Soft Matter*, 2016, **12**, 9030-9038.

28. V.S. Meka, M.K.G. Sing, M.R. Pichika, S.R. Nali, V.R.M. Kolapalli and P. Kesharwani, *Drug Discovery Today*, 2017, **22**, 1697-1706.

29. P.K. Jha, P.S. Desai, J. Li and R.G. Larson, *Polymers*, 2014, **6**, 1414-1436.

30. V. Starchenko, M. Müller and N. Lebovka, *J. Phys. Chem. B*, 2012, **116**, 14961-14967.

31. J. Koetz and S. Kosmella, Interactions between poly(diallyldimethylammonium chloride) and poly(acrylic acid) in dependence on polymer concentration, presented in part at the International Conference on Scaling Concepts and Complex Fluids, Italy, 1994.

32. P. Atkins and J. de Paula, *Atkins' Physical Chemistry*, 9th edn., Oxford University Press, Oxford, 2010, p. 647.

33. S. Nimesh, A. Saxena, A. Kumar and R. Chandra, *J. Appl. Polym. Sci.*, 2012, **124**, 1771-1777.

34. D.S. Williams, S. Koga, C. Rohaida, C. Hak, A. Majrekar, A.J. Patil, A.W. Perriman and S. Mann, *Soft Matter*, 2012, **8**, 6004-6014.

35. Y. Ishimuro and K. Ueberreiter, *Colloid Polym. Sci.*, 1980, **258**, 928-931.

36. A. Forgiarini, J. Esquena, C. González and C. Solans, *Langmuir*, 2001, **17**, 2076-2083.

37. A.S. Prata and C.R.F. Grosso, *J. Am. Oil Chem. Soc.*, 2015, **92**, 1063-1072.

38. N.R. Pallas and Y. Harrison, *Colloids Surf.*, 1990, **43**, 169-194.

39. B.P. Binks and J.H. Clint, *Langmuir*, 2002, **18**, 1270-1273.

CHAPTER 5 – MIXTURE OF WEAK CATIONIC, PAH, AND STRONG ANIONIC, PSSNa, POLYELECTROLYTES

5.1 Introduction

The polyelectrolyte system reported here is that formed between a weak (PAH) and a strong (PSSNa) polyelectrolyte. As for the system PDADMAC-PAANa discussed in Chapter 4, the pH will play an important role on the strength of the interaction as the degree of ionisation of PAH varies with pH while PSSNa remains fully charged.

The same systematic approach was followed to evaluate the influence of parameters such as the mole fraction of the anionic polyelectrolyte, [PEL] and pH for aqueous PEC dispersions. The type of associative phase separation across the pH range was identified visually and from optical microscope images. PEC particles are obtained at low pH when the oppositely charged polyelectrolytes interact strongly. On the other hand, coacervate droplets are detected at high pH when the electrostatic interaction is considerably weaker. Moreover, the amount of unreacted PEL in aqueous PEC dispersions containing PEC particles was quantified through fluorescence measurements.

The same parameters as for the dispersions were evaluated for emulsions together with the oil volume fraction (ϕ_o). Regarding the x_{PSSNa}, the most stable emulsions possessing the smallest droplet diameter and the lowest amount of oil coalesced, are obtained around charge neutrality. Moreover, emulsions prepared with PEC particles are more stable than those containing coacervate droplets. High internal phase emulsions (HIPEs) up to a ϕ_o equal to 0.85 with high viscosity were prepared with PEC particles as emulsifiers. The formation of HIPEs is not abound in particle-stabilised systems, where catastrophic phase inversion is the usual phenomenon encountered upon increasing the oil:water ratio. Taking advantage from the inherent fluorescence of each PEL, PEC particles could be visualised with any further modification through confocal laser scanning microscopy (CLSM). The interface of dispersed drops was found to be sparsely covered by PEC particles at high ϕ_o, as observed by CLSM and cryo-SEM.

5.2 Potentiometric titration of PAH and degree of ionisation

PSSNa is a strong polyacid and therefore fully ionised at all pH. However, PAH is a weak polybase and consequently its degree of ionisation varies with the pH. A potentiometric titration of a 1 g L^{-1} PAH solution was carried out against NaOH as described in the experimental section. From that, the curve of the degree of ionisation as a function of pH and the pK_a were obtained (Figure 5.1). The black line that connects the filled points corresponds to the derivative of the pH as a function of the volume of titrating agent (dpH/dV). The inset plot in Figure 5.1 displays the curve of the degree of ionisation against the pH and it is obtained from the data of the titration curve. In order to do so, PAH is considered to be fully ionised (degree of ionisation = 100%) at pH = 4.4 (first inflection point) and fully protonated (degree of ionisation = 0%) at pH = 11.6 (when the plateau is reached). Intermediate points at different degrees of ionisation were selected and interpolated in the titration curve to build the full ionisation curve.

The pK_a value for this sample was found to be 8.1, consistent with the literature values ranging from 8 to 9[1,2] but lower than the typical pK_a of an aliphatic amine, *i.e.* its low molecular weight analogue, which is around 10.7.[3] The behaviour of weak polyelectrolytes upon increasing or decreasing the charge density is not comparable to that of simple electrolytes. For PAH, due to the electrostatic repulsion between positively charged groups within the polymer chain, as the amount of protonated amine groups increases it becomes progressively more difficult to protonate.

Figure 5.1. Potentiometric titration of a 1 g L^{-1} PAH solution against 0.1 M NaOH solution (open points). The pH of the initial PAH solution was decreased to ≈ 2.7 with HCl to evaluate the full pH range. The curve that connects the filled points corresponds to the derivative of the pH as a function of the volume of titrating agent (dpH/dV). Inset plot: degree of ionisation *versus* pH obtained from the titration curve together with the structures present at each pH extreme.
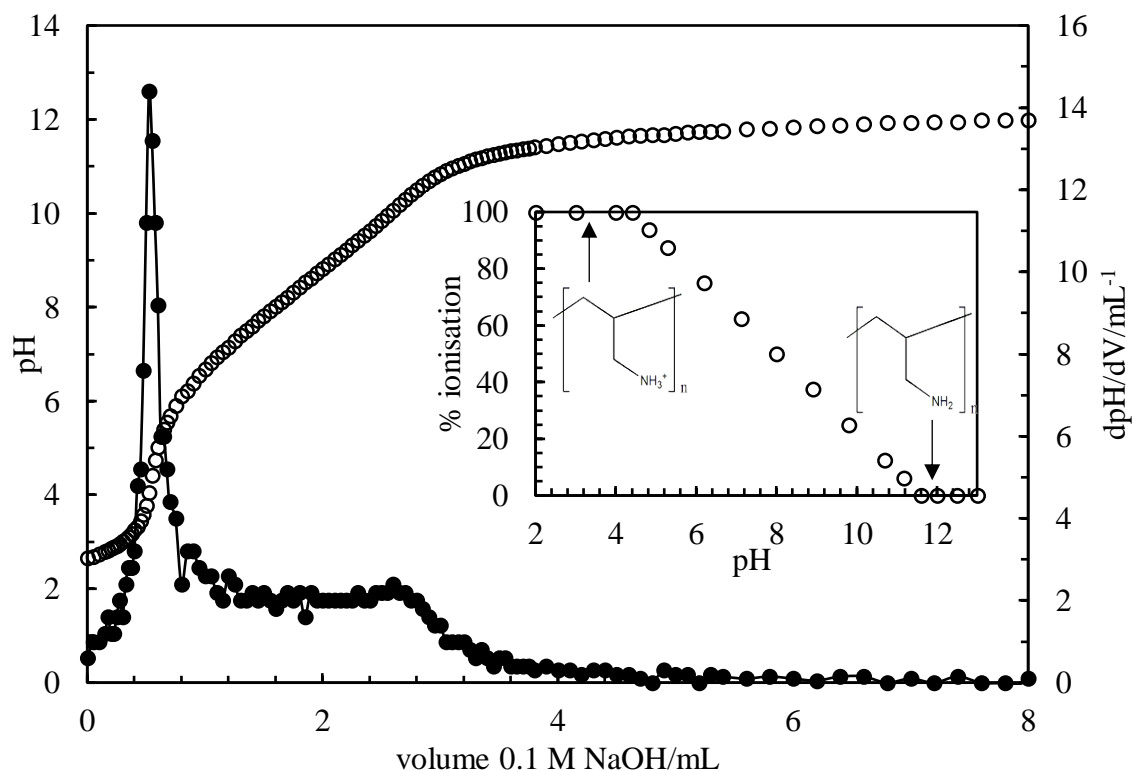
5.3 Characterisation of aqueous PEC dispersions at different pH

5.3.1 Dispersions at low PEL concentration

5.3.1.1 Effect of pH and mole fraction of anionic polyelectrolyte

As mentioned above, the charge of PAH varies with the pH. Consequently, its interaction with PSSNa to form the so-called polyelectrolyte complexes will be significantly affected. This was already posed in Chapter 4 for the system constituted by a strong polybase (PDADMAC) and a weak polyacid (PAANa) after a systematic and comprehensive study over a wide pH range (2 to 10). Therefore, for the analysis of this system at low PEL concentration, three different pH were selected to cover the entire pH range. These were: pH = 2, unmodified pH and pH = 10. The % ionisation of PAH is considered to be 100% and 25% for pH = 2 and 10, respectively, taken from

the curve of the degree of ionisation in Figure 5.1. The pH of a 0.1 g L^{-1} PAH solution at unmodified pH is 4.80, which relates to a degree of ionisation of ~ 93%. Across all pH, PSSNa will be fully ionised (100%).

Aqueous PEC dispersions were first characterised in terms of their average diameter and zeta potential. The appearance of aqueous PEC dispersions prepared from 0.1 g L^{-1} PEL solutions at different x_{PSSNa} and pH is shown in Figure 5.2. In general, all aqueous PEC dispersions and solutions of the neat polymers are transparent and colourless. However, at pH = 10 a few dispersions appear bluish (x_{PSSNa} = 0.34 and 0.47) or show signs of precipitation (x_{PSSNa} = 0.67). The pH of the resulting aqueous PEC dispersions was measured after preparation. For pH = 2 and 10 the pH did not vary considerably compared to that of the individual PEL solutions. In contrast, for aqueous PEC dispersions prepared at unmodified pH, the pH varied from 5.09 to 5.84 due to the differences in the pH of each PEL solution (pH = 5.68 for the 0.1 g L^{-1} PSSNa solution). However, for sake of simplicity, a pH ~ 5.5 and consequently a degree of ionisation of PAH of ~ 85% was assigned to all aqueous PEC dispersions at unmodified pH.

Figure 5.2. Appearance of aqueous PEC dispersions prepared at different pH and x_{PSSNa} (given) from 0.1 g L^{-1} PEL solutions of PAH and PSSNa. Photos taken after preparation. Scale bar = 1 cm.
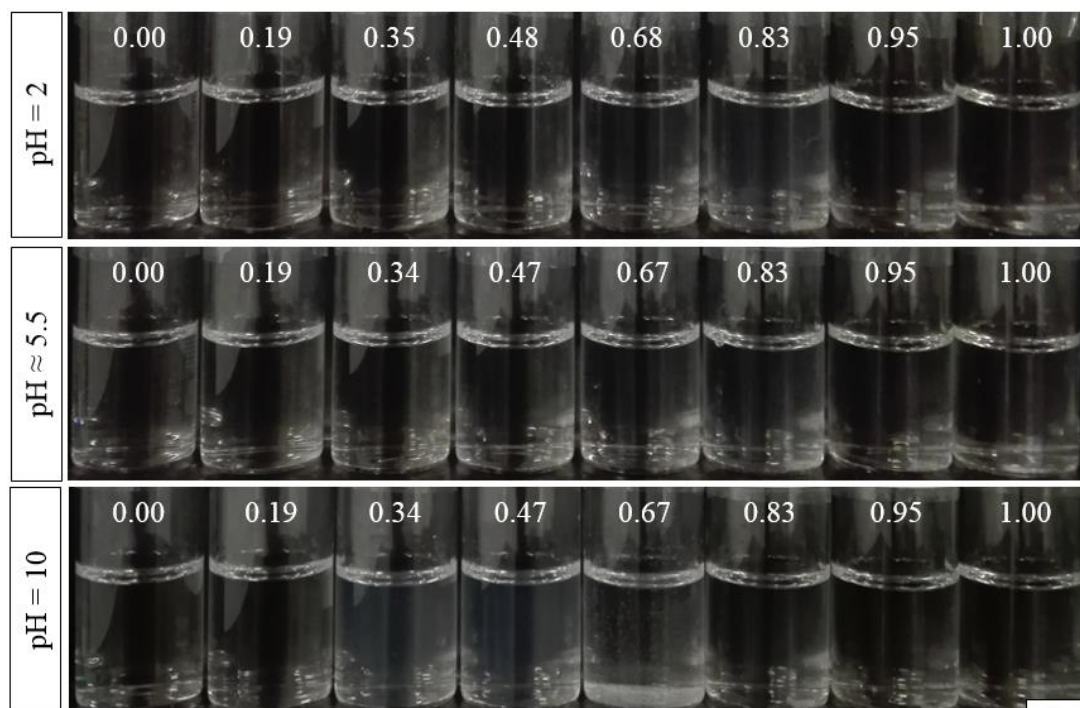
The average diameter and zeta potential of the entities present in the above dispersions was measured and are shown in Figure 5.3 at different pH. For the three pH, the plot of the average diameter *versus* the x_{PSSNa} displays a maximum. At unmodified pH (~ 5.5), the result for the $x_{PSSNa} = 0.83$ was not included as the value obtained from the three repetitions was not reproducible, despite being higher than the rest (~ 450 nm). As mentioned in Chapter 3 and 4, after carefully examine the literature dealing with different polyelectrolyte combinations, one can come to the conclusion that there is no full agreement about the dependence of the particle size on the mixing ratio. In some cases,[4,5] the plot displays a minimum around the point of charge neutralization, while other authors[6,7] report that the largest size is achieved when all the charges are compensated.

The plot of the zeta potential against the x_{PSSNa}, displays a sigmoidal shape with positive and negative values for the three pH (Figure 5.4). The sign reversal occurs at a relatively high x_{PSSNa} and it is linked to the maximum displayed in the average diameter plot. This could be explained by the differences in the molecular weight of the two polyelectrolytes (Table 2.1). The M_w of PSSNa (75 kDa) is half of that of PAH (120-200 kDa) so a higher amount of sulfonate groups must be available to achieve charge neutralisation. This is in line with the results presented in Chapter 3. The zeta potential was measured for the system PDADMAC-PSSNa to assess the effect of the M_w of PSSNa (148 kDa and 976 kDa) by keeping constant the M_w of PDADMAC (160 kDa). The x_{PSSNa} of sign reversal occurred at a lower value when the differences in the M_w between the two polyelectrolytes were high. Moreover, for the system shown here it is worth noting that the change in the sign of the zeta potential shifts to a lower x_{PSSNa} by increasing the pH, as expected. At pH = 10, the degree of ionisation of PAH is 25%, therefore, a higher amount of protonated amine groups are needed to overcome all the negative charges of PSSNa compared to the situation at pH = 2, where both polyelectrolytes are fully ionised. This supports the findings presented in Chapter 4 for the system PDADMAC-PAANa, where the change in the sign of the zeta potential occurred at lower x_{PAANa} as the pH increased.

Figure 5.3. Variation of the average particle diameter with x_{PSSNa} for aqueous PEC dispersions prepared from 0.1 g L^{-1} PEL solutions at different pH (given).
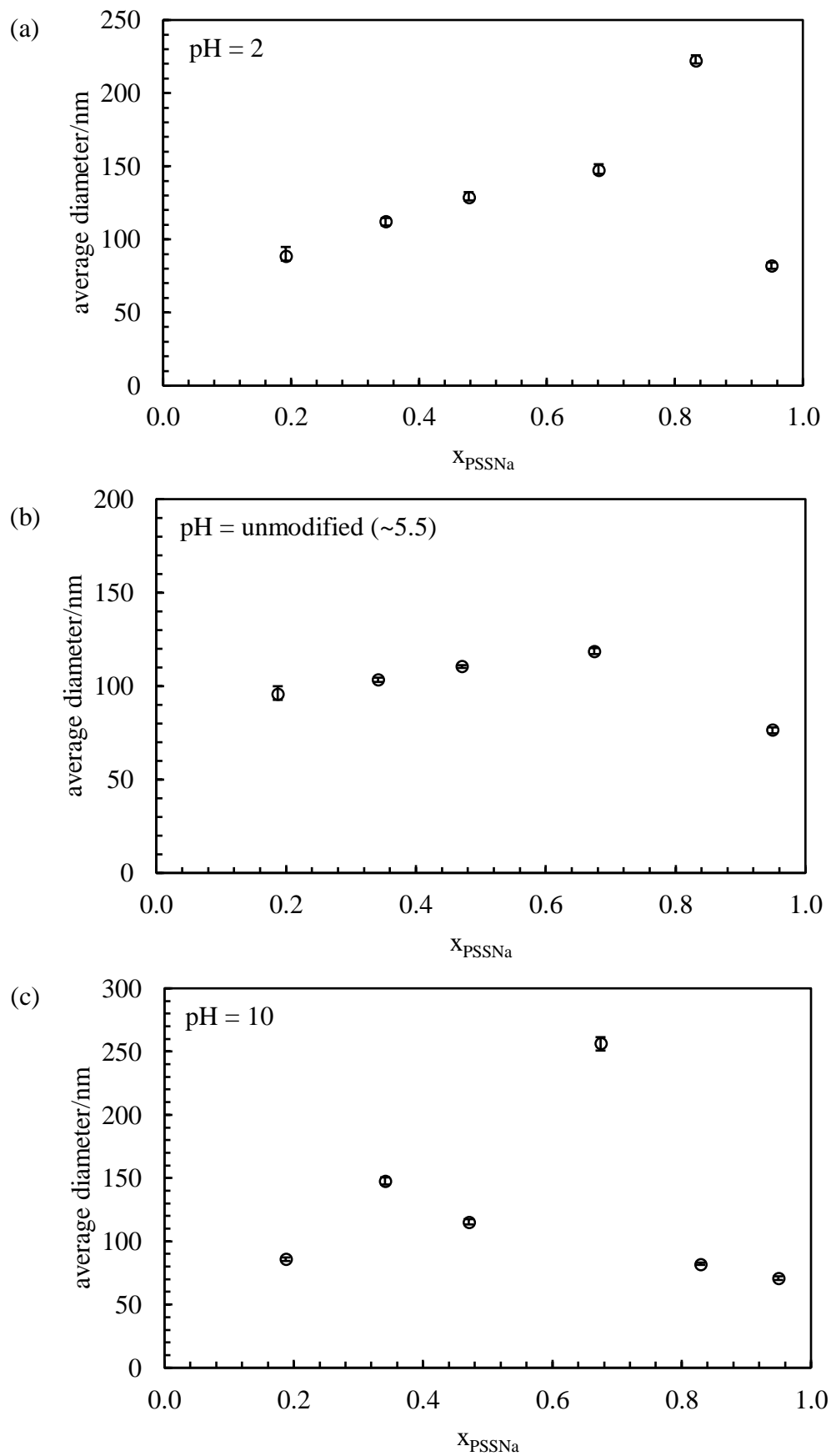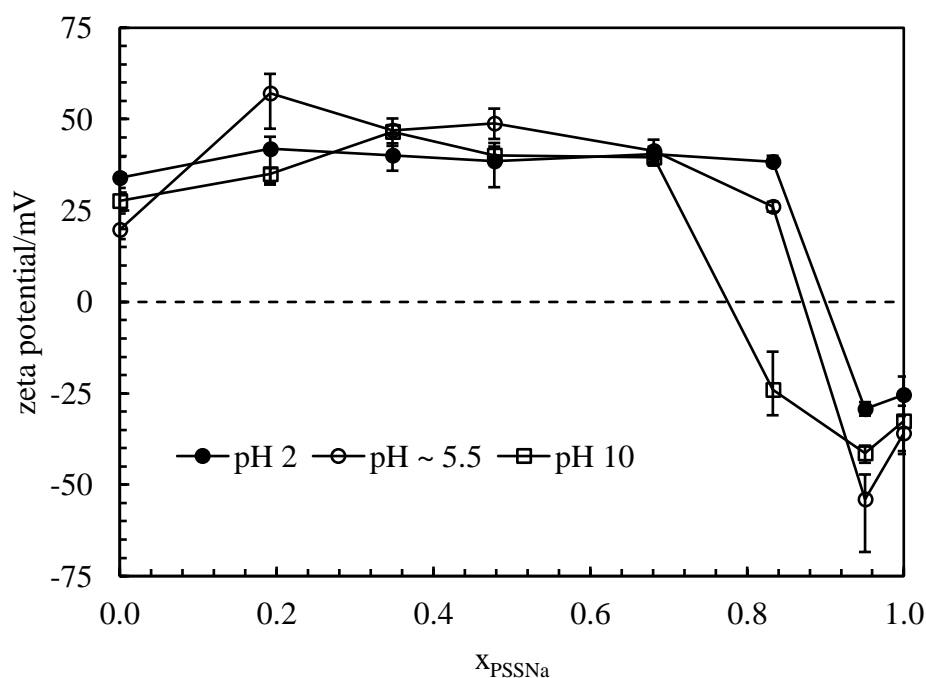
Figure 5.4. Variation of zeta potential with x_{PSSNa} for aqueous PEC dispersions prepared from 0.1 g L^{-1} PEL solutions at different pH (given).


5.3.2 Dispersions at high PEL concentration

5.3.2.1 Effect of pH and mole fraction of anionic polyelectrolyte

The effect of pH and x_{PSSNa} was investigated at high [PEL]. After increasing the [PEL] to 10 g L^{-1}, the appearance of aqueous PEC dispersions in terms of visual inspection at pH = 2, unmodified and 10 changed significantly compared to the one at low [PEL], shown in Figure 5.2. At pH = 2 and unmodified pH (pH of a PSSNa and a PAH solution at this concentration is 4.49 and 3.59, respectively), the appearance is similar so the data for unmodified pH is shown only, Figure 5.5(a). After preparation, at these pH (2 and unmodified) dispersions look turbid, the one prepared at a x_{PSSNa} = 0.83 being the most turbid. This implies a higher volume fraction of PEC compared to the other x_{PSSNa}. Moreover, this mole fraction corresponds to charge neutralisation as probed previously from zeta potential measurements.

Figure 5.5. Appearance of aqueous PEC dispersions prepared from 10 g L^{-1} PEL solutions at pH (a) unmodified (~ 4) and (b) 10 at different x_{PSSNa} (given) for two times. Scale bars = 1 cm. (c) Selected optical microscope images of aqueous PEC dispersions (x_{PSSNa} = 0.48) taken after preparation for unmodified pH (left) and pH = 10 (right).
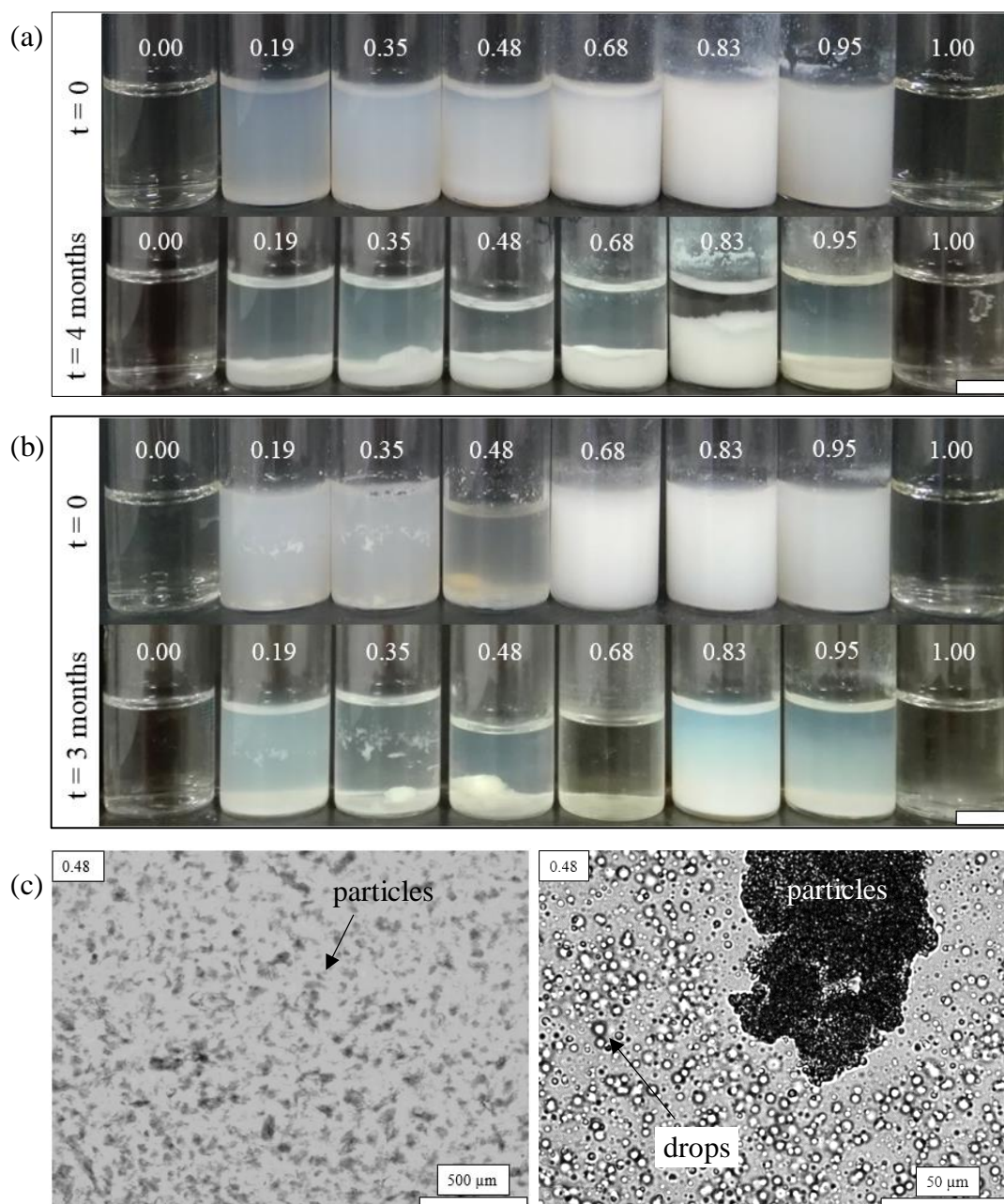
Optical micrographs were taken from all the dispersions and solid particles with irregular shape were observed. An example is shown in Figure 5.5(c, left) for a x_{PSSNa} = 0.48. After two months, particles sediment. The highest sediment is obtained at x_{PSSNa} = 0.83 (as expected), however particles do not seem to be really dense as they

remain partially in suspension. At these pH (2 and unmodified), both PAH and PSSNa are fully ionised. Therefore, a strong electrostatic interaction is expected to occur which is entirely consistent with the formation of a solid-liquid type of phase separation (precipitate).

The appearance of aqueous PEC dispersions prepared at pH = 10 differs significantly to the previous studied pH. A close inspection of the dispersions after preparation through optical microscopy reveals two different types of associative phase separation (precipitation and complex coacervation). At $x_{PSSNa} < 0.83$, both precipitates and coacervate droplets were detected. Moreover, at specific x_{PSSNa} (0.35 and 0.48) PEC particles are highly aggregated and remain glued at the bottom of the vial and around the walls (Figure 5.5(b)). An example showing the coexistence of both solid particles and coacervate droplets is shown in Figure 5.5(c, right). Precipitates have irregular shape while coacervate droplets are spherical and liquid in nature. Co-existence of both coacervate droplets and solid particles was also identified for the system PDADMAC-PAANa at low pH (Chapter 4). Finally, at $x_{PSSNa} = 0.83$ and 0.95, coacervate droplets were detected only. At pH = 10, the degree of ionisation of PSSNa and PAH is 100% and 25%, respectively. Therefore, a weak electrostatic interaction occurs, in line with the formation of coacervate droplets.

Another interesting feature to highlight for the dispersions at pH = 10 is the remarkable change in the stability of PEC coacervates along the time observed at specific mole fractions. For instance, the dispersion at a $x_{PSSNa} = 0.68$, despite initially being the most turbid, only after four hours (data not shown) it turned completely transparent. This is explained by the coalescence of coacervate droplets forming the so-called coacervate phase (a viscous and concentrated polymer phase) that settled down at the bottom of the vial. This x_{PSSNa} is close to charge neutralisation from zeta potential measurements. Moreover, it is worth noting the enhanced stability against coalescence of coacervate droplets in aqueous PEC dispersions prepared at a $x_{PSSNa} = 0.83$ and 0.95. The appearance of the dispersions after two months is still turbid although a clear liquid depleted in coacervate droplets is revealed on the top. Despite the coacervate droplets settling down gently, they are not coalescing with each other as they easily re-disperse recovering the appearance of the initial dispersion. Probably, at a $x_{PSSNa} = 0.68$, coacervate droplets are uncharged so this enhances their coalescence. However, at higher x_{PSSNa}, the surface of coacervate droplets might be negatively charged due to

the excess of PSSNa and this could prevent their coalescence due to electrostatic repulsion. This distinct behaviour regarding the stability of coacervate droplets was already posed in Chapter 4 for the system PDADMAC-PAANa. At pH = 6 coalescence of coacervate droplets occurred with time while from pH = 7 to 10 coacervate droplets were stable to coalescence.

The same study was carried out for two different polyelectrolyte concentrations (1 and 5 g L^{-1} in Figures 5.6 and 5.7, respectively) and the same pattern of behaviour was observed despite the amount of entities was lower *cf.* 10 g L^{-1}.

Figure 5.6. Appearance of aqueous PEC dispersions prepared from 1 g L^{-1} PEL solutions at pH (a) unmodified (~ 5) and (b) 10 at different x_{PSSNa} (given) for two times. Scale bars = 1 cm. (c) Selected optical microscope images of the above aqueous PEC dispersions taken after preparation for unmodified pH (left) and pH = 10 (right) ($x_{PSSNa} = 0.68$).
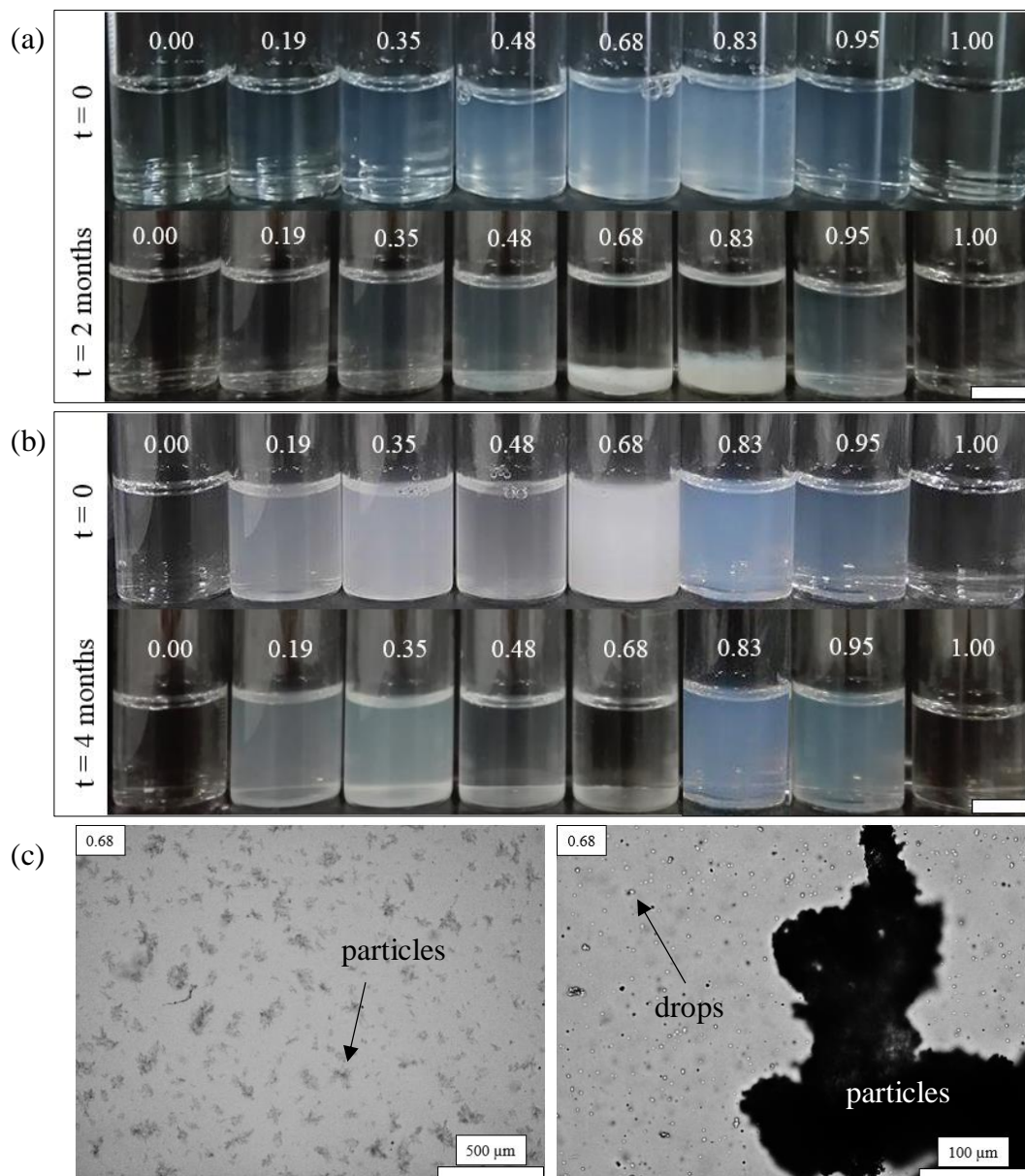
Figure 5.7. Appearance of aqueous PEC dispersions prepared from 5 g L^{-1} PEL solutions at pH (a) unmodified ($\sim$ 4.5) and (b) 10 at different x_{PSSNa} (given) for two times. Scale bars = 1 cm. (c) Selected optical microscope images of the above aqueous PEC dispersions taken after preparation for unmodified pH (left) and pH = 10 (right) (x_{PSSNa} = 0.48).
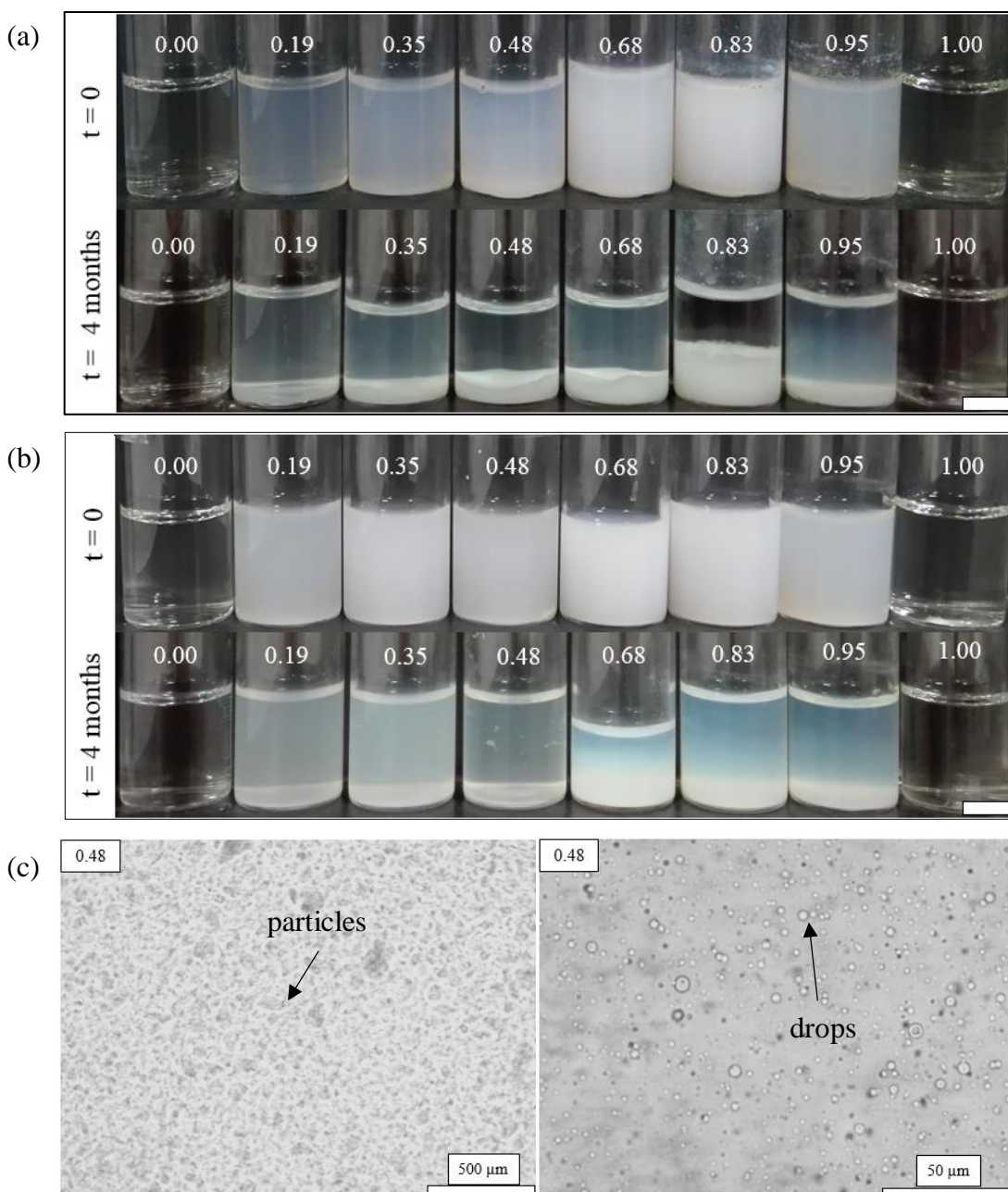
As seen from Figures 5.5(a) and 5.7(a), the amount of PEC particles is maximum at a $x_{PSSNa} = 0.83$ (around charge neutrality) and decreases drastically around this value. It has been decided to determine the amount of unreacted PAH or PSSNa in the supernatant of selected aqueous PEC dispersions to get some information, from an indirect method, about the yield of PEC formation across the x_{PSSNa}. The studied x_{PSSNa} were 0.68, 0.83 and 0.95. Three different volumes (0.5, 1 and 2 mL) of PSSNa and PAH solutions of different concentrations (0.1, 1 and 5 g L^{-1}) were added to the supernatant. For a $x_{PSSNa} = 0.68$, free PSSNa does not seem to be present in the supernatant as it remained completely transparent after the addition of a PAH solution (Figure 5.8(a)). On the contrary, unreacted PAH appears to be in the supernatant as high amounts of PEC particles were formed after the addition of a 5 g L^{-1} PSSNa solution (Figure 5.8(b)). The amount of free PAH was quantified *via* fluorescence measurements by interpolating in the calibration curve the intensity of the sample at $\lambda_{em} = 405$ nm (Figure 5.9). The amount of free PAH was found to be 90.4%.

Figure 5.8. Appearance of vials after the addition of different volumes (given) of (a) PAH and (b) PSSNa solutions of different concentrations (0.1, 1 and 5 g L^{-1} for each line, respectively) into the supernatant separated from an aqueous PEC dispersion ($x_{PSSNa} = 0.68$, [PEL] = 5 g L^{-1}, pH = unmodified) to determine the presence of free PSSNa or PAH in the supernatant. Scale bars = 1 cm.
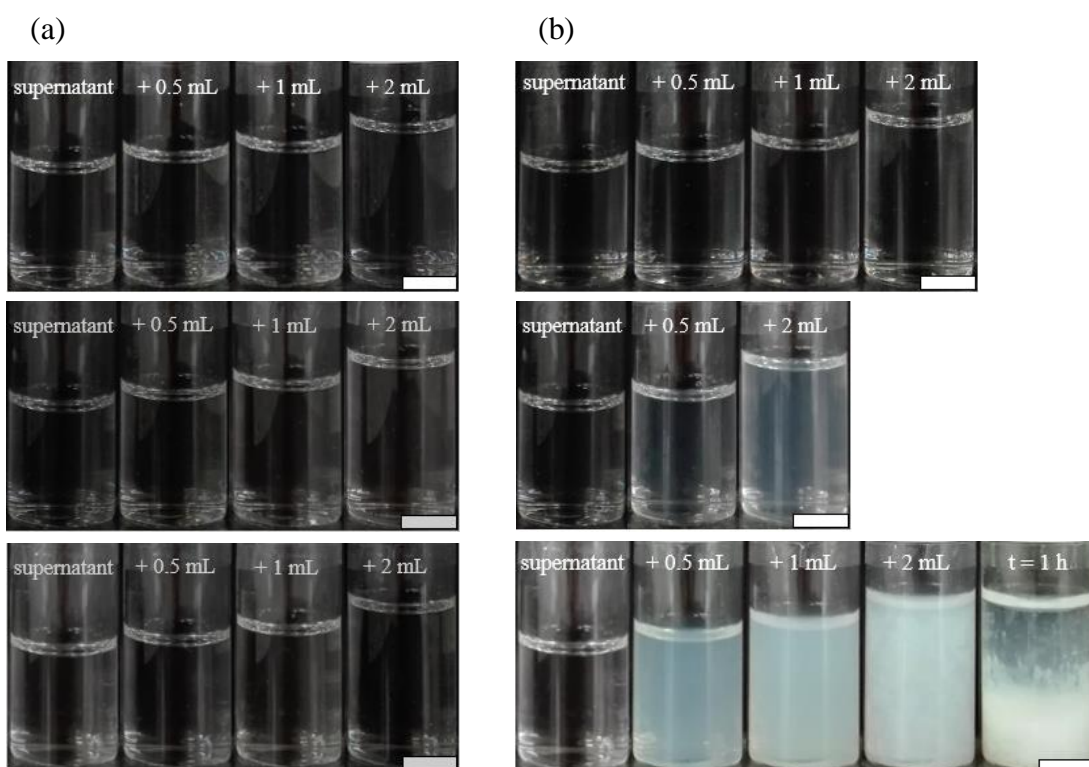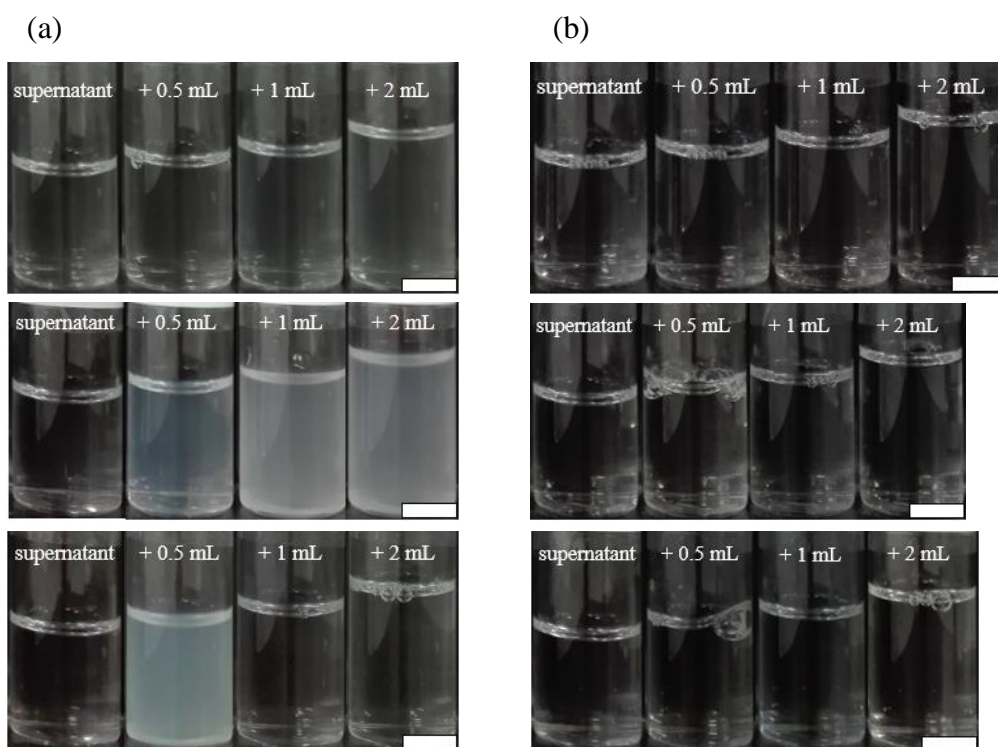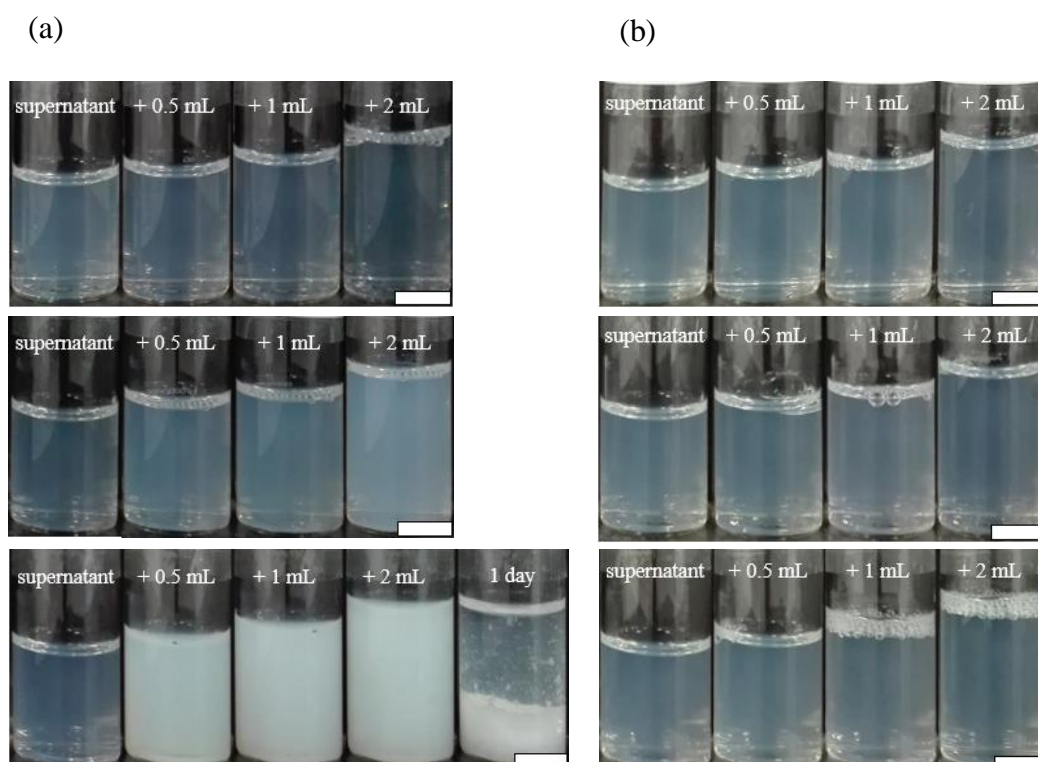
Figure 5.9. (a) Plot of intensity ($\lambda_{ex} = 300$ nm) *versus* wavelength for PAH solutions of different concentrations prepared at unmodified pH. (b) Calibration curve for PAH by plotting the intensity at $\lambda_{em} = 405$ nm against [PAH]. (c) Plot of intensity ($\lambda_{ex} = 300$ nm) *versus* wavelength for the supernatant separated after centrifugation from an aqueous PEC dispersion ($x_{PSSNa} = 0.68$, [PEL] = 5 g L^{-1} pH = unmodified).
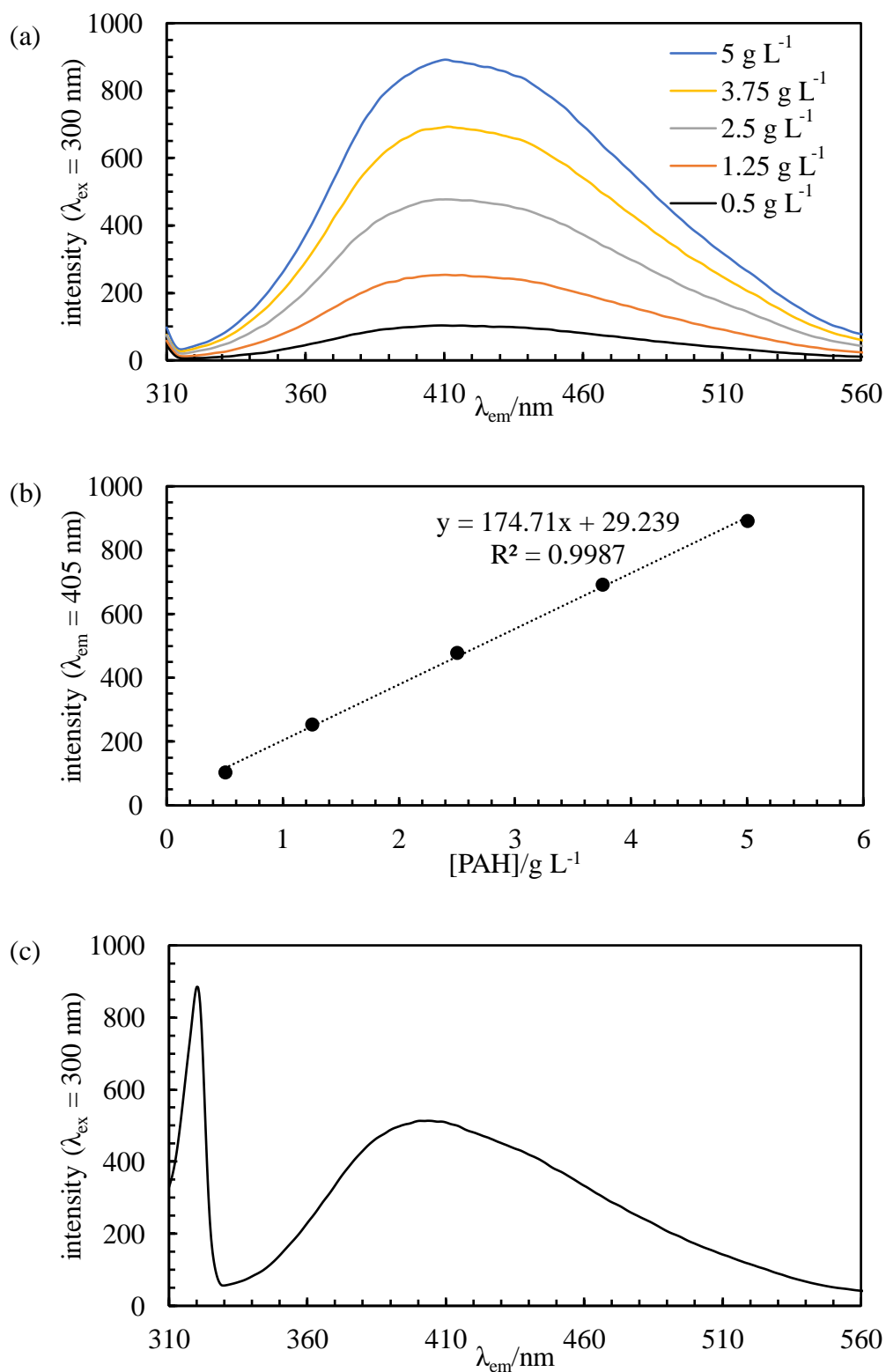
For a x_{PSSNa} = 0.83, residual PSSNa is found in the supernatant as the dispersion turns slightly bluish after the addition of specific volumes and concentrations of PAH (Figure 5.10(a)). The amount of free PSSNa was estimated to be 0.4% from fluorescence measurements (Figure 5.11). Therefore, virtually almost all PSSNa is complexed with PAH.

Figure 5.10. Appearance of vials after the addition of different volumes (given) of (a) PAH and (b) PSSNa solutions of different concentrations (0.1, 1 and 5 g L^{-1} for each line, respectively) into the supernatant separated from an aqueous PEC dispersion (x_{PSSNa} = 0.83, [PEL] = 5 g L^{-1}, pH = unmodified) to determine the presence of free PSSNa or PAH in the supernatant. Scale bars = 1 cm.

Figure 5.11. (a) Plot of intensity (λ_{ex} = 300 nm) *versus* wavelength for PSSNa solutions of different concentrations prepared at unmodified pH. (b) Calibration curve for PSSNa by plotting the intensity at λ_{em} = 382 nm against [PSSNa]. (c) Plot of intensity (λ_{ex} = 300 nm) *versus* wavelength for the supernatant separated after centrifugation from an aqueous PEC dispersion (x_{PSSNa} = 0.83, [PEL] = 5 g L^{-1}, pH = unmodified).
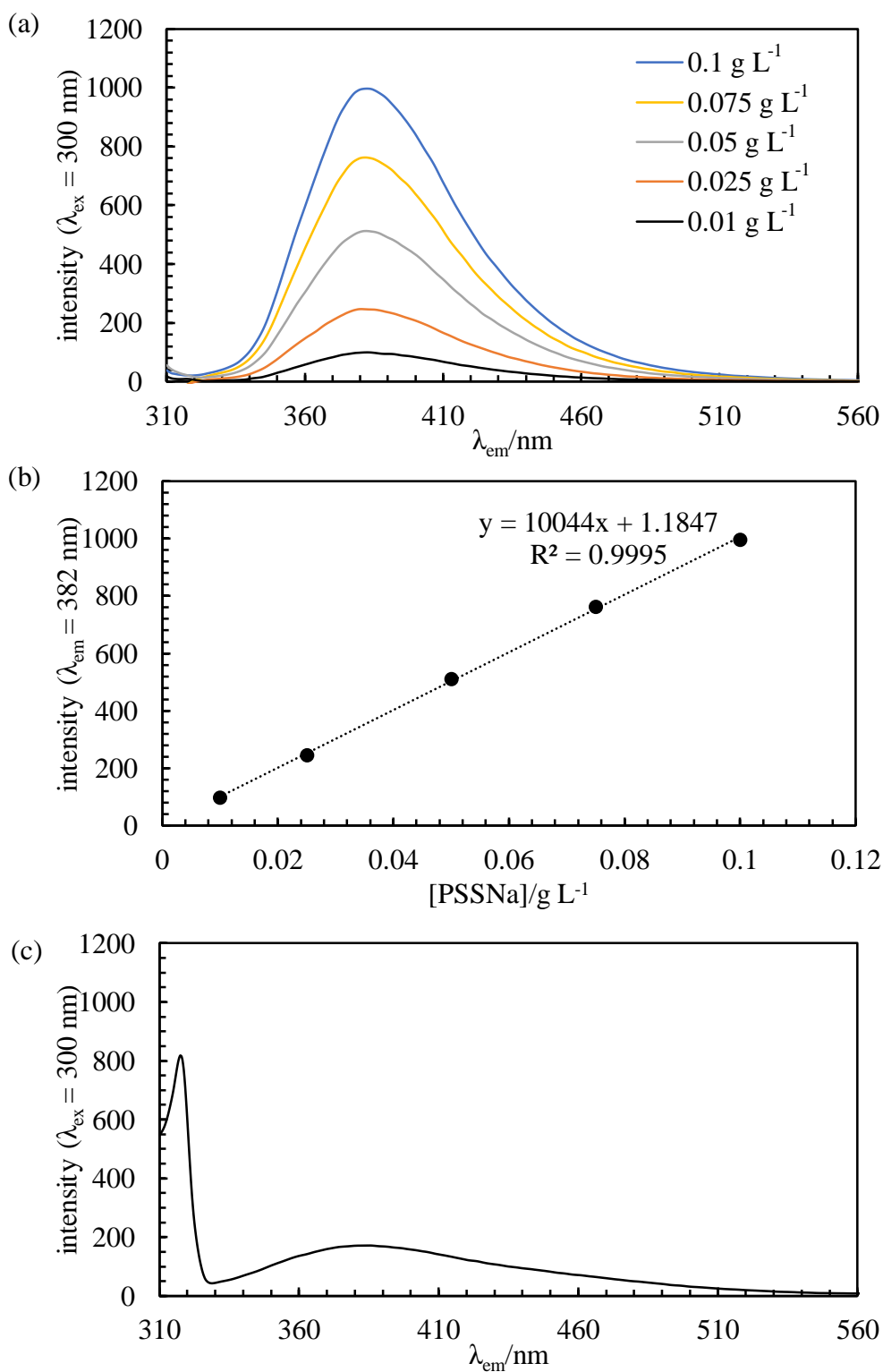
Finally, for a $x_{PSSNa} = 0.95$ unreacted PSSNa is detected in the supernatant, as after the addition of PAH high amounts of PEC particles are formed (Figure 5.12). Unlike the other supernatants (Figure 5.8 and 5.10), this one was already a bit bluish. The amount of free PSSNa estimated from fluorescence measurements was found to be 66%.

Therefore, for a x_{PSSNa} equal to 0.68, 0.83 and 0.95, the amount of free PSSNa is found to be 0%, 0.4% and 66%, respectively.

Figure 5.12. Appearance of vials after the addition of different volumes (given) of (a) PAH and (b) PSSNa solutions of different concentrations (0.1, 1 and 5 g L^{-1} for each line, respectively) into the supernatant separated from an aqueous PEC dispersion ($x_{PSSNa} = 0.95$, [PEL] = 5 g L^{-1}, pH = unmodified) to determine the presence of free PSSNa or PAH in the supernatant. (c) Plot of intensity ($\lambda_{ex} = 300$ nm) *versus* wavelength for the supernatant separated from the above aqueous PEC dispersion. The supernatant was diluted 50 times.

(a)　　　　　　　　　　　　　　　　　　(b)

(c)

Figure axis labels: intensity (λ_{ex} = 300 nm) on y-axis (0 to 1200), λ_{em}/nm on x-axis (310, 360, 410, 460, 510)
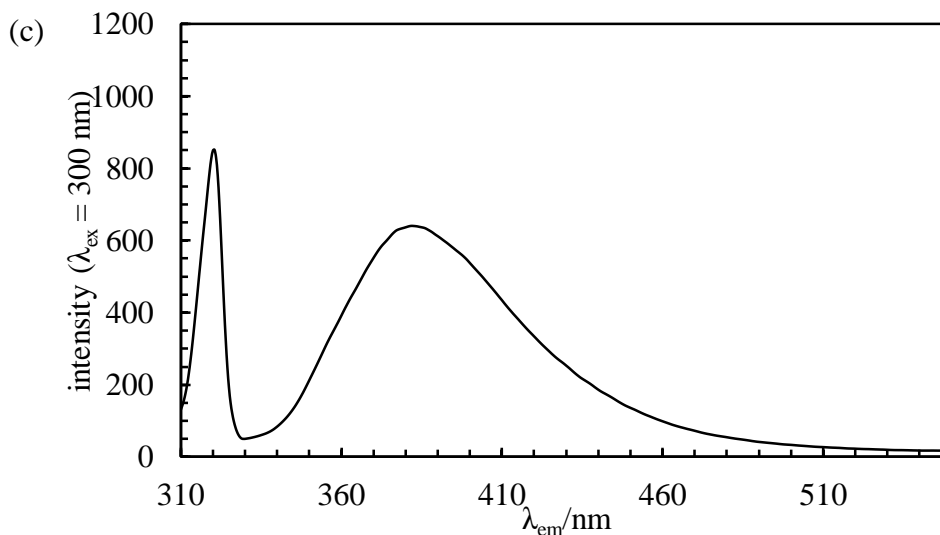
5.3.2.2 Effect of pH at fixed mole fraction of anionic polyelectrolyte

The influence of pH on the formation of PEC was studied in more detail by working at a fixed [PEL] (5 g L^{-1}) and x_{PSSNa} (0.83). The appearance of dispersions prepared at six different pH one day and two months after preparation is shown in Figure 5.13.

Three different patterns of behaviour can be distinguished. From pH 2 to 6, solid particles were only detected both visually and under the optical microscope. Their appearance is the same as the one described previously for aqueous PEC dispersions prepared at pH = 2 and unmodified pH at different x_{PSSNa}. As discussed in the previous section, the degree of ionisation of PAH at these pH is 100%. Consequently, a strong electrostatic interaction is expected to occur with the oppositely charged polyelectrolyte resulting in precipitate formation. At pH = 8 both precipitate and coacervate droplets were identified while at pH = 10 coacervate droplets only were formed. The degree of ionisation of PAH at these pH is lower than 100% and as discussed previously, this weak electrostatic interaction could explain the formation of coacervate droplets. Finally, at pH = 12 a transparent solution is recovered. The degree of ionisation of PAH is 0% so no electrostatic interaction is expected to occur and individual polymer chains remain in solution.

Figure 5.13. Appearance of aqueous PEC dispersions prepared from 5 g L^{-1} PEL solutions ($x_{PSSNa} = 0.83$) at different pH (given). Photos taken (a) 1 day and (b) 2 months after preparation. Scale bars = 1 cm.
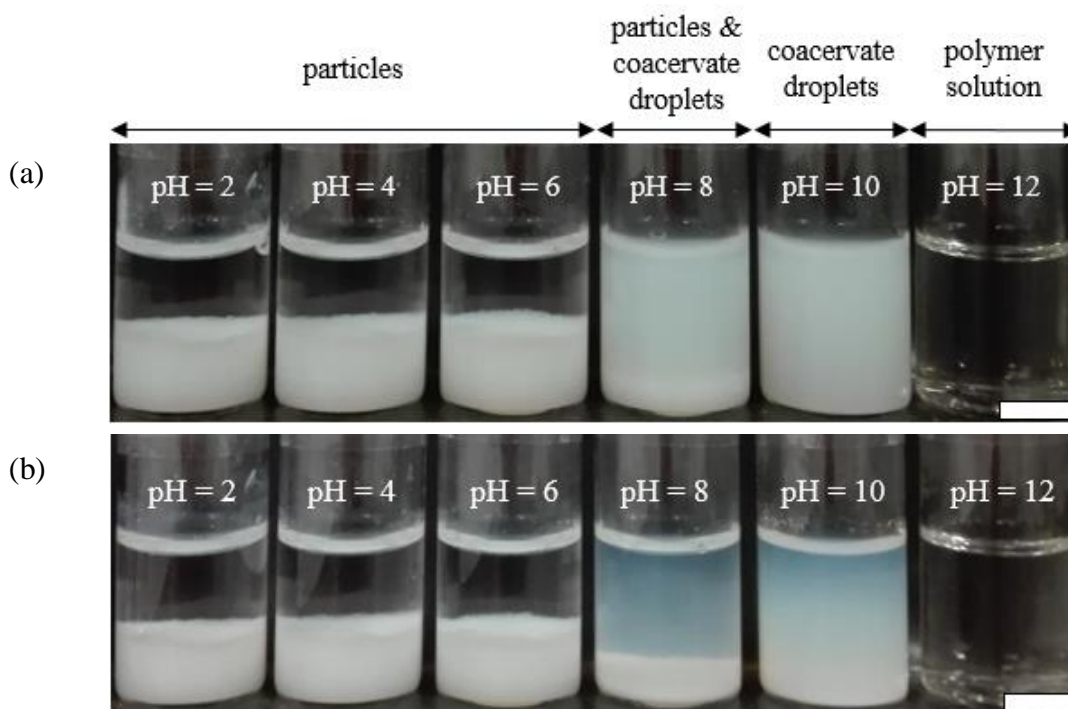
The size distribution of PEC (particles and coacervate droplets) prepared at different pH was measured with the Mastersizer and the Zetasizer. The average particle diameter for each pH is summarized in Table 5.1. From pH 2 to 6, the size distribution is relatively monomodal (span values ~ 1.1) and centred around 16 μm. Moreover, there is not a significant effect of pH. The distribution obtained for pH = 2 is shown in Figure 5.14(a) as an example. Interestingly, the average diameter measured for the PEC obtained at pH = 2 at low polyelectrolyte concentration was in the nanometre range, in contrast to the micrometre range reported here. By increasing the concentration of PEL, the number of complexes can increase at a constant size, larger aggregates can form at fixed number or both scenarios can occur simultaneously. Starchenko *et al.* found that by increasing the PEL concentration for the system PDADMAC-PSSNa, the aggregation of primary particles is accelerated giving rise to an increase in the size of secondary particles.[8] At pH = 8, two distributions were obtained, in agreement with the two types of associative phase separation identified through optical microscopy. The band centred on 202 nm is related to coacervate droplets whereas the second distribution (maximum at 11.2 μm) corresponds to solid

particles (Figure 5.14(b)). At pH = 10 only one band at ~150 nm is displayed, attributed to coacervate droplets (Figure 5.14(c)) while at pH = 12 no distribution was revealed as no complex is formed.

Table 5.1. Average diameter of PEC aggregates obtained from 5 g L^{-1} PEL solutions ($x_{PSSNa} = 0.83$) at different pH.

pH	Average diameter
2	17.9 ± 0.3 μm
4	14.5 ± 0.9 μm
6	14.6 ± 1.3 μm
8	202 ± 48 nm; 11.2 ± 0.6 μm
10	148.7 ± 6.1 nm
12	-

Figure 5.14. Size distributions of PEC obtained from 5 g L^{-1} PEL solutions ($x_{PSSNa} = 0.83$) at pH (a) 2, (b) 8 and (c) 10.

(c)

Size Distribution by Intensity
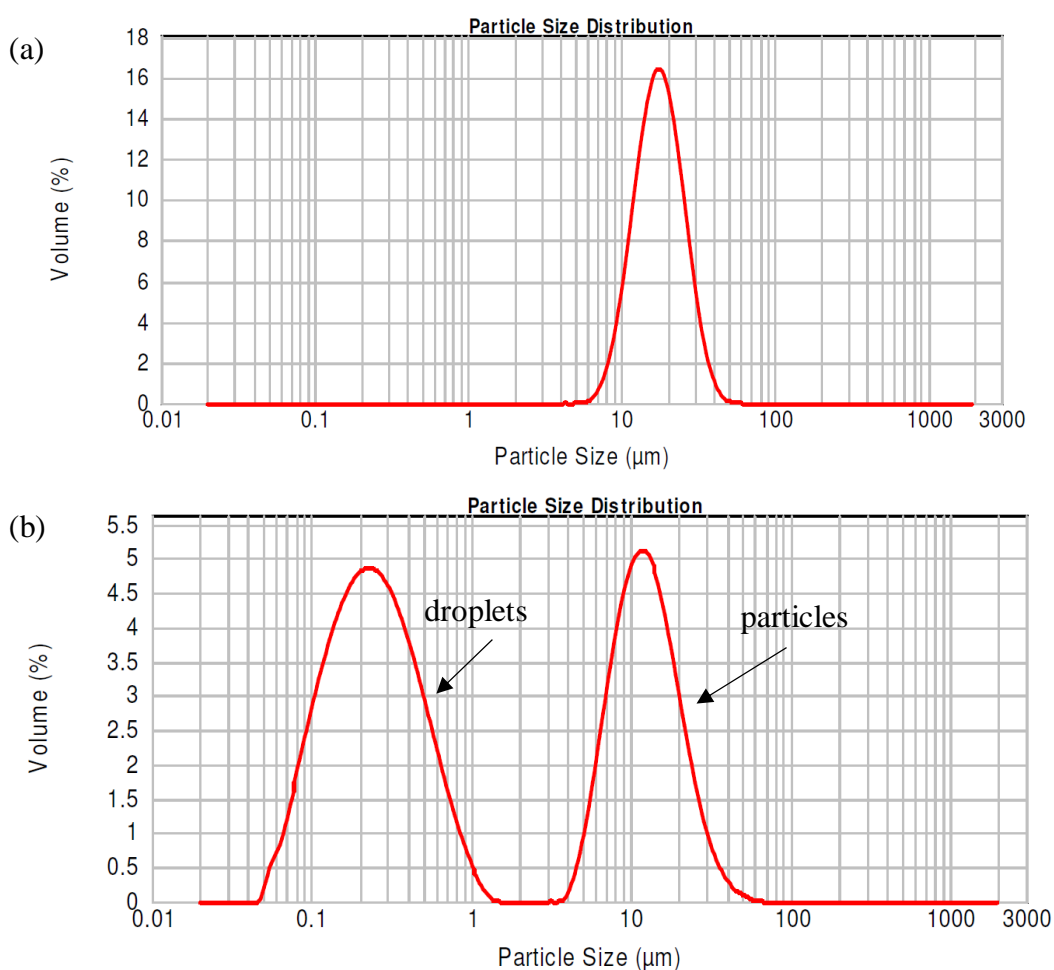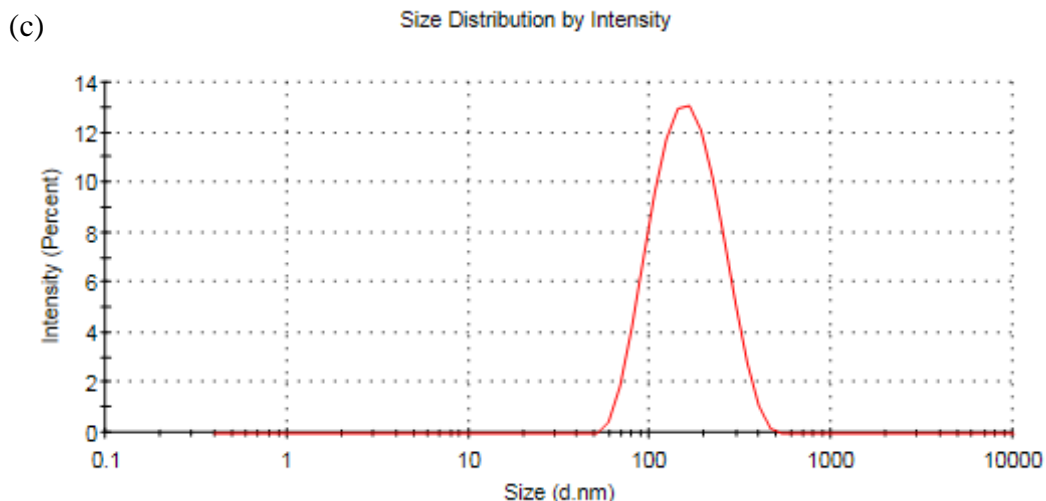
Therefore, as gleaned from this study, the transition precipitate – precipitate and coacervate – coacervate – polymer solution is observed by progressively removing the charge of PAH (increasing the pH). This is the transition expected from the theory. However, for the system PDADMAC-PAANa (Chapter 4), this behaviour was not fully followed as coacervate droplets were formed at high pH when both polyelectrolytes were expected to be fully ionised.

Regarding the long term stability of these aqueous PEC dispersions (Figure 5.13(b)), from pH 2 to 6 particles settled down and the height of the sediment is comparable. At pH = 8 particles sediment but the amount of particles is lower compared to acidic pH. Dispersions at pH = 8 and 10 remain bluish despite a clear liquid depleted in coacervate droplets appears on the top. Therefore, at these two pH coacervate droplets stable to coalescence are formed, in line with the results shown previously.

At the selected x_{PSSNa} (0.83), the charge of the aggregates is expected to change across the pH. Therefore, zeta potential measurements were carried out from these solutions but prepared at lower [PEL] (0.1 g L^{-1}). The zeta potential changes from positive to negative by increasing the pH, as expected (Figure 5.15). At low pH, when both PEL are fully ionised, an excess of positive charge is present as the M_w of PAH is twice that of PSSNa. Then it decreases slightly until it turns negative at pH = 8. From this point onwards, the excess charge is negative as PAH becomes less charged.

Figure 5.15. Plot of zeta potential against pH for aqueous PEC dispersions prepared from 0.1 g L^{-1} PEL solutions ($x_{PSSNa} = 0.83$).
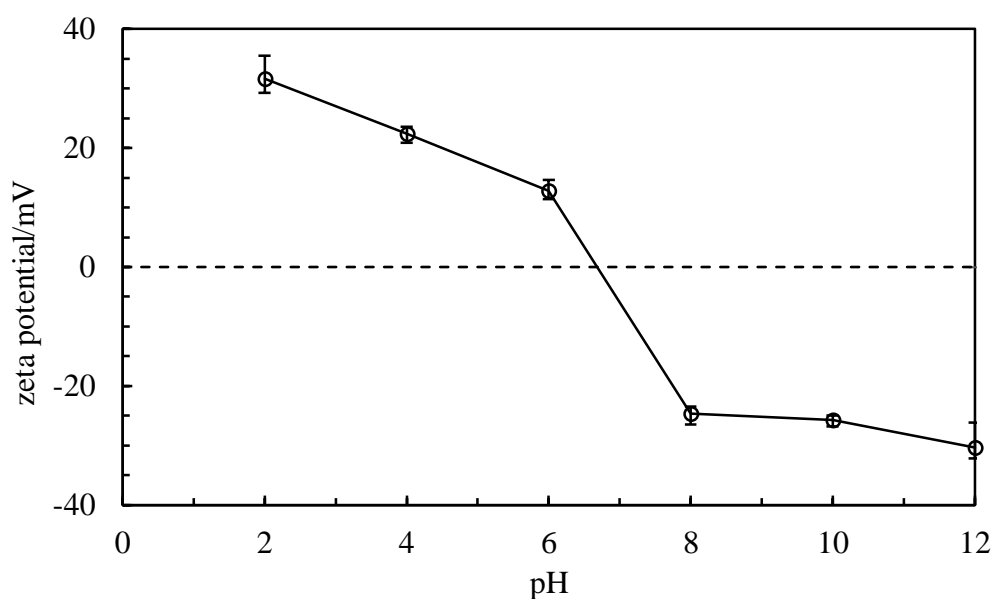
5.3.3   Summary of aqueous PEC dispersions

For aqueous PEC dispersions prepared with PSSNa and PAH, a strong and a weak PEL, respectively, the following behaviour was observed. By increasing the pH, the transition precipitate − precipitate/coacervate − coacervate − polymer solution was found, in agreement with the predicted behaviour. At low pH, both PEL are fully ionised and therefore precipitates arise as a result of strong electrostatic interactions. By increasing the pH, the degree of ionisation of PAH decreases and weak electrostatic interactions ensue, which supports the formation of coacervate droplets. At high pH no complex is formed as PAH is not ionised. For dispersions prepared at a fixed pH and [PEL], the highest amount of PEC entities is obtained around charge neutrality. The amount of complexes formed also increases by increasing the initial polyelectrolyte concentration.

5.4 Oil-in-water emulsions prepared from polymer mixtures

After the complete study identifying the different types of phase separation across the x_{PSSNa} and pH, the ability of preparing emulsions with these dispersions and *n*-dodecane was assessed. Therefore, the parameters evaluated for emulsions are the [PEL], x_{PSSNa} and pH as well as the oil volume fraction. From these results, together with the ones obtained from previous systematic investigations of other polyelectrolyte combinations, we put forward the challenge of envisioning the best conditions to obtain emulsions stabilised with PEC.

5.4.1 Effect of mole fraction of anionic polyelectrolyte on emulsion stability

Emulsions were prepared with *n*-dodecane ($\phi_o = 0.2$) and aqueous PEC dispersions at different x_{PSSNa} from 10 g L^{-1} PEL solutions at unmodified pH as well as with individual PEL solutions (Figure 5.16).

All emulsions were oil-in-water as inferred from the drop test after preparation. Regarding the emulsion stability of the individual PEL, PAH ($x_{PSSNa} = 0$) is not surface-active as the emulsion completely phase separates after homogenisation. On the contrary, despite PSSNa ($x_{PSSNa} = 1$) showing some surface activity initially, after two months the amount of oil coalesced is 46%. On the contrary, stable emulsions (to different extents) were prepared from aqueous PEC dispersions. The most stable emulsions were obtained around charge neutrality ($x_{PSSNa} \sim 0.8$). At these mole fractions (0.79 and 0.83) all the particles migrate to the cream as the aqueous solution resolved remains completely transparent with no evidence of complexes. Moreover, and more crucial for the stability study, the fraction of cream generated is higher and the average droplet diameter (Figure 5.16(c)) is the lowest and remains unaltered after two months, compared to the other x_{PSSNa}. The oil resolved after two months was measured by weight for all emulsions. The amount of oil released for emulsions prepared close to charge neutrality, $x_{PSSNa} = 0.79$ and 0.83, was 3.8% and 1.1%, respectively. For the other x_{PSSNa}, this value was substantially higher and varied from 4% to 12%, although the emulsion with a $x_{PSSNa} = 0.48$ displayed a relatively higher value (37%). Therefore, PEC enable long term emulsion stability compared to the individual PEL, the most stable emulsion being the one prepared around charge neutrality. This is in agreement with the results obtained for the system PDADMAC-PSSNa (Chapter 3).

Figure 5.16. (a) Appearance of emulsions prepared with *n*-dodecane ($\phi_o = 0.2$) and aqueous PEC dispersions ([PEL] = 10 g L^{-1}, pH = unmodified) at different x_{PSSNa} given (a) after preparation once creaming stopped and (b) two months after preparation. Scale bars = 1 cm. (c) Plot of average droplet diameter *versus* x_{PSSNa} for the above emulsions.
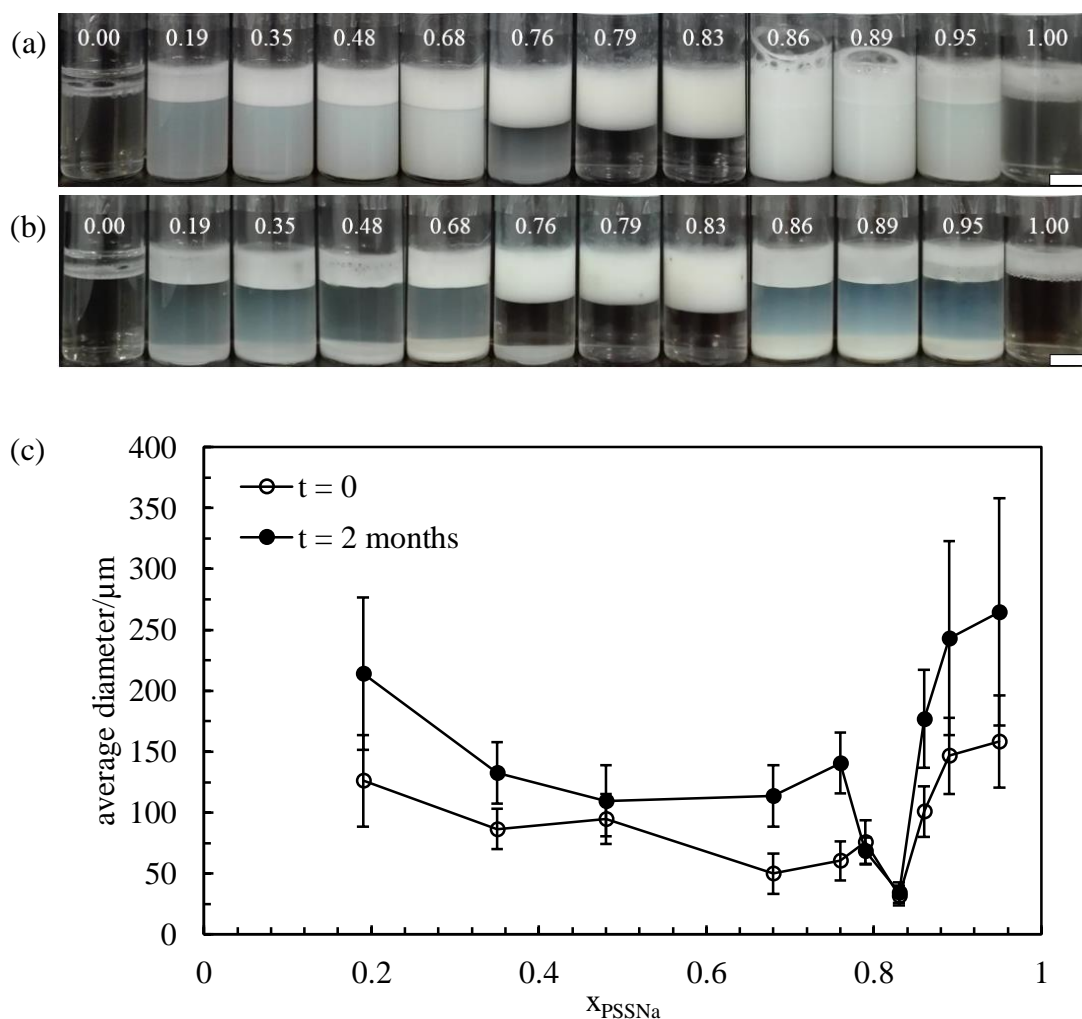
The study was repeated for pH = 2 and 10 for selected x_{PSSNa} (Figure 5.17). For pH = 2, the results are similar to the ones obtained at unmodified pH, as expected. The most stable emulsion with the smallest average droplet diameter (29 ± 8 μm), the highest fraction of cream and the lowest amount of oil coalesced after two months (3%) was obtained at a $x_{PSSNa} = 0.83$.

Figure 5.17. Appearance of emulsions prepared with *n*-dodecane ($\phi_o = 0.2$) and aqueous PEC dispersions at different x_{PSSNa} (given) and for two times prepared from 10 g L^{-1} PEL solutions at (a) pH = 2 and (b) pH = 10. Scale bars = 1 cm. (c) Selected optical microscope images of the above emulsions taken two months after preparation at pH = 10 at different x_{PSSNa} (given).
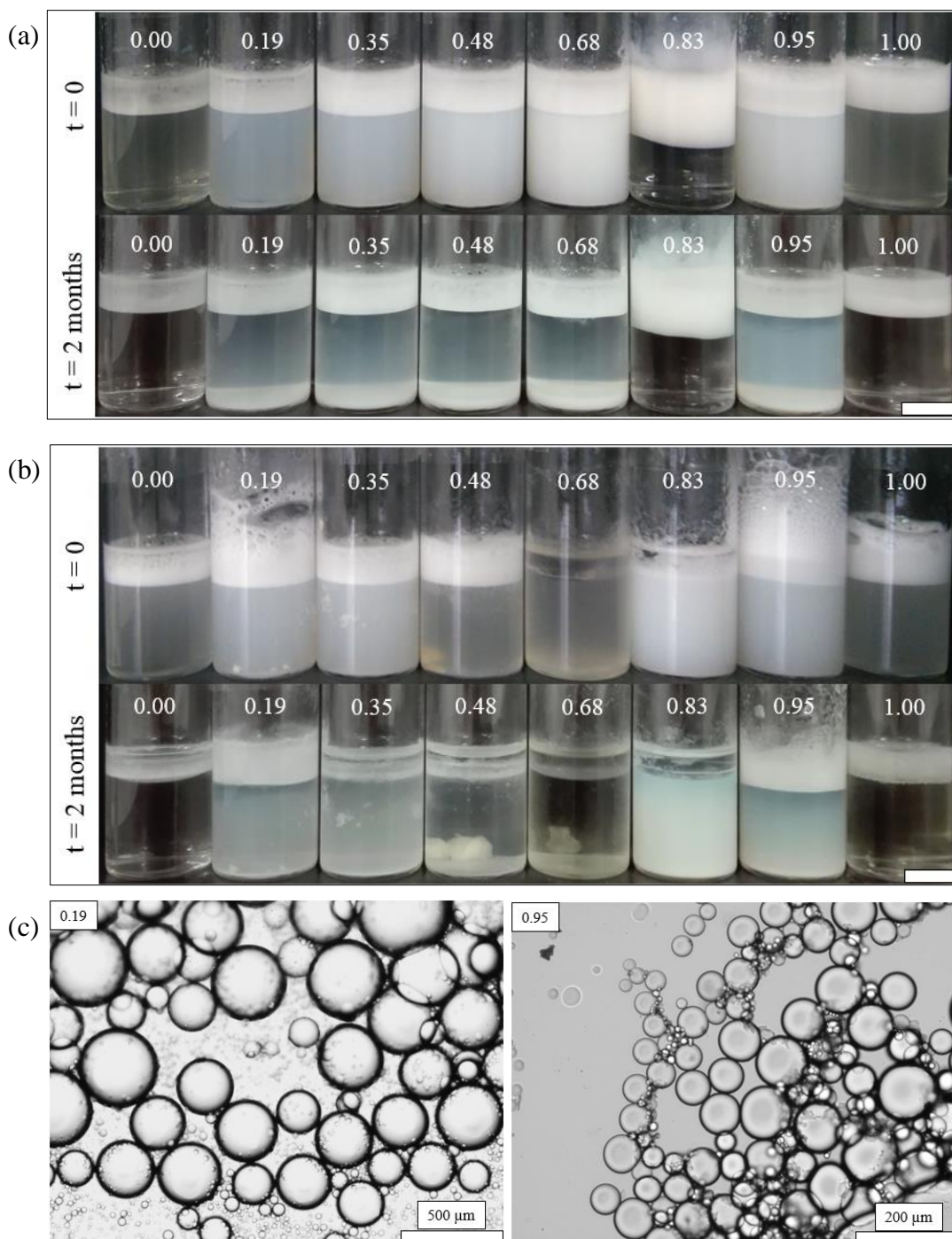
However, at pH = 10 the observed behaviour was different. The majority of emulsions completely coalesce and only the ones obtained close to the x_{PSSNa} extremes seem to be stable in the long term. The ability of coacervate droplets to stabilise emulsions was assessed in Chapter 4 for the system PDADMAC-PAANa. However, the experimental conditions in that case had to be optimised in order to obtain stable emulsions against coalescence. Many parameters such as the viscosity or the spreading of one phase over another have to be considered which makes this system difficult to fully understand. In conclusion, the stability of emulsions prepared with PEC particles is higher than that obtained with dispersions containing coacervate droplets.

5.4.1.1 Preparation of PEC disks for contact angle measurements

As discussed in Section 5.4.1, there is a dramatic change in emulsion stability upon increasing the x_{PSSNa} for unmodified pH. Long term stable emulsions were obtained in a narrow x_{PSSNa} range around charge neutrality (0.76 - 0.83), while more unstable emulsions with high amounts of oil coalesced were found outside this range. This could be driven by the fact that a higher amount of PEC particles are formed within this narrow x_{PSSNa} range, as shown from the results discussed in Section 5.3.2.1. On the other hand, this could also be due to a change in the particle hydrophilicity across the x_{PSSNa}. If that is the case, one would expect that particles with a $x_{PSSNa} = 0.68$ are too hydrophilic and prefer to remain dispersed in water while particles with a $x_{PSSNa} = 0.83$ could have a higher contact angle. In order to prove this hypothesis, contact angle measurements on PEC disks prepared at two different x_{PSSNa} (0.68 and 0.83) were suggested to check whether any change in the particle hydrophilicity was detected.

As explained in the experimental section, in order to obtain PEC disks, aqueous PEC dispersions at two x_{PSSNa} (0.68 and 0.83) were prepared. PEC particles were separated from the supernatant by filtration and the remaining water was left to evaporate at room temperature until constant weight. After filtration, PEC particles were white (first images, Figure 5.18(a and b)). However, after complete water removal, yellow crystals were left (last images, Figure 5.18(a and b)). PEC particles obtained at two different x_{PSSNa} were ground up with a mortar and pestle until a fine powder was obtained. Figure 5.19 shows the appearance of PEC particles ($x_{PSSNa} = 0.83$) before and after grinding.

Figure 5.18. Residue left after filtration and water removal at room temperature with time (given) for an aqueous PEC dispersion ([PEL] = 5 g L^{-1}, pH = unmodified) at different x_{PSSNa}: (a) 0.68 and (b) 0.83.
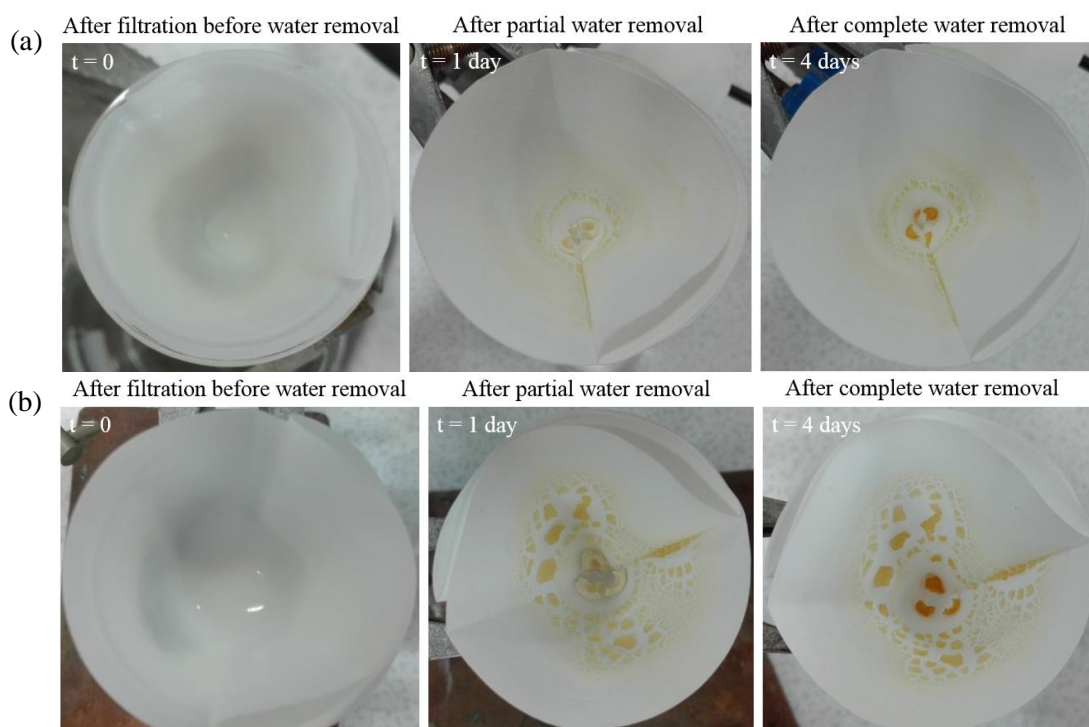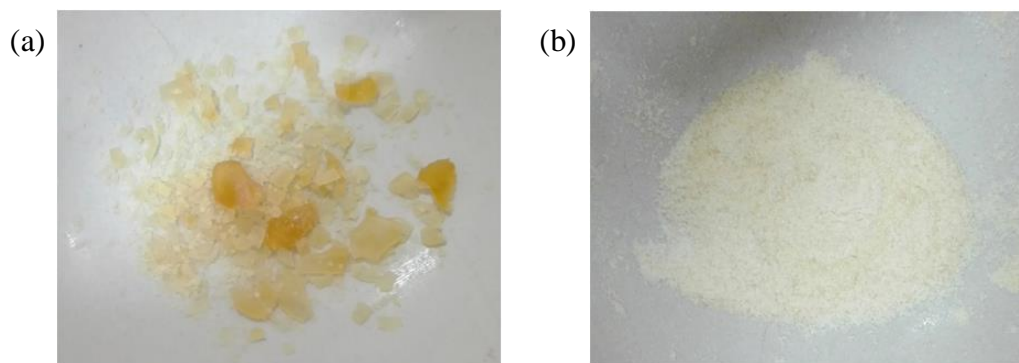

Figure 5.19. Appearance of PEC particles (x_{PSSNa} = 0.83, [PEL] = 5 g L^{-1}, pH = unmodified) (a) before and (b) after grinding.

Once PEC particles were ground into a fine powder, disks were prepared with a hydraulic press using almost all the powder obtained. Both disks were really compact and smooth as shown in Figure 5.20. The diameter was 13 mm in both cases while the thickness was 1 mm and 2.5 mm for x_{PSSNa} = 0.68 and 0.83, respectively. This is due to the different amount of powder used in each preparation.

Figure 5.20. Appearance of disks prepared with the powders obtained at different x_{PSSNa} (a) 0.68 and (b) 0.83 after compressing them in a steel die with a hydraulic press with 10^{10} tones.
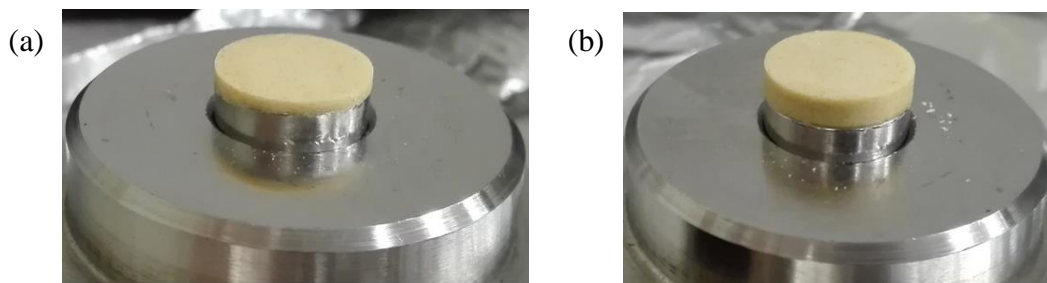
Unfortunately, the air-water contact angle could not be measured as the drop of water penetrated inside the disk displacing some of the particles from the surface (Figure 5.21), probably due to the high porosity. Probably particles were too big and upon compression pores were left between them. Therefore, the hypothesis suggested regarding the change in particle hydrophilicity across the x_{PSSNa} could not be proved.

Figure 5.21. Image taken after placing a drop of water (pH = 4) on a PEC disk (x_{PSSNa} = 0.83).
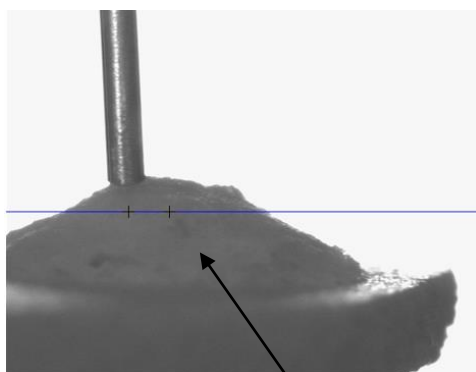
particles are displaced from the disk surface upon deposition of a drop of water

5.4.2 Effect of PEL concentration on emulsion stability

In particle-stabilised emulsions the particle concentration plays an important role in emulsion stabilisation.[9] At low stabiliser concentration (emulsifier-poor régime) droplets are partially covered so they coalesce to a limited extent. By increasing the particle concentration, the degree of surface coverage increases and this results in the decrease of the mean droplet size. Finally, at high emulsifier concentration (emulsifier-rich régime) the average droplet size remains unaltered.

Aqueous PEC dispersions (x_{PSSNa} = 0.83) were prepared from PEL solutions of different concentrations at unmodified pH. Afterwards, emulsions were prepared with n-dodecane (ϕ_o = 0.2) in order to evaluate the influence of the [PEL] on emulsion stability. The appearance of emulsions after preparation once creaming stopped is shown in Figure 5.22(a). Two different behaviours can be distinguished. From a [PEL] of 1 to 10 g L^{-1}, all the particles migrate to the cream, the fraction of cream increases slightly and the average droplet diameter decreases first and then remains unaltered by increasing the polyelectrolyte concentration. From [PEL] = 11 to 20 g L^{-1}, not all the particles migrate to the cream, the average droplet diameter increases and the fraction of cream decreases slightly compared to the emulsion prepared with the aqueous PEC dispersion from 10 g L^{-1} PEL solutions. The amount of oil coalesced after two months is less than 2% for emulsions with PEC particles prepared with a [PEL] between 1 and 10 g L^{-1} and slightly higher but lower than 7.5% for emulsions prepared at higher [PEL].

Figure 5.22. Appearance of emulsions prepared with *n*-dodecane ($\phi_o = 0.2$) and aqueous PEC dispersions ($x_{PSSNa} = 0.83$, pH = unmodified) at different [PEL] given in g L^{-1} (a) after preparation once creaming stopped and (b) two months after preparation. Scale bars = 1 cm. (c) Plot of average droplet diameter and (d) fraction of cream two months after preparation *versus* [PEL] for the above emulsions.
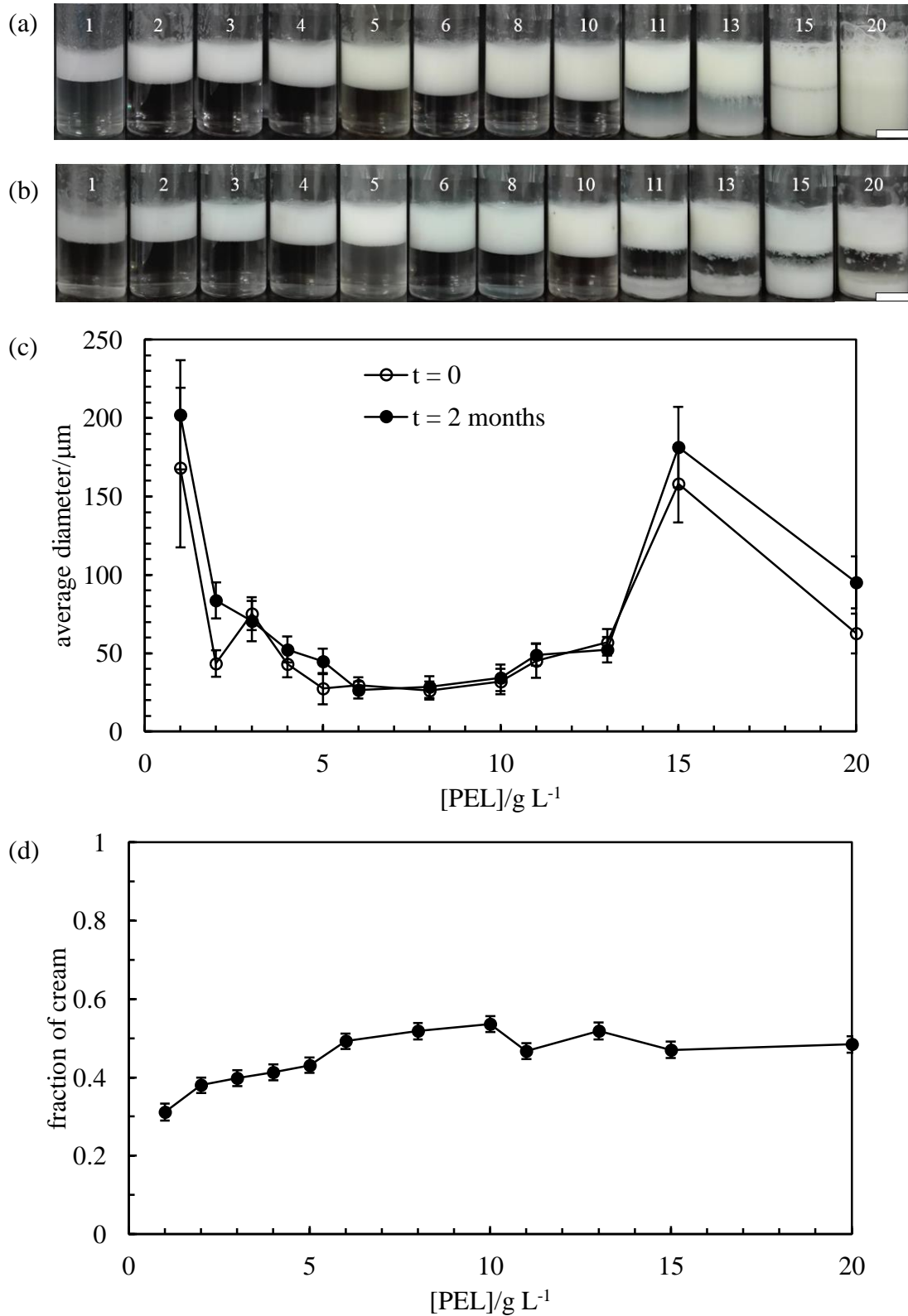
Selected optical microscope images of emulsions prepared at different [PEL] are shown in Figure 5.23. For the first [PEL] range, the system behaves in the same way as described by the limited coalescence model for particle-stabilised emulsions, *i.e.* the average droplet diameter decreases with the polyelectrolyte concentration until it reaches a point where emulsion drops are fully covered by particles so the excess particles form a network at the continuous phase and the droplet diameter does not decrease further. Some examples of emulsions stabilised by various kinds of particles following this pattern of behaviour are encountered in the literature.[9-11] However, for emulsions prepared with aqueous PEC dispersions from polyelectrolyte concentrations higher than 10 g L^{-1} the behaviour differs from the one expected by the limited coalescence model. We have to be aware, however, that here particles are formed from the interaction of two oppositely charged polyelectrolytes, unlike the case of traditional solid particles. Therefore, at high polyelectrolyte concentrations, entanglements of polymer chains are expected to be greater and this can induce further aggregation of the complexes.

The average diameter of the aqueous complexes prepared at selected [PEL] were measured with the Mastersizer. In Figure 5.24(a), particle size distributions are shown for PEC particles in aqueous PEC dispersions prepared at four [PEL]. The values of d(0.1), d(0.5) and d(0.9) together with the span value are plotted in Figure 5.24(b) at different [PEL]. PEC particles obtained at a [PEL] of 1 and 5 g L^{-1} are relatively monodisperse in size (narrow distributions given by low span values). However, as soon as the [PEL] increases, the distribution gets wider and bigger particles are present. Larger particles are dislodged easily from the oil-water interface. This would explain the decrease in emulsion stability for emulsions prepared with a [PEL] higher than 10 g L^{-1}.

Figure 5.23. Microscopy of emulsions prepared with *n*-dodecane ($\phi_o = 0.2$) and aqueous PEC dispersions ($x_{PSSNa} = 0.83$, pH = unmodified) at different [PEL] (given) two months after preparation.
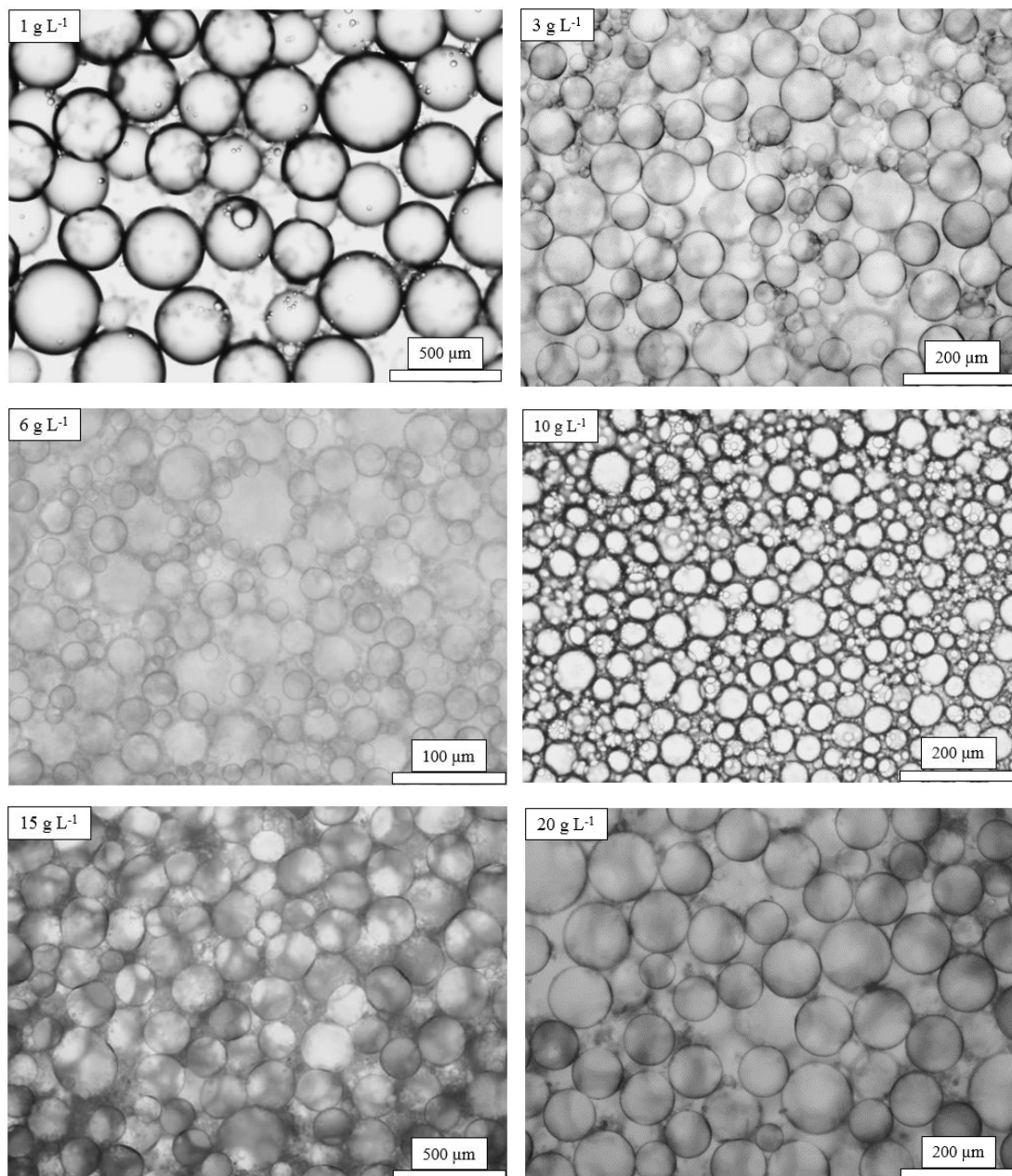
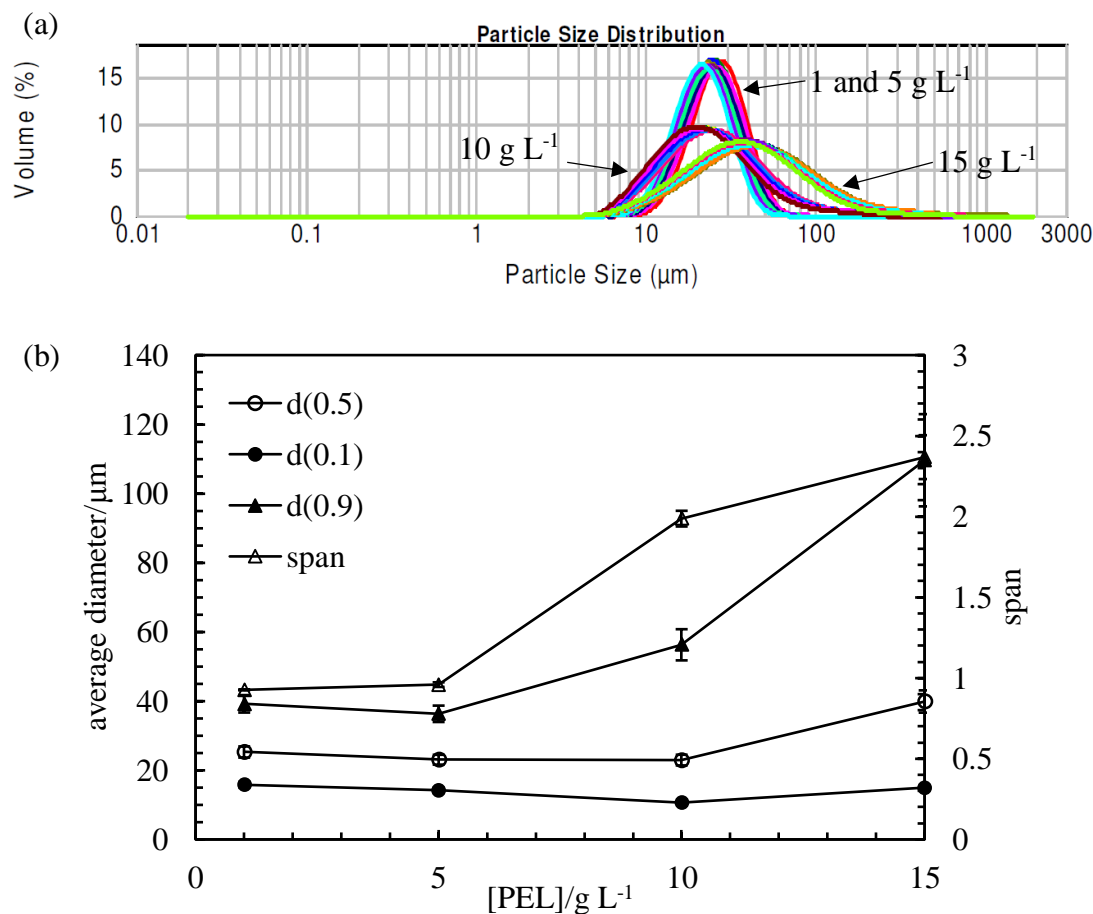**Figure 5.24.** (a) Particle size distributions from aqueous PEC dispersions (x_{PSSNa} = 0.83, pH = unmodified) prepared at different [PEL] (given). (b) Plot of average diameter and span *versus* [PEL] for the above aqueous PEC dispersions.

For the system reported in Chapter 3 between two strong polyelectrolytes (PDADMAC-PSSNa), the influence of [PEL] was assessed on emulsion stability for a wider range of concentrations (1 to 50 g L^{-1}). Unlike the results presented here, emulsions prepared with a [PEL] $\geq$ 20 g L^{-1} showed no sign of creaming or coalescence.

5.4.3   Effect of pH on emulsion stability

As reported in the section dealing with the characterisation of aqueous PEC dispersions, the pH shows a remarkable influence on the type of associative phase separation (precipitation and coacervation). Therefore, the effect of pH on emulsion stability was evaluated by working at a fixed [PEL] (5 g L^{-1}) and x_{PSSNa} (0.83).

Emulsions were prepared with *n*-dodecane ($\phi_o = 0.2$) and aqueous PEC dispersions shown in Figure 5.13. For emulsions (Figure 5.25), three different behaviours were found which can be related to the types of phase separation described previously for each aqueous PEC dispersion.

For emulsions prepared at pH = 2 to 6, all the particles migrate to the cream, the average droplet diameter is about 30 μm and the amount of oil coalesced after two months is lower than 1.5% in all the cases. Moreover, the average droplet diameter remains unaltered with time. When coacervate droplets are present in dispersions (pH = 8 and 10), the average droplet diameter increases, the cream height decreases and the amount of oil released also increases (2% and 5%, respectively). The average droplet diameter changes more with time and droplets appear to be deformed at pH = 10 compared to the ones obtained at other pH (Figure 5.26(a)). Finally, at pH = 12 the average droplet diameter decreases to the same level as the one reported for low pH. In this case, however, the stabilisation is given by free polymer chains of PAH as it is expected to be fully protonated. In order to check this assumption, emulsions were prepared from 5 g L^{-1} PEL solutions (Figure 5.26(b)). During homogenisation, both emulsions generated high amount of foam which completely collapsed a few minutes after preparation. PAH (0% ionised) is surface-active and the emulsion remains stable for at least two months with a relatively low amount of oil coalesced (8.8%). The same behaviour was noted for a 5 g L^{-1} PAANa solution at pH = 2 (0% ionised) in Chapter 4. On the contrary, PSSNa (100% ionised) despite being surface-active initially, the amount of oil coalesced after two months is 40.3%. Therefore, to sum up, emulsion stabilisation is more remarkable for PEC particles than for PEC coacervates.

Figure 5.25. Appearance of emulsions prepared with *n*-dodecane ($\phi_o = 0.2$) and aqueous PEC dispersions ($x_{PSSNa} = 0.83$, [PEL] = 5 g L^{-1}) at different pH (given). Photos taken (a) 1 day and (b) 2 months after preparation. (c) Plot of average droplet diameter *versus* pH at two different times.
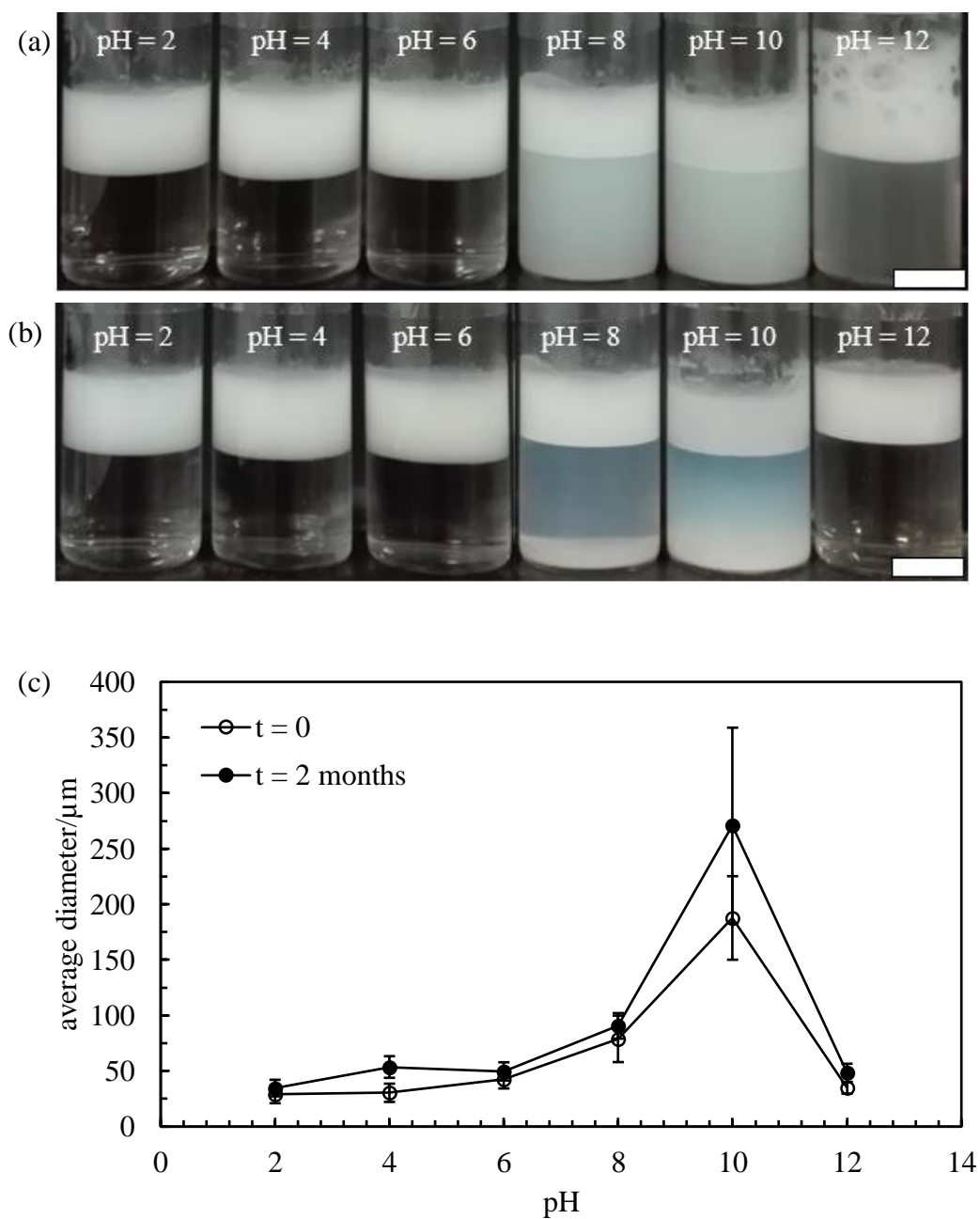
Figure 5.26. (a) Selected optical microscope images of emulsions prepared with *n*-dodecane (ϕ_o = 0.2) and aqueous PEC dispersions (x_{PSSNa} = 0.83, [PEL] = 5 g L^{-1}) at different pH (given) two months after preparation. (b) Appearance of emulsions prepared with the individual PEL solutions (pH = 12, [PEL] = 5 g L^{-1}) (1) several minutes after preparation once the foam collapsed and (2) two months after preparation. Scale bars = 1 cm.
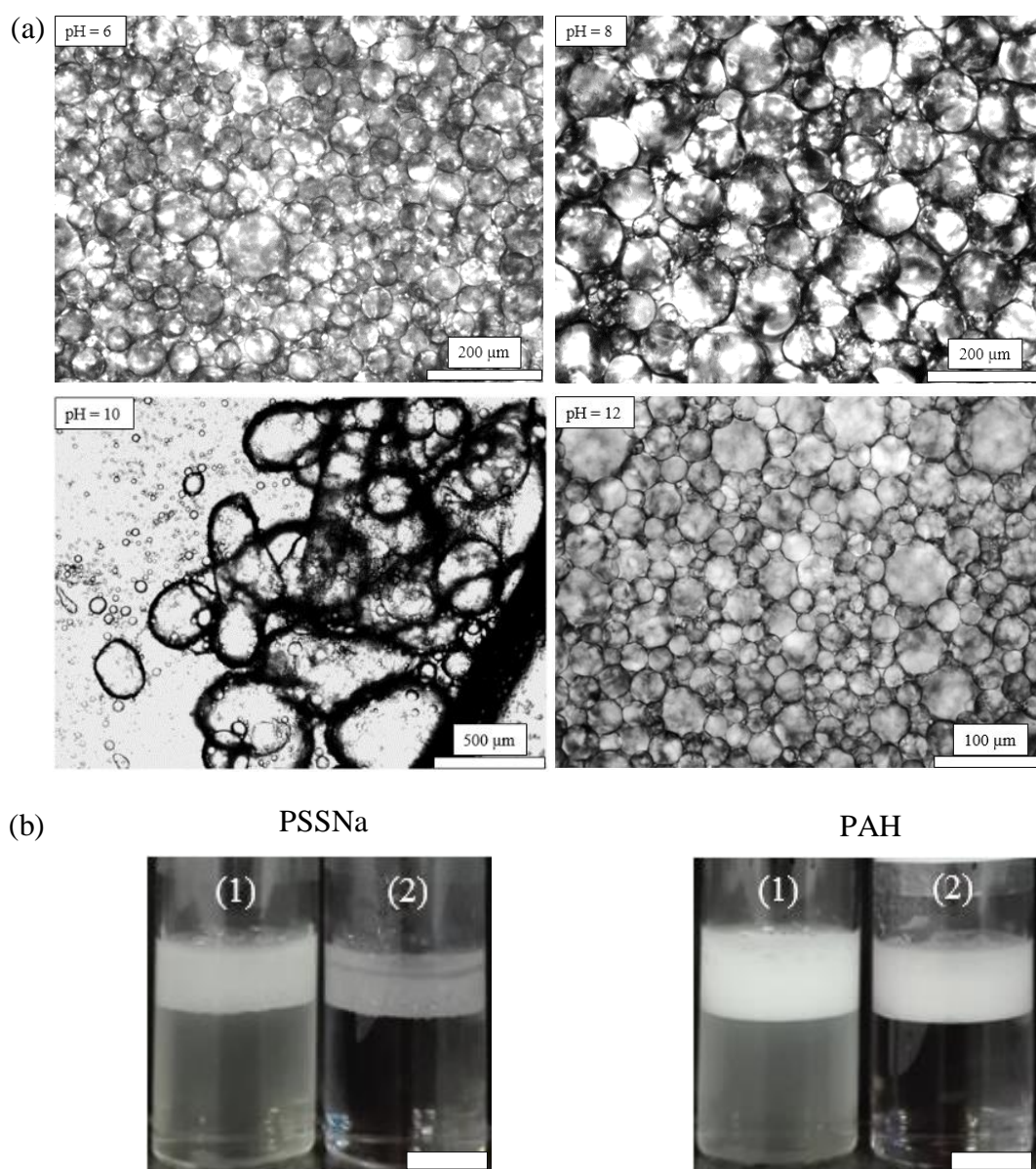
5.4.4 Effect of oil volume fraction: high internal phase emulsions (HIPEs)

In general, emulsions stabilised by solid particles undergo catastrophic phase inversion, *i.e.* change in emulsion type, by varying the oil:water ratio.[12,13] In order to evaluate the influence of this parameter in our system, emulsions with *n*-dodecane at

different ϕ_o were prepared with an aqueous PEC dispersion ($x_{PSSNa} = 0.83$, [PEL] = 10 g L^{-1} and pH = 2). Due to the experimental design, the amount of particles was not kept constant along the oil volume fraction range, unlike in Chapter 3 where the [PEL] in the final emulsion was the same for all oil volume fractions. The appearance of emulsions at different volume fractions of the dispersed phase after preparation once creaming stopped is shown in Figure 5.27(a). The average droplet diameter from the above emulsions was measured from optical microscope images. Selected micrographs are shown in Figure 5.27(c). The average droplet diameter increases with the oil volume fraction as shown in Figure 5.28(a) as the particle concentration in the system decreases as ϕ_o increases. Moreover, at high oil volume fractions droplets appear to be deformed and the viscosity of emulsions increases considerably and to such an extent that they lose their ability to flow by tilting the vial. This indicates the formation of high internal phase emulsions (HIPEs) which are emulsions that contain a high volume fraction of disperse phase.[14,15]

For monodisperse spheres arranged in face centered cubic (FCC) crystalline structure, the maximum close packing fraction that can be accomplished is 0.74.[15] However, for emulsions, this value can be exceeded and fractions of disperse phase up to 0.95 have been reported.[16] Spherical liquid droplets, unlike solid spheres, can be compressed and transformed into polyhedra separated by thin films of continuous phase.[14] For this system, HIPEs were obtained up to a $\phi_o = 0.85$ as no emulsion could be prepared at a $\phi_o = 0.9$, probably due to the lack of particles.

The formation of HIPEs is not common in particle-stabilised systems and only a few examples are found in the literature.[10,17-20] Moreover, it is difficult to predict which type of emulsifier will render high internal phase emulsions. However, the film of emulsifier must be rigid enough to resist breaking but flexible and reversible enough to adjust to changing conditions in the environment.[15] Ikem *et al.* reported the stabilisation of Pickering o/w HIPEs up to a volume fraction of 0.92 using silica nanoparticles hydrophobized by adsorption of oleic acid.[19]

Regarding the long term stability of emulsions, their visual appearance remains almost unaltered after two months (Figure 5.27(b)). The average droplet diameter does not significantly change at low ϕ_o whereas at $\phi_o = 0.8$ and 0.85, it increases substantially. Figure 5.28(b) shows the fraction of oil and water released two months after

preparation for the above emulsions. The amount of oil released is lower than 6% apart from the emulsion prepared with a $\phi_o = 0.8$, in which it raises up to 16%. Moreover, creaming was fully inhibited at $\phi_o \geq 0.7$ as no aqueous phase was resolved after two months.

Figure 5.27. Appearance of emulsions prepared with an aqueous PEC dispersion ($x_{PSSNa} = 0.83$, [PEL] = 10 g L^{-1}, pH = 2) and *n*-dodecane at different oil volume fractions given (a) after preparation once creaming has stopped and (b) two months after preparation. Scale bars = 1 cm. (c) Selected optical microscope images at different ϕ_o (given) taken after preparation.
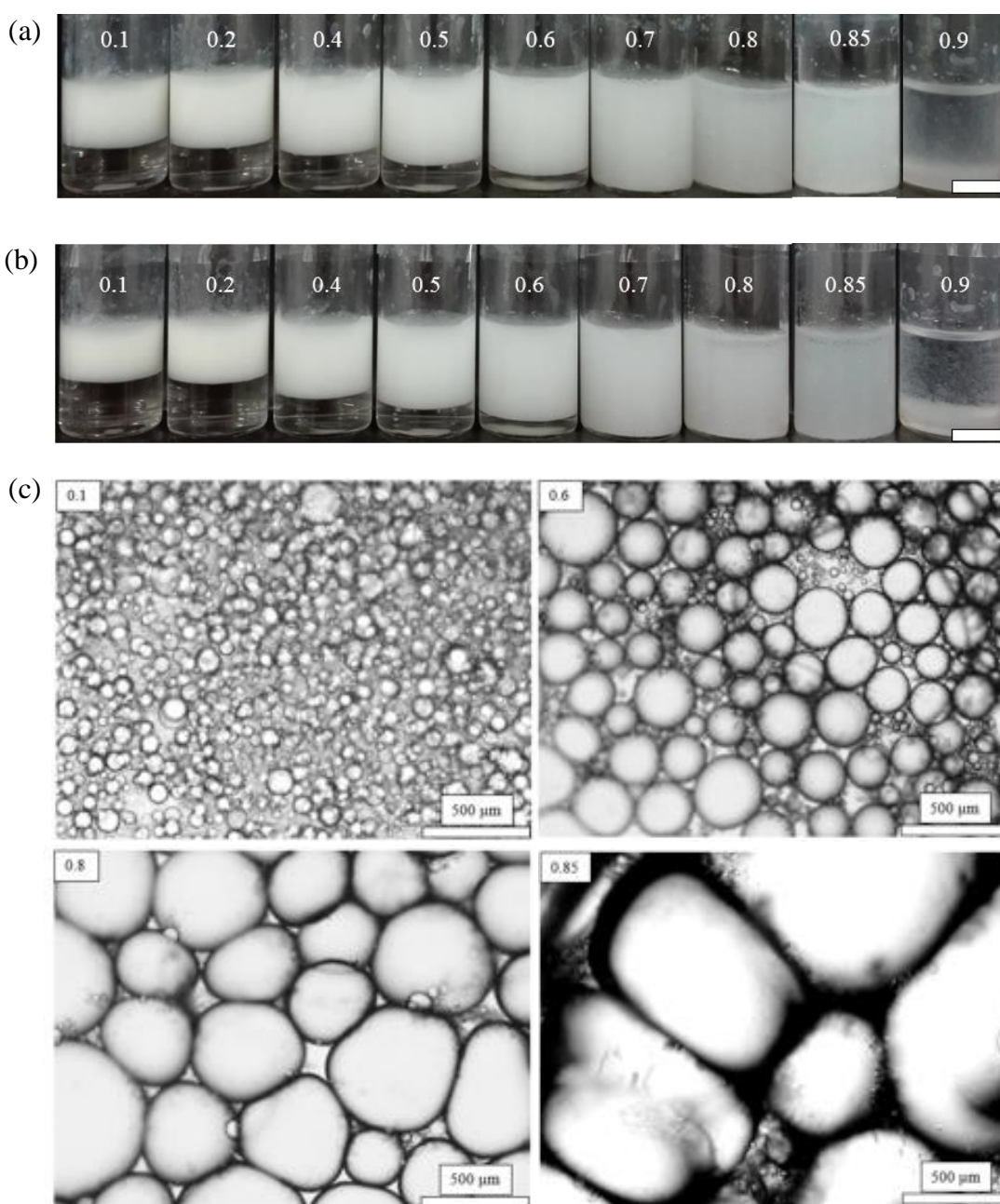
Figure 5.28. (a) Plot of average diameter *versus* volume fraction of oil (ϕ_o) for emulsions prepared with an aqueous PEC dispersion ($x_{PSSNa} = 0.83$, [PEL] = 10 g L^{-1}, pH = 2) and *n*-dodecane after preparation and 2 months after preparation. (b) Variation of fraction of oil (filled points) and water (open points) resolved after two months as a function of ϕ_o.
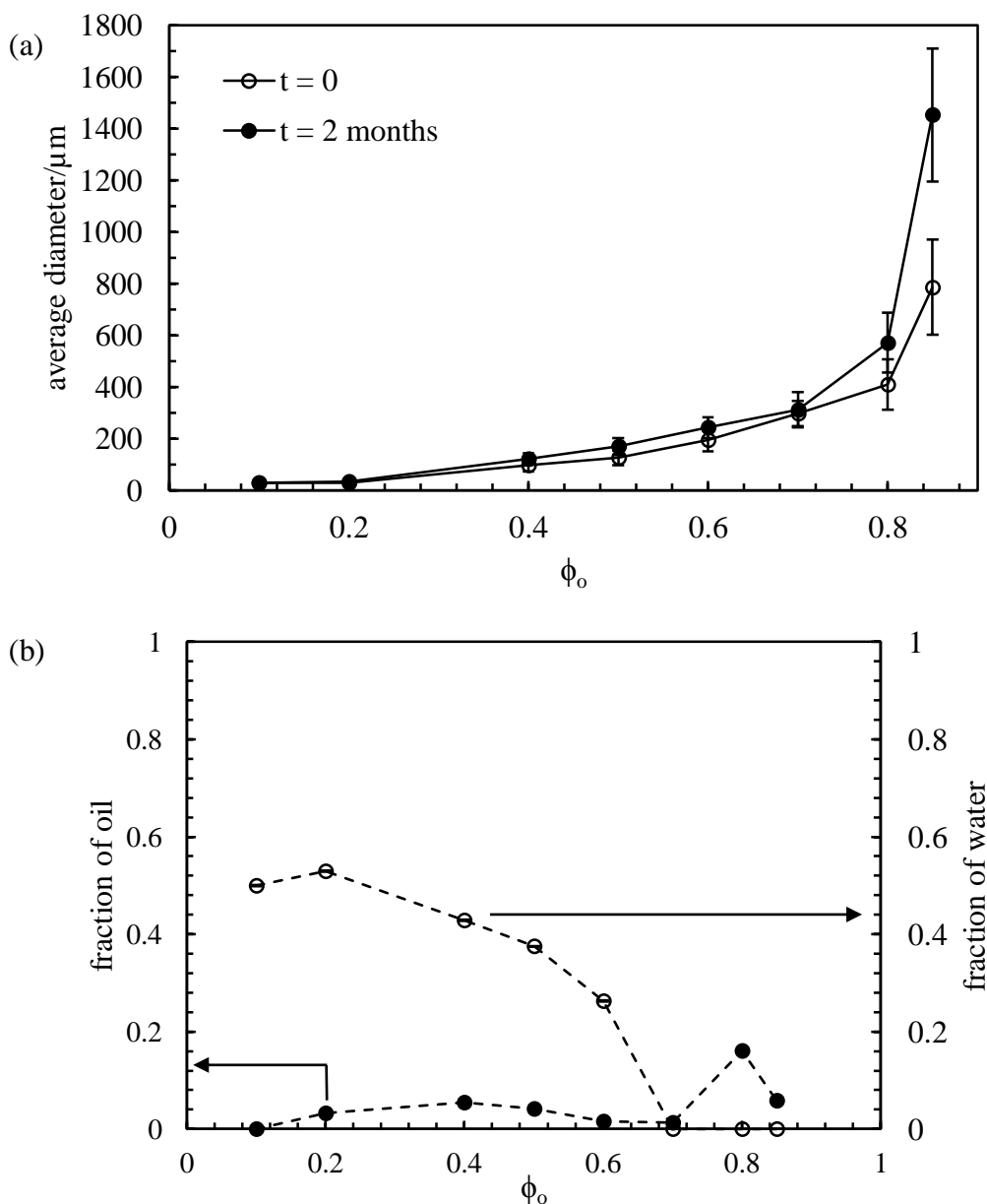
As a control, emulsions with individual PEL solutions at the same conditions ([PEL] = 10 g L^{-1}, pH = 2) were prepared and the long term stability was assessed. Plots for the fraction of oil and water released after two months for emulsions prepared with PSSNa and PAH are shown in Figure 5.29. From this analysis, it was found that PAH is not surface-active. The amount of oil and water released is close to 100% for the

majority of ϕ_o. However, for emulsions with a $\phi_o = 0.1$ and 0.2, the amount of oil released represented 28% and 78%, respectively. PSSNa, despite being surface-active initially, two months after preparation the fraction of oil and water released (Figure 5.29(b)) is higher compared with emulsions prepared from aqueous PEC dispersions (Figure 5.28(b)). Therefore, PEC particles enable long term emulsion stability unlike the individual PEL solutions and HIPEs are formed at high fractions of disperse phase.

Figure 5.29. Variation of fraction of oil (filled points) and water (open points) resolved after two months as a function of the initial oil volume fraction (ϕ_o) for emulsions prepared with 10 g L^{-1} solutions of (a) PAH and (b) PSSNa at pH = 2.
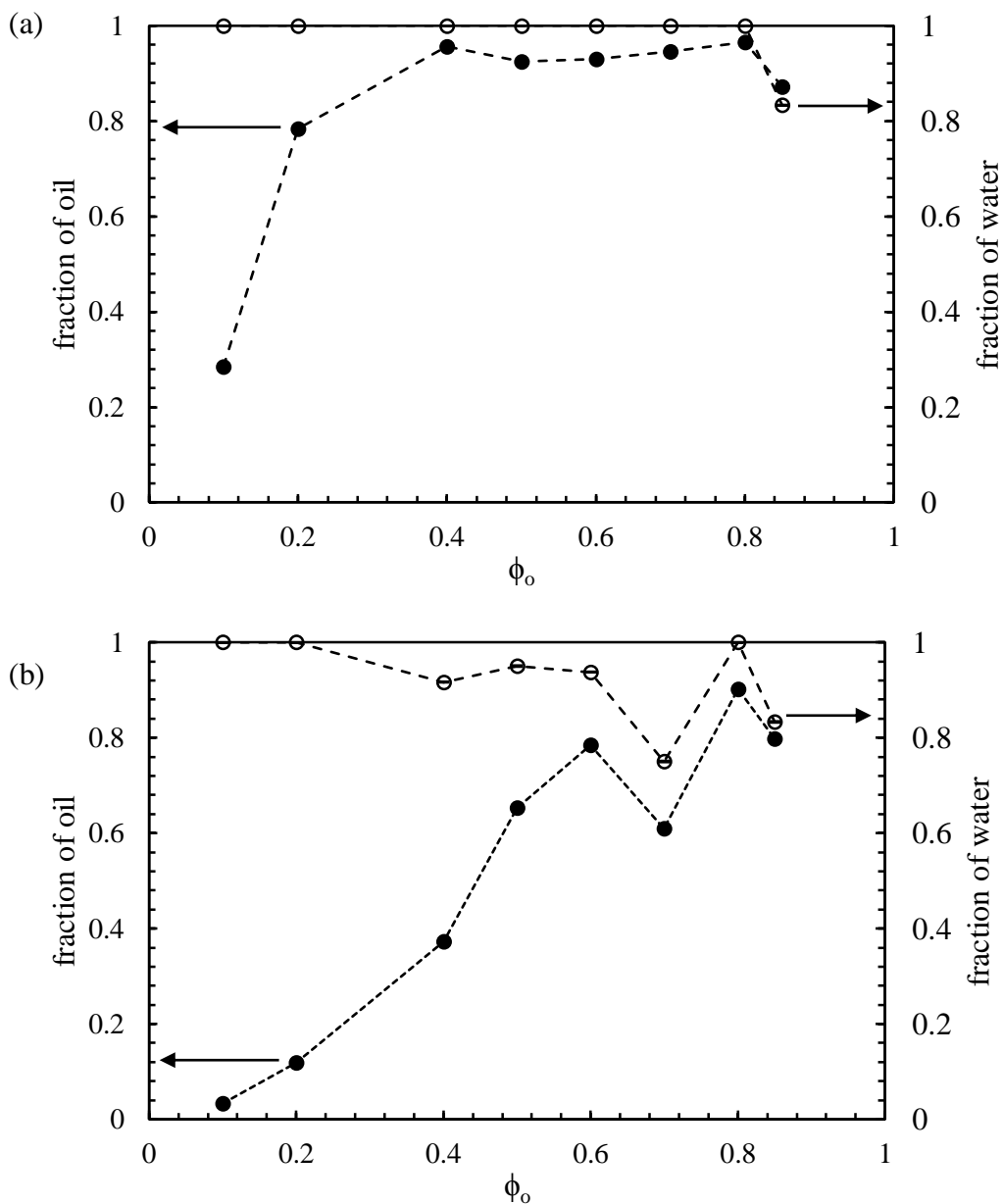
5.4.4.1 Rheology measurements

To prove the increase in the viscosity by increasing the oil volume fraction, rheology measurements were carried out for the above emulsions as detailed in the experimental section.

Curves for viscosity *versus* shear stress are shown in Figure 5.30(a). The viscosity of emulsions with a $\phi_o = 0.8$ and 0.85 could not be measured because the gap size was close to the average droplet diameter. By plotting the viscosity at a specific shear stress (10 Pa) *versus* ϕ_o, (Figure 5.30(b)) it can be concluded that the viscosity increases markedly from a $\phi_o = 0.1$ to 0.5 and then it decreases for $\phi_o = 0.6$ and 0.7. This drop in the viscosity of about 10 orders of magnitude compared with $\phi_o = 0.5$ could be explained by two facts. On the one hand, the amount of particles decreases with ϕ_o because of the experimental design. It is known that the particle concentration influences the viscosity of a solution.[21] The higher the amount of particles, the higher the viscosity. Moreover, an increase of the average droplet diameter takes place by increasing the amount of disperse phase in the emulsion. There are several clear evidences showing that rheological properties are strongly influenced by the droplet size.[22,23] Pal showed that fine emulsions (small droplet diameter) have much higher viscosities than the corresponding coarse emulsions (bigger droplet diameter) at the same volume fraction of oil.[23] Regarding the influence of the fraction of oil, Pal concludes in another publication that the viscosity of an emulsion increases with the fraction of oil at constant droplet diameter.[24] Therefore this effect, together with the decrease in the number of particles, could result in the viscosity decreasing slightly from its expected value for high fractions of oil.

Figure 5.30. (a) Viscosity *versus* shear stress (σ) for emulsions prepared with aqueous PEC dispersions ($x_{PSSNa} = 0.83$, $[PEL] = 10$ g L^{-1}, pH = 2) and *n*-dodecane at different oil volume fractions (ϕ_o) given. (b) Viscosity at a shear stress = 10 Pa *versus* oil volume fraction (ϕ_o) for above emulsions.
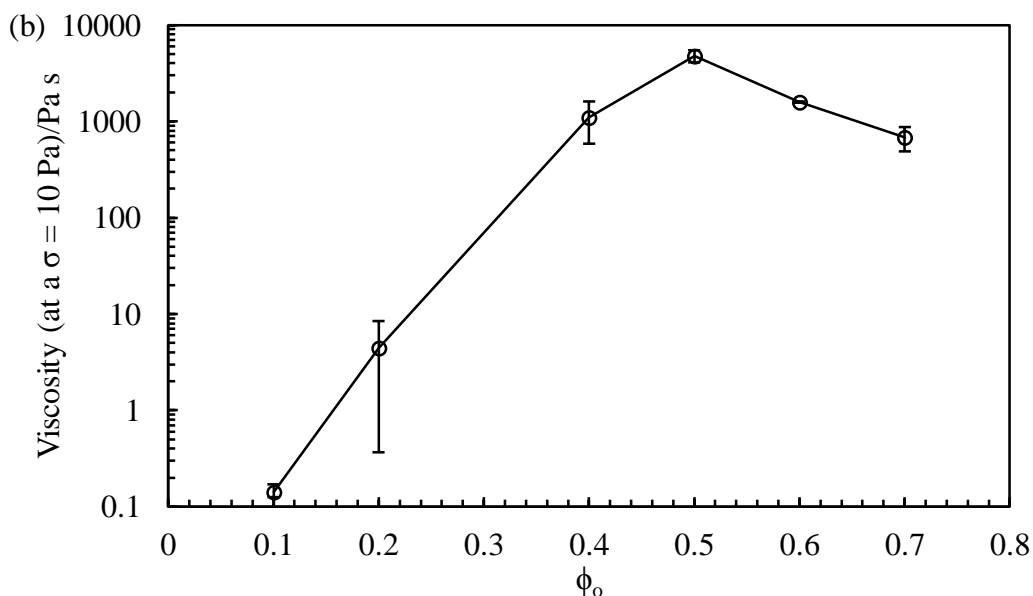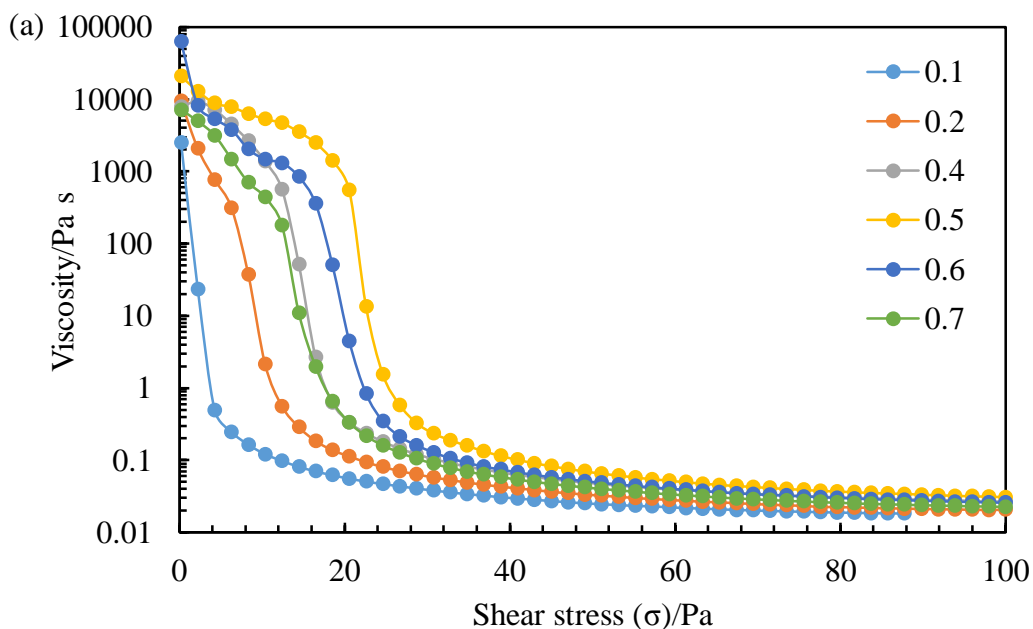
5.4.4.2 Cryo-SEM images of emulsions

Cryo-SEM images of emulsions across the oil volume fraction range were taken. In Figure 5.31, images for emulsions with a (a) $\phi_o = 0.5$ and (b) 0.6 are shown. For a $\phi_o = 0.5$ (right picture), spherical and monodisperse entities of a diameter around 110 nm are detected both at the interface (left-hand side of the picture) and in the aqueous continuous phase (right-hand side of the picture). Surprisingly, at a $\phi_o = 0.6$, elongated structures were detected (length ~ 600 nm; diameter ~ 130 nm). It is worth noting that the diameter of the rod-like shape entities is of the same order as the spherical entities observed at lower ϕ_o. This can suggest that the elongated structures are formed by few spherical entities merged together. Due to this intriguing observation, images of emulsions prepared at other ϕ_o (0.7 and 0.8) were taken. For the emulsions with a $\phi_o = 0.7$ (Figure 5.32) both spherical and rod-like shape entities were observed with approximately the same dimensions as the ones presented earlier. At a $\phi_o = 0.8$ only spherical entities were detected (Figure 5.33). Moreover, the surface is not fully covered as in the previous cases due to a lower amount of particles present in the emulsion.

The change in the morphology of the PEC entities still remains unresolved as the aqueous PEC dispersion used to prepare the above emulsions is the same for all the ϕ_o. We have to bear in mind that PEC particles could be considered as soft particles as they form through an electrostatic interaction between two charged polymers. Some hypothesis arise regarding this change in the morphology, despite any of them having been proved. Due to their soft nature, PEC particles could hold oil in their structures or the combination of shear and a specific oil volume fraction during emulsification might be plausible explanations regarding the change in shape. Moreover, a discrepancy regarding the size of the PEC can be detected by comparing cryo-SEM images with optical microscope images (Figure 5.5(c)) and the results from size measurements of aqueous PEC dispersions (Figure 5.24). Nanometer-sized particles are identified from cryo-SEM images of emulsions while particles in the micrometer range are measured with the Mastersizer and from optical microscope images of aqueous dispersions. PEC particles are aggregated structures. Therefore, the high shear used during homogenisation might have broken them into smaller entities.

Figure 5.31. Cryo-SEM images of a freshly prepared emulsion with an aqueous PEC dispersion (x_{PSSNa} = 0.83, [PEL] = 10 g L^{-1}, pH = 2) and *n*-dodecane for (a) ϕ_o = 0.5 and (b) ϕ_o = 0.6 at different magnifications.

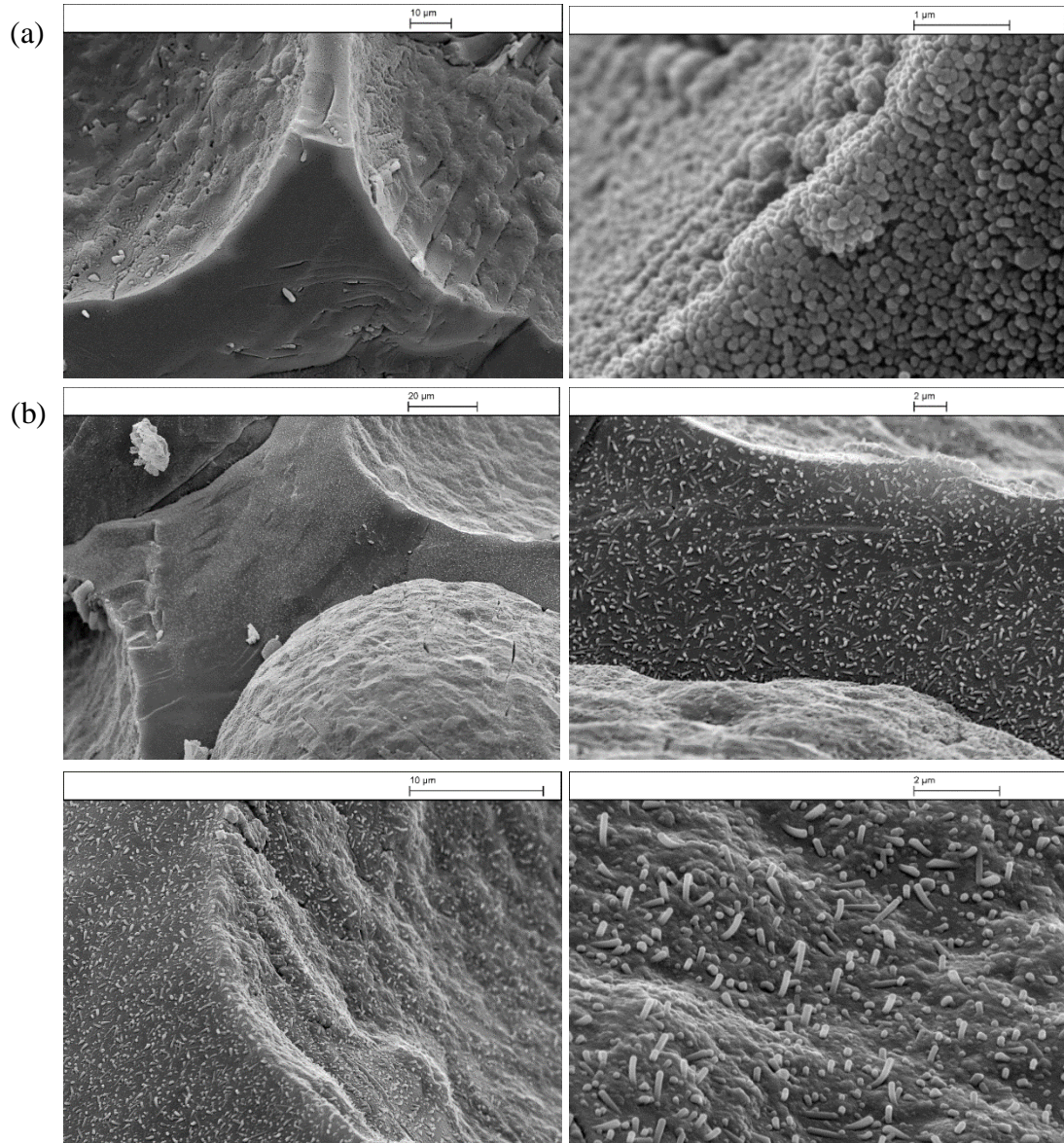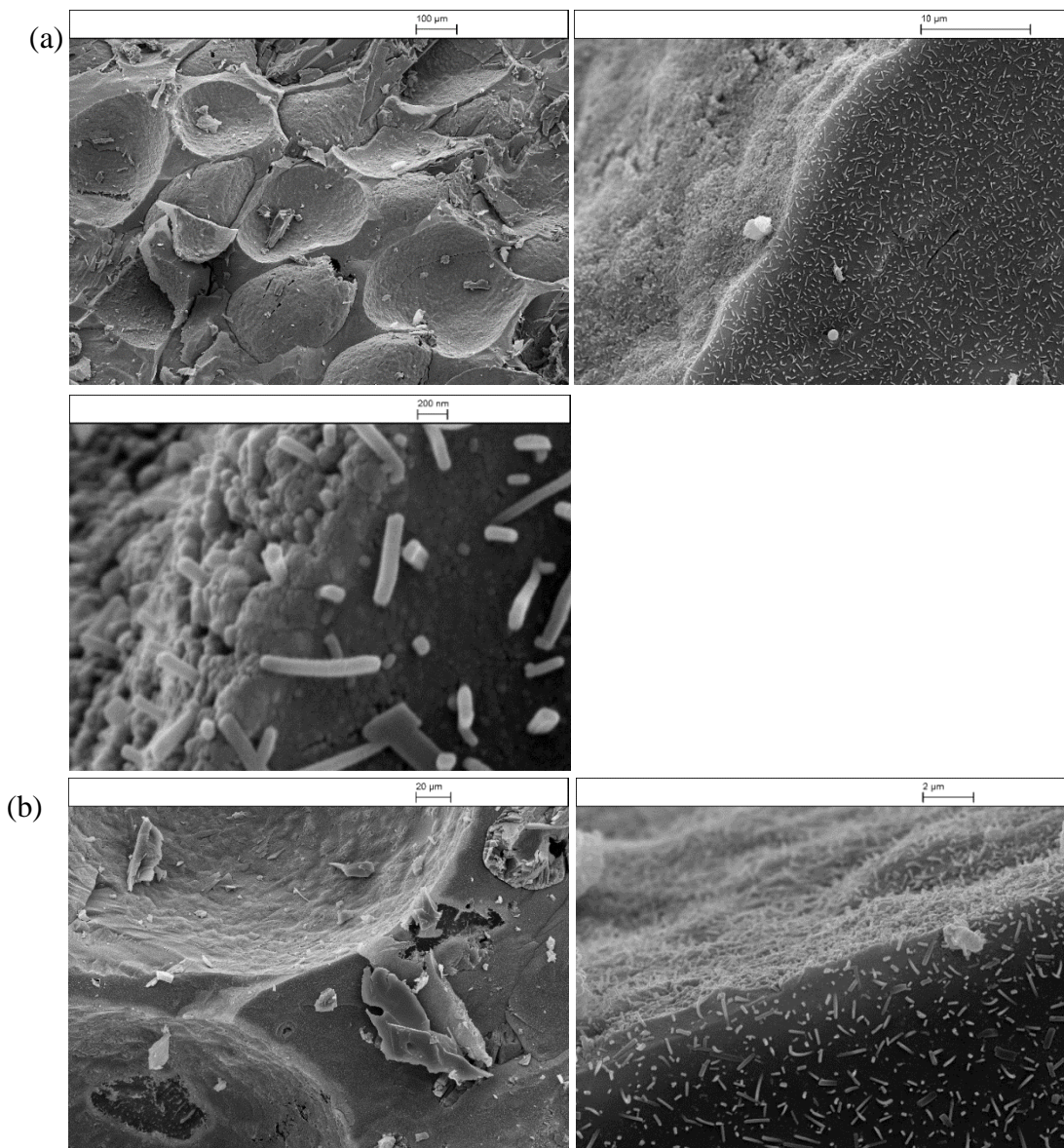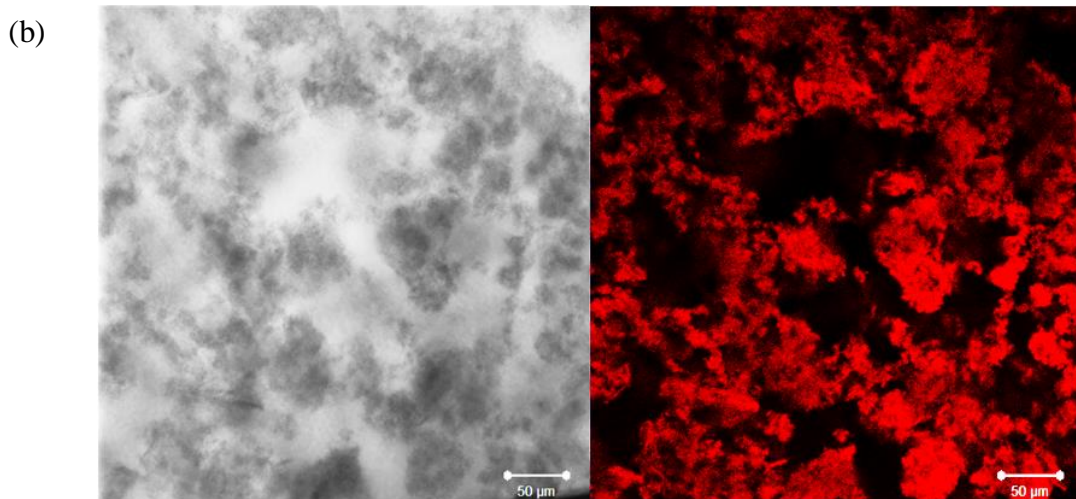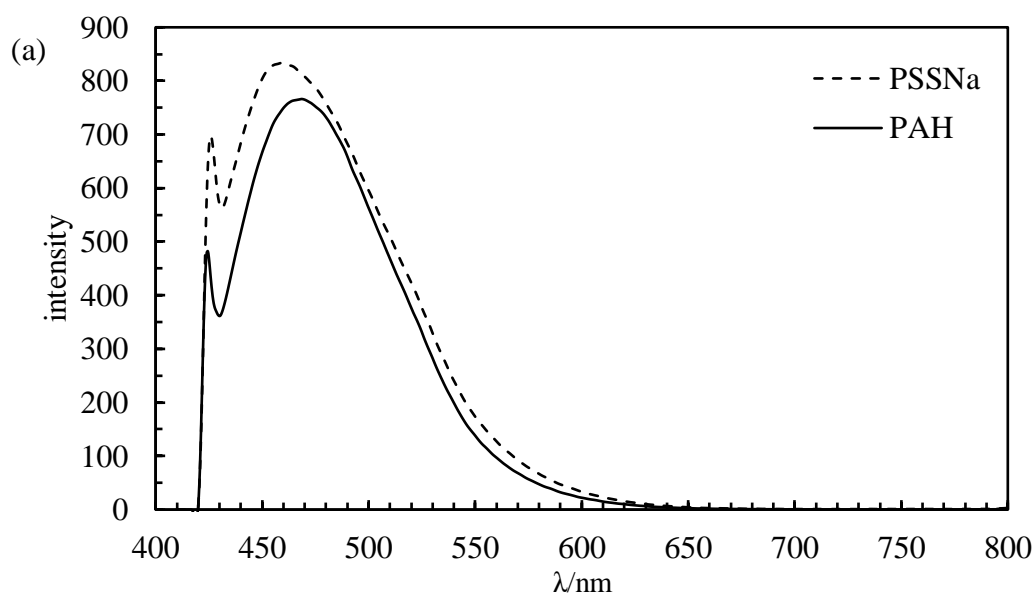**Figure 5.32.** Cryo-SEM images of freshly prepared emulsions with an aqueous PEC dispersion ($x_{PSSNa} = 0.83$, [PEL] = 10 g L^{-1}, pH = 2) and n-dodecane ($\phi_o = 0.7$). (a) and (b) show two different areas of the emulsion at different magnifications.

Figure 5.33. Cryo-SEM images of freshly prepared emulsions with an aqueous PEC dispersion ($x_{PSSNa} = 0.83$, $[PEL] = 10$ g L^{-1}, pH = 2) and n-dodecane ($\phi_o = 0.8$) at different magnifications.
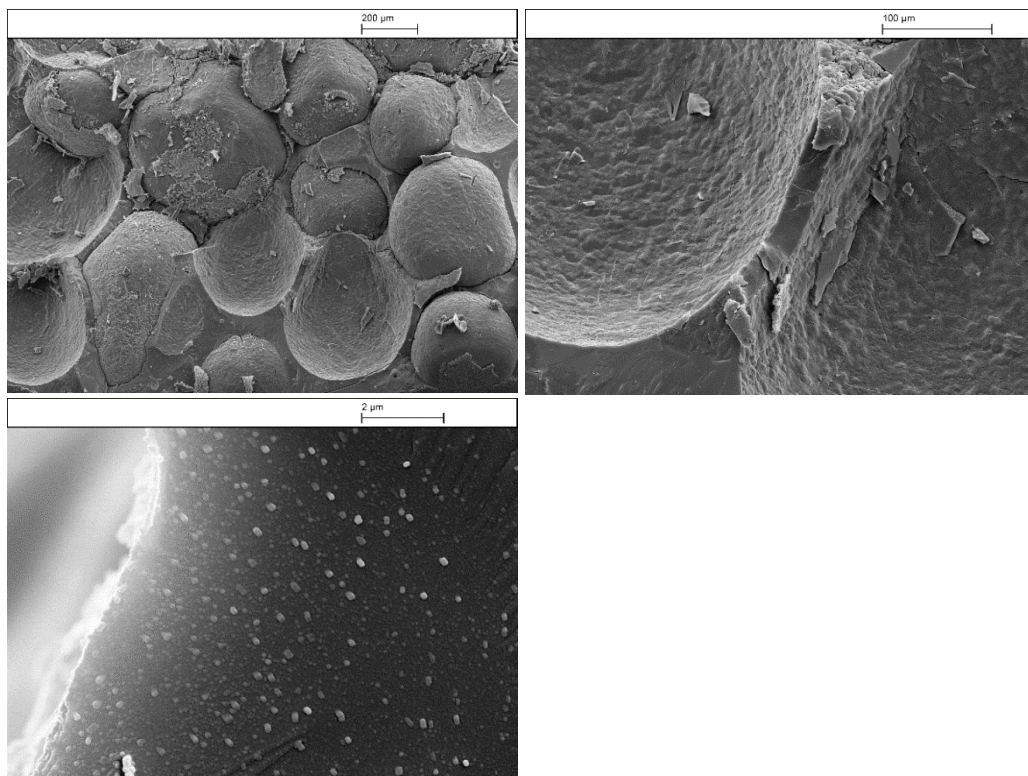
5.4.4.3 Confocal laser scanning micrographs of emulsions

Taking advantage from the fact that each PEL is fluorescent after being excited at 405 nm (Figure 5.34(a)), confocal micrographs of emulsions prepared with PEC particles were taken in order to visualise where particles are placed after emulsification with a different technique. Optical images and the corresponding confocal micrographs of an aqueous PEC dispersion ($x_{PSSNa} = 0.83$) and emulsions prepared at different ϕ_o are shown in Figure 5.34(b) and Figure 5.35, respectively. As shown in Figure 5.34(b), PEC particles (shown in red) are fluorescent on their own after being excited at 405 nm.

Figure 5.34. (a) Fluorescence emission spectra at λ_{ex} = 405 nm of the individual PEL solutions (10 g L^{-1}). Measurements taken in a 1 cm path length quartz cuvette with four optically clear sides. Milli-Q water was used as reference. (b) Optical (left) and confocal (right) micrographs of an aqueous PEC dispersion (x_{PSSNa} = 0.83, [PEL] = 10 g L^{-1}, pH = unmodified) after being excited at λ = 405 nm.

Regarding emulsions stabilised with those PEC particles at ϕ_o = 0.2, particles are found at the interface of disperse drops and excess particles form a network in the aqueous continuous phase (Figure 5.35(a)). At higher oil volume fractions (Figure 5.35(b and c)), and especially at ϕ_o = 0.8, particles are detected only at the oil-water interface.

Figure 5.35. Optical (left) and confocal (right) micrographs of freshly prepared emulsions with an aqueous PEC dispersion (x_{PSSNa} = 0.83, [PEL] = 10 g L^{-1}, pH = 2) and *n*-dodecane at different ϕ_o: (a) 0.2, (b) 0.6 and (c) 0.8.
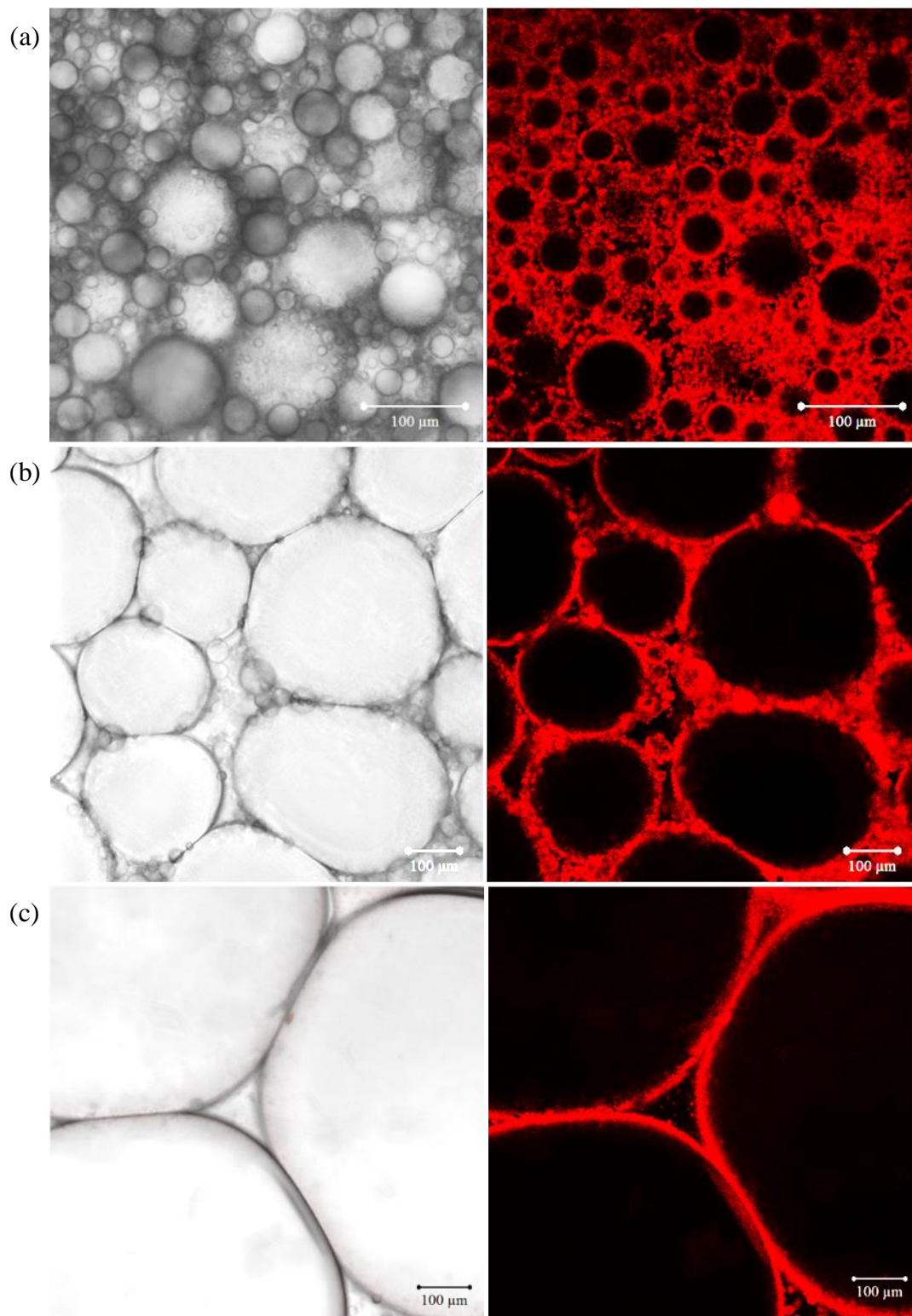
A 3D image of emulsion drops prepared at a ϕ_o = 0.8 (Figure 5.36(b)) was obtained by taking a series of confocal micrographs at different depths of the sample (Figure 5.36(a)). Particles are only visible at the oil-water interface and oil droplets appear to be partially covered, in agreement with cryo-SEM images at this oil volume fraction. At high oil volume fractions, the long term mechanical stability of droplets and their gel-like rheology is thought to arise from the occurrence of particle bridging.[25-27] In relation to this, stable emulsions have been prepared even if droplets are sparsely covered.[28,29] In this case, particles accumulate spontaneously at the point of contact between two droplets preventing coalescence.[27] In the light of these findings, the occurrence of particle bridging in this system at high oil volume fraction (ϕ_o = 0.8) was checked using the highest magnification available in the CLSM. Lee *et al*. used the same technique to report particle bridging in emulsions stabilised by fluorescent silica microspheres.[30] Unfortunately, as shown in Figure 5.37, in this case the individual PEC particles cannot be detected in the thin liquid film between two drops (due to their small diameter) and a red halo is observed instead.

Figure 5.36. (a) Confocal micrographs of a freshly prepared emulsion with n-dodecane ($\phi_o = 0.8$) and an aqueous PEC dispersion ($x_{PSSNa} = 0.83$, [PEL] = 10 g L^{-1}, pH = 2) at different depths. The fist image of the series corresponds to the top of the emulsion drop and the last image to the bottom. The depth scan goes down the emulsion droplet from left to right on each line. Scale bars = 200 μm (b) 3D images built from images in (a) taken from different perspectives. x and y = 800 μm, z = 400 μm.
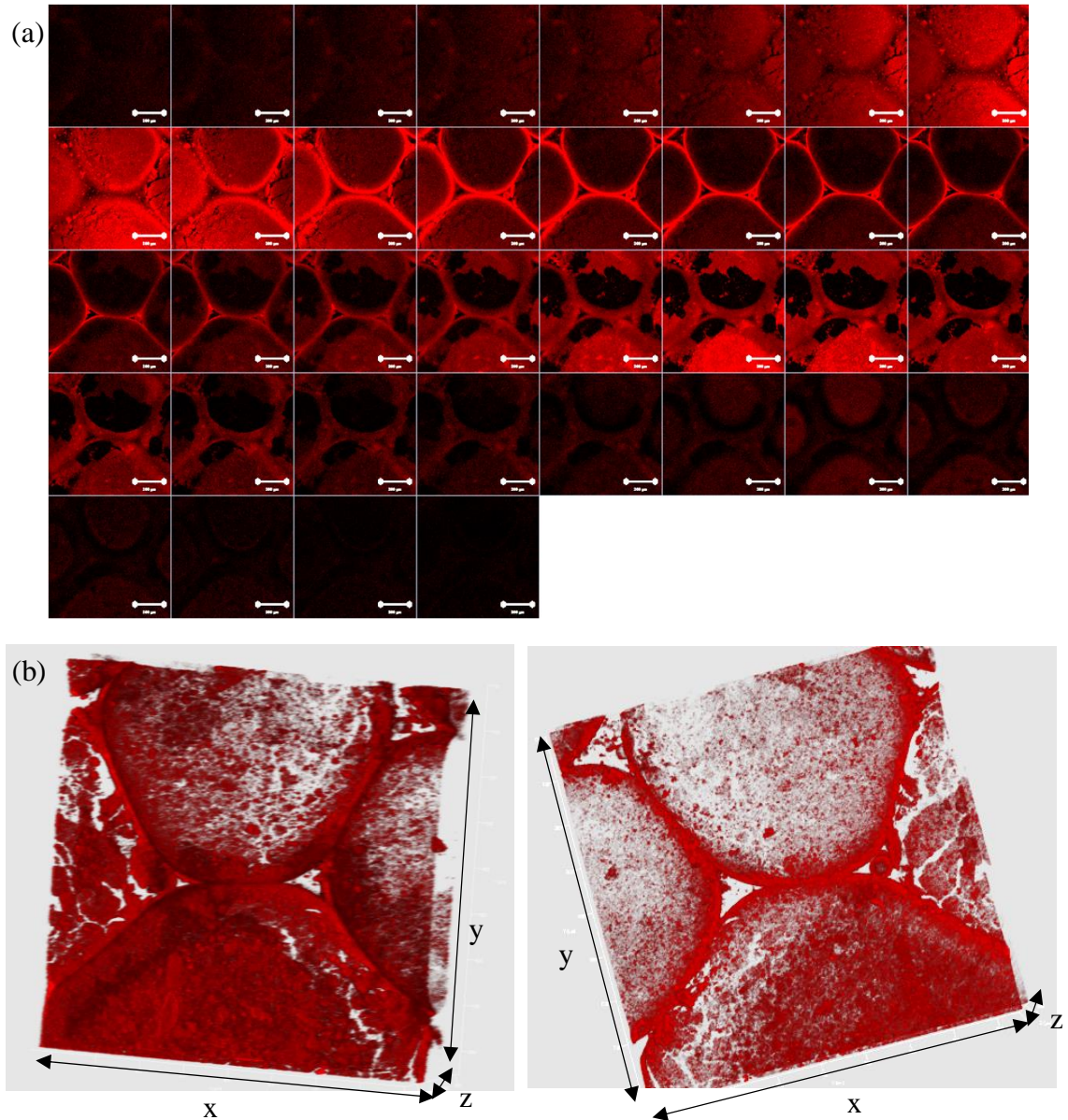
Figure 5.37. Optical (left) and confocal (right) micrographs of an emulsion prepared with n-dodecane ($\phi_o = 0.8$) and an aqueous PEC dispersion ($x_{PSSNa} = 0.83$, [PEL] = 10 g L^{-1}, pH = 2) at two different areas: (a) Plateau border and (b) thin film.
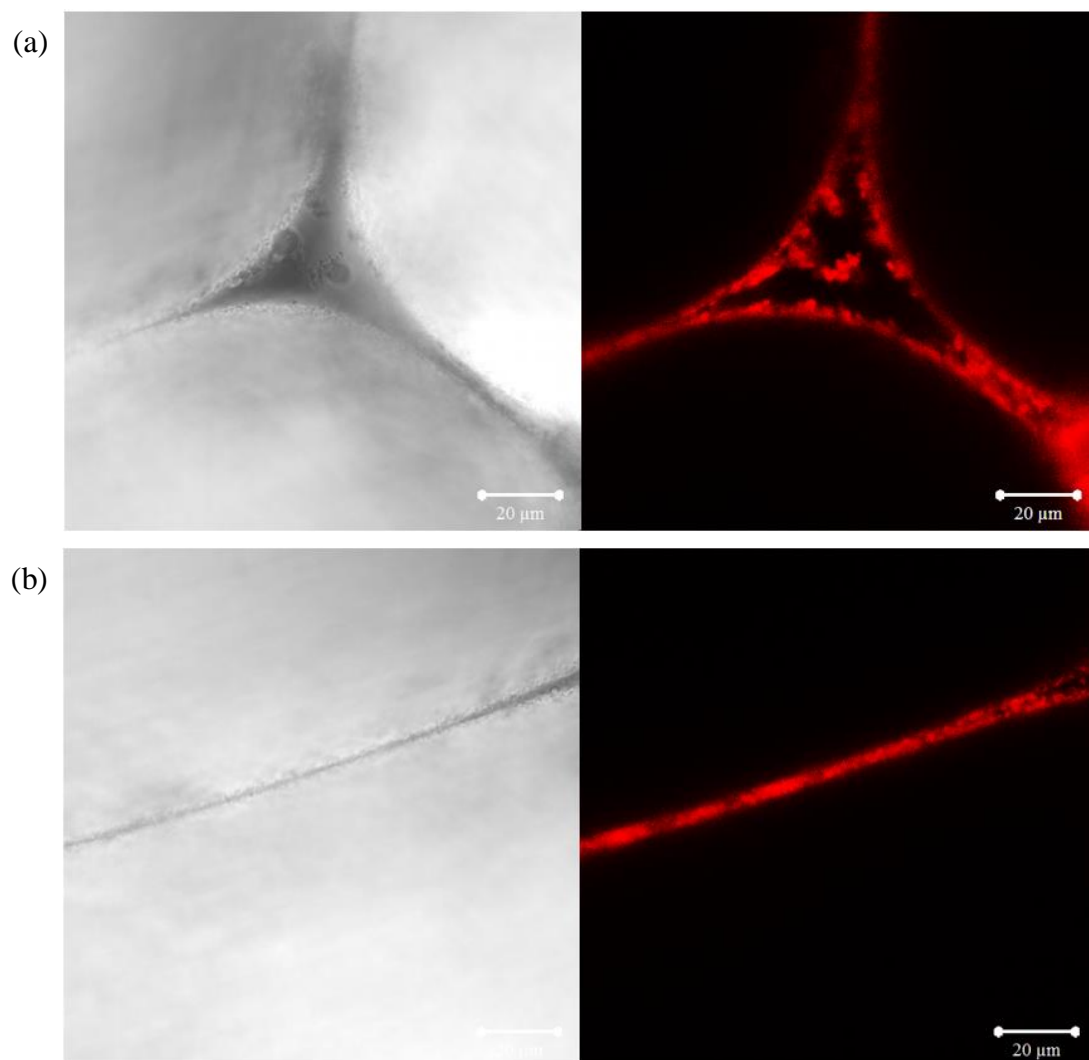
5.4.5 Emulsions prepared with dried PEC particles

Until now, oil-in-water emulsions were prepared under all conditions. In a very recent publication, Zanini *et al*. found out that for their own synthesised particles with specific surface roughness, depending in which phase particles were first dispersed, either oil-in-water or water-in-oil emulsions could be prepared.[31] For the emulsions prepared throughout this thesis, PEC particles were formed *in situ* in water and therefore they were firstly dispersed in this phase. To check whether the other emulsion type could be prepared, PEC particles from an aqueous PEC dispersion ($x_{PSSNa} = 0.83$, [PEL] = 5 g L^{-1}, pH = unmodified) were dried, ground with a pestle and a mortar and dispersed in n-dodecane. PEC particles disperse well by a gentle

hand-shake but completely sediment after a few minutes (Figure 5.38), probably due to the relatively large crystals and their higher density compared to PEC particles prepared in water. Water was then added and the two phases were homogenised with an Ultra-turrax at 13,200 rpm for 2 min ([particles] in the overall emulsion = 2.9 wt.%, $\phi_w = 0.2$). Photos of the emulsion after preparation are shown in Figure 5.39. From the drop test the emulsion type was found to be o/w. Therefore, this suggest that particles are not hydrophobic enough to render the other emulsion type. However, few points are noteworthy. Oil droplets were bigger compared to when particles were initially dispersed in water (Figure 5.40). This is probably due to the larger size of the particles as with the manual grinding the size could not be reduced further. This could be improved by reducing their size further with a different method, such as the ball mill or by applying ultrasounds. Moreover, it is worth mentioning that the amount of particles in the overall emulsion were obtained from the equivalent of twenty five aqueous PEC dispersions. However, the emulsion stability was better when the emulsion was prepared with the particles present in one aqueous PEC dispersion. Regarding the long term stability, the emulsion cream was stable at least one month after preparation.

Figure 5.38. (1) *n*-dodecane added to dried and ground PEC particles, (2) appearance after hand-shaking and (3) appearance of the dispersion in (2) after settling down for 30 seconds. Scale bar = 1 cm. (4) Optical microscope image of PEC particles after drying and grinding in air.
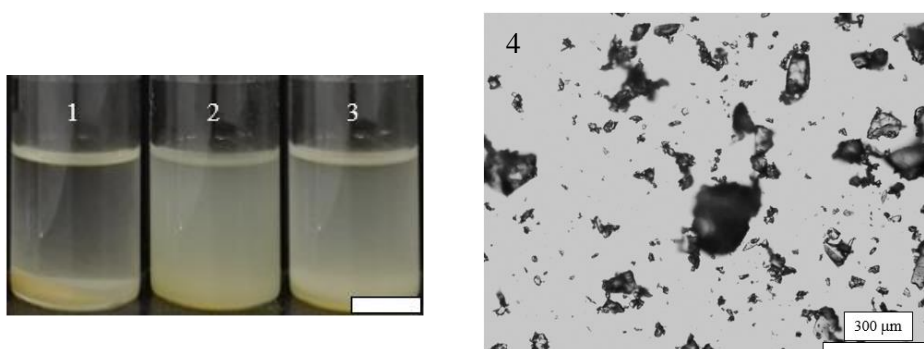
Figure 5.39. (a) Appearance of vial containing the dry particles in Figure 5.38(4) dispersed in *n*-dodecane (upper phase) and water at unmodified pH (lower phase) (ϕ_w = 0.2). (b) Appearance of emulsion prepared with an Ultra-turrax (13,200 rpm for 2 min) by homogenising the phases in (a) at different times (given). Scale bar = 1 cm.
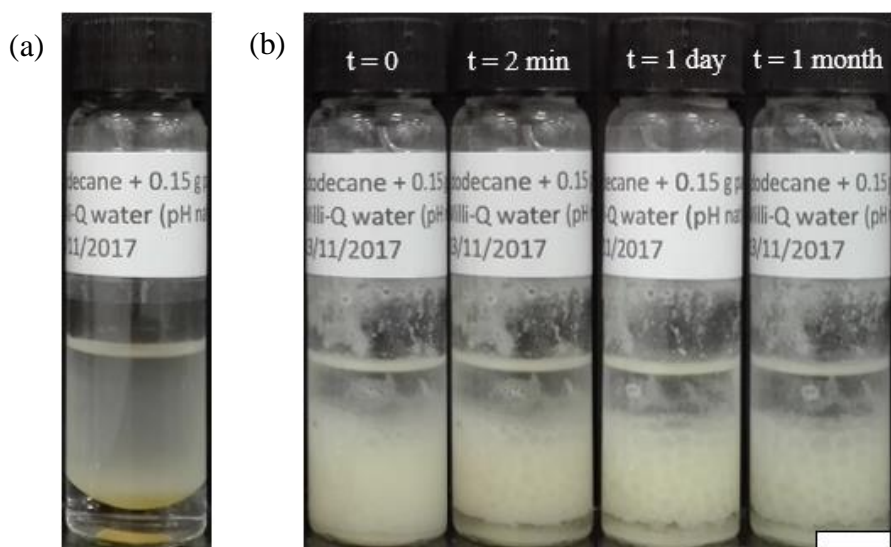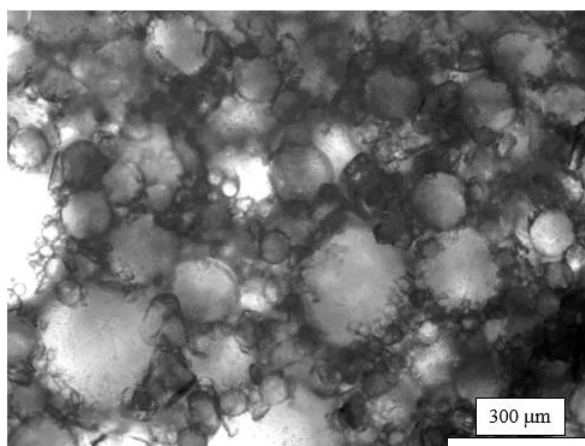

Figure 5.40. Optical microscope image of the emulsion in Figure 5.39(b) after preparation.

5.5 Conclusions

In the present chapter, the characterisation of aqueous PEC dispersions and emulsions has been carried out for the PEC system between a weak cationic (PAH) and a strong anionic (PSSNa) polyelectrolyte. For aqueous PEC dispersions, the transition precipitate – precipitate/coacervate – coacervate – polymer solution occurs by increasing the pH. At low pH, both PEL are fully ionised and therefore precipitates are formed as a result of strong electrostatic interactions. By increasing the pH, the degree of ionisation of PAH decreases and weak electrostatic interactions ensue, which supports the formation of coacervate droplets.

For the emulsion study, the influence of parameters such as x_{PSSNa}, [PEL], pH and oil volume fraction were evaluated. Oil-in-water emulsions were prepared in all cases. The most stable emulsions with PEC particles are obtained around charge neutralisation ($x_{PSSNa} = 0.83$) probably due to a large number of PEC particles compared to the other x_{PSSNa}. As neither PAH nor PSSNa are surface-active in the long term (coalescence after two months is 100% and 46%, respectively) it can be claimed that emulsion stability is attributable to PEC particles. Regarding the influence of [PEL] used to prepare aqueous PEC dispersions, the average droplet diameter decreases and the fraction of cream in the emulsion increases by increasing the [PEL]. On the other hand, at relatively high [PEL] the stability of emulsions is slightly reduced, probably due to high aggregation levels of PEC particles. Emulsion stabilisation decreases considerably when coacervate droplets are present in the dispersion. Therefore, the stability of emulsions prepared with PEC particles is enhanced compared to those prepared with PEC coacervates. High internal phase emulsions, identified by the occurrence of deformed droplets and gel-like emulsions with high viscosities, are obtained at high oil volume fractions, which is unusual in particle-stabilised systems. From CLSM, at low ϕ_o, both the aqueous continuous phase and the oil-water interface are fully covered by PEC particles. Conversely, at high ϕ_o, particles were placed only at the interface of dispersed droplets, which were sparsely covered.

5.6 References

1. M. Fang, C.H. Kim, G.B. Saupe, H. Kim, C.C. Waraksa, T. Miwa, A. Fujishima and T.E. Mallouk, *Chem. Mater.*, 1999, **11**, 1526-1532.

2. J. Choi and M.F. Rubner, *Macromolecules*, 2005, **38**, 116-124.

3. D.D. Perrin, B. Dempsey and E.P. Serjeant, *pKa Prediction for Organic Acids and Bases*, Chapman and Hall, New York, 1981.

4. M. Sotiropoulou, C. Cincu, G. Bokias and G. Staikos, *Polymer*, 2004, **45**, 1563-1568.

5. A. Matralis, M. Sotiropoulou, G. Bokias and G. Staikos, *Macromol. Chem. Phys.*, 2006, **207**, 1018-1025.

6. L. Gärdlund, L. Wågberg and M. Norgren, *J. Colloid Interface Sci.*, 2007, **312**, 237-246.

7. M. Mende, G. Petzold and H. Buchhammer, *Colloid Polym. Sci.*, 2002, **280**, 342-351.

8. V. Starchenko, M. Müller and N. Lebovka, *J. Phys. Chem. B*, 2012, **116**, 14961-14967.

9. S. Tcholakova, N.D. Denkov and A. Lips, *Phys. Chem. Chem. Phys.*, 2008, **10**, 1608-1627.

10. S. Arditty, C.P. Whitby, B.P. Binks, V. Schmitt and F. Leal-Calderon, *Eur. Phys. J. E*, 2003, **11**, 273-281.

11. M. Destribats, M. Rouvet, C. Gehin-Delval, C. Schmitt and B.P. Binks, *Soft Matter*, 2014, **10**, 6941-6954.

12. B.P. Binks and S.O. Lumsdon, *Langmuir*, 2000, **16**, 2539-2547.

13. B.P. Binks and J.A. Rodrigues, *Langmuir*, 2003, **19**, 4905-4912.

14. N.R. Cameron and D.C. Sherrington, in *Biopolymers Liquid Crystalline Polymers Phase Emulsion*, Advances in Polymer Science, Springer, Berlin, Heidelberg, 1996, vol. 126, ch. 4.

15. K.J. Lissant, in *Emulsions and Emulsion Technology part 1*, ed. K.J. Lissant, Marcel Dekker Inc., New York, 1974, ch. 1.

16. S. Zhang, Y. Zhu, Y. Hua, C. Jegat, J. Chen and M. Taha, *Polymer*, 2011, **52**, 4881-4890.

17. Y. Hu, S. Yin, J. Zhu, J. Qi, J. Guo, L. Wu, C. Tang and X. Yang, *Food Hydrocolloids*, 2016, **61**, 300-310.

18. V.O. Ikem, A. Menner and A. Bismarck, *Langmuir*, 2010, **26**, 8836-8841.

19. V.O. Ikem, A. Menner and A. Bismarck, *Angew. Chem., Int. Ed.*, 2008, **47**, 8277-8279.

20. I. Capron and B. Cathala, *Biomacromolecules*, 2013, **14**, 291-296.

21. C.W. Macosko, *Rheology: Principles, Measurements and Applications*, Wiley-VCH, New York, 1994, p. 449.

22. A.Y. Malkin, I. Masalova, P. Slatter and K. Wilson, *Rheol. Acta*, 2004, **43**, 584-591.

23. R. Pal, *AIChE J.*, 1996, **42**, 3181-3190.

24. R. Pal, *J. Colloid Interface Sci.*, 2000, **255**, 359-366.

25. P. Thareja and S. Velankar, *S. Rheol. Acta*, 2007, **46**, 405-412.

26. P. Thareja and S. Velankar, *S. Rheol. Acta*, 2008, **47**, 189-200.

27. T.S. Horozov and B.P. Binks, *Angew. Chem.*, 2006, **118**, 787-790.

28. B.R. Midmore, *Colloids Surf., A*, 1998, **132**, 257-265.

29. E. Vignati and R. Piazza, *Langmuir*, 2003, **19**, 6650-6656.

30. M.N. Lee, H.K. Chan and A. Mohraz, *Langmuir*, 2012, **28**, 3085-3091.

31. M. Zanini, C. Marschelke, S.E. Anachkov, E. Marini, A. Synytska and L. Isa, *Nat. Commun.,* 2017, **8**, 15701.

CHAPTER 6 – MIXTURE OF WEAK CATIONIC, PAH, AND WEAK ANIONIC, PAANa POLYELECTROLYTES

6.1 Introduction

In this chapter, the polyelectrolyte combination formed by two weak polyelectrolytes of similar molecular weight (PAH, 160 kDa, and PAANa, 131.2 kDa) is investigated. Due to their nature, the degree of ionisation varies with the pH in both cases. The experiments presented here have been designed taking into consideration the results of the previously investigated systems so the outcome can help to elucidate a general pattern of behaviour of emulsions stabilised by polyelectrolyte complexes.

Firstly, aqueous PEC dispersions at different pH are characterised in terms of size and zeta potential. Afterwards, the type of associative phase separation at different pH values is identified visually and from optical microscope images at two different [PEL]. Co-existence of precipitates and coacervate droplets is detected across the x_{PAANa} at low and intermediate pH, while at high pH coacervate droplets only are formed.

After some preliminary studies at different pH, the emulsion stability was evaluated in detail at pH = 5.5 as none of the PEL appears to be surface-active, *i.e.* they do not stabilise emulsions on their own. The emulsion with highest stability (smallest average droplet diameter and lowest amount of oil coalesced) is obtained with aqueous PEC dispersions prepared with a x_{PAANa} around charge neutrality. The influence of the oil volume fraction (ϕ_o) was also investigated. High internal phase emulsions (HIPEs) up to a fraction of oil equal to 0.85 with high viscosity are prepared with PEC particles as emulsifiers, in line with the results obtained for the system PAH-PSSNa. Taking advantage from the inherent fluorescence of PAH at pH = 5.5, PEC particles could be visualised without any further modification through confocal laser scanning microscopy (CLSM). At high oil volume fractions, droplet surfaces are partially coated and the continuous aqueous phase appears to be depleted in particles.

6.2 Degree of ionisation PAH and PAANa

As already presented in Chapters 4 and 5, PAH and PAANa are weak polyelectrolytes. Curves of the degree of ionisation against the pH obtained from potentiometric titrations of each polyelectrolyte are shown together in Figure 6.1. At low pH, PAH will be fully ionised and PAANa will be fully protonated; while at high pH, PAANa will be fully charged and PAH will be uncharged. Therefore, unlike the three previous systems, at any pH both polyelectrolytes will be fully charged.

Figure 6.1. Curves of the degree of ionisation *versus* pH for PAH (squares) and PAANa (circles) together with the structures present at each pH extreme. Taken from Figures 4.5 and 5.1.
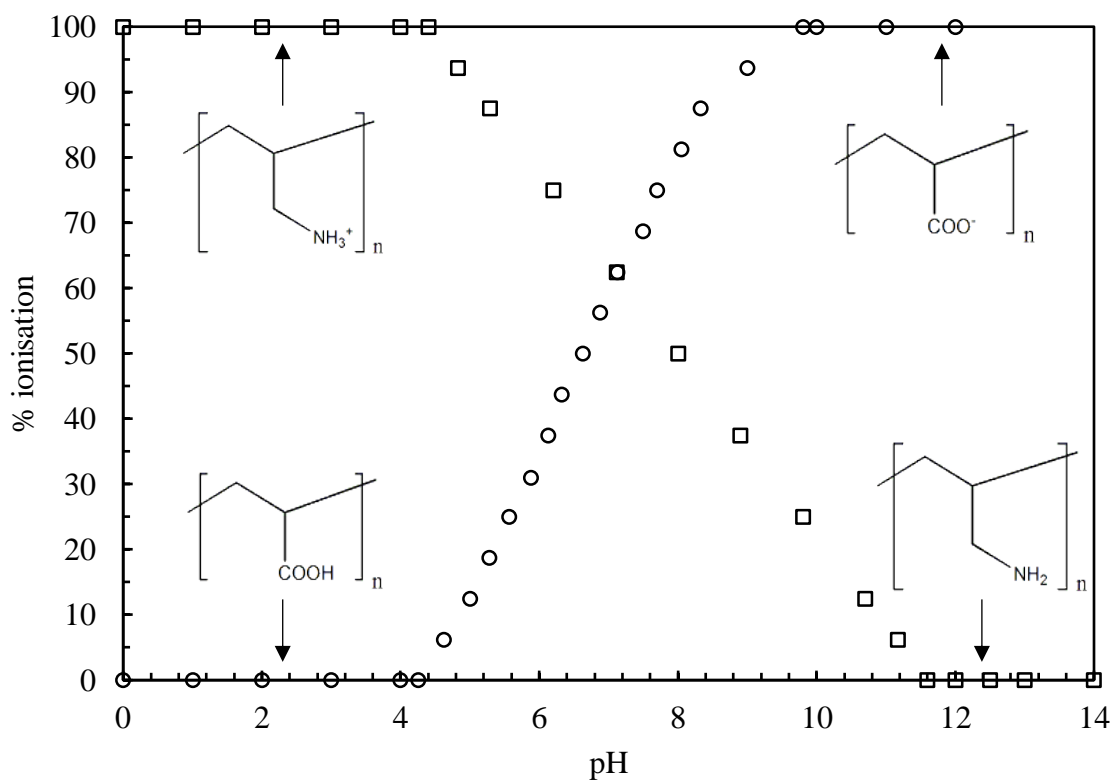
6.3 Characterisation of aqueous PEC dispersions

6.3.1 Dispersions at low PEL concentration

For the characterisation of aqueous PEC dispersions at low polyelectrolyte concentration, seven pH were selected to cover the entire pH range. The selected pH,

together with the degree of ionisation of each polyelectrolyte taken from the curves in Figure 6.1, are shown in Table 6.1.

Table 6.1. % of ionisation of each polyelectrolyte at selected pHs.

pH	% ionisation PAH	% ionisation PAANa
2	100	0
4	100	0
5.5	85	22
7	62	62
8.4	44	87
10	22	100
12	0	100

Aqueous PEC dispersions were prepared from 0.1 g L^{-1} PEL solutions at different pH and x_{PAANa}. Selected dispersions are shown in Figure 6.2. All dispersions were transparent despite few of them being bluish or containing precipitates.

The average diameter of the formed complexes was measured in triplicate for each set of aqueous PEC dispersions at different pH and x_{PAANa} (Figure 6.3). At pH extremes (2, 11 and 12), the average diameter was not measurable. The polydispersity was too high for cumulant analysis and/or the measurement was not reproducible even in a single run. Moreover, in the majority of cases, more than one peak was observed in the size distribution plot or the peak was not monomodal. For this PEL system, at pH extremes complexes are not expected to be formed *via* electrostatic interactions as one of the polyelectrolytes is not charged. For intermediate pH values, when both PEL are partially ionised, a relatively monomodal distribution was observed for dispersions prepared at all x_{PAANa} (PDI < 0.2). At the mole fractions where precipitation occurred, size measurements were not carried out and this occurrence is indicated in the average diameter plot with red crosses. It is worth noting that the maximum in the average diameter plot shifts to lower values of x_{PAANa} by increasing the pH and this maximum matches with the most bluish aqueous PEC dispersions or when precipitation occurred. At pH = 4, despite complexes through electrostatic interactions not being expected to

be formed, both monomodal distributions in the average diameter and precipitation were observed across the x_{PAANa} range.

Upon the interaction, the pH of the dispersion changes and this can modify the degree of ionisation of each polyelectrolyte. In fact, the pH of aqueous PEC dispersions at different x_{PAANa} was measured after preparation and varied, for example, from 3.7 to 4.1 at pH = 4, from 4.3 to 5.8 at pH = 5.5 and from 6.8 to 7.2 at pH = 7. Although Petrov et al.[1] and Vitorazi et al.[2] measured the reduction in pH after mixing due to proton release around the pK_a, we note that the majority of work in this area makes no mention of this.[3-5] Therefore, as done for the previous PEL systems, we quote the initial pH before mixing in all cases.

Figure 6.2. Appearance of selected freshly prepared aqueous PEC dispersions from 0.1 g L^{-1} PEL solutions at different x_{PAANa} and pH (given). Scale bars = 1 cm.
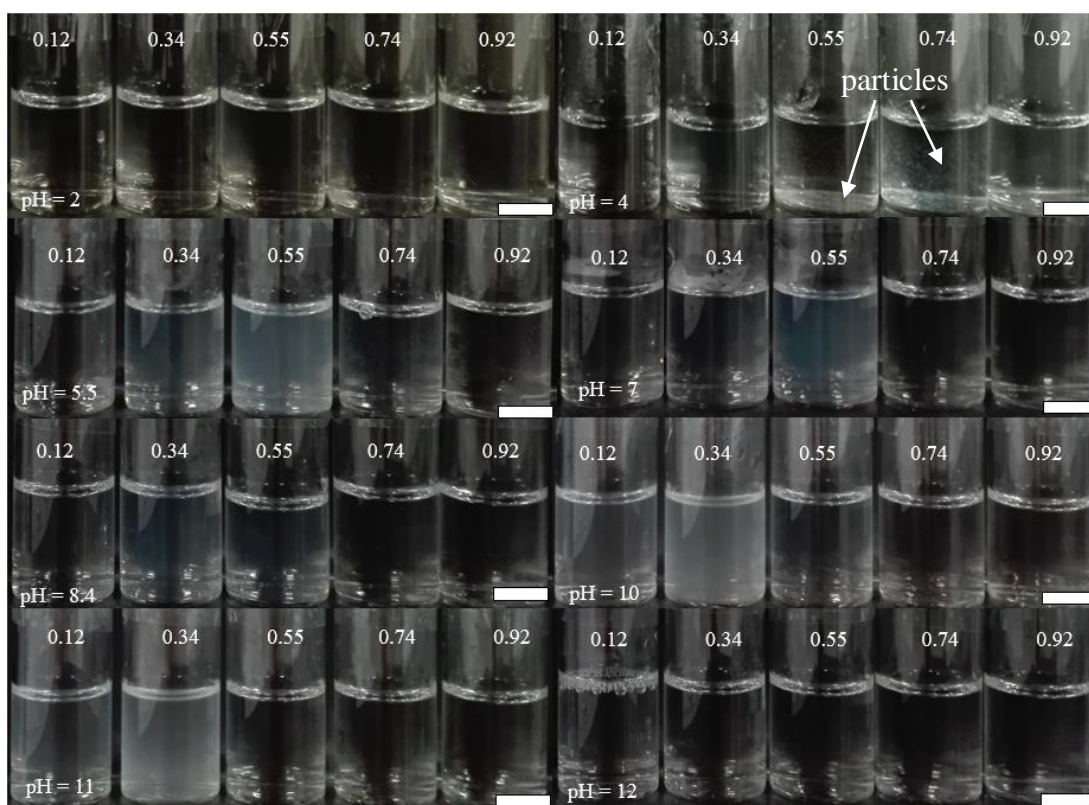
Figure 6.3. Variation of the average particle diameter with x_{PAANa} for aqueous PEC dispersions prepared from 0.1 g L^{-1} PEL solutions at different pH (given). Black circles represent the values measured with the Zetasizer while red crosses indicate the x_{PAANa} where visible precipitates appeared (size meaningless). The dashed vertical lines are drawn as guidance.
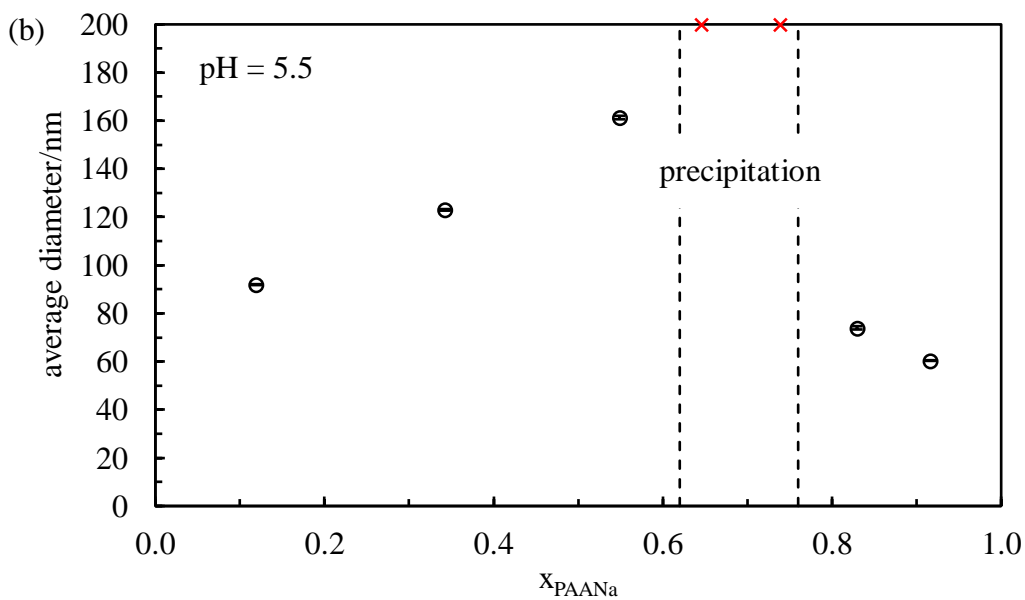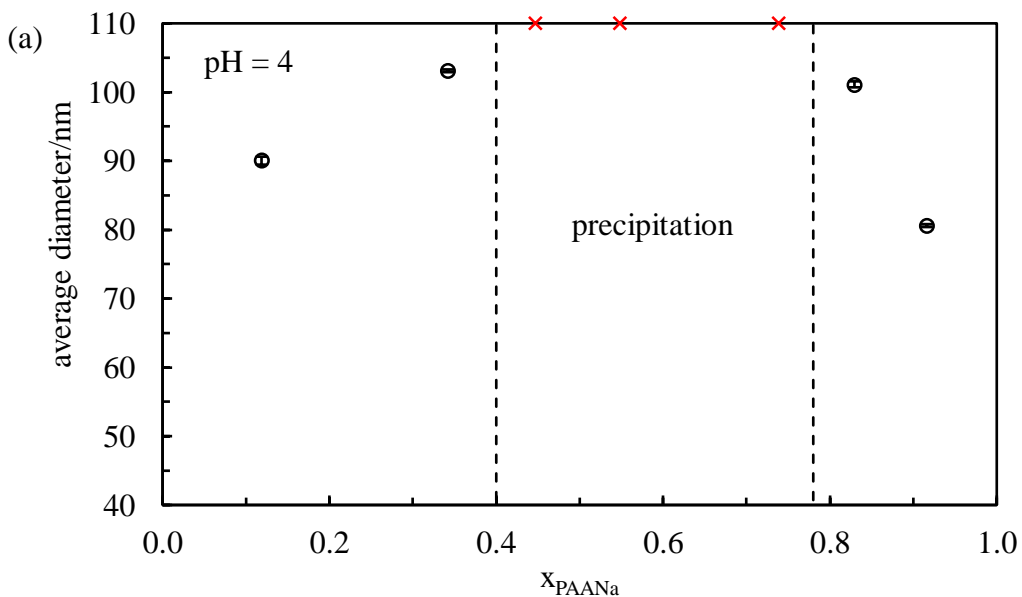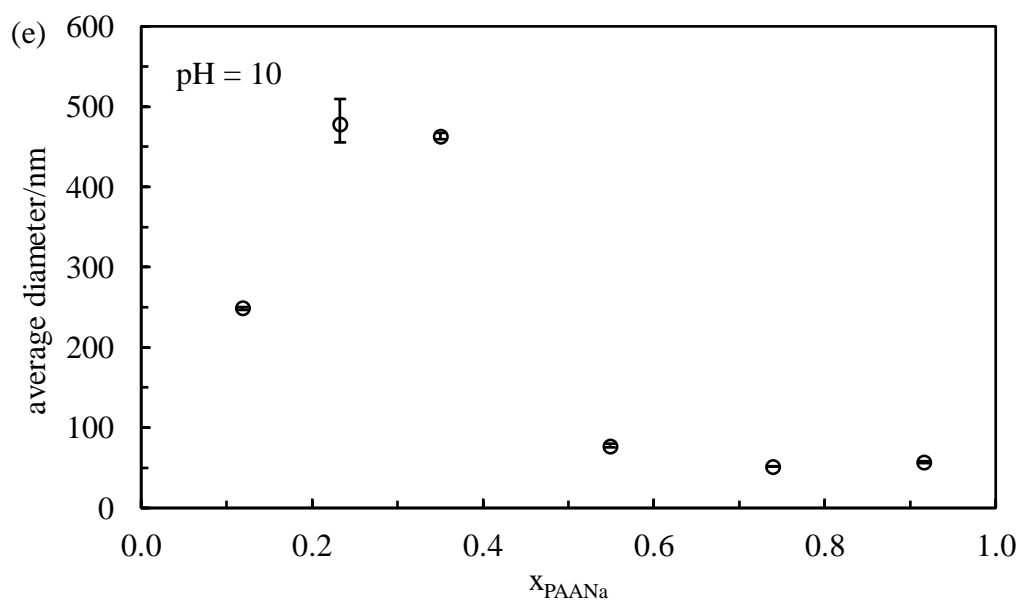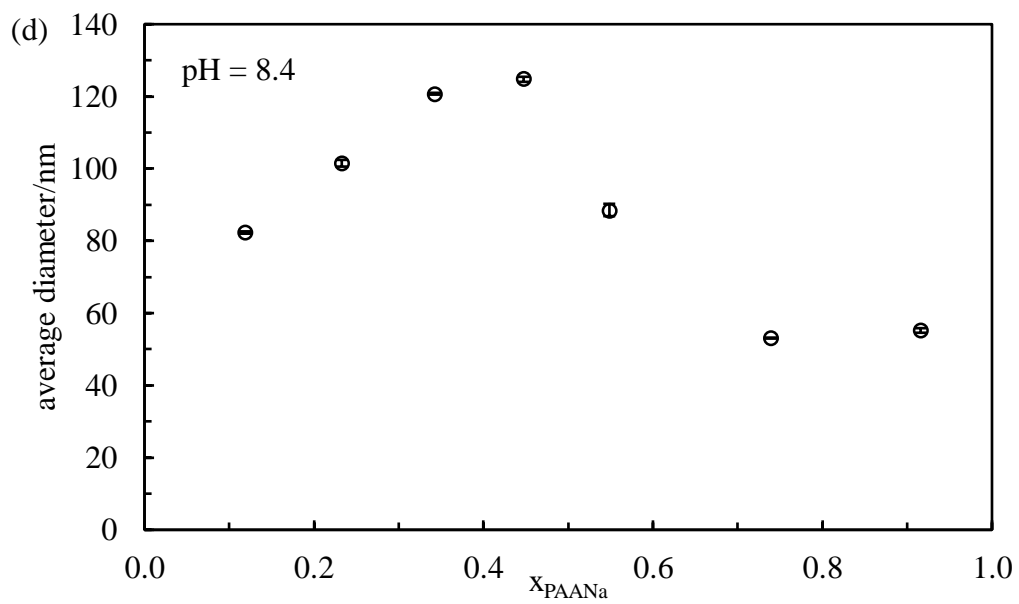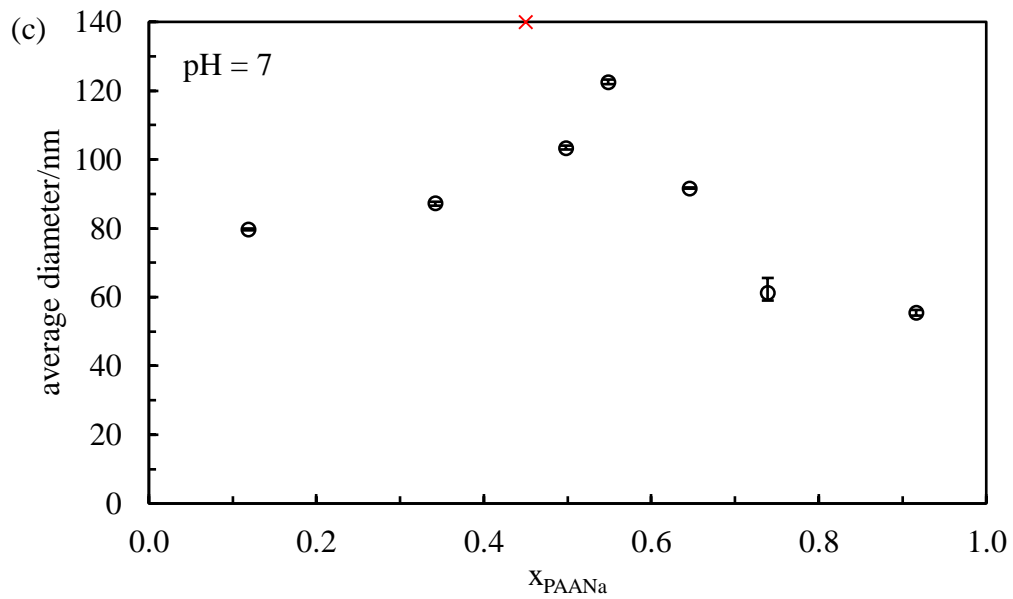
Zeta potential measurements were carried out for aqueous PEC dispersions at different pH and x_{PAANa} (Figure 6.4). The results are separated in two plots. Figure 6.4(a) shows zeta potential curves at the pH where the degree of ionisation of PAH is higher than that of PAANa and Figure 6.4(b) displays the zeta potential when the degree of ionisation of PAH is lower than that of PAANa. At pH extremes (2 and 12), the curve exhibits only either positive (PAH fully charged) or negative (PAANa fully charged) values. At intermediate pH, a sigmoidal curve with positive and negative values is obtained.

Figure 6.4. Variation of the zeta potential with x_{PAANa} for aqueous PEC dispersions prepared from 0.1 g L^{-1} PEL solutions at different pH. In (a) the degree of ionisation of PAH is $\geq$ than that of PAANa, while in (b) it is lower than that of PAANa.
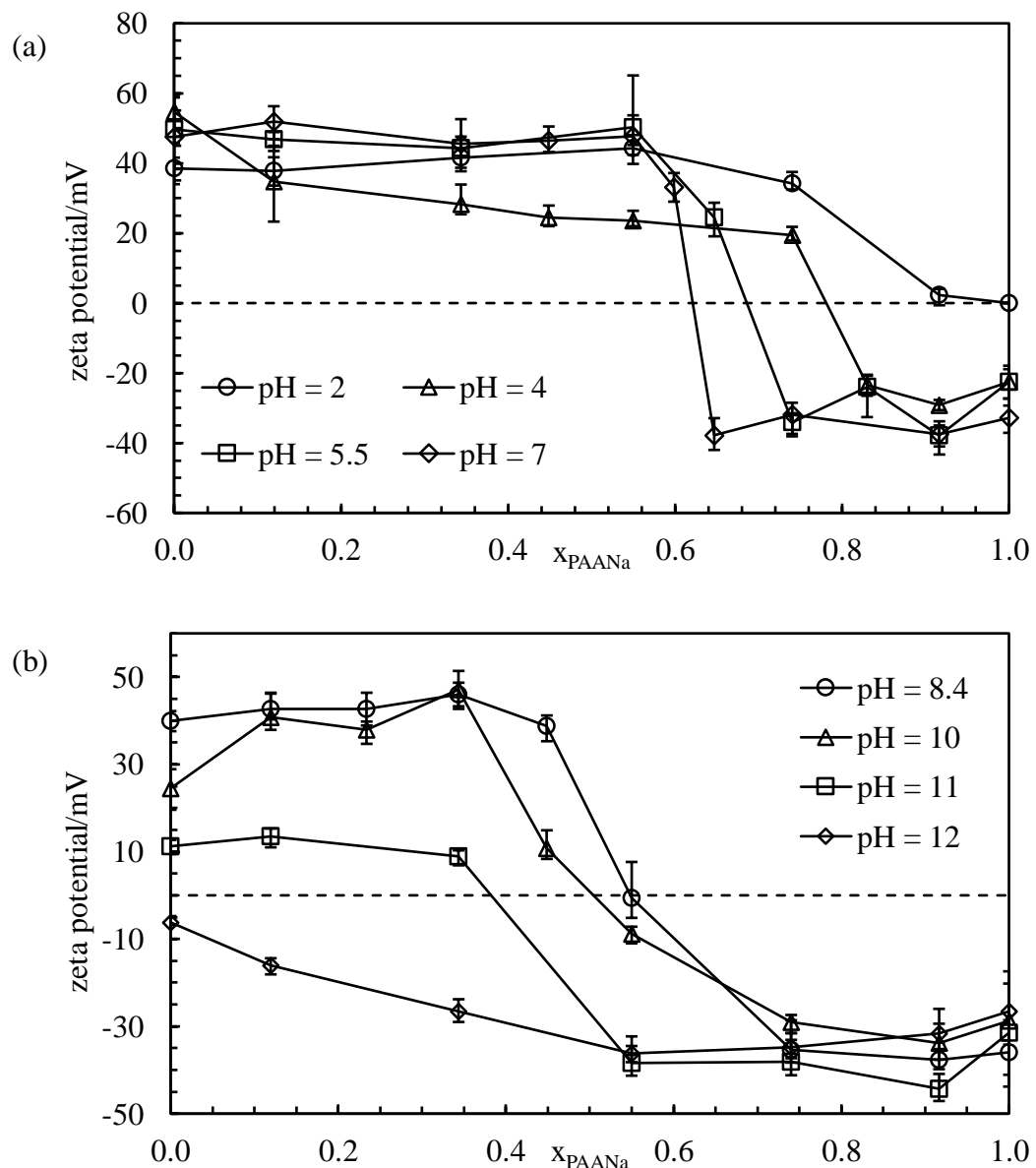
The x_{PAANa} where the zeta potential is zero decreases as the pH increases, as expected (Figure 6.5). As soon as the pH increases, the amount of ionised PAANa increases and PAH gets less charged. Therefore, less PAANa is needed to neutralise the positive charges on PAH. The same conclusions were taken from the system PDADMAC-PAANa (Chapter 4).

Figure 6.5. Variation of x_{PAANa} at zeta potential = 0 with pH for aqueous PEC dispersions prepared from 0.1 g L^{-1} PEL solutions.
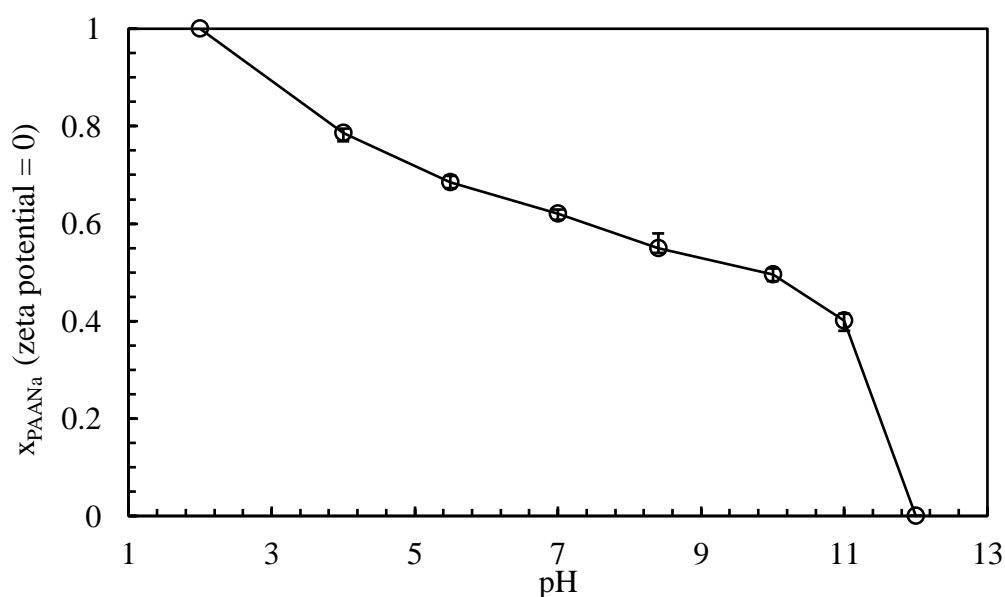
6.3.2 *Dispersions at high PEL concentration*

6.3.2.1 Effect of pH and mole fraction of anionic polyelectrolyte on the type of associative phase separation

Three pH (4, 7 and 10) were studied at higher [PEL] (1 g L^{-1}) to evaluate the type of associative phase separation at various pH and across the x_{PAANa} range. At pH = 4, PEC particles were obtained at intermediate mole fractions as shown in Figure 6.6. Moreover, few coacervate droplets were detected at the x_{PAANa} extremes. Despite the fact that at this pH no electrostatic interaction is expected to occur as PAANa is fully protonated, as mentioned previously, upon complexation the pH of the dispersion can change and this can modify the strength of the interaction.

Figure 6.6. Appearance of aqueous PEC dispersions prepared from 1 g L^{-1} PEL solutions at pH = 4 at different x_{PAANa} (given). Images taken one hour after preparation. Scale bar = 1 cm. (b) Optical microscope images of a drop of dispersion at selected x_{PAANa} (given). The inset figure for a x_{PAANa} = 0.26 shows an image of the dispersion at higher magnification to show the presence of coacervate droplets.
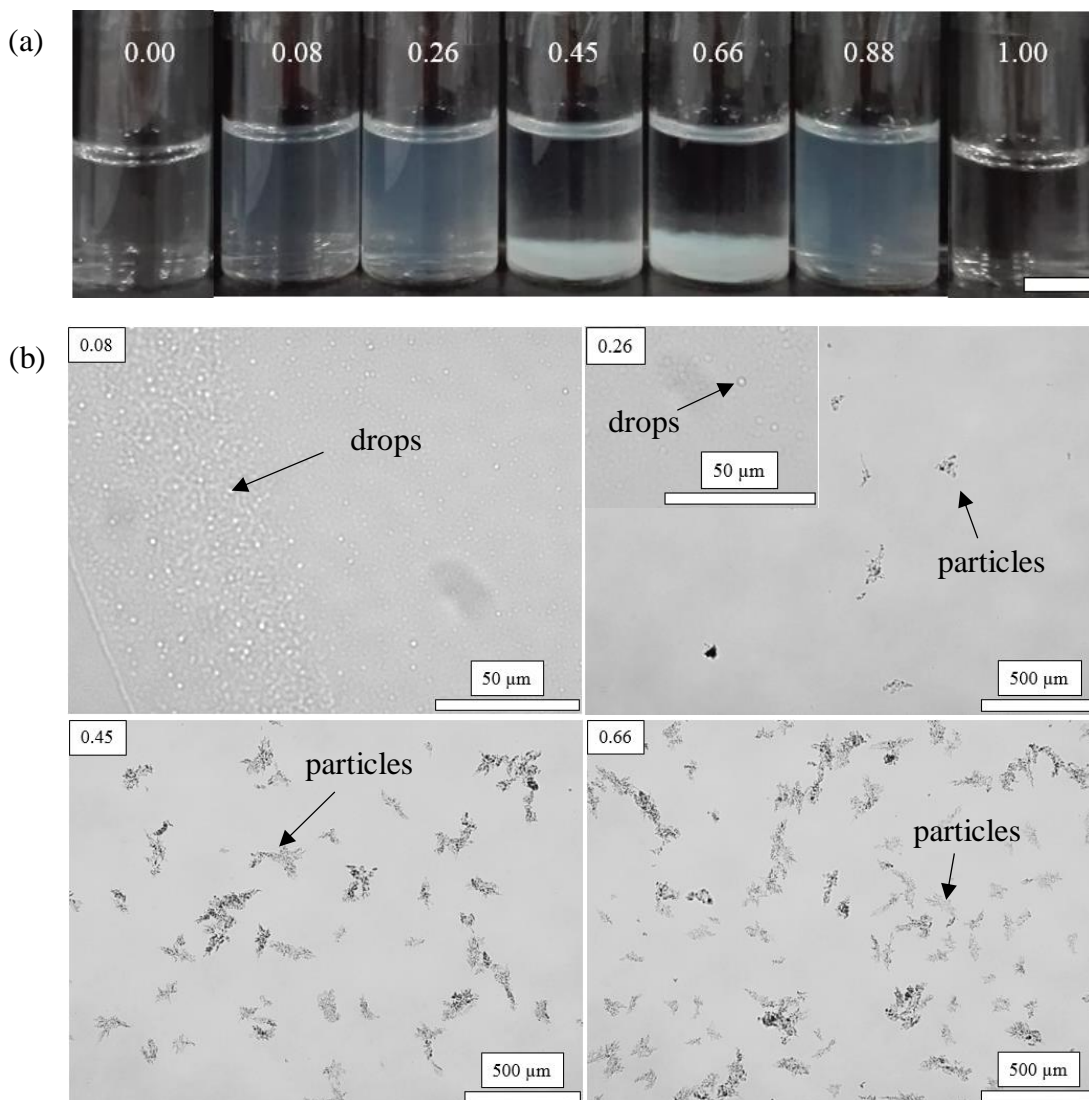
At pH = 7, coacervate droplets are detected at all mole fractions (Figure 6.7). At this pH both PEL are 62% ionised. The weak electrostatic interaction could explain the formation of coacervate droplets. The highest amount of complexes is obtained at x_{PAANa} = 0.45 as the dispersion is the most whitish one. The pH of the dispersions varied from 5.5 to 7.0 at this pH and [PEL].

Figure 6.7. Appearance of aqueous PEC dispersions prepared from 1 g L^{-1} PEL solutions at pH = 7 at different x_{PAANa} (given). Images taken four hours after preparation. Scale bar = 1 cm. (b) Optical microscope images of a drop of dispersions at selected x_{PAANa} (given).
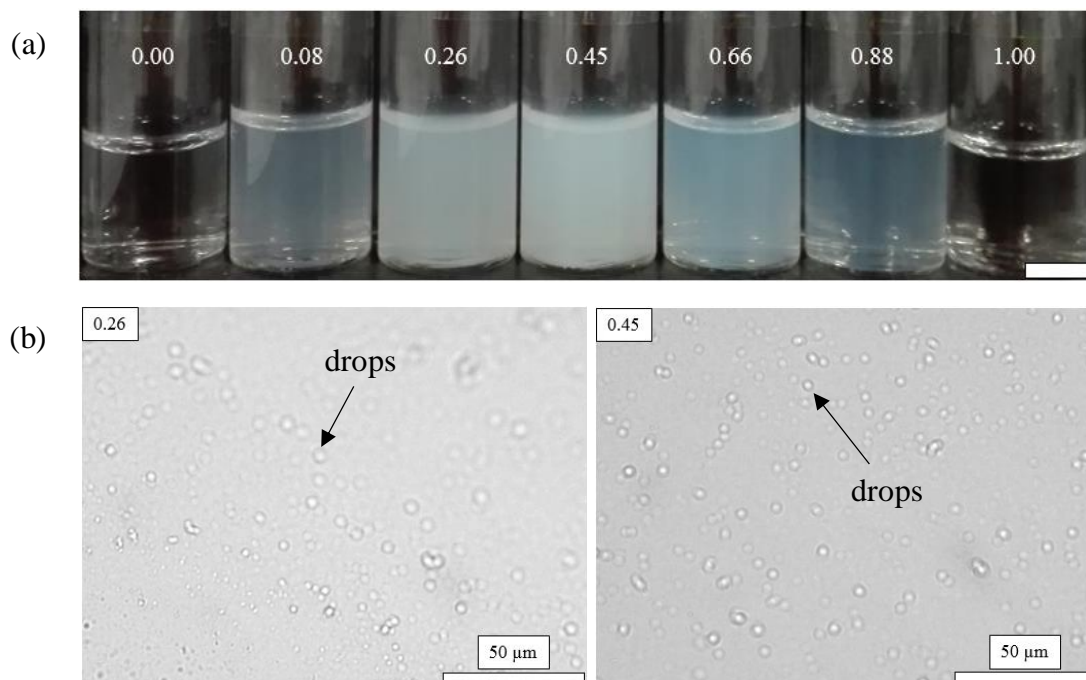
At pH = 10, only coacervate droplets were detected (Figure 6.8). No precipitate formation was identified, neither visually nor *via* optical micrographs. At this pH, the degree of ionisation of PAH and PAANa is 22% and 100%, respectively. Therefore, the weak electrostatic interaction would explain the formation of coacervate droplets. The appearance of the dispersions is shown after preparation and after four hours. It is noteworthy the change in the turbidity of the aqueous PEC dispersion with a x_{PAANa} = 0.26. This dispersion, despite initially being the most whitish one, after four hours it turned almost completely transparent (Figure 6.8(b)). Aqueous PEC dispersions prepared with the systems PDADMAC-PAANa and PAH-PSSNa at specific pH and mole fraction of anionic polyelectrolyte showed the same behaviour. This is attributable to the coalescence of coacervate droplets forming the so-called coacervate phase. The pH of the dispersions varied from 10.1 to 11.2 at this pH and [PEL].

In general, from the study at these three pH, it can be observed that by increasing the pH, the most turbid dispersion or that with the highest amount of PEC precipitates is obtained at a lower x_{PAANa} (0.66, 0.45 and 0.26 for a pH of 4, 7 and 10, respectively).

This tendency is in agreement with the zeta potential plot obtained at a lower [PEL] (Figure 6.5), despite the value of x_{PAANa} corresponding to charge neutrality occurs at a higher x_{PAANa} (0.78, 0.62 and 0.50 for a pH of 4, 7 and 10, respectively).
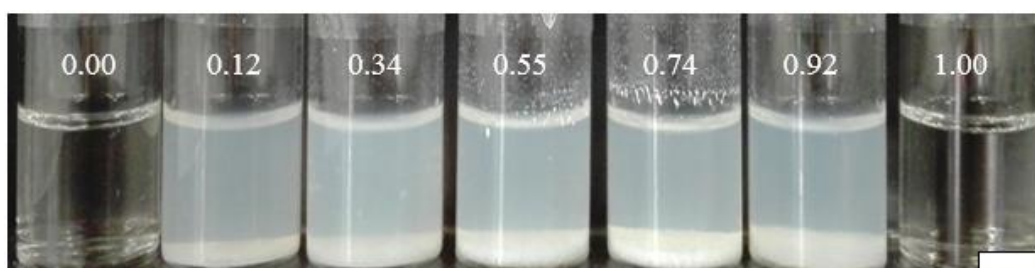
Figure 6.8. Appearance of aqueous PEC dispersions prepared from 1 g L^{-1} PEL solutions at pH = 10 at different x_{PAANa} (given). Images taken (a) after preparation and (b) four hours after preparation. Scale bars = 1 cm. (c) Optical microscope images of a drop of dispersion at selected x_{PAANa} (given).
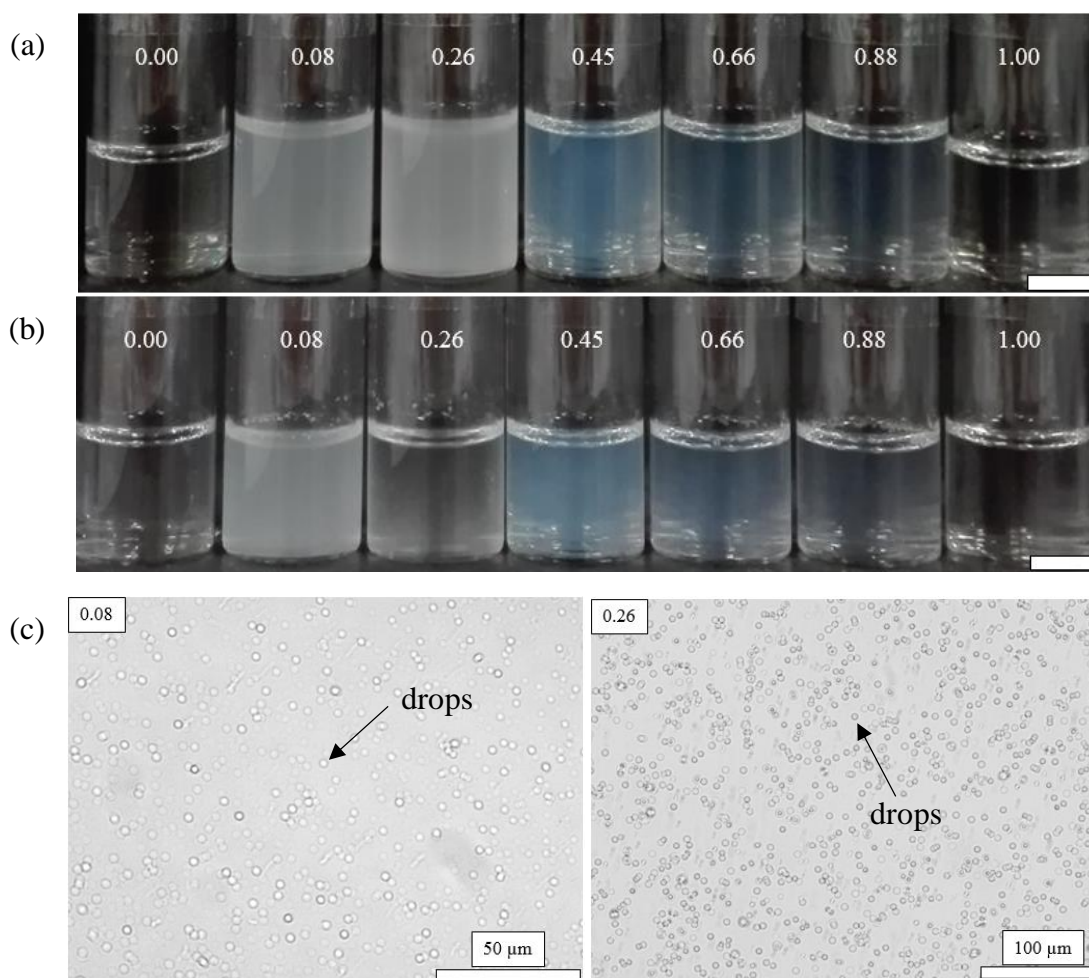
The same study was carried out by increasing the [PEL] to 5 g L^{-1} at four pH (4, 5.5, 7 and 10). At pH = 4 and 5.5, PEC particles and coacervate droplets were formed as shown in Figures 6.9 and 6.10, in aggrement with the results obtained for a [PEL] = 1 g L^{-1}. For a pH of 5.5, the x_{PAANa} range was studied in more detail and both particles and coacervate droplets were detected at all x_{PAANa} except for a x_{PAANa} = 0.74, where PEC particles only were formed (Figure 6.11). Moreover, the amount of PEC particles

increases drastically at this x_{PAANa}, while the height of the particles at the other x_{PAANa} is comparable. Furthemore, the appearance of PEC particles at a $x_{PAANa} = 0.74$ is fluffy compared to the other x_{PAANa}, which have a more compact structure. Moreover, complexes at a $x_{PAANa} = 0.74$ do not fully sediment probably due to their relatively low density. This mole fraction corresponds to the value of charge neutralisation from the zeta potential curves, which could explain the formation of precipitates. These results are similar to the ones presented for the system PAH-PSSNa at pH = 2 (Chapter 5).

Figure 6.9. Appearance of aqueous PEC dispersions prepared from 5 g L^{-1} PEL solutions at pH = 4 at different x_{PAANa} (given). Images taken two hours after preparation. Scale bar = 1 cm.

Figure 6.10. Appearance of aqueous PEC dispersions prepared from 5 g L^{-1} PEL solutions at pH = 5.5 at different x_{PAANa} (given). Images taken (a) after preparation and (b) two months after preparation. Scale bars = 1 cm.
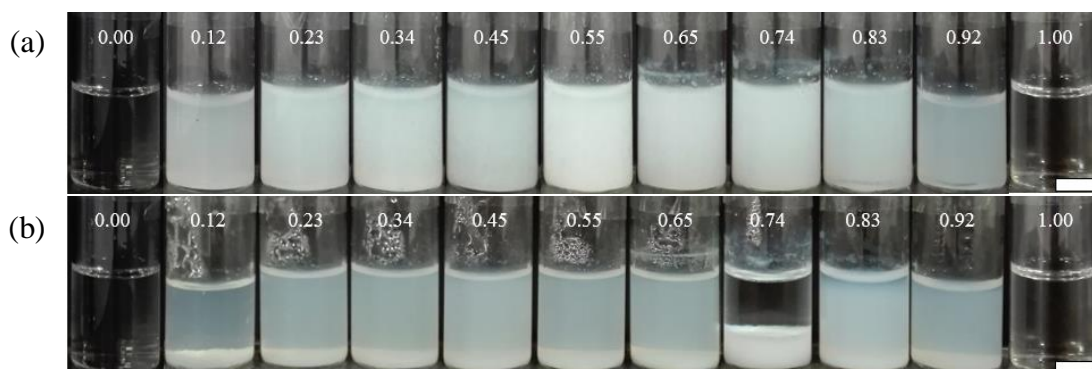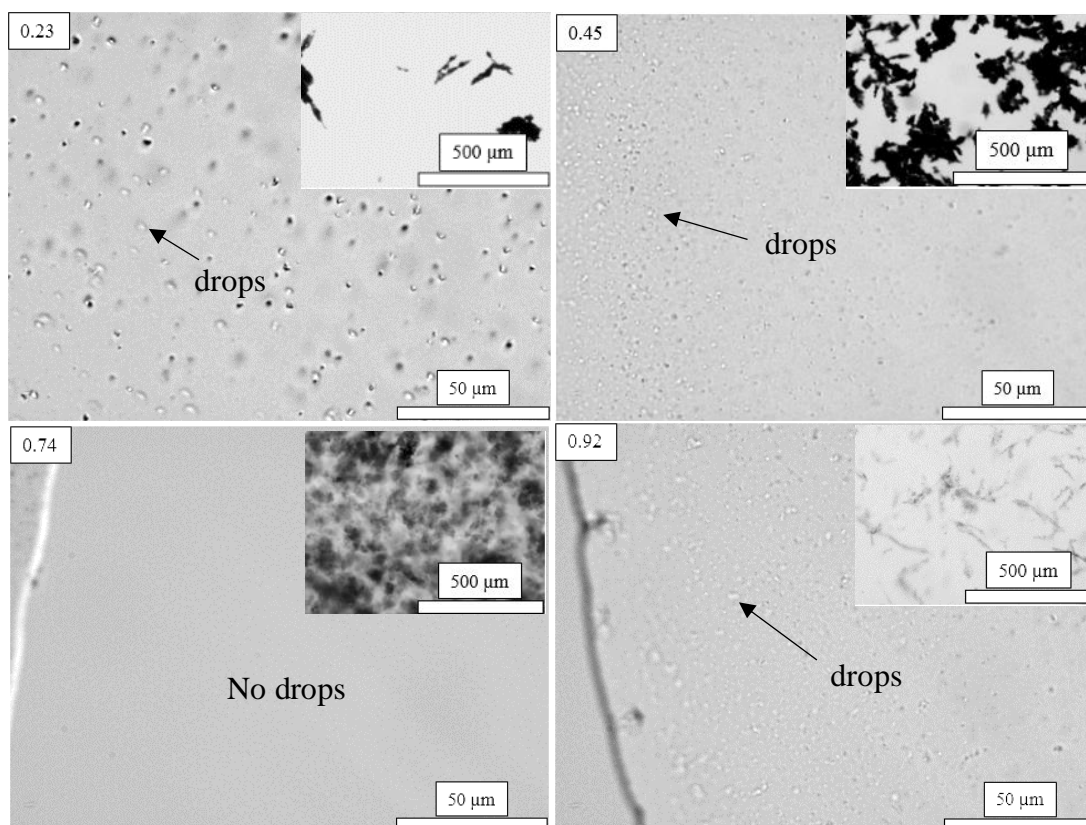
Figure 6.11. Selected optical microscope images of aqueous PEC dispersions in Figure 6.10 at different x_{PAANa} (given). Images at two different magnifications for each x_{PAANa} are shown to check the formation of coacervate droplets (picture at high magnification) and particles (inset at lower magnification).

For pH = 7 at a [PEL] = 5 g L^{-1} (Figure 6.12), both particles and coacervate droplets were formed, despite coacervate droplets only being detected at a lower [PEL] (1 g L^{-1}) (Figure 6.7). Therefore, the transition PEC coacervates to PEC precipitates is detected by increasing the [PEL]. This transition was not observed for the previously studied systems by increasing the [PEL]. In the literature, the transition from precipitate to coacervate was observed in some cases by increasing the salt concentration[6,7] and the molecular weight of the polyelectrolytes.[8] Koetz and Kosmella observed that complexes prepared with low molecular weight polyelectrolytes gave coacervation, while precipitates were obtained with PEL of high molecular weight.[8] The pH of these dispersions at high [PEL] were not measured. However, the formation of precipitates might be explained by the fact that upon complexation at this high [PEL] the pH of the final dispersion could have been reduced down to pH values between 4 and 5 so precipitates arised. In fact, by comparing the

pH of dispersions prepared at a [PEL] = 0.1 and 1 g L^{-1}, by increasing the [PEL] the lowest pH measured was reduced to 6.8 and 5.5, respectively.

Figure 6.12. Appearance of aqueous PEC dispersions prepared from 5 g L^{-1} PEL solutions at pH = 7 at different x_{PAANa} (given). Images taken after preparation. Scale bar = 1 cm.
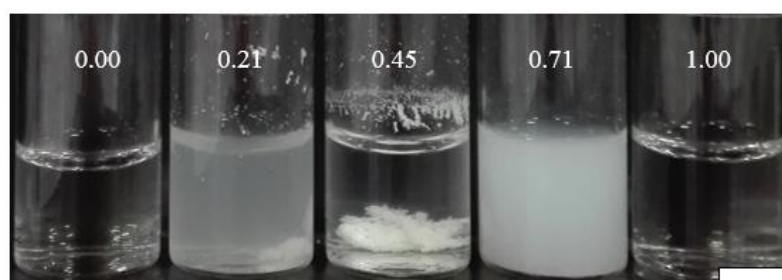
At pH = 10, the transition mentioned above for pH = 7 was not observed. Instead, coacervate droplets only were detected (Figure 6.13(c, left)). As for the lower [PEL] (1 g L^{-1}), the turbidity of the most whitish dispersion (x_{PAANa} = 0.21) decreased considerably three hours after preparation (Figure 6.13(b)). Dispersions at the other mole fractions were completely transparent, unlike the ones prepared at lower [PEL] (1 g L^{-1}) and coacervate droplets were not detected (Figure 6.13(c, right).

Figure 6.13. Appearance of aqueous PEC dispersions prepared from 5 g L^{-1} PEL solutions at pH = 10 at different x_{PAANa} (given) (a) after preparation and (b) three hours after preparation. Scale bars = 1 cm. (c) Optical microscope images of a drop of dispersions at selected x_{PAANa} (given).

(a)

(b)
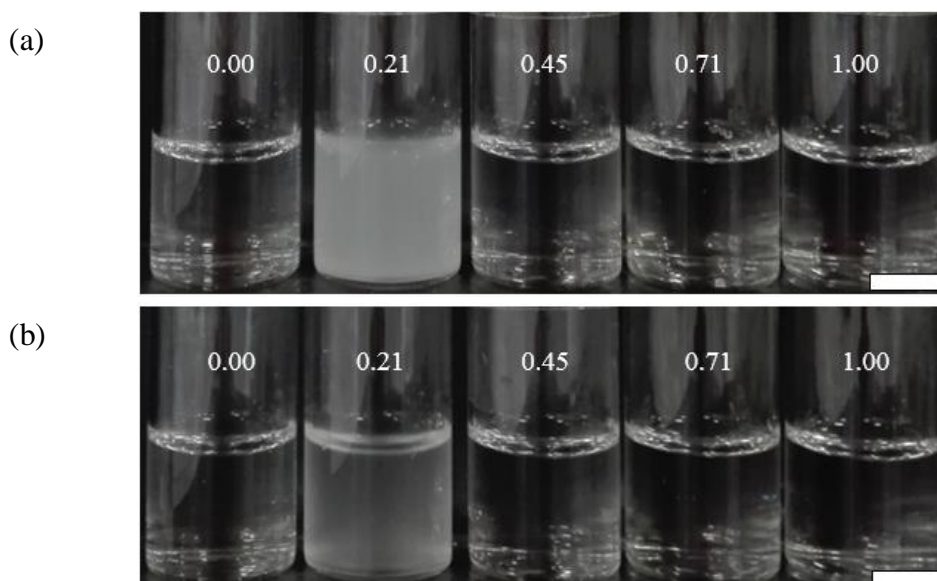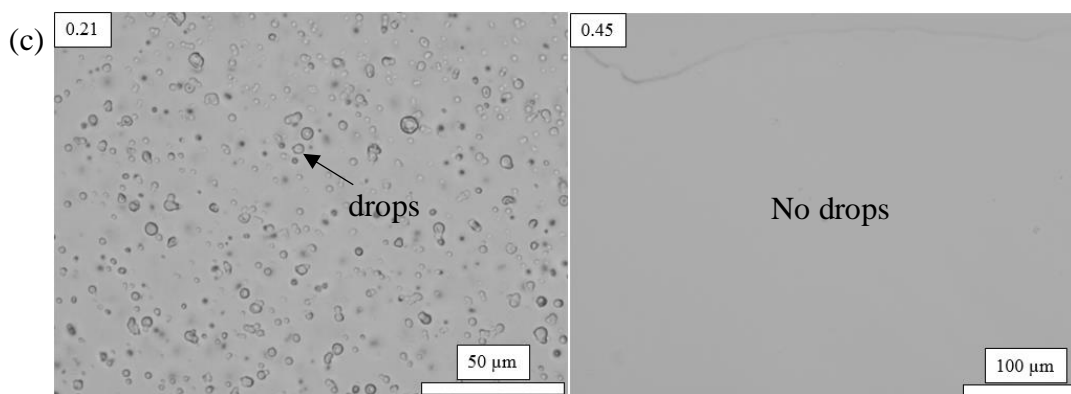
In this section the effect of x_{PAANa}, pH and [PEL] was evaluated on the type of associative phase separation (precipitation and coacervation). In general, by increasing the pH from 4 to 10 the transition precipitate/coacervate – coacervate occurred. By increasing the [PEL] from 1 to 5 g L^{-1}, the formation of PEC particles was extended to more x_{PAANa} at pH = 4 and 5.5, and particles were formed at intermediate pH (7) at specific x_{PAANa}, despite only coacervate droplets were formed at this pH at low [PEL] (1 g L^{-1}).

6.3.3 Summary of aqueous PEC dispersions

The results presented in this first part of the chapter correspond to the characterisation of aqueous dispersions of the PEL system constituted by two weak polyelectrolytes. The effect of pH and x_{PAANa} was evaluated for the average diameter and the charge of complexes prepared in water. At pH extremes, no complexes are formed as one polyelectrolyte is fully protonated. Therefore, polyelectrolyte complexes are formed only at pH where both polyelectrolytes are partially ionised. The size of the complexes falls into the nanometer range despite at specific x_{PAANa} aggregation of particles lead to precipitate formation. At high [PEL], both precipitates and coacervates were identified visually and from optical microscope images at low and intermediate pH, while coacervate droplets are only formed at relatively high pH and specific x_{PAANa}. In any case, the amount of PEC is higher at a x_{PAANa} around charge neutralisation.

6.4 Oil-in-water emulsions prepared from polymer mixtures

6.4.1 Effect of pH and mole fraction of anionic polyelectrolyte on emulsion stability

The effect of pH and x_{PAANa} was evaluated on emulsion stability. A preliminary study at four pH (4, 5.5, 7 and 10) was carried out to select the pH and x_{PAANa} at which the complete study of emulsion stability will be centered.

At pH = 4, emulsions were prepared with n-dodecane (ϕ_o = 0.2) and aqueous PEC dispersions prepared from 5 g L^{-1} PEL solutions (Figure 6.9). As seen from Figure 6.14, PAH (x_{PAANa} = 0.00) is not surface-active as complete phase separation occurred after homogenisation. On the other hand, PAANa (x_{PAANa} = 1.00) stabilises an oil-in-water emulsion alone and high amounts of foam were produced upon homogenisation, as already pointed out for the system PDADMAC-PAANa at low pH (Chapter 4). For emulsions prepared at intermediate x_{PAANa}, PEC particles seem to have migrated partially to the cream after emulsification, as few particles sediment in the aqueous phase resolved five days after preparation (Figure 6.14(b)). Optical microscope images of emulsions were taken after preparation and are shown in Figure 6.15. Oil droplets are polydisperse in size in emulsions prepared with a x_{PAANa} lower than 0.92. The average droplet diameter for these x_{PAANa} is around 150 μm. Five days after preparation, the emulsion with a x_{PAANa} = 0.74 almost completely breaks, probably due to the large size of PEC particles as seen from optical microscope images.

Figure 6.14. Appearance of emulsions prepared with n-dodecane (ϕ_o = 0.2) and aqueous PEC dispersions ([PEL] = 5 g L^{-1}, pH = 4) at different x_{PAANa} (given) (a) after preparation and (b) five days after preparation. Scale bars = 1 cm.

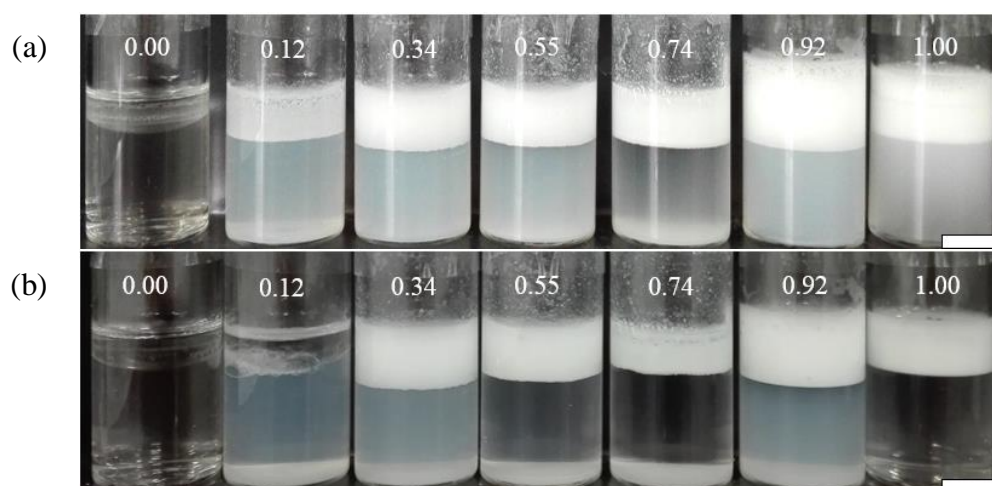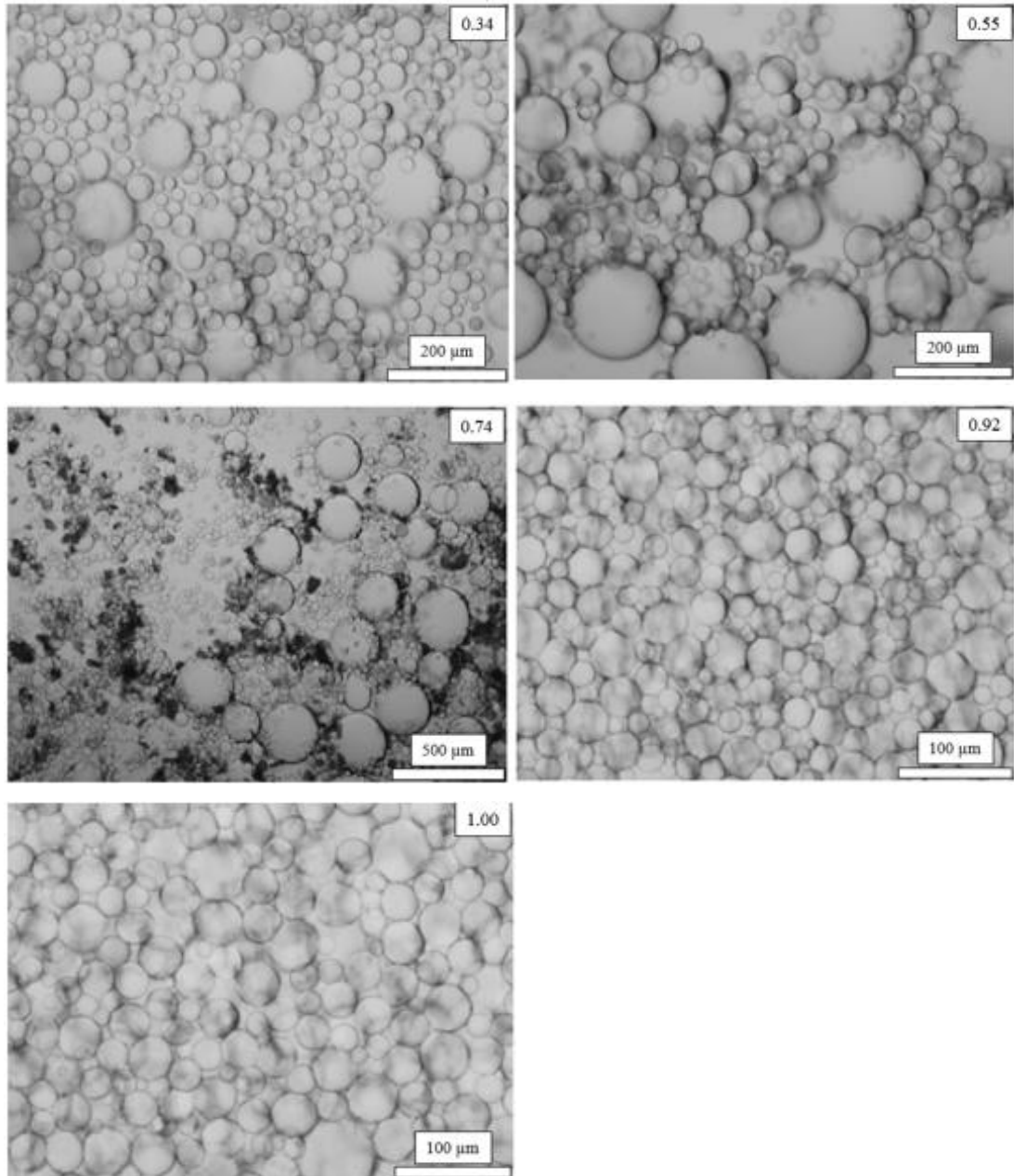**Figure 6.15.** Optical microscope images of emulsions prepared with n-dodecane (ϕ_o = 0.2) and aqueous PEC dispersions ([PEL] = 5 g L^{-1}, pH = 4) at different x_{PAANa} (given) after preparation.

At pH = 7 and 10 no emulsions could be prepared by addition of oil in one step (Figure 6.16). However, PAANa and PAH are not surface-active on their own at none of those pH as complete phase separation occurred after homogenisation.

Figure 6.16. Appearance of emulsions prepared with *n*-dodecane ($\phi_o = 0.2$) and aqueous PEC dispersions ([PEL] = 5 g L^{-1}) at different x_{PAANa} (given) at (a) pH = 7 and (b) pH = 10, after preparation. Scale bars = 1 cm.
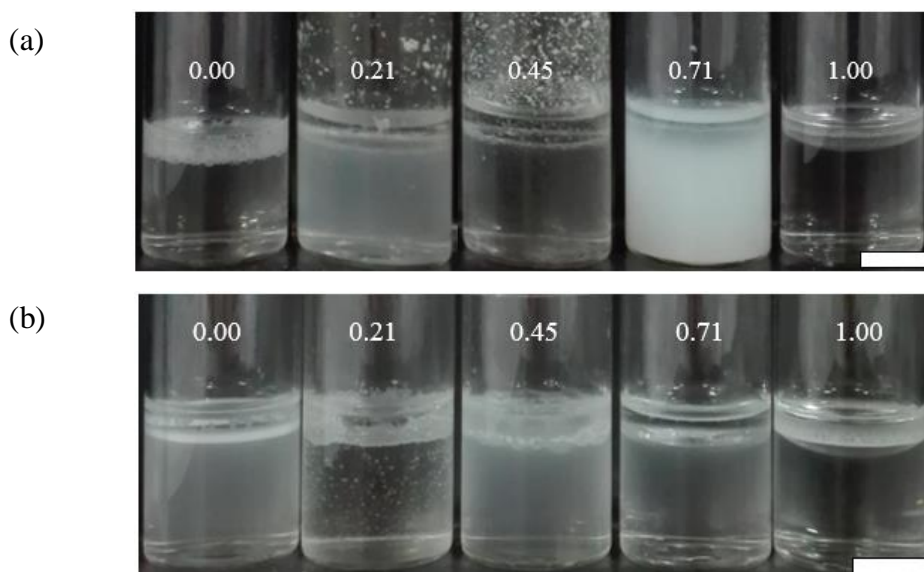
Therefore, from these preliminary results, it was suggested to prepare emulsions with aqueous PEC dispersions prepared with a pH in between 4 and 7, to see whether stable emulsions could be prepared with PEC, while emulsions with individual PEL solutions were completely unstable. In order to do so, emulsions were prepared with *n*-dodecane ($\phi_o = 0.2$) and aqueous PEC dispersions prepared from 5 g L^{-1} PEL solutions at pH = 5.5. Individual PEL are not surface-active on their own as complete phase separation occurred few hours after preparation in both cases (Figure 6.17(b)). However, stable emulsions could be prepared with specific aqueous PEC dispersions around charge neutrality. In the long term (t = 2 months), only stable emulsions with a x_{PSSNa} of 0.74 and 0.83 remained stable (Figure 6.17(c)).

Figure 6.17. Appearance of emulsions prepared with *n*-dodecane ($\phi_o = 0.2$) and aqueous PEC dispersions ([PEL] = 5 g L^{-1}, pH = 5.5) at different x_{PSSNa} (given) (a) after preparation, (b) one day after preparation and (c) two months after preparation. Scale bars = 1 cm.
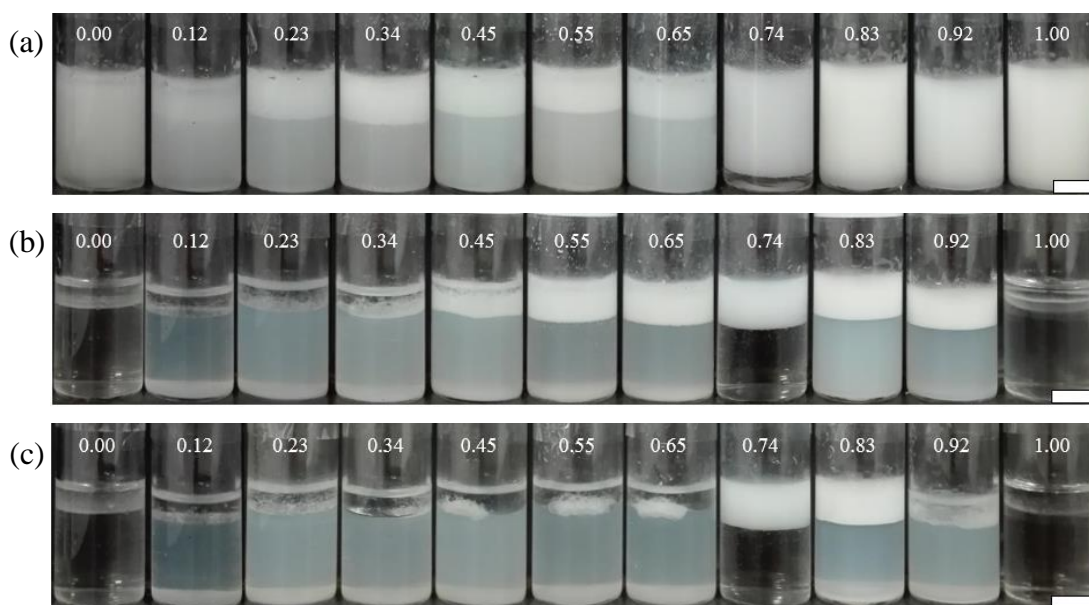
Optical microscope images were taken after preparation once creaming stopped and after two months (Figure 6.18). The average droplet diameter after preparation for emulsions with a x_{PAANa} = 0.74, 0.83 and 0.92 was 250, 20 and 26 μm, respectively (Figure 6.18(a)). Two months after preparation, the emulsion prepared with a x_{PAANa} = 0.92 completely coalesced, while the average droplet diameter remained almost unaltered for the emulsion with a x_{PAANa} = 0.83 (22 ± 4 μm) and increased slightly for that with a x_{PAANa} = 0.74 (305 ± 86 μm). The fraction of oil released after two months is 0.05 and 0.01 for the x_{PAANa} = 0.74 and 0.83, respectively.

Therefore, this system is comparable to the systems PDADMAC-PSSNa and PAH-PSSNa, where emulsion stability improved remarkably around charge neutrality. Moreover, as for the system PAH-PSSNa, the emulsion stability is centred in a narrow mole fraction range around charge neutrality.

Figure 6.18. Selected optical microscope images of emulsions prepared with *n*-dodecane (ϕ_o = 0.2) and aqueous PEC dispersions ([PEL] = 5 g L^{-1}, pH = 5.5) at different x_{PAANa} (given) (a) after preparation once creaming has stopped and (b) two months after preparation.
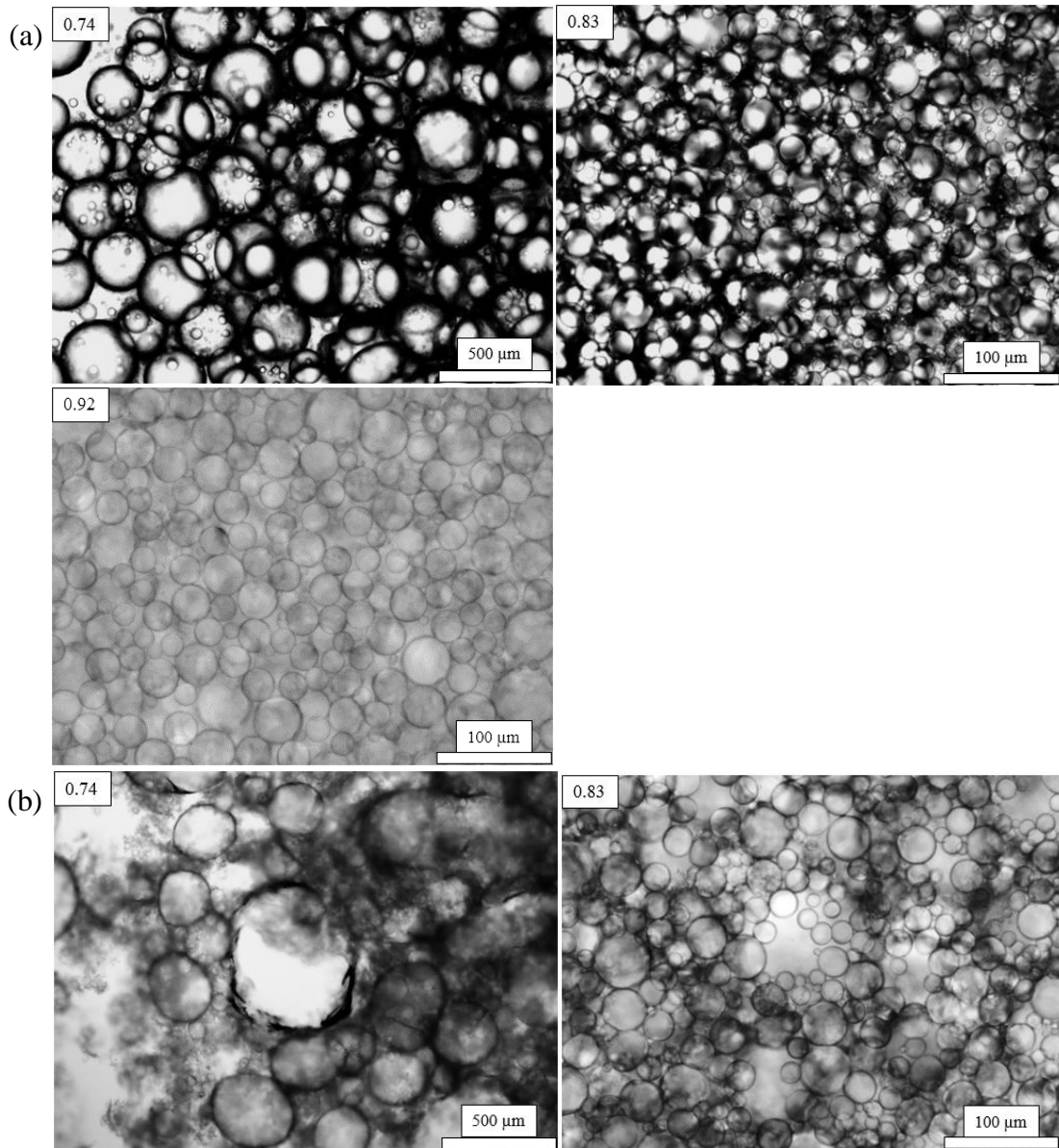
6.4.2   Effect of oil volume fraction on emulsion stability

From the results in section 6.4.1, it has been found that the most stable emulsion, with the lowest amount of oil coalesced and a stable average droplet diameter with time was the one prepared with an aqueous PEC dispersion with a x_{PAANa} = 0.83 at pH = 5.5. Therefore, the influence of the oil volume fraction was investigated in detail at this x_{PAANa}.

As shown in Figure 6.19, by increasing the fraction of oil, the height of the cream increases until a $\phi_o \geq 0.7$ where creaming was fully inhibited. Moreover, the average droplet diameter increases as shown in Figure 6.20 and 6.21(a) and the viscosity increases substantially at high oil volume fractions as the emulsion does not flow by titling the vial. Moreover, from optical microscope images at high oil volume fractions ($\phi_o = 0.8$ and 0.85), oil droplets appear deformed two months after preparation (Figure 6.20). The non-spherical morphology of oil droplets together with the increase in the viscosity of emulsions at high ϕ_o point out the occurrence of high internal phase emulsions (HIPEs). It is important to highlight that from optical micrographs taken after preparation at high oil volume fractions (0.8 and 0.85), oil droplets were spherical and really polydisperse (Figure 6.22). This polydispersity induces that oil droplets are not deformed even if the system contains more than 75% internal phase.[9] With time, small droplets might have coalesced with bigger ones and as a result they deform due to an increase in the monodispersity. The average droplet diameter increases after two months for all ϕ_o, as shown in Figure 6.21(a).

The amount of oil and water resolved two months after preparation was measured for the above emulsions and is plotted *versus* ϕ_o (Figure 6.21(b)). The amount of oil coalesced is lower than 15% for all oil volume fractions. The fraction of water resolved after preparation decreases by increasing ϕ_o until a $\phi_o \geq 0.7$, where creaming was completely inhibited.

The results presented here are fully in agreement with those obtained for the system PAH-PSSNa described in Chapter 5. HIPEs are formed in both systems at high ϕ_o, creaming was fully inhibited at a $\phi_o \geq 0.7$ and the amount of oil coalesced after two months is really low and increases slightly at high ϕ_o. The main difference between these two systems lies in the polydispersity of the droplet diameter, as for the system PAH-PSSNa oil droplets were more monodisperse in size from optical microscope images.

Figure 6.19. Appearance of emulsions prepared with an aqueous PEC dispersion (x_{PSSNa} = 0.83, [PEL] = 5 g L^{-1}, pH = 5.5) and *n*-dodecane at different ϕ_o (given) (a) after preparation once creaming has halted and (b) two months after preparation. Scale bars = 1 cm.
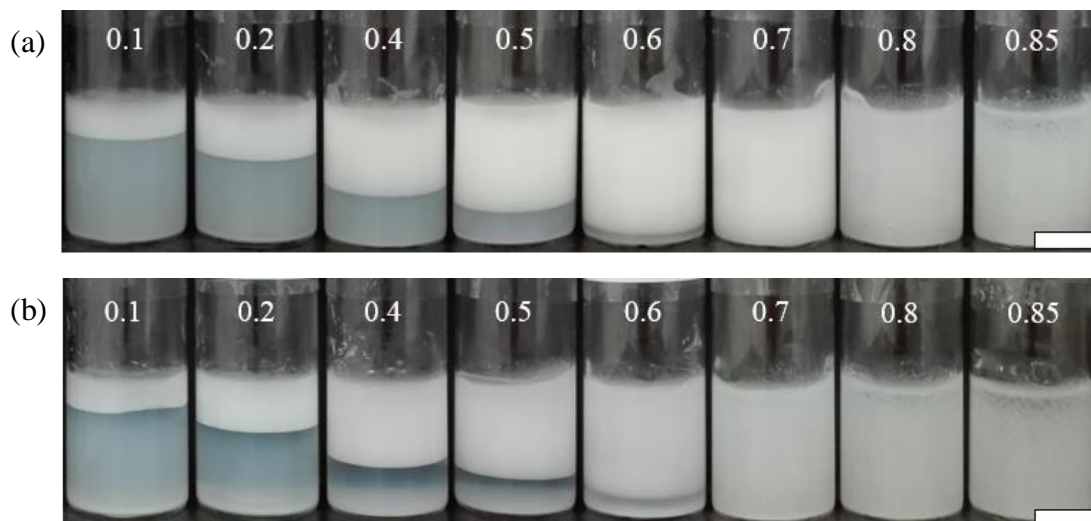
Figure 6.20. Optical microscope images of emulsions in Figure 6.19 at selected ϕ_o (given). Images taken two months after preparation.
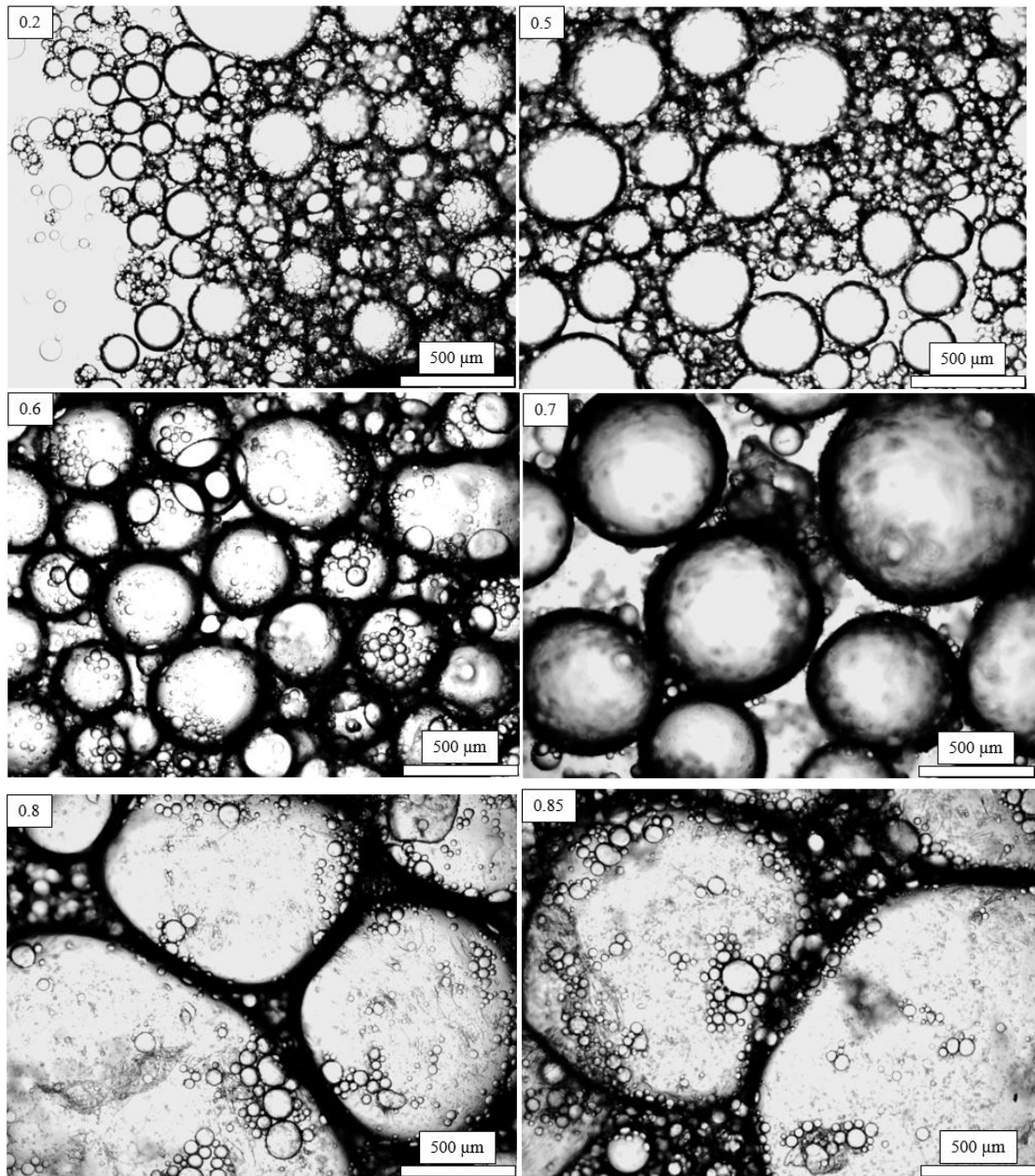
Figure 6.21. (a) Plot of average diameter *versus* the volume fraction of oil (ϕ_o) for emulsions prepared with an aqueous PEC dispersion ($x_{PSSNa} = 0.83$, [PEL] = 5 g L^{-1}, pH = 5.5) and *n*-dodecane after preparation and two months after preparation. (b) Variation of fraction of oil (filled points) and water (open points) resolved after two months as a function of the initial oil volume fraction (ϕ_o).
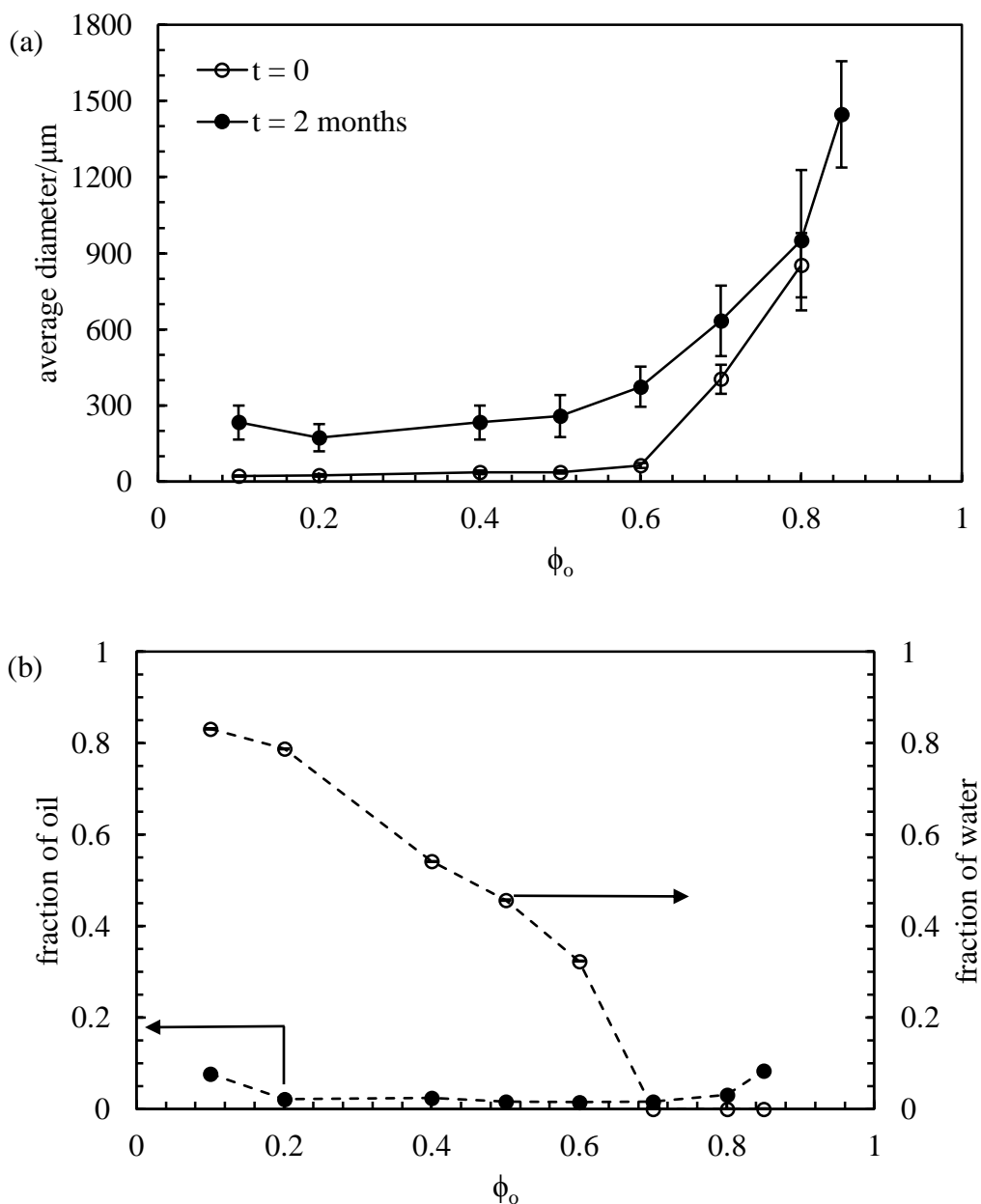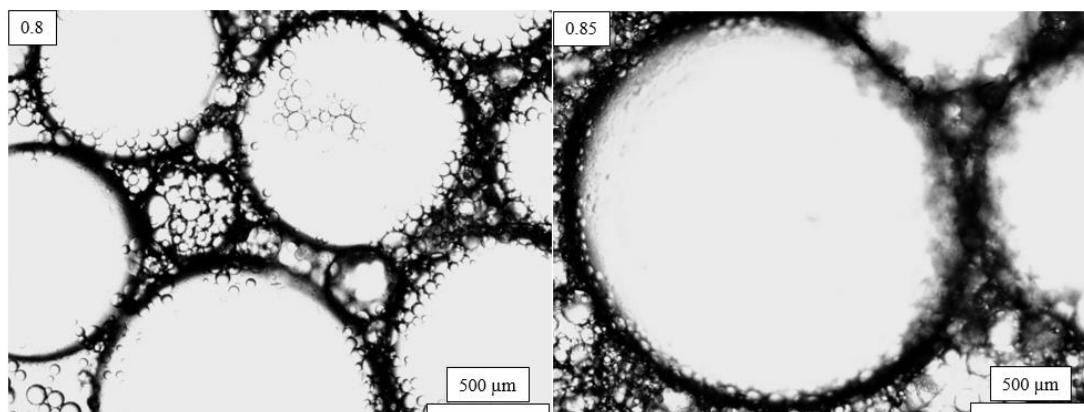
Figure 6.22. Optical microscope images of emulsions in Figure 6.19 at selected ϕ_o (given). Images taken after preparation.

As a control, emulsions with individual PEL solutions (5 g L^{-1}, pH = 5.5) and n-dodecane (ϕ_o = 0.8) were prepared. In both cases, emulsions completely phase separated after homogenisation as shown in Figure 6.23. Therefore, PEC are enabling emulsion stabilisation, unlike the individual PEL.

Figure 6.23. Appearance of emulsions prepared with a PEL solution (given) ([PEL] = 5 g L^{-1}, pH = 5.5) and n-dodecane (ϕ_o = 0.8) after preparation. Scale bar = 1 cm.
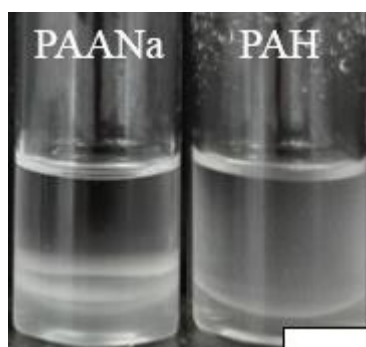
A brief study of the influence of the oil volume fraction (ϕ_o) was carried out for aqueous PEC dispersions prepared with a x_{PAANa} = 0.74 at pH = 5.5, despite the emulsion stability being worse than that with a x_{PAANa} = 0.83. Emulsions were prepared at selected ϕ_o = 0.2, 0.6 and 0.8 (Figure 6.24). The emulsion prepared with a ϕ_o = 0.8 completely coalesced after preparation. However, stable emulsions with a ϕ_o = 0.2 and 0.6 were obtained with an average droplet diameter measured after preparation once creaming stopped of 87 ± 15 μm and 760 ± 197 μm, respectively (Figure 6.25). As expected, average droplet diameters are higher compared to the ones

measured for emulsions prepared at the same ϕ_o but different x_{PAANa} (0.83) (Figure 6.20).

Figure 6.24. Appearance of emulsions prepared with an aqueous PEC dispersion (x_{PAANa} = 0.74, [PEL] = 5 g L^{-1}, pH = 5.5) and *n*-dodecane at different ϕ_o (given). Images taken after preparation once creaming has stopped. Scale bar = 1 cm.
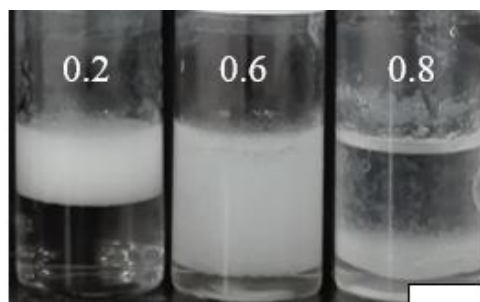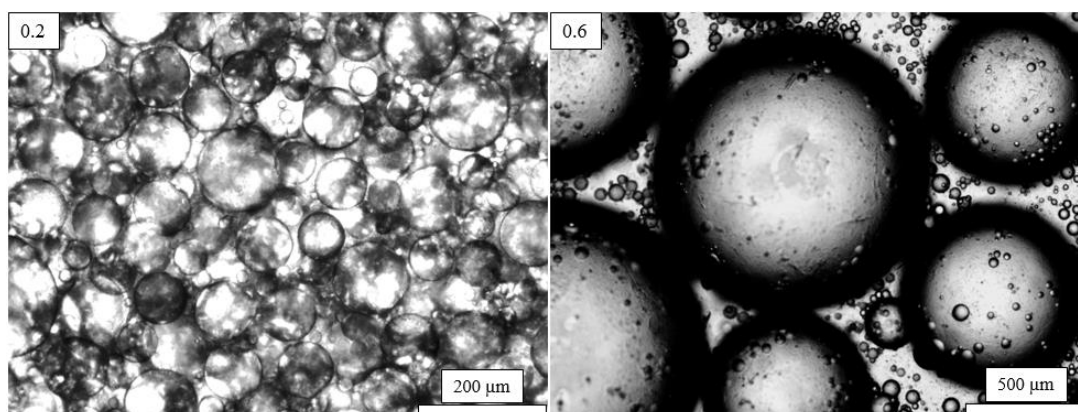

Figure 6.25. Optical micrographs of emulsions in Figure 6.24 at different ϕ_o (given). Images taken after preparation once creaming has stopped.

6.4.2.1 Cryo-SEM images of emulsions

Cryo-SEM images of emulsions prepared with an aqueous PEC dispersion (x_{PAANa} = 0.83, [PEL] = 5 g L^{-1}, pH = 5.5) and *n*-dodecane at two oil volume fractions (ϕ_o = 0.6 and 0.8) were taken. For a ϕ_o = 0.6 (Figure 6.26(a)), both spherical (150 nm) and elongated structures were detected (length ~ 740 nm; diameter ~ 170 nm). At a ϕ_o = 0.8 spherical entities were observed, although few rod-like structures were also present (Figure 6.26(b)). This change in the morphology of PEC entities was also observed from cryo-SEM images for the system PAH-PSSNa (Chapter 5) and still remains intriguing.

**Figure 6.26.** Cryo-SEM images of an emulsion prepared with *n*-dodecane (a) $\phi_o = 0.6$ and (b) $\phi_o = 0.8$ and an aqueous PEC dispersion ($x_{PSSNa} = 0.83$, [PEL] = 5 g L^{-1}, pH = 5.5) at different magnifications.

(a)

(b)
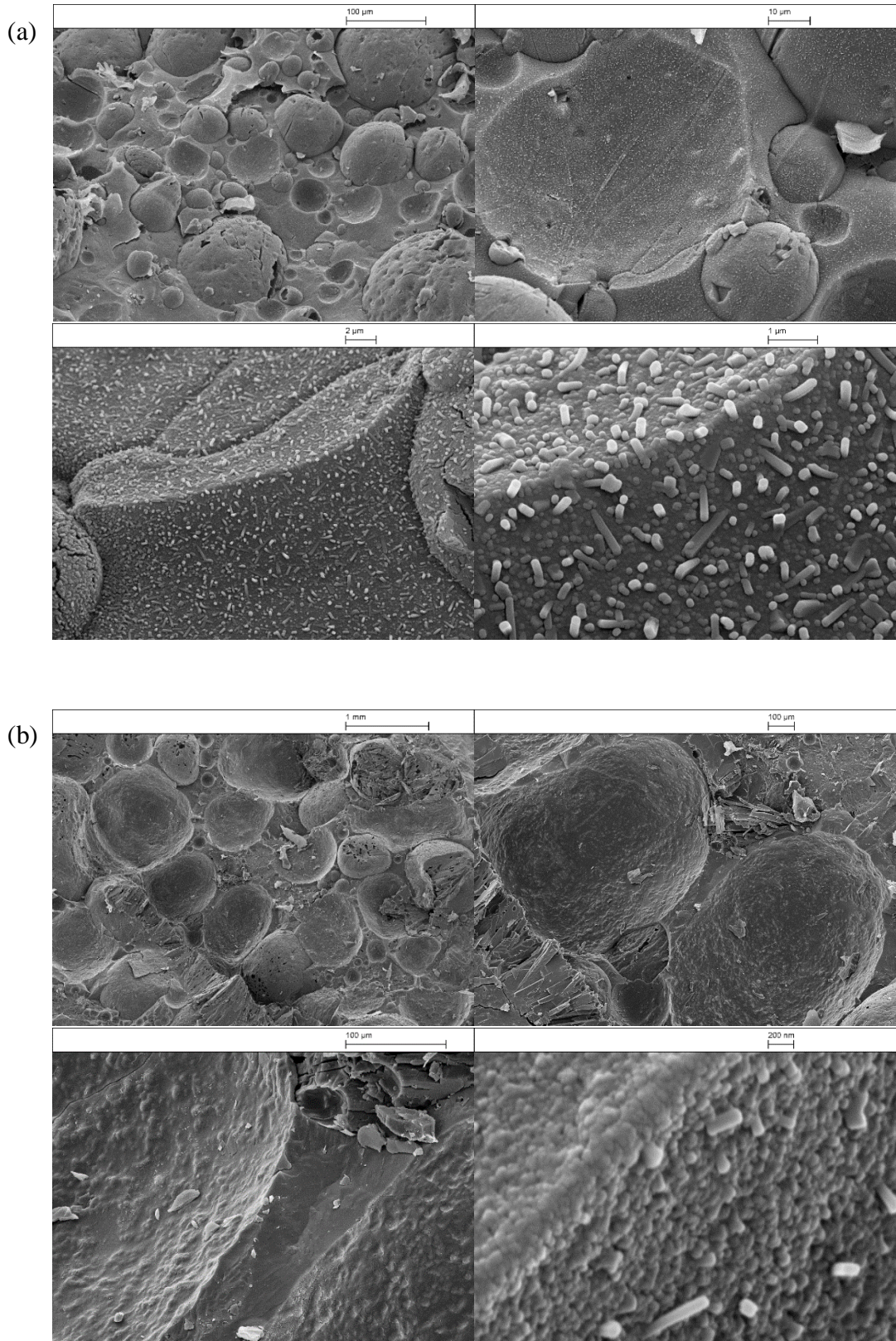
As for the system PAH-PSSNa, CLSM was used to visualise where particles were placed upon emulsification. Firstly, fluorescence measurements were carried out for each PEL solution at pH = 5.5 to check whether each polyelectrolyte is fluorescent after being excited at $\lambda = 405$ nm. As seen from Figure 6.27, PAH is fluorescent while PAANa is not. Even though the existence of some units with large π-conjugated systems and rigid planar structures are necessary prerequisites according to the classical theory,[10] in recent years strong fluorescence from several types of amine-containing polymers without conventional fluorophores was observed.[11] The photoluminescence mechanism of amine containing compounds differs from that of the current fluorescent materials and the presence of the lone-pair electrons on the nitrogen atoms of amine groups are thought to be responsible for the fluorescence emission.[11] Pastor-Pérez *et al.* studied the luminescence of hyperbranched and linear polyethylenimines.[12] The inherent luminescence exhibited in that case was linked to the creation of amine rich nanocluster and electron-hole recombination processes.[12] This has not been studied in detail in this work as it is not in the scope of the current research.

**Figure 6.27.** Fluorescence emission spectra of 5 g L^{-1} PAH and PAANa solutions at pH = 5.5 after being excited at 405 nm. Measurements taken in a 1 cm path length quartz cuvette with four optically clear sides. Milli-Q water was used as reference.
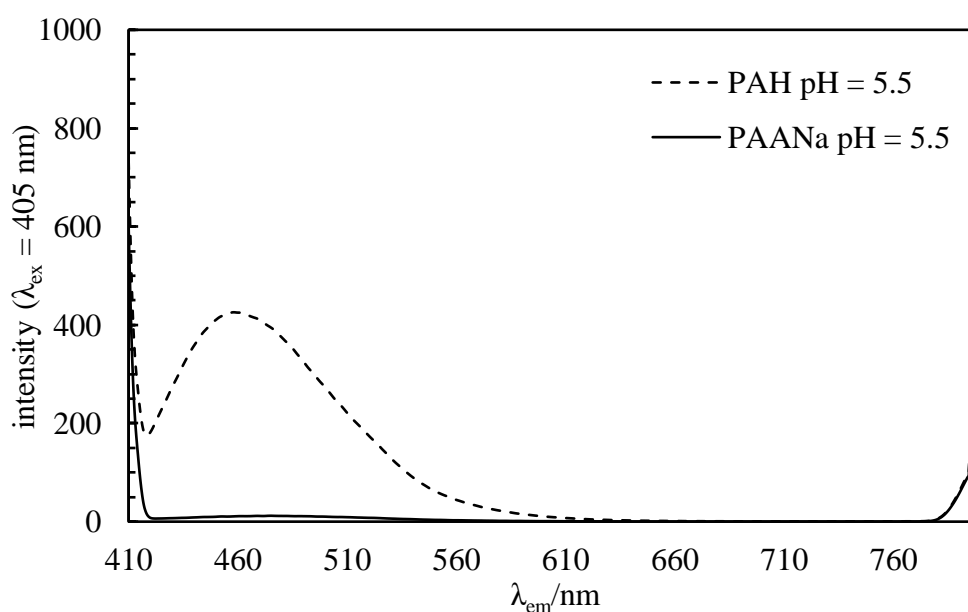
In order to confirm that PEC particles are fluorescent after being excited at 405 nm, confocal micrographs of an aqueous PEC dispersion prepared at $x_{PAANa} = 0.74$ were taken. As shown in Figure 6.28, particles are fluorescent as they appear in red in the confocal micrograph. Despite only PAH being fluorescent, black regions within the particles could not be identified by comparing the optical with the confocal micrograph.

Emulsions at selected oil volume fractions ($\phi_o = 0.2$ and 0.6) were prepared with *n*-dodecane and an aqueous PEC dispersion ($x_{PAANa} = 0.74$, [PEL] = 5 g L^{-1}, pH = 5.5). Confocal microscope images of emulsions in Figure 6.24 were taken and are shown in Figures 6.29 and 6.30. As shown for both ϕ_o, particles were observed at the oil-water interface while the continuous phase was depleted in particles.

Figure 6.28. Optical (left) and confocal micrographs (right) of an aqueous PEC dispersion ($x_{PAANa} = 0.74$, [PEL] = 5 g L^{-1}, pH = 5.5) after being excited at $\lambda = 405$ nm.
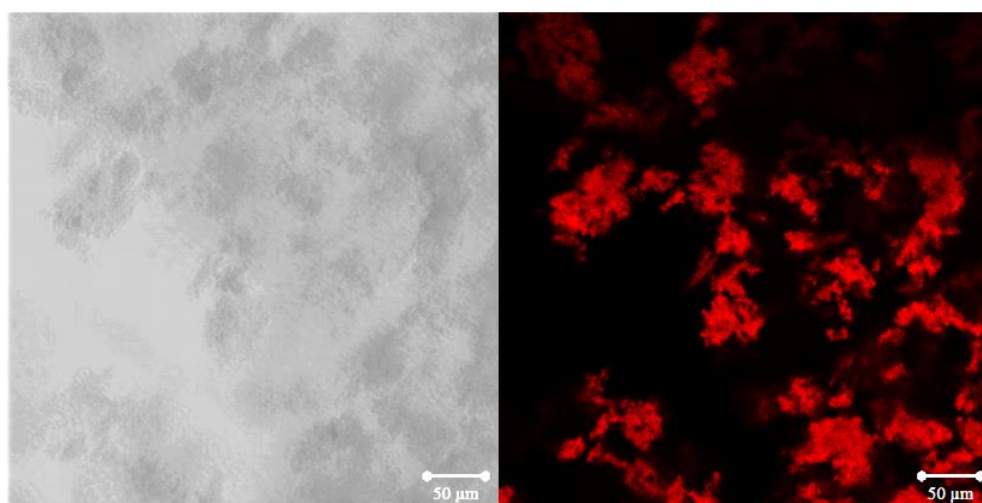
A 3D image was built for the emulsion with a $\phi_o = 0.6$ by taking a series of images at different depths (Figure 6.31). Droplets appear to be partially coated by PEC particles from the 3D reconstruction. This is explained by the fact that at high oil volume fractions, the amount of PEC particles was substantially reduced due to the experimental design.

Therefore, the same conclusions can be taken from the CLSM images as for the system PAH-PSSNa (Chapter 5) at high ϕ_o.

Figure 6.29. Optical (left) and confocal (right) micrographs of an emulsion prepared with an aqueous PEC dispersion (x_{PAANa} = 0.74, [PEL] = 5 g L^{-1}, pH = 5.5) and n-dodecane (ϕ_o = 0.2) taken after preparation once creaming has stopped. (a) and (b) show images taken at different magnifications.

(a)

(b)
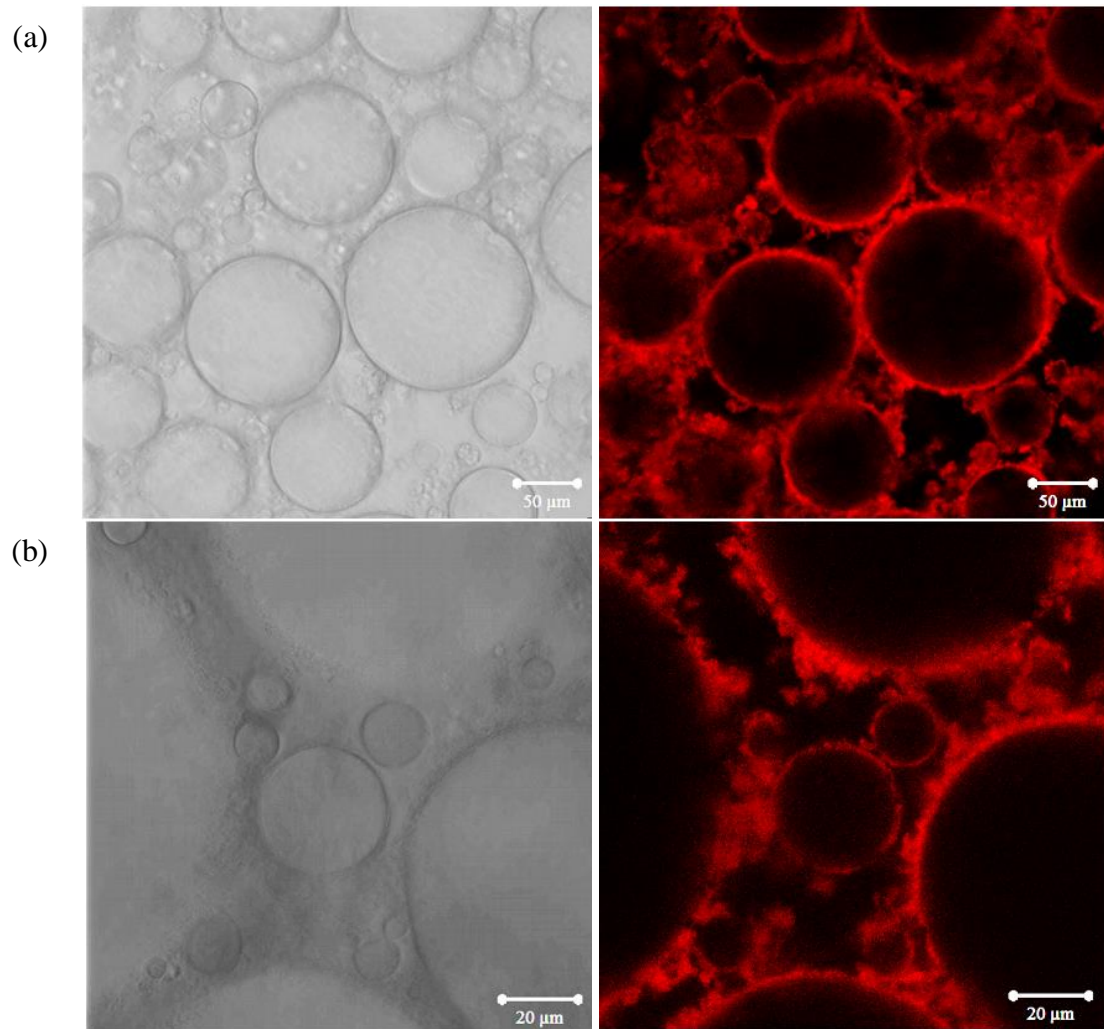
Figure 6.30. Optical (left) and confocal (right) micrographs of an emulsion prepared with an aqueous PEC dispersion (x_{PAANa} = 0.74, [PEL] = 5 g L^{-1}, pH = 5.5) and n-dodecane (ϕ_o = 0.6). Images taken after preparation once creaming has stopped.

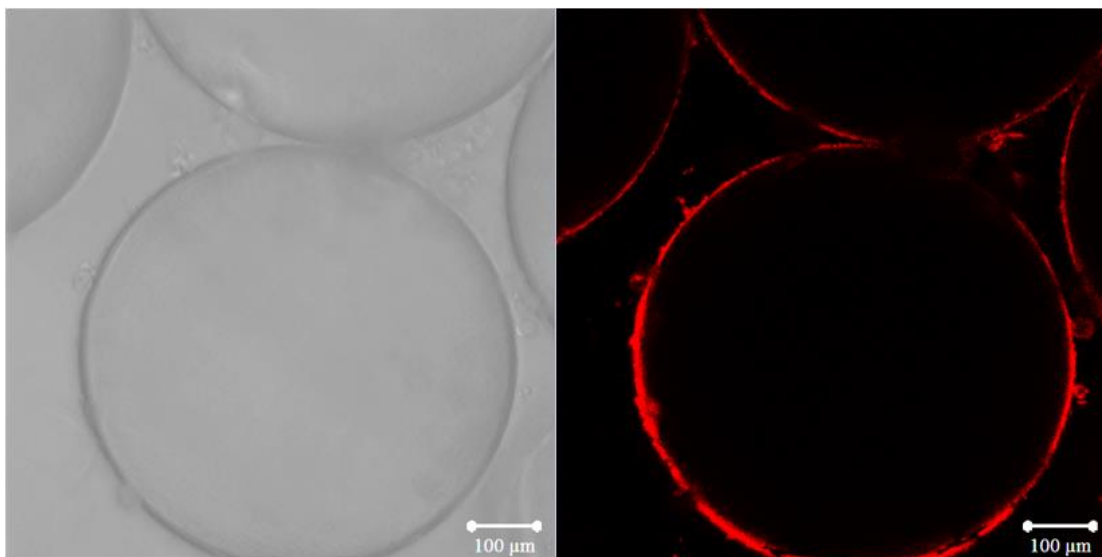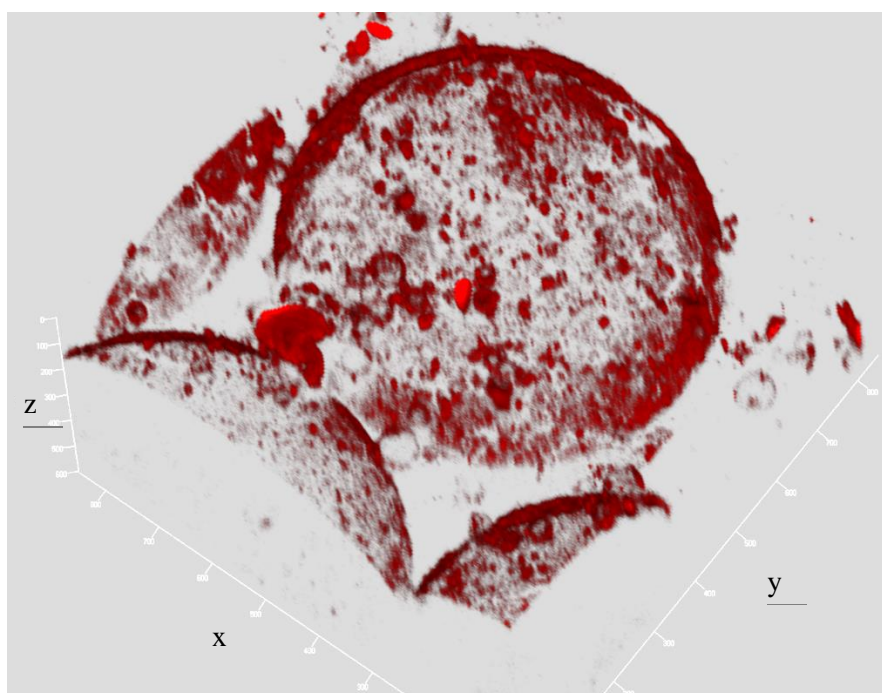**Figure 6.31.** 3D image taken for an emulsion prepared with an aqueous PEC dispersion (x_{PAANa} = 0.74, [PEL] = 5 g L^{-1}, pH = 5.5) and n-dodecane (ϕ_o = 0.6) (dimensions: x and y = 800 μm, z = 600 μm).

6.5 Conclusions

The characterisation of aqueous PEC dispersions has been carried out for the PEL system formed between two oppositely charged weak polyelectrolytes (PAH and PAANa) of similar molecular weight. The effect of pH and x_{PAANa} was evaluated for the average diameter and the charge of complexes prepared in water. At pH extremes, no complexes are formed as one polyelectrolyte is fully protonated. Therefore, polyelectrolyte complexes are formed only at pH where both polyelectrolytes are partially ionised. The size of the complexes falls into the nanometer range despite at specific x_{PAANa} aggregation of particles lead to precipitate formation. At high [PEL], both precipitates and coacervates were identified visually and from optical microscope images at low and intermediate pH, while coacervate droplets are only formed at relatively high pH and specific x_{PAANa}. In any case, the amount of PEC is higher at a x_{PAANa} around charge neutralisation.

For the emulsion study, the investigation was centred at pH = 5.5 as the individual PEL were not surface-active while complexes prepared at specific x_{PAANa} (around charge neutralisation) enabled emulsion stabilisation. Stable emulsions could not be prepared with dispersions containing coacervate droplets in this case (pH = 7 and 10). Regarding the influence of the oil volume fraction on emulsions prepared with *n*-dodecane and an aqueous PEC dispersion at pH = 5.5, high internal phase emulsions, identified by the occurrence of deformed droplets and gel-like emulsions with high viscosities, are obtained at high volume fractions of dispersed phase. They are stable in the long term, despite some oil coalescence after two months. From confocal micrographs taken at low ϕ_o, PEC particles are located only at the interface of dispersed droplets, which were sparsely covered. By increasing ϕ_o to 0.6, less particles were detected in the micrographs as the concentration of particles in the overall emulsion decreased due to the experimental design.

6.6 References

1. A.I. Petrov, A.A. Antipov and G.B. Sukhorukov, *Macromolecules*, 2003, **36**, 10079-10086.

2. L. Vitorazi, N. Ould-Moussa, S. Sekar, J. Fresnais, W. Loh, J.-P. Chapel and J.-F. Berret, *Soft Matter*, 2014, **10**, 9496-9505.

3. X. Liu, M. Haddou, I. Grillo, Z. Mana, J.-P. Chapel and C. Schatz, *Soft Matter*, 2016, **12**, 9030-9038.

4. P.K. Jha, P.S. Desai, J. Li and R.G. Larson, *Polymers*, 2014, **6**, 1414-1436.

5. J. Požar and D. Kovačević, *Soft Matter*, 2014, **10**, 6530-6545.

6. R. Chollakup, J.B. Beck, K. Dirnberger, M. Tirrell and C.D. Eisenbach, *Macromolecules*, 2013, **46**, 2376-2390.

7. Q. Wang and J.B. Schlenoff, *Macromolecules*, 2014, **47**, 3108-3116.

8. J. Koetz and S. Kosmella, Interactions between poly(diallyldimethylammonium chloride) and poly(acrylic acid) in dependence on polymer concentration, presented in part at the International Conference on Scaling Concepts and Complex Fluids, Italy, 1994.

9. K.J. Lissant, in *Emulsions and Emulsion Technology part 1*, ed. K.J. Lissant, Marcel Dekker Inc., New York, 1974, ch. 1.

10. H. Itagaki, in *Experimental Methods in Polymer Science*, ed. T. Tanaka, Academic Press, San Diego, USA, 2000, ch. 3.

11. D. Jia, L. Cao, D. Wang, X. Guo, H. Liang, F. Zhao, Y. Gu and D. Wang, *Chem. Commun.*, 2014, **50**, 11488-11491.

12. L. Pastor-Pérez, Y. Chen, Z. Shen, A. Lahoz, S.-E. Stiriba, *Macromol. Rapid Commun.*, 2007, **28**, 1404-1409.

CHAPTER 7 – SUMMARY OF CONCLUSIONS, FUTURE WORK AND PRELIMINARY EXPERIMENTS

7.1 Summary of conclusions

In this study, our primary goal is to prepare emulsions stabilised with mixtures of oppositely charged polyelectrolytes, in the case where none of the polyelectrolytes are surface-active alone. For this reason, both aqueous PEC dispersions and emulsions were carefully investigated by evaluating the influence of parameters such as the mole fraction of the anionic polyelectrolyte, [PEL], pH, [salt] and oil volume fraction (ϕ_o). By analysing the results obtained from four polyelectrolyte combinations, the final aim is to elucidate a general pattern of behaviour that could predict the conditions to prepare stable emulsions with polyelectrolyte complexes. The conclusions raised from each individual system are summarised below. Afterwards, general conclusions are included.

The system constituted by two strong polyelectrolytes (PDADMAC and PSSNa) is discussed in Chapter 3. PEC particles are obtained across the mole fraction range as a result of a strong electrostatic interaction and the highest amount of entities is obtained around charge neutrality. By increasing the [PEL] upon the preparation of aqueous dispersions, both aggregation of primary particles and an increase in the number of PEC was achieved. For the emulsion study, the most stable emulsion to both creaming and coalescence is formed at around equal mole fraction of the two polymers, and it possesses the smallest average droplet diameter. On the contrary, emulsions prepared with the individual PEL complete phase separate. By increasing the initial polyelectrolyte concentration, the average droplet diameter decreases fitting with the emulsifier-poor régime of the limited coalescence model for particle-stabilised emulsions. Using cryo-SEM, particles are visualised at the oil-water interface of emulsion drops. At low polyelectrolyte concentrations their distribution is not uniform, whereas at high concentrations a layer of close-packed particles covers the interfaces and excess particles aggregate in the aqueous continuous phase enhancing emulsion stability. By increasing the salt concentration in aqueous particle dispersions, the transition: stable dispersions – aggregated and unstable dispersions – solutions of individual polymer molecules is found. The corresponding emulsions are initially destabilized completely at intermediate salt concentrations and subsequently re-

stabilised at high salt concentrations by adsorbed polymer molecules. Therefore, emulsions stabilised by PEC are stimuli-responsive by addition of salt. Stable emulsions could be prepared with aqueous PEC dispersions and various oils with no significant differences regarding their stability, while emulsions prepared with PEL solutions were completely unstable. The behaviour at air-water and oil-water planar interfaces was briefly investigated and no reduction of either the surface or interfacial tension was detected when particles were present in water. Therefore, an external force is required to bring the particles to the interface.

Chapter 4 includes the results for the strong cationic (PDADMAC) – weak anionic (PAANa) system. In aqueous mixtures of this polyelectrolyte combination, both precipitation and complex coacervation occurred as a result of an associative phase separation phenomenon which is dependent on pH. The progression coacervate – precipitate/coacervate – coacervate ensued upon increasing the pH as PAANa becomes ionised. Although precipitates are expected to be formed at high pH when both polyelectrolytes are fully charged, complex coacervation resulted. TEM images of coacervate droplets revealed the presence of no internal structure, in agreement with the few electron micrographs of coacervate droplets in the literature. For a dispersion containing coacervate droplets, salt induces first their coalescence, followed by a dissolution of the complex when the salt content is really high. Regarding emulsions prepared from aqueous PEC dispersions, no stable emulsion was possible at low and intermediate pH where coacervate droplets or coacervate droplets and solid particles coexist due to their relatively low amount, their considerable size or their intrinsic hydrophilicity. By contrast, at high pH, stable dodecane-in-water emulsions could be prepared from the coacervate phase of near neutral charge by addition of oil stepwise, while emulsions with PEL solutions were unstable. The morphology of the oil droplets coated by the coacervate phase (complete engulfing, partial engulfing or non-engulfing) is compared with theoretical predictions using equilibrium spreading coefficients for a range of oils. Despite the agreement for dodecane and toluene, a discrepancy is found for the other oils. This disagreement could be related to kinetic aspects linked to the viscosity of the coacervate phase which are not considered in the calculation of equilibrium spreading coefficients but could play a role in the encapsulation process.

The results for the system prepared with a weak cationic (PAH) and a strong anionic (PSSNa) polyelectrolyte are included in Chapter 5. By increasing the pH, the transition precipitate – precipitate/coacervate – coacervate – polymer solution was observed, in agreement with the predicted behaviour. At low pH, both PEL are fully ionised and therefore precipitates arise as a result of strong electrostatic interactions. By increasing the pH, the degree of ionisation of PAH decreases and weak electrostatic interactions ensue, which supports the formation of coacervate droplets. The most stable emulsions, *i.e.* lowest average droplet diameter, highest fraction of cream and lowest amount of oil coalesced were prepared around charge neutralisation and emulsion stability occurred in a narrow mole fraction range of the anionic polyelectrolyte. Emulsions with coacervate droplets could be prepared but the stability was worse compared to that with PEC particles. By increasing the initial [PEL], the average droplet diameter decreases and the fraction of cream in the emulsion increases for emulsions prepared with PEC particles, following the limited coalescence model. However, at high [PEL] the stability of emulsions is slightly worse probably due to high aggregation levels of PEC particles compared to the case at low [PEL]. By increasing the oil volume fraction, the average droplet diameter of emulsions prepared with aqueous PEC dispersions increased. At high oil volume fractions, oil droplets appear to be deformed and the viscosity of emulsions increased considerably, indicating the formation of HIPEs. From confocal micrographs of emulsions at high ϕ_o, PEC particles are only detected at the oil-water interface. At low oil volume fractions, excess particles form a network in the aqueous continuous phase giving extra stability against coalescence.

Chapter 6 encompasses the system formed between two weak polyelectrolytes (PAH and PAANa). The transition precipitate/coacervate – coacervate ensued by increasing the pH from 4 to 10. By increasing the [PEL], higher amount of PEC particles or coacervate droplets arise as well as an increase in the aggregation levels. The most stable emulsions with the lowest average droplet diameter, highest fraction of cream and lowest amount of oil coalesced were prepared in a narrow mole fraction range around charge neutrality at intermediate pH, when both particles and coacervate droplets coexist. Moreover, at this pH, individual PEL are not surface-active as complete phase separation occurred one day after preparation. Formation of HIPEs at high oil volume fractions was confirmed by the occurrence of gel-like emulsions and

deformed oil droplets. From confocal micrographs of emulsions at high ϕ_o, PEC entities were detected at the oil-water interface.

Therefore, by identifying the common findings among the studied systems, the following general conclusions can be formulated. For aqueous PEC dispersions, the highest amount of PEC (particles or coacervate droplets) is obtained around charge neutralisation. In general, strongly interacting PEL give rise to precipitates while weakly interacting PEL form coacervates. By increasing the initial polyelectrolyte concentration, higher amounts of PEC and higher aggregation levels ensue. Salt has an important effect in the complexation process of both precipitates and complex coacervates. For both types of associative phase separation, by increasing the salt content complexes first aggregate and finally dissolve releasing individual PEL chains, which remain in solution. Regarding the emulsion behaviour, oil-in-water emulsions are prepared under any condition and those with highest stability are obtained around charge neutralisation. This could suggest the following stabilisation mechanism: at the x_{PEL} extremes, particles are highly charged due to the presence of the polyelectrolyte in excess at their surfaces. Therefore, they are really hydrophilic and prefer to remain dispersed in water. By approaching a x_{PEL} close to charge neutrality, the hydrophobicity of the particles increases enabling them to stay at the oil-water interface. This explanation was already posed for emulsions stabilised with mixtures of particles of opposite charge.[1] Emulsions prepared with particles are more stable than those stabilised with coacervates. For emulsions with PEC particles, the oil type does not significantly affect the emulsion stability and the preparation procedure does not need to be optimised as in the case of emulsions stabilised with coacervate droplets. By increasing the [PEL], the emulsion stability is improved. However, at relatively high concentrations, high aggregation levels can slightly worsen the stability as large particles can easily be dislodged from droplet interfaces. As for aqueous PEC dispersions, the presence of salt has an impact on emulsion stability. For emulsions stabilised with PEC particles, by increasing the aggregation level, emulsions become completely unstable. However, at a relatively high salt content, emulsions re-stabilise due to the presence of free polymer molecules. HIPEs are formed at high oil volume fractions, which is not common in particle-stabilised systems, where catastrophic phase inversion is the usual phenomenon.

Despite this work being a complete starting point for the basic understanding of emulsions stabilised by mixtures of oppositely charged polymers, we are not yet in a position to predict definite rules of behaviour in both aqueous PEC dispersions and emulsions containing them. Further investigation of other polyelectrolyte combinations is required to develop a better understanding of this area.

7.2 Future work and preliminary experiments

7.2.1 Future work

In this research, four polyelectrolyte combinations were studied. In order to confirm the general behaviour summarised in the conclusions section, the investigation should be extended to other polyelectrolyte mixtures of strong and weak polyelectrolytes. Moreover, as shown in Chapter 3, the concentration of NaCl (a monovalent salt) had an important effect on the behaviour of aqueous PEC dispersions and emulsions. Hence, future work could also focus on the effect of divalent salts, *i.e*. $CaCl_2$.

The two oppositely charged polyelectrolytes selected for the systems studied throughout this thesis were water-soluble. Therefore, it could be of interest to mix an oil-soluble polyelectrolyte with a water-soluble one. With this, the complex would be formed at the oil-water interface upon homogenisation. Hence, the characterisation of the complex dispersion will be more difficult. Monteillet *et al*. carried out complexation studies between poly(fluorine-*co*-benzothiadiazole-*co*-benzoic acid) (oil-soluble anionic polyelectrolyte) and poly(diallyldimethylammonium) chloride or poly(L-lysine) (water-soluble cationic polyelectrolytes).[2] They proved the formation of the complex at the oil-water interface *via* tensiometry and confocal microscopy. Moreover, a brief emulsion study was carried out.

Following up this idea, oil-in-oil and water-in-water emulsions stabilised by polyelectrolyte complexes could be investigated by mixing two oil-soluble or two water-soluble polyelectrolytes, respectively. The advantage of these two systems is that each polyelectrolyte could be in a different phase and the complex could be formed upon homogenisation at the oil-oil or water-water interface; or the complexation could occur either in one of the oil or water phases and the oil-in-oil or water-in-water emulsion would be prepared after the subsequent addition of the

second oil or water phase, respectively. Additionally, both preparation procedures could be compared in terms of their stability.

Another interesting point to study is whether polyelectrolyte complexes can stabilise Janus emulsions. Preliminary experiments with the system PAH-PSSNa are included in the following section. Both, the influence of total oil volume fraction in the emulsion and the ratio of the two oils within the oil phase could be investigated.

The process of PEC formation in water has been widely studied using Monte Carlo simulations,[3-5] including the effects of adding salt.[6] However, simulations dealing with the behaviour of polyelectrolyte complexes at fluid interfaces are lack in the literature.

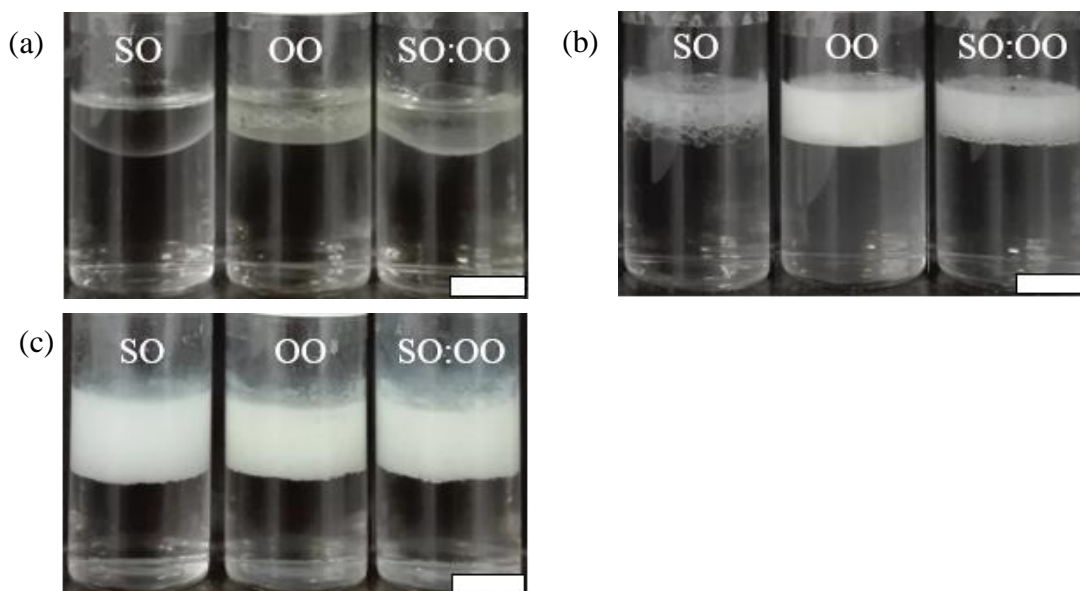### 7.2.2 *Janus emulsions prepared with polyelectrolyte complexes*

Janus emulsions are a class of emulsions whose droplets are composed of two lobes of immiscible oils dispersed in a continuous aqueous medium. Examples of immiscible oils are given in Table 1 of ref. 7. The concept of Janus was coined by de Gennes and it is named after the two-faced god in the Roman mythology.[8] Janus emulsions were first produced with microfluidic devices.[9] Afterwards, the use of traditional medium energy vibrational methods (Mini Vortex)[10,11] and high-energy mixing (Ultra-turrax)[12] extended their application to a greater area.

Stabilisation of Janus emulsions has been accomplished with various surfactants such as the nonionic surfactant Tween 80,[13] amphoteric surfactants,[14] magnetic nanoparticles[15] and even polyelectrolyte complexes (gelatin and chitosan).[16,17] For Janus emulsions stabilised with polyelectrolyte complexes from a protein and a polysaccharide, the individual components can also stabilise Janus emulsions. However, the mixture of the two polyelectrolytes improves the droplet stability.[16,17] Inspired from this work, we decided to prepare emulsions with oppositely charged synthetic polyelectrolytes, in the case where the individual PEL are not surface-active. Preliminary results were carried out for the system PAH-PSSNa. The selected immiscible oils – silicone oil (50 cSt at 25°C) and olive oil (highly refined, low acidity) – were purchased from Sigma-Aldrich and were filtered twice through a basic alumina column to remove polar impurities.

Before generating Janus emulsions, simple emulsions were prepared with both PEL solutions (5 g L^{-1}, pH = unmodified) and an aqueous PEC dispersion (x_{PSSNa} = 0.83,

[PEL] = 5 g L^{-1}, pH = unmodified) to check whether emulsions could be prepared with the individual oils. As shown in Figure 7.1(a), PAH is not surface-active as emulsions with either silicone oil or olive oil complete phase separate after homogenisation. Despite PSSNa being partially surface-active, a high amount of oil coalesces after two months (Figure 7.1(b)). On the other hand, emulsions prepared with an aqueous PEC dispersion are stable in the long term with a small amount of oil coalesced (Figure 7.1(c)). Optical microscope images of simple emulsions with aqueous PEC dispersions are taken after preparation once creaming halted and are shown in Figure 7.2. Oil droplets of olive oil appear to be darker than those of silicone oil and contained air bubbles created during homogenisation. Confocal microscope images of freshly prepared emulsions with silicone oil and olive oil are shown in Figure 7.3 (a) and (b), respectively. The same pattern of behaviour is observed.

Figure 7.1. Appearance of emulsions two months after preparation with either silicone oil (SO), olive oil (OO) or a mixture 1:1 of silicone oil and olive oil (SO:OO) (ϕ_o = 0.2) and (a) 5 g L^{-1} PAH solution, (b) 5 g L^{-1} PSSNa solution or (c) an aqueous PEC dispersion prepared with the system PAH-PSSNa (x_{PSSNa} = 0.83, [PEL] = 5 g L^{-1}, pH = unmodified). Scale bars = 1 cm.

Afterwards, Janus emulsions were prepared by mixing equal volumes of both oils with either a polyelectrolyte solution (5 g L^{-1}) or an aqueous PEC dispersion (x_{PSSNa} = 0.83, [PEL] = 5 g L^{-1}, pH = unmodified). As seen from Figure 7.1(a) (last vial), complete phase separation is achieved when PAH is used as emulsifier. PSSNa is surface-active

(Figure 7.1(b), last vial) but some oil coalesces after two months. When preparing the emulsion with an aqueous PEC dispersion, a stable Janus emulsion is obtained (Figure 7.1(c) last vial). Droplets are spherical and divided in two hemispheres each of them containing a different oil (Figure 7.2). Confocal micrographs of the emulsion at two different magnifications are shown in Figure 7.3(c,d). The hemisphere containing olive oil can be identified by comparing confocal micrographs of the Janus emulsion with those obtained from the simple emulsion with olive oil, as they both appear in red.

Figure 7.2. Selected optical microscope images of emulsions prepared with either silicone oil (SO), olive oil (OO) or a mixture 1:1 of silicone oil and olive oil (SO:OO) ($\phi_o = 0.2$) and an aqueous PEC dispersion prepared with the system PAH-PSSNa ($x_{PSSNa} = 0.83$, [PEL] = 5 g L^{-1}, pH = unmodified). Images taken after preparation once creaming has halted.

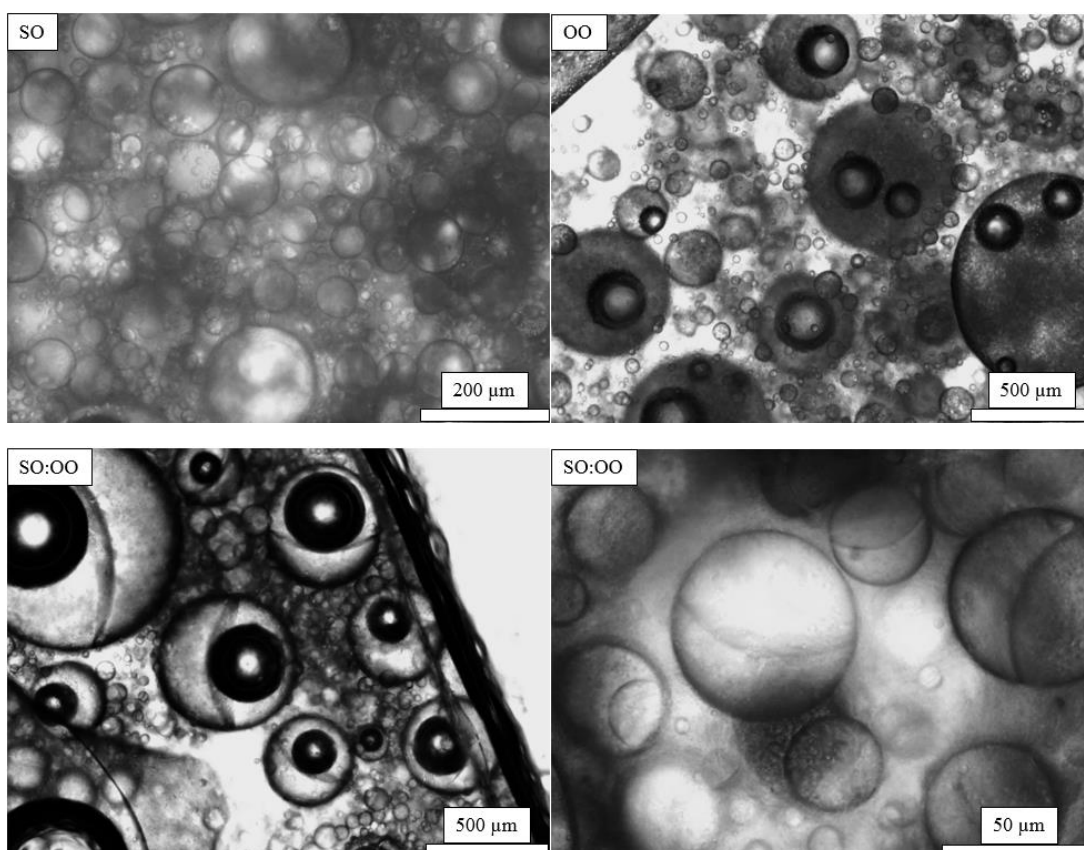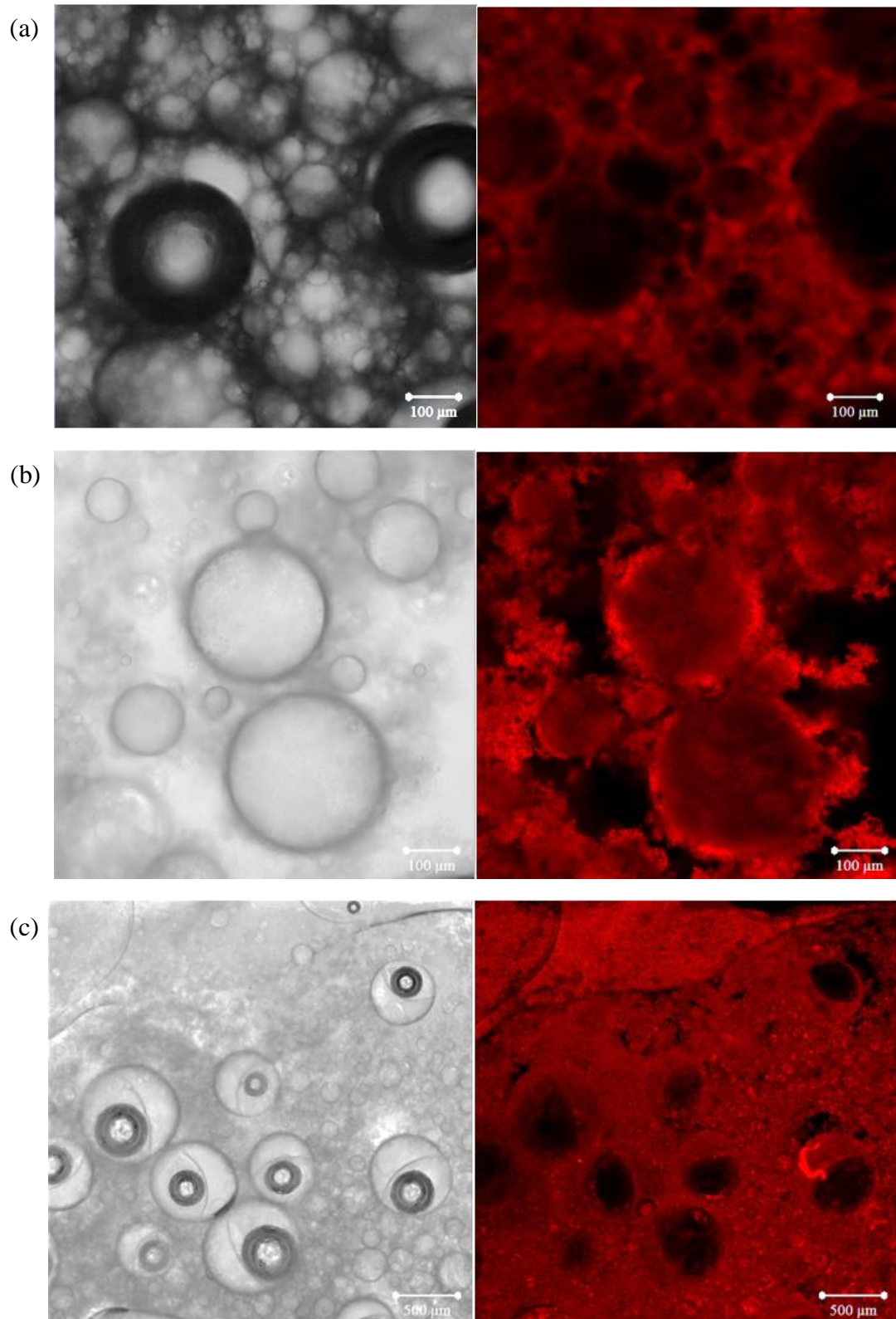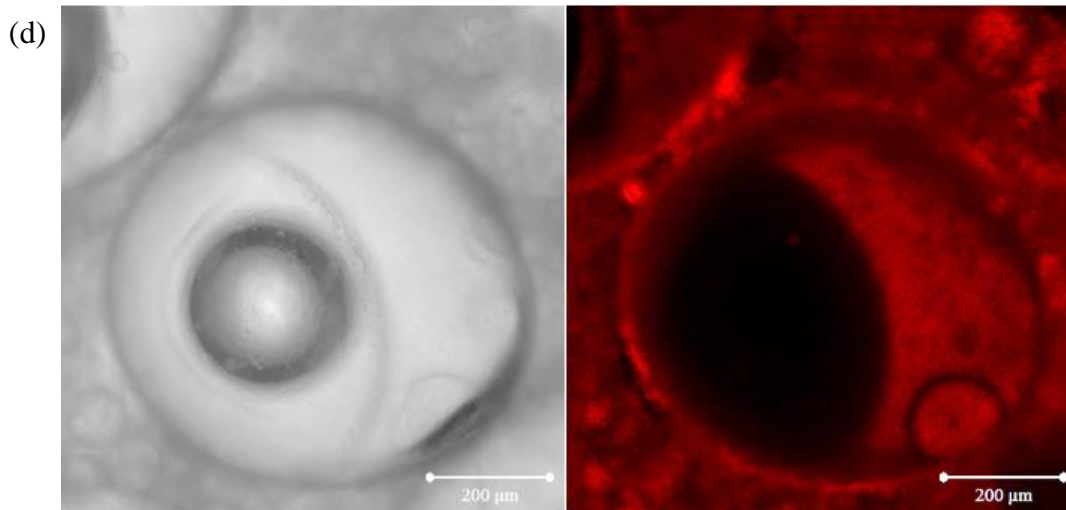**Figure 7.3.** Optical (left) and confocal (right) micrographs of freshly prepared emulsions with an aqueous PEC dispersion (x_{PSSNa} = 0.83, [PEL] = 5 g L^{-1}, pH = unmodified) and (a) silicone oil, (b) olive oil or (c,d) a mixture 1:1 of silicone oil and olive oil. In all cases the oil volume fraction in the emulsion (ϕ_o) is 0.2.

(a)

(b)

(c)

(d)

At low oil volume fraction ($\phi_o = 0.2$), PSSNa is a little surface-active. From the results discussed in Chapter 5 for the system PAH-PSSNa with *n*-dodecane, it was found that at high oil volume fractions, none of the PEL were surface-active in the long term. Therefore, the same study was carried out at an oil volume fraction of 0.8. As shown in Figure 7.4(a) and (b), neither PAH nor PSSNa are surface-active as both simple and Janus emulsions prepared with the mixture of the two oils complete phase separate after two months. For simple emulsions prepared with PSSNa, a few drops remain but they are mainly around the walls of the vial. On the other hand, simple and Janus emulsions prepared with aqueous PEC dispersions are stable in the long term (Figure 7.4(c)). Optical microscope images of these emulsions are shown in Figure 7.5. They have the same appearance as the ones obtained at low oil volume fraction despite being larger in size. Moreover, unlike emulsions prepared with *n*-dodecane at $\phi_o = 0.8$, in these cases oil droplets do not appear to be deformed.

Figure 7.4. Appearance of emulsions two months after preparation with either silicone oil (SO), olive oil (OO) or a mixture 1:1 of silicone oil and olive oil (SO:OO) (ϕ_o = 0.8) and (a) 5 g L^{-1} PAH solution, (b) 5 g L^{-1} PSSNa solution or (c) an aqueous PEC dispersion prepared with the system PAH-PSSNa (x_{PSSNa} = 0.83, [PEL] = 5 g L^{-1}, pH = unmodified). Scale bars = 1 cm.
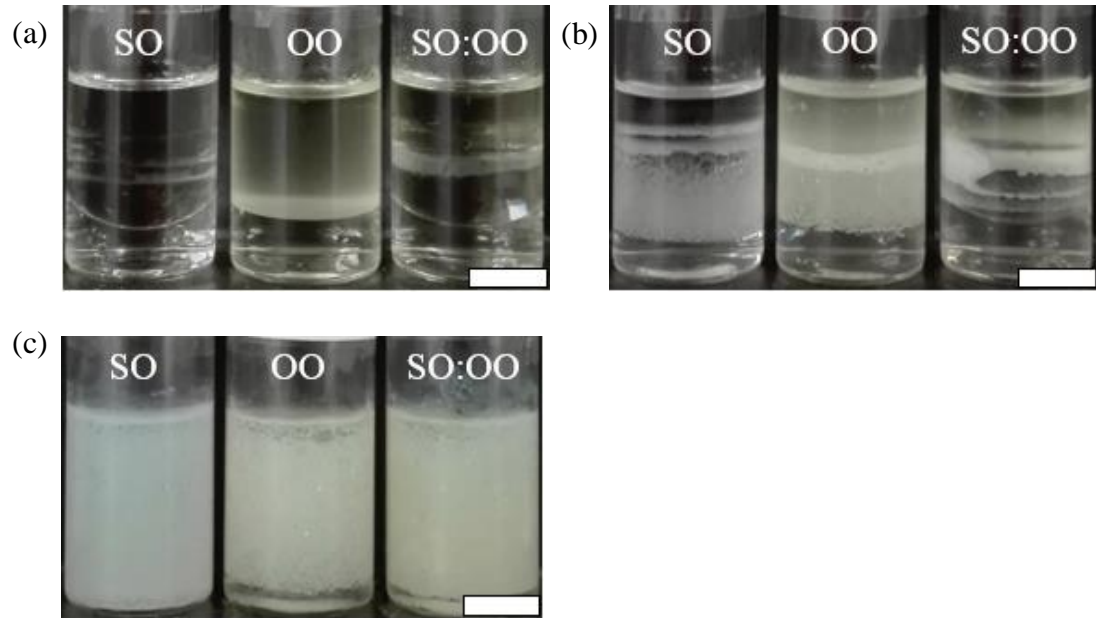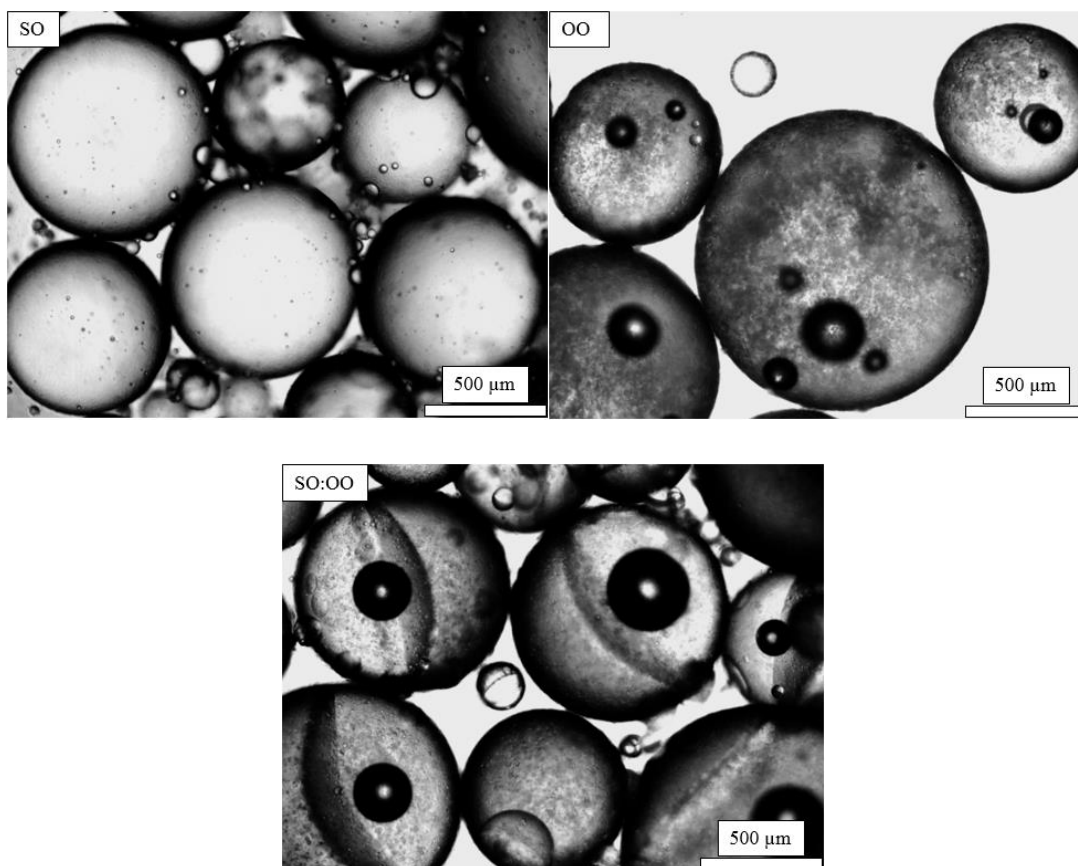
Figure 7.5. Selected optical microscope images of emulsions prepared with either silicone oil (SO), olive oil (OO) or a mixture 1:1 of silicone oil and olive oil (SO:OO) ($\phi_o = 0.8$) and an aqueous PEC dispersion prepared with the system PAH-PSSNa ($x_{PSSNa} = 0.83$, [PEL] = 5 g L^{-1}, pH = unmodified). Images taken after preparation once creaming has halted.

7.3 References

1. T. Nallamilli, B.P. Binks, E. Mani and M.G. Basavaraj, *Langmuir*, 2015, **31**, 11200-11208.

2. H. Monteillet, F. Hagemans and J. Sprakel, *Soft Matter, 2013, 9, 11270-11275.*

3. C.F. Narambuena, E.P.M. Leiva, M. Chávez-Páez and E. Pérez, *Polymer*, 2010, **51**, 3293-3302.

4. V. Starchenko, M. Müller and N. Lebovka, *J. Phys. Chem. C*, 2008, **112**, 8863-8869.

5. J. Rydén, M. Ullner and P. Linse, *J. Chem. Phys.*, 2005, **123**, 034909.

6. Y. Hayashi, M. Ullner and P. Linse, *J. Phys. Chem. B*, 2003, **107**, 8198-8207.

7. B.P. Binks and A.T. Tyowua, *Soft Matter*, 2016, **12**, 876-887.

8. P.G. de Gennes, *Rev. Mod. Phys.*, 1992, **64**, 645-648.

9. J. Guzowski, P.M. Korczyk, S. Jakiela and P. Garstecki, *Soft Matter*, 2012, **8**, 7269-7278.

10. H. Hasinovic and S.E. Friberg, *J. Colloid Interface Sci.*, 2011, **361**, 581-586.

11. H. Hasinovic and S.E. Friberg, *Langmuir*, 2011, **27**, 6584-6588.

12. L. Ge, S. Lu, J. Han and R. Guo, *Chem. Commun.*, 2015, **51**, 7432-7434.

13. H. Hasinovic, S.E. Friberg and G. Rong, *J. Colloid Interface Sci.*, 2011, **354**, 424-426.

14. I. Kovach, J. Koetz and S.E. Friberg, *Colloids Surf. A*, 2014, **441**, 66-71.

15. R.R. Raju, F. Liebig, B. Klemke and J. Koetz, *Colloid Polym. Sci.*, 2018, **296**, 1039-1046.

16. R.R. Raju, S. Kosmella, S.E. Friberg and J. Koetz, *Colloids Surf. A,* 2017, **533**, 241-248.

17. I. Kovach, J. Won, S.E. Friberg and J. Koetz, *Colloid Polymer. Sci.*, 2016, **294**, 705-713.